Removal of Enteric Viruses By Ultrafiltration Membranes

by

Ahmed El-Hadidy

A thesis
presented to the University of Waterloo
in fulfillment of the
thesis requirement for the degree of
Master of Applied Science
in
Civil Engineering

Waterloo, Ontario, Canada, 2011

AUTHOR'S DECLARATION

I hereby declare that I am the sole author of this thesis. This is a true copy of the thesis, including any required final revisions, as accepted by my examiners.

I understand that my thesis may be made electronically available to the public.

Abstract

Application of low pressure membranes in drinking water treatment, including both microfiltration (MF) and ultrafiltration (UF), have witnessed a rapid increase in the past decades. Low pressure membranes are considered a good technology in retrofitting existing conventional drinking water treatment plants or in newly constructed plants to meet the stringent regulations for drinking water treatment that aim at preventing health risks of waterborne diseases. Enteric viruses are one of the major types of waterborne pathogens, and they can be commonly found and are persistent in the environment. Both the United States and Canada require a 99.99% (4-log) removal of viruses during the drinking water treatment train.

Unlike MF membranes, UF membranes have a very good potential for removing enteric viruses from the water due to their smaller pores comparable to the size of viruses. Drinking water regulations/guidelines in both the United States and Canada do not grant UF membranes any removal credit for viruses by default; however they have the provision that, in certain cases, virus removal credit may be granted based on pilot scale challenge testing. A better understanding of the interaction between the UF membranes and virus rejection can help to establish a removal credit for UF membranes. An essential part of this will be the effect of the membrane operation on the rejection of viruses to determine if UF membranes can offer a consistent removal of viruses. Membrane fouling is one of the major problems in membrane operation and it can affect the rejection characteristics of the membrane and improve its performance.

The aim of this study was to investigate the removal of virus surrogates (MS2 and φX174 bacteriophage) using a commercial UF membrane under different conditions, to obtain information about the removal mechanisms of viruses. The experimental filtration unit was designed to have similar conditions like the full scale membrane treatment plants. The UF membrane used in this study provided very good removal of both MS2 and φX174 bacteriophage. The obtained results were consistent and in agreement with the expected removals based on the membrane characterization results and types of virus surrogate. As part of this work, a detailed study to improve methods for characterizing the pore size distribution of membranes was conducted.

In the second part of the study, two different types of surface waters were used to study the effect of membrane fouling on virus removal. It was found that mainly hydraulically irreversible fouling could significantly improve the virus removal by UF membranes. Different cleaning regimes that are

used in treatment plants had varying effects on virus removal. After maintenance cleaning, virus removal remained higher than that of clean membranes, and only chemical cleaning was effective for completely removing membrane foulants and returning virus removal back to base levels. Advanced analytical techniques were used to define the nature of the fouling layer on the membrane surface and how the foulants affected the rejection of viruses.

Finally, our study showed that UF membranes are a robust treatment technology for removing different types of enteric virus surrogates from water under different operational conditions. Close monitoring of the UF unit performance and direct integrity testing can possibly detect membrane problems that can affect the rejection of viruses. Based on the virus physical characteristics and a detailed study of the membrane surface characteristics, especially the pore size distribution of the membrane, the removal of the specific virus can be closely estimated.

Acknowledgements

First, all praises to Allah (God) for all his blessings and for helping me to tread the path in search of knowledge.

I wish to thank my supervisors Dr. Peter M. Huck, Dr. Sigrid Peldszus and Dr. Michele Van Dyke for their guidance and continuous support throughout this research from the initial to final level of this work. Also I would like to thank all the other members of the NSERC chair team of water treatment at the University of Waterloo for their help and advice.

This research project was funded by the Walkerton Clean Water Center (WCWC), Ontario, Canada. NSERC chair in water treatment at the University of Waterloo and its partners kindly supported this project by providing the required lab facilities and their technical support. Thanks to the City of Waterloo and the Town of Collingwood for their help in providing the surface waters used in this research project.

Thanks to Terry Ridgway, Mark Sobon and Mark Merlau for their technical support at the University of Waterloo and Nina Heinig at the Waterloo Advanced Technology Lab (WETLAB) for her help with FE-SEM work. Thanks for everyone who helped me during this work: Cynthia Hallé, Jan Benecke, Vishal Luniya, Curtis Fang, and Mohamed Hamouda.

Finally, I would like to express my gratitude to my parents for their continuous support and unlimited love. They had endless faith in me and always encouraged me to achieve my dreams. Also I want to thank my wife Heba for all the joy and hope she added to my life.

Table of Contents

List of Figures

List of Tables

Chapter 1
Introduction

1.1 Problem Statement

Addressing microbiological hazards through drinking water treatment is of major concern for drinking water providers in order to meet stringent water quality regulations worldwide. Enteric viruses are one of the main categories of microbiological contaminants in raw water sources and current Canadian Drinking Water Quality Guidelines require more than 99.99% removal of viruses through employing different treatment technologies (Health Canada 2004). Although enteric viruses can be disinfected by chlorine efficiently, it is prudent to achieve removals in other treatment processes so that multiple barriers are in place to achieve overall adequate virus removal. Fairly high fluences are required to inactive viruses, and due to their small size, virus removal by filtration is challenging.

Membrane filtration is a promising technology for drinking water treatment due to its ability to efficiently remove turbidity and different types of microbiological contaminants in addition to their economical benefits (AWWA 2005, Jacangelo et al. 1995). Low pressure ultrafiltration (UF) membranes have a pore size range of 1 to 100 nm and, hence, they have the potential to remove enteric viruses from water (Jacangelo et al. 1995, Jacangelo et al. 2006, Langlet et al. 2009, Urase et al. 1994). Removal of viruses by UF membranes is believed to be mainly due to the size exclusion; however, other removal mechanisms such as adsorption or electrostatic interactions are contributing to their removal as well (Jacangelo et al. 1995).

One problem of using UF membranes in drinking water treatment is membrane fouling. The filtration units suffer from a gradual drop in their productivity due to the accumulation of different foulant materials from the feed water on the membrane surface and/or within its porous structure (Crittenden and Montgomery Watson Harza (Firm) 2005). Foulant materials include different fractions of the natural organic matter (NOM) and colloids (Hallé et al. 2009, Jucker and Clark 1994, Lee et al. 2005, Lee et al. 2006). Fouled membranes can be cleaned either mechanically using hydraulic backwashing accompanied with air sparging or chemically using different cleaning agents such as chlorine, sodium hydroxide and citric acid (AWWA 2005). However, membrane fouling remains a major limitation for employing membranes as a drinking water treatment technology, although UF can achieve high enteric virus removals (Jacangelo et al. 1995, Jacangelo et al. 2006).

There is no clear understanding though how the different types of membrane fouling can affect virus removal and how this may be related to feed water quality. Also, there is no mechanistic model available that correlates the characteristics of the virus and of the membrane to the removal efficiency and incorporates the different removal mechanisms mentioned previously.

1.2 Objectives

Through a literature review, different research gaps were identified and they were the motive behind this work. The major objective was to evaluate the removal efficiency of different enteric virus surrogates by a commercial UF membrane. In depth study of the UF membrane surface characteristics, in addition to using two viruses in the same size range but with different surface charges would be useful to study the removal mechanisms of both viruses and how virus characteristics other than size affected removal.

The second objective was to compare removal of both viruses after membrane fouling was developed using different representative surface waters from Ontario. A better understanding of the contributions of different types of membrane fouling on the removal of viruses, in addition to the effect of cleaning regimes on membrane fouling and virus removal were investigated.

An overarching general objective was to provide a mechanistic model for the rejection of viruses by UF membranes and how this would be affected by changes in membrane surface characteristics due to fouling.

1.3 Thesis structure

The literature review in Chapter 2 includes an overview of published information related to the research area outlined above. A summary of different research gaps and detailed objectives of this research project are provided at the end of Chapter 2. The remainder of the thesis is in integrated-article format as each chapter was written as a separate article.

Chapter 3 represents a detailed study of the porous structure of the UF membrane used. Different surface characterization techniques were used and a new data analysis technique was developed to obtain representative information about the pore size distribution of the UF membrane. These pore size distributions were used in Chapter 4 and 5 to account for size exclusion which was expected to be a very important mechanism in virus removal. Surface characterization together with the new developed data analysis technique was also used on other commercially available membranes.

Chapter 4 represents the results of UF virus removal studies under non fouling conditions thus establishing base line removals of the two virus surrogates investigated - namely MS2 bacteriophage and φX174 bacteriophage. This chapter also includes the detailed design and the operation protocol of the UF bench scale unit employed. In addition, the protocols used for sample collection and analysis are provided.

Chapter 5 provides the results of the fouling experiments. Water quality results including NOM characterization for the two different surface waters from Ontario (Grand River water and Georgian Bay water) are given. Then virus removal results at different degrees of membrane fouling are presented for each of the waters followed by an in depth mechanistic interpretation. Finally, based on the results of this thesis, general recommendations for drinking water providers and legislators are given at the end of this chapter.

Chapter 2
Literature Review

2.1 Membranes used for drinking water treatment

The major objective of drinking water treatment is to provide microbiologically and chemically safe water for the consumers. Membrane filtration is one of the treatment technologies that can provide such high quality standards and meet the regulatory requirements. Membranes can be viewed as an absolute barrier to the different types of contaminants that will be physically larger than the largest pore on the membrane. Due to the recent advances in the membrane industry and the rapid growth in membrane manufacturing and knowledge about membrane characteristics and performance, membranes have become a preferred technology for drinking water treatment and are replacing conventional drinking water treatment systems. Based on the rejection characteristics of the membrane they can be divided into different categories as shown in Figure 2-1. Both ultrafiltration (UF) and microfiltration (MF) are categorized as low pressure membranes while reverse osmosis (RO) and nanofiltration (NF) are categorized as high pressure membranes. Low pressure membranes and especially UF membranes are capable of removing most of the waterborne pathogens and colloidal matter to provide safe water and minimize the required footprint compared with conventional filtration processes (Pearce 2007). Low pressure membranes have became more widely used in drinking water treatment over the past decades to guarantee the production of high water quality and decrease the amount of chemicals used in the treatment process. The major limiting factor in membrane technology was the cost, but recently membrane filtration has became a cost effective option (Adham 2005).

UF membranes have a pore size range from 1 to 100 nm and this allows them to be an absolute barrier for bacteria and protozoa including *Giardia lamblia* cysts and *Cryptosporidium parvum* oocysts, and membranes will even have a very good potential for removing viruses (Jacangelo *et al.* 1995, Jacangelo *et al.* 2006). Another method to characterize UF membranes is the molecular weight cut off (MWCO), which is the molecular weight of a solute that will be rejected by the membrane at a certain ratio, commonly above 90% (Zeman and Zydney 1996). UF membranes have a MWCO range from 1 to 100 KDa (Kennedy *et al.* 2008). UF membranes widely used in the drinking water industry are commonly made from polymeric materials such as polysulfone (PS), polyethersulfone (PES), polyacrylonitrile (PAN), polyvinylidene fluoride (PVDF) or polyamide (PA) due to the thermal

stability and low biodegradability of these materials (Khulbe *et al.* 2008). UF membranes have an asymmetric structure with a thin active layer on the feed side that will have membrane pores with a high pore density, and this layer is responsible for the rejection characteristics of the membrane. Beneath this a more open porous structure exists to improve total permeability of the membrane and provide the required mechanical strength (Pearce 2007). A more detailed discussion of the UF membrane structure and pore size is available in Chapter 3 (section 3.1).

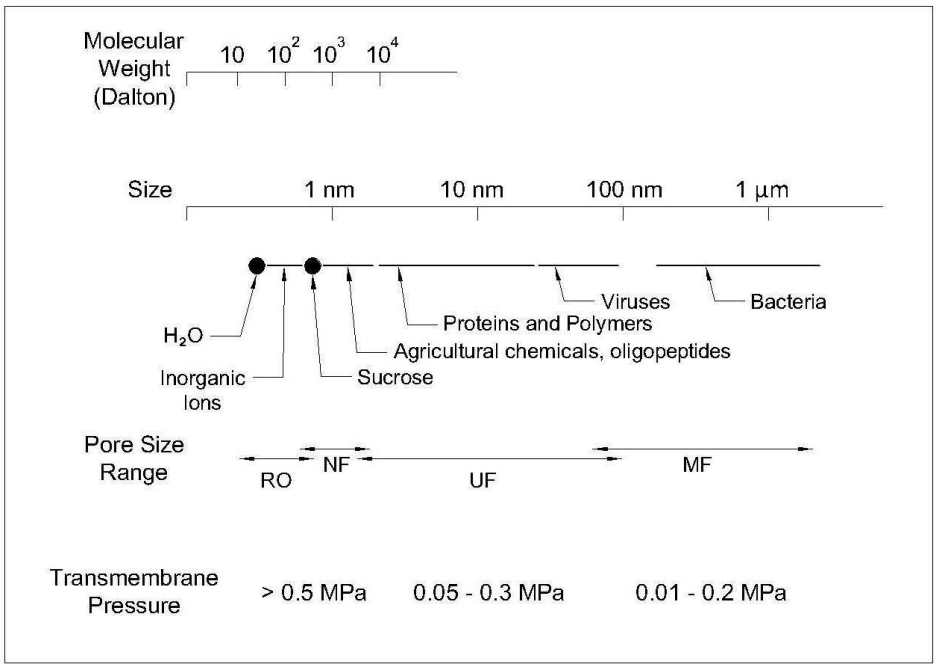

Figure 2-1 Pore rating of different types of membranes along with the size of different contaminants rejected (adapted from Li 2008).

The most common configuration of the UF membranes is the hollow fiber configuration. Membranes are made as fibers with an external diameter ranging between 0.5 and 1.5 mm. The water flow direction is either perpendicular to the membrane skin layer in a dead end flow regime or parallel to it in a cross flow regime. Depending on the type of applied pressure across the membrane, the membrane will be a submerged membrane if a negative pressure is employed or a pressurized membrane if positive pressure is used (Kennedy *et al.* 2008). Selecting the best configuration and flow regime will be dependent on the application.

2.2 Enteric viruses

Enteric viruses are a common type of waterborne pathogens and they usually reach surface waters due to contamination by sewage. Enteric viruses can survive for extended times in the environment under a wide range of pH and temperatures and they grow only inside their host cell. The health effect of enteric viruses is usually gastrointestinal upset, and for individuals with lowered immunity it can cause severe gastrointestinal illness and even cause chronic or fatal illness (Health Canada 2004).

Table 2-1 Common enteric viruses found in water (Fong and Lipp 2005) and their approximate dimensions (Carrillo-Tripp *et al.* 2009)

Virus family	Genera	Nucleic acid	Size
Picornaviridae	Poliovirus	ssRNA	32 nm
	Enterovirus	ssRNA	28-30 nm
	Coxsackievirus A Coxsackievirus B	ssRNA	33 nm
	Echovirus	ssRNA	32 nm
	Hepatitis A virus	ssRNA	27 nm
Adenoviridae	Adenovirus	dsDNA	94 nm
Caliciviridae	Norovirus	ssRNA	40 nm
	Calicivirus	ssRNA	41 nm
	Astrovirus	ssRNA	27 – 30 nm
Reoviridae	Reovirus	dsRNA	75 nm
	Rotavirus	dsRNA	50 nm core with a 80 nm envelope

The detection of enteric viruses in surface water is expensive, time consuming and imprecise as they exist at low concentrations in the environment. A large volume of water (10 to 1000 L) needs to be filtered to concentrate the viruses prior to analysis (Health Canada 2004). The final concentrate is enumerated either using cultural or molecular techniques. In cultural methods, enteric viruses are used to inoculate tissue cultures of mammalian cell lines, which are then incubated and checked for damage to the host cells that will indicate the virus presence. For molecular methods like polymerase chain reaction (PCR) amplification, the nucleic acid will be amplified and detected to measure the virus concentration. PCR is typically less time consuming and more accurate than cell culture techniques, but it can detect both infectious and non-infectious cells (Fong and Lipp 2005).

2.2.1 Enteric viruses in drinking water treatment regulations

In The Guidelines for Canadian Drinking Water Quality issued by Health Canada on 2003, a multi barrier approach is used to limit the risk of enteric viruses. A 4 log removal (i.e. 99.99% removal) of enteric viruses is required when treatment of source water is required. Similarly, the United States environmental protection agency (USEPA) Long Term 2 Enhanced Surface Water Treatment Rule (LT2ESWTR) (USEPA, 2003), also state that a 4-log virus removal is required for surface water or ground water under the influence of surface water. Different treatment technologies are granted a log removal credit for enteric viruses if they can meet the turbidity limits prescribed in the Guidelines for Canadian Drinking Water Quality. These technologies include conventional filtration, direct filtration and slow sand or diatomaceous earth filtration. For technologies that are not given log removal credits in the regulations, there are provisions that additional virus removal credits can be applied based on challenge experiments done on the specific treatment technology to prove its efficiency. Both MF and UF do not get any credit for the removal of enteric viruses. Therefore, for drinking water systems that incorporate membrane filtration, a higher disinfectant dose may be required to reach the required log removal for disinfection of the viruses. Ontario Ministry of the Environment Safe Drinking Water Act (2002) also requires drinking water treatment system to obtain a minimum 4 logs removal of enteric viruses with 0 to 2.0 enteric virus log removal credits based on challenge testing. On May 2010, Health Canada issued proposed guidelines for enteric viruses in drinking water for public comment. UF will be granted a removal credit based on the challenge testing and the full scale plant will be required to continuously perform direct integrity testing to detect any integrity problems with the system. No log credit was given to MF membranes in this proposed guideline (Health Canada 2010).

2.2.2 Bacteriophage as a virus surrogate

Viruses that can only infect bacterial cells are defined as bacteriophage. Bacteriophage are commonly used as a surrogate for enteric viruses in various research studies as they are not considered a risk to human health and they can be more easily cultivated in laboratories than enteric viruses (Grabow 2001, Schijven and Hassanizadeh 2000). Different strains of bacteriophage have been used in numerous virus removal studies in the literature. The major types of bacteriophage are listed in Table 2-2 along with some of their characteristics. Understanding the nature of the viruses is an essential step in understanding their removal properties.

Viruses consist mainly of nucleic acid surrounded by a protein coat. The protein coat usually possesses a surface charge due to the different chemical groups present such as carboxyl and amino

groups. The isoelectric point of a virus is the pH at which the total surface charge of the virus as denoted from its electrophoretic mobility will be equal to zero. Also, the type of proteins on the virus surface can cause the viruses to have some hydrophobic characteristics.

Table 2-2 Different strains of bacteriophage most often used as models for enteric viruses in the literature from (Dowd et al. 1998)

Bacteriophage Strain	Shape	Size (diameter)	Isoelectric point
MS2	Icosahedral capsid (T*=3)	27 nm	3.5
ϕX174	Icosahedral capsid (T=1)	27 nm	6.6
Qβ	Icosahedral capsid (T=3)	24 – 26 nm	5.3
PM2	Icosahedral capsid (T=12)	60 nm	7.3
PRD1	Pseudo lattice (T=25)	63 nm	3 – 4
*T is the triangulation number of the protein capsid, which is equal to the number of protein subunits in the unit of symmetry of the protein capsid			

2.3 Removal of enteric virus surrogates by UF membranes

Bacteriophage have commonly been used as enteric virus surrogates for studies on virus removal by UF membranes. In these studies, MS2 was the predominant type of virus surrogate used, followed by Qβ and then φX174. UF membranes provided good removal for enteric viruses according to the literature shown in Table 2-3. However, no direct relationship was observed between the type of water or the membrane material and the removal of viruses. For the few studies where the removal of different types of viruses were tested, MS2 bacteriophage had a higher removal than either Qβ or φX174 bacteriophage. The obtained removal values were also not correlated with the MWCO characteristics of the membranes. The main reason for this is that the rejection characteristics of UF membranes is complex and also includes mechanisms other than size exclusion, including adsorption and electrostatic repulsion (Zeman and Zydney 1996). Different removal mechanisms of enteric viruses by UF membrane will include size exclusion, electrostatic repulsion between charged membrane and charged virus and adsorption of viruses to the membrane material as shown in Figure 2-2.

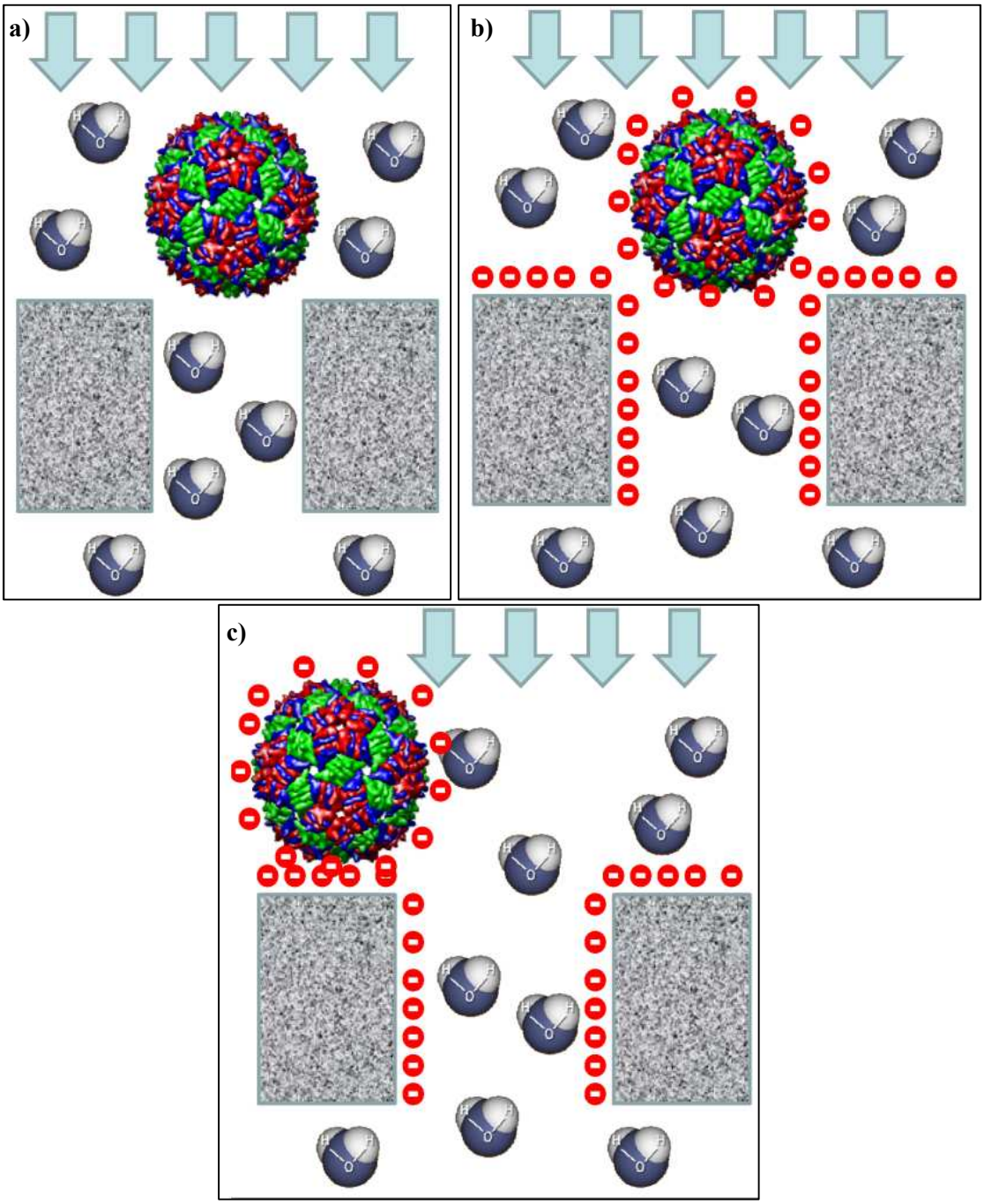

Figure 2-2 A schematic for the different removal mechanisms of enteric viruses,(a) size exclusion, (b) electrostatic repulsion and (c) adsorption

Table 2-3 Removal of enteric virus surrogates by different types of UF membranes in published studies. Pore rating is either defined as MWCO (KDa) or nominal pore size (nm) as reported by manufacturer.

Study	UF Material	Pore Rating	Feed water [a]	Phage	Log Removal
Jacangelo *et al.* 1995	PS	500 KDa	LW at pH=7	MS2	1.5
	Ceramic	300 KDa	LW at pH=7	MS2	4
	Cellulose ester	100 KDa	LW at pH=7	MS2	> 6
Madaeni 1997	PS	30 KDa	LW at pH=7	MS2	>DL*
Otaki *et al.* 1998	PAN	13 KDa	SW	Qβ	>6
Langlet *et al.* 2009	PES	100 KDa	LW at pH=7	MS2	3.54
				Qβ	1.54
	PES	150 KDa	LW at pH=7	MS2	>4.9
				Qβ	3.25
	Cellulose	100 KDa	LW at pH=7	MS2	>DL*
				Qβ	>DL*
Urase *et al.* 1994	PS	20 KDa	LW	Qβ	5 -6
	Polylefin	20 KDa	LW	Qβ	6 -7
	PAN	20 KDa	LW	Qβ	6 - 8
	PVDF	40 KDa	LW	Qβ	4 - 8
	Sulfontaed PS	20 KDa	LW	Qβ	6 -7
Hu *et al.* 2003	Polyamide	Not reported	LW	MS2	2
	PS	Not reported	LW	MS2	1
Zodrow *et al.* 2009	PS	Not reported	LW	MS2	3
Hirasaki *et al.* 2002	Regenerated cellulose	35 nm pore	LW	φX174	>DL*
		50 nm pore	LW	φX174	>DL*
		75 nm pore	LW	φX174	2
Fiksdal and Leiknes 2006	polypropylene	30 KDa	SW at pH=9	MS2	< 1
Arkhangelsky and Gitis 2008	PES	20 KDa	LW at pH=7	MS2	2.9
			LW at pH=7	φX174	2.5
Jacangelo *et al.* 2006	PS	10 KDa	LW at pH=7	MS2	3.8
	PS	100 KDa		MS2	>5.7
	PS	300 KDa		MS2	>5.5
	PVDF	35 nm pore		MS2	3.8
	PVDF	100 nm pore		MS2	0.34
	PS	300 nm pore		MS2	0.45

>DL*: Larger than detection limit of Viruses
[a] Feed water types were grouped as lab water (LW) and surface water (SW)

2.3.1 Size exclusion of viruses by UF membranes

It is assumed that size exclusion or physical straining will be the major removal mechanism of viruses by UF membranes. In other words viruses are too large to enter the membrane pores and are therefore

rejected. MWCO is commonly used to represent rejection characteristics in terms of pore sizes of a membrane when assessing whether size exclusion is taking place.

However, there are many problems with using a MWCO pore size rating to predict virus removal. The nature of a bacteriophage particle is different from the organic molecules that are used to calculate the MWCO of the membranes. The organic molecules have either a coiled or branched configuration while a bacteriophage will have a known three dimensional structure making them similar to colloids. The MW of the phage can be nearly three logs higher than the membrane MWCO and yet pass through the membrane pores. This makes organic molecule rejection, described in terms of MWCO value, not representative of bacteriophage rejection.

Another problem is that the reported pore size values of the UF membranes reported in Table 2-3, described as MWCO or the average or nominal pore size, are values reported by the manufacturer. This information does not typically provide the experimental conditions or the characteristics of the molecules that were used to determine the membrane pore size or MWCO. This raises questions about the important characteristics of the membrane that will help in evaluating its potential for the rejection of viruses. These characteristics will affect the removal mechanisms of viruses by UF membranes. Madaeni *et al.* (1995) studied MS2 bacteriophage removal by UF membranes and assumed that size exclusion was the only removal mechanism in their experiments. Hirasaki *et al.* (2002) came to a similar conclusion using φX174 bacteriophage and a UF membrane. Urase *et al.* (1994) and (1996) also assumed that size exclusion was the predominant mechanism for virus removal by UF membranes after using different types of viruses. These authors explained the failure of the low MWCO UF membranes in rejecting Qβ bacteriophage by assuming that the skin layer had defects in the form of larger pores, and this allowed viruses to pass to the permeate. A similar hypothesis was also assumed by Hu *et al.* (2003) for RO membranes, and in order to verify it some defects were seen in microscopic studies of the membranes.

However, other studies have proven that size exclusion is not the only mechanism involved in virus removal by membranes. Size exclusion alone cannot explain the higher removal observed for MS2 compared to the other types of bacteriophage of similar size like Qβ and φX174 (Arkhangelsky and Gitis 2008, Langlet *et al.* 2009). In addition, Pontius *et al.* (2009) compared the rejection of 26 nm fluorescence spheres to MS2 bacteriophage using two different flat sheet UF membranes. The microspheres and the MS2 phage have similar size but with different charge and hydrophobic properties, and they found that removal was affected by pH and membrane surface area, confirming

that rejection was not completely due to size exclusion. Size exclusion seems to be the main removal mechanism but it cannot fully explain the interactions between the membrane and the viruses. A narrow pore size distribution with only a small number of pores larger than the size of the enteric viruses would be necessary to achieve high removals of viruses. Although physical sieving is believed to be the major removal mechanism for viruses by UF membranes, contributions from adsorption and steric repulsion also occur (Jacangelo *et al.* 1995).

2.3.2 Adsorption of viruses

Another possible mechanism for retaining viruses by the membrane can be the adsorption of viruses to the membrane surface, the more porous support structure or to the walls of large pores. The protein capsid of viruses is composed of amino acids, and it can contain hydrophobic sites that can enhance the adsorption of viruses to surfaces by hydrophobic interactions. Also, viruses can have an opposite surface charge to the membrane surface which can enhance electrostatic adsorption (Schijven and Hassanizadeh 2000).

If hydrophobic adsorption sites are available on the membrane surface, viruses can exhibit hydrophobic adsorption and be removed from the water. This is believed to be the most important adsorption mechanism (Urase *et al.* 1996). Various studies reported hydrophobic interactions especially with regard to removal of viruses by soil passage (Schijven and Hassanizadeh 2000). A hydrophobic MF membrane was found to be a better barrier for MS2 bacteriophage than a hydrophilic membrane with similar pore rating (van Voorthuizen *et al.* 2001). Virus hydrophobicity will depend on the structure of the protein capsid of the virus. Lytle and Routson (1995) found that φX174 was the least hydrophobic virus among different types of bacteriophage (including MS2 bacteriophage) tested on a variety of materials.

Similar to stable colloids, the electrostatic adsorption or adsorption due to Van der Waals forces will be governed by the Derjaguin, Landau, Verwey, Overbeek (DLVO) theory. Most of the viruses will be negatively charged at the pH of surface waters (pH 7 to 8) (van Voorthuizen *et al.* 2001) and commonly polymeric UF membranes will also be negatively charged (Khulbe *et al.* 2008) which will cause a repulsive interaction force i.e. electrostatic repulsion to exist. The attractive force will be the London Van der Waals forces, which are believed to be lower between organic molecules compared to inorganic molecules (Schijven and Hassanizadeh 2000). The large repulsive energy barrier would need to be overcome to deposit the virus onto the membrane surface, and a reduction of this energy

barrier can improve the electrostatic adsorption of viruses on the membrane surface. This could be done by:

- Decreasing the pH of the solution, which can decrease the negative surface charge of the virus or make it positively charged depending on the isoelectric point of the virus (van Voorthuizen *et al.* 2001).
- Blocking the surface charge of the membrane by surface modification, or membrane fouling may decrease the surface charge of the membrane (Yamamura *et al.* 2007).
- Increasing ionic strength of the solution would compress the adsorbed double layer of the virus particles according to the DLVO theory and hence decrease the repulsive energy barrier and improve adsorption of viruses to the membrane surface. Jacangelo *et al.* (2006) showed that at very high ionic strength values, MS2 bacteriophage removal increased by more than 2 log units as the concentration of NaCl was increased from 0 to 170 mM with a membrane of 0.1 μm pore size.
- For viruses with high isoelectric point, they will possess a neutral or a slight negative charge, at pH values typical in surface water i.e. 6-8.5 so repulsion will be at a minimum and more adsorption should happen.
- Divalent cations like calcium can complex with two different organic ligands (Costa et al. 2006) and calcium may therefore complex the virus capsid proteins to the membrane or the membrane fouling layer. Calcium was reported to improve MS2 phage binding to a silica bed coated with organics by complexing capsid proteins to carboxylic groups in the organic (Pham et al. 2009).

2.3.3 Electrostatic repulsion

A negative charge on the membrane surface or within its pores and a negative charge on a virus surface will lead to electrostatic repulsion of viruses. The membrane surface charge is usually due to either ionization of surface chemical groups such as carboxylic or amino groups or due to adsorption of specific ions (Zeman and Zydney 1996). For viruses, the surface charge exists on the outside of the protein capsid. The capsid proteins contains both carboxyl and amino groups that would give the virus its total surface charge with localized positions of positive or negative charges (Schijven and Hassanizadeh 2000). The surface charge of MS2 bacteriophage was approximated by accounting for the amino and carboxylic residues on the exterior of the capsid, and this was found to be in good agreement with experimentally determined electrophoretic mobility (Penrod *et al.* 1996).

Different studies on protein rejection by ultrafiltration membranes have denoted the importance of the electrostatic repulsion between negatively charged protein molecules and the UF membrane. The rejection of different types of proteins was found to decrease with increasing the ionic strength of the solution (Mehta and Zydney 2006, Pujar and Zydney 1997). In a different study, lower rejections of protein molecules were observed for a modified membrane with a positive charge compared to the original negatively charged membrane (Burns and Zydney 2001).

Viruses may be represented as small charged particles and hence, the mass transport model provided by Smith and Deen (1983) describing the transport of spherical colloids inside cylindrical pores of the membrane can also be applied to viruses. According to this model colloid transport within the pore will be affected by the surface charge on the membrane and the colloid. An opposite surface charge on both the cylinder walls and the colloid will affect the partitioning of the colloid between the bulk solution and the pore wall (Smith and Deen 1983). The major parameters governing rejection of the colloid in this model considering electrostatic repulsion are 1) the ratio of the particle radius to the pore radius, 2) the charge on either the particle or the membrane surface, and 3) the solution ionic strength (Burns and Zydney 2001).

2.3.4 Proposed mechanistic model for the rejection of viruses

According to the different removal mechanisms previously mentioned, a proposed mechanistic model for the rejection of a mono dispersed feed solution of viruses can be reached as shown in Figure 2-3. For pores smaller than the size of the virus, they will physically strain the viruses (size exclusion) and provide a minimum removal for a particular membrane regardless of the experimental conditions. For the pores larger than the size of the virus, initially electrostatic repulsion will be the dominant mechanism for rejection until the pore size becomes large enough to diminish the effect of electrostatic repulsion For the largest pores, removal can only be due to adsorption to the membrane surface or pore walls, and this will depend on the diffusivity of the virus particle inside the pore. Once this adsorption mechanism fails, virus breakthrough will occur.

The rejection process may be modeled for viruses similarly to particle rejection. For a spherical particle large enough to enter a pore and moving along a cylindrical pore, its transport either by diffusion or convection will be hindered causing the particle to be strained (Deen 1987). The contribution of each of these transport mechanisms will depend mainly on the relative size of the sphere with regard to the pore size in addition to the properties of the membrane and the virus such as surface charge and flow velocity (Dechadilok and Deen 2006). The assumptions used to develop this

rejection model are that the pore length to its diameter is large and no additional hindrance will exist at pore entrance or exit (Deen 1987). A proper approximation for the asymptotic sieving coefficient for convective flow of a spherical particle in a cylindrical pore was provided by Zeman and Zydney (1996) and is shown in equation (2-1). In this equation, λ is the ratio of the solute radius to the pore radius. This expression can be extended to a membrane with a continuous pore size distribution function f(r) as shown in equation (2-2), to measure the average asymptotic sieving coefficient of the membrane.

$$S_a(\lambda) = (1-\lambda)^2(2-(1-\lambda)^2)e^{-0.7146\lambda^2} \quad \text{.....Equation (2-1)}$$

$$S_a = \frac{C_{permeate}}{C_{feed}} = \frac{\int_0^\infty S_a(\lambda).f(r).r^4\,dr}{\int_0^\infty f(r).r^4\,dr} \quad \text{..... Equation (2-2)}$$

According to this, the size exclusion properties of the membrane will not only depend on the size of the pores larger than the virus but will depend on their density (i.e probability of having this pore size in the membrane) as well. By only using MWCO pore density is neglected which can greatly affect removal. Removals of a virus with a size comparable to that of the larger pore sizes of a membrane pore size distribution, will be higher for more narrow distributions compared to a wider pore size distribution (Zeman and Zydney 1996). This rejection model was successful in predicting the rejection of protein molecules, but one limitation is that it neglects long range interactions like van der Waals forces and electrostatic repulsion (Mehta and Zydney 2005).

Size exclusion is a characteristic of the membrane and the virus, while both electrostatic repulsion and adsorption will in addition to these factors depend on the experimental conditions as well. Solution pH, ionic strength, presence of specific ions or membrane surface modification (hydrophobicity or charge) will affect both electrostatic repulsion and adsorption. Some of these effects will be discussed in the following section.

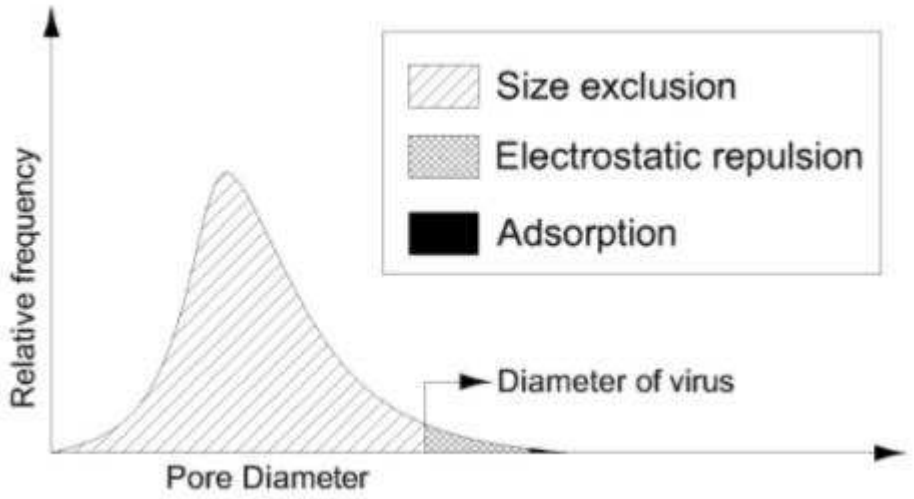

Figure 2-3 A schematic for the contribution of different removal mechanisms of viruses for different pore size ranges within the pore size distribution of the membrane

2.4 Effect of operational parameters on virus removal

2.4.1 Solution pH

The pH of the feed solution will affect the ionization of chemical groups in both the membrane surface and the protein capsid of the virus. For viruses, this effect will be based on the pKa values for the different amino acids residues that determine the isoelectric point of the virus. At pH values below the isoelectric point the virus will be positively charged, and at pH values above the isoelectric point the virus will be negatively charged. At the pH levels of natural waters (around 6 to 9), most viruses will be negatively charged and the charge level will be based on the characteristics of the virus. Increasing pH will generally make the virus more negatively charged, which can affect different membrane removal mechanisms. For membranes that are negatively charged, an increase in pH will increase the electrostatic repulsion between the virus and the membrane and improve virus removal. However, an increase in pH will also decrease adsorption by for example Van der Waals forces since larger electrostatic repulsive forces have to be overcome before adsorption can take place and virus removals through adsorption will therefore decrease. The interplay between the opposing effects of electrostatic repulsion and adsorption, and the chemical characteristics of the membrane itself, will determine the extent to which pH affects virus removal.

The removal of MS2 bacteriophage was found to be greatly affected by increases in pH of the feed water for two different MF membranes (van Voorthuizen *et al.* 2001). Even with the presence of different salt concentrations, a pH increase from 3.9 to 7 resulted in a decrease in the rejection of MS2 bacteriophage from 4 to 0.5 log removal. In a different study using a 50 nm MF membrane, MS2 removal decreased from 70% to 30% with a pH increase from 4 to 6, compared with Qβ bacteriophage in which removal decreased from 90% to 25% log with a pH increase from 4 to 8. As pH was increased above 6 and 8 for MS2 and Qβ, respectively, the rejection was nearly stable (Herath *et al.* 1999). These results were attributed to the higher isoelectric point for Qβ (5.3) compared to MS2 (3.9). Results of both of these studies suggest that electrostatic repulsion prevented adsorption onto the membrane surface as solution pH increased. However, electrostatic repulsive forces were not large enough to prevent passage of the viruses through the relatively large MF membrane pores compared with either MS2 or Qβ bacteriophage of approximately 27 nm diameter. Another hypothesis for the improved removal at lower pH values was that the viruses were aggregated near or below their isoelectric point and removed by size exclusion.

However, solution pH does not always affect virus removal by membranes. For example, Jacangelo *et al.* (2006) found no significant effect of increasing the feed water pH from 5 to 9 for MS2 bacteriophage removal by a 0.1 μm PVDF MF membrane. Also, for 3 different UF membranes with varying degrees of hydrophobicity, the rejection of MS2 bacteriophage was similar at feed water pH values of 6.5 and 8.5. These results may be because MS2 is less affected by an increase of pH above 6 compared with other viruses. This can be attributed to the constant surface charge of MS2 in this pH range (Penrod *et al.* 1996), and would result in constant electrostatic repulsion or adsorption to membranes. Not much information is available in the literature for the other types of viruses with different isoelectric points. This would be necessary to verify the effect of surface charge of the virus on the removal mechanism.

2.4.2 Effect of solution ionic strength

The ionic strength of the solution is believed to have an effect on the rejection of viruses. Increasing the ionic strength of the solution compresses the electrostatic double layer and decreases its thickness around the charged viruses and also on the membrane surface and within pores. This will decrease the electrostatic repulsion of the charged viruses by the membrane (Smith and Deen 1983), resulting in reduced virus removal. However, decreasing the double layer thickness can also improve aggregation of charged particles, as it will allow attractive Van der Waals forces to aggregate the two particles

before their double layer start to interact leading to removal of aggregates by size exclusion (Crittenden and Montgomery Watson Harza (Firm) 2005). In addition, decreasing the electrostatic double layer thickness on membranes will likely improve the adsorption of viruses to the membrane as it is easier to overcome electrostatic repulsive forces hindering adsorption and virus removal will therefore improve. This hypothesis is supported by the fact that attachment of viruses to soil particles was found to increase with increasing the ionic strength (Schijven and Hassanizadeh 2000).

These mechanistic interpretations are supported by the following study results. Increasing the solution ionic strength, by adding either sodium or calcium chloride at 0.2 M and 0.5 mM, respectively, was found to be effective in improving removal of MS2 bacteriophage with a MF membrane when tested at pH values between 4 and 7 (van Voorthuizen *et al.* 2001). Similar results were reported by Jacangelo *et al.* (2006), as MS2 and PRD1 bacteriophage removal with a 0.1 μm MF membrane was improved by 3 logs when conductivity was raised to 3,700 μS/cm using sodium chloride. The ionic solution concentrations used in these studies were higher than what is experienced in surface waters and a moderate increase in ionic strength may therefore not have such an effect in real systems. For example, improved virus removal through a 50 nm MF membrane was not observed for MS2 and Qβ bacteriophage when sodium chloride was used to raise the conductivity in the range of 100 to 500 μS/cm (Herath *et al.* 1999). Comparison of these studies is complicated by the difference in ion concentrations and the use of membranes with different pore sizes. However, it is expected that the improvement in removal reported for MF membranes can be attributed to adsorption, as this is believed to be the dominant mechanism for this type of membrane. Whereas for UF membranes it is expected that size exclusion is the dominant mechanism due to their smaller pores that will have a similar size to the small bacteriophage such as MS2 bacteriophage. A big portion of the membrane rejection of viruses will be due to the size exclusion and both electrostatic repulsion and adsorption will improve the removal as explained earlier in section 2.3.4.

2.4.3 Effect of feed concentration

Increasing the concentration of viruses in the feed solution is believed to have an effect on the obtained removal of viruses by membranes. Increasing the concentration of MS2 bacteriophage in the feed solution from 10^6 to 10^9 pfu.mL^{-1} caused a more than 1 log drop in removal using a 500 KDa UF membrane (Jacangelo *et al.* 1995). Similar findings were noticed for 10 and 100 KDa UF membranes at MS2 loadings higher than 10^5 pfu/cm^2 (Jacangelo *et al.* 2006). This is important in designing virus removal experiments, and means that the feed concentration should be constant for different

experiments and below a threshold of 10^5 pfu/cm^2 since otherwise the removal can be impacted. This threshold value would also change based on the used membrane material and characteristics. A possible explanation for this phenomenon is the concentration polarization effect. During an experiment, the viruses will be retained at the surface of the membrane due to rejection and results in an increased virus concentration in the boundary layer on the membrane surface compared to the bulk of the feed solution. This will cause a decrease in the apparent rejection of the viruses when feed concentration is used as the influent value.

Increasing transmembrane pressure for clean membranes under non-fouling conditions did not have an effect on virus removal for different UF membranes (Jacangelo *et al.* 1995, Jacangelo *et al.* 2006). For MF membranes or UF membranes with pores larger than the virus size, flow regime (i.e. cross or dead end flow) can have varying effects. For example, stirring or cross flow conditions can disturb virus adsorption and lower the virus removal (van Voorthuizen *et al.* 2001). Another hypothesis is that stirring can decrease the concentration polarization effect to improve the measured virus removal (Madaeni *et al.* 1995).

2.5 Membrane fouling

Membranes experience a loss of productivity during operation that is generally known as membrane fouling. This results from either a drop in permeate flux or increase in operating transmembrane pressure (TMP) which will increase the energy requirements (Crittenden and Montgomery Watson Harza (Firm) 2005). This effect can be due to different mechanisms such as complete or partial pore blocking, and also adsorption of different types of materials to the membrane surface or inside the pores (Hermia 1982).

Fouling can be classified according to the reversibility of fouling. Membranes are usually backwashed between short filtration cycles using permeate water and/ or air to remove a part of the developed fouling which is called hydraulically reversible fouling. The remaining fouling will be denoted as hydraulically irreversible fouling. Hydraulically irreversible fouling develops with unit operation, and when high degrees of hydraulically irreversible fouling are present, the membrane unit undergoes chemical cleaning using oxidants or surfactants to remove the membrane fouling layer and recover original permeability. The final part that will remain after chemical cleaning is the chemically irreversible fouling or membrane aging (AWWA 2005). Different components of the surface water matrix can cause these effects and this differentiation can also be used to classify membrane fouling.

Organic fouling

The natural organic matter (NOM) is a major element in any surface water matrix. NOM consists of different fractions with varying characteristics such as hydrophobicity, molecular weight, molecular shape, and surface charge (Cho *et al.* 2000). NOM fractions can be characterized according to their molecular weight using size exclusion techniques such as liquid chromatography organic carbon detector (LC-OCD) (Huber *et al.* 2011) or due to their fluorescence excitation emission (Peiris *et al.* 2010). Two fractions of NOM that are mainly suspected in UF membrane fouling include biopolymers and humic substances. The fouling potential of these two fractions varies with different types of waters and with differences in membrane characteristics and operational conditions. Biopolymers are believed to be the major fraction of NOM responsible for UF membrane fouling (Haberkamp *et al.* 2008, Hallé *et al.* 2009, Lee *et al.* 2004, Zheng *et al.* 2010). Biopolymers are larger molecular weight organic molecules (i.e. >10KDa) and include polysaccharides and proteins with mainly a hydrophilic nature (Huber *et al.* 2011). This fraction is believed to have a more neutral surface charge compared to humic substances (Cho *et al.* 2000). They will be deposited on the membrane forming a cake layer causing a decrease in surface roughness (Lee *et al.* 2006) and/or blockage of larger pores in the membrane resulting in complete blocking or pore narrowing (Costa *et al.* 2006, Haberkamp *et al.* 2008). The smaller MW humic substances have a hydrophobic nature and negative charge, and may contribute to fouling in the early stages of unit operation. Humic substances probably adsorb to pore walls to narrow them, and also may enhance fouling by the larger MW biopolymer fraction due to pore blockage (Yamamura *et al.* 2007, Yuan and Zydney 1999). The adsorption of humic substances can cause an increase in the zeta potential or negative surface charge of different UF membranes and a decline in hydrophobicity, especially in the prescience of divalent cations (Jucker and Clark 1994). Pre-filtration using UF membranes of different MWCO showed that all the different size fractions of NOM can cause membrane fouling in different degrees, and that degree of fouling was proportional to the MWCO of the pre-filter with the NOM in the MW range of 100 to 3 KDa was the major contributor to membrane fouling. Pre-filtering larger MW NOM could essentially decrease the degree of fouling, and membrane fouling is decreased by decreasing the MWCO of the pre-filter (Howe and Clark 2002).

Inorganic fouling

Inorganic fouling of membranes is due to precipitation of inorganic salts (i.e. scale) on the membrane surface. This occurs when the salt concentration exceeds the solubility limit in the region near the

membrane surface. Inorganic fouling is common for high pressure membranes due to their ability to reject divalent and monovalent ions depending on the membrane properties (Jarusutthirak *et al.* 2007). This would be less pronounced for low pressure membranes as their larger pores will not be able to reject these ions.

Colloidal fouling

Inorganic colloids can also contribute to membrane fouling. These particles can deposit on the membrane surface to eventually form a cake layer (AWWA 2005) that often can be easily removed by backwashing due to the weak bond to the membrane surface (Huang *et al.* 2009).

Biofouling

Microbial cells found in the feed water can adsorb to the membrane surface according to different types of intermolecular forces. Under favorable conditions the attached cells will start replicating and will produce extra polymeric substances (EPS), creating a biofilm that will foul the membrane and cause a significant drop in performance (Flemming *et al.* 1997). Without preventative measures and cleaning regimes, the biofilm can grow over the membrane surface to cause a thick fouling layer (Lewandowski and Beyenal 2005).

2.5.1 Effect of membrane fouling on virus removal

All the different types of membrane fouling can either interfere or enhance the removal of viruses by UF membranes. Complete or partial pore blockage would largely improve the virus removal by physical straining, especially for UF membranes with smaller pore size ranges. The fouling layer can also affect other virus removal mechanisms. Adsorption of neutral fouling material (i.e. biopolymers) to the membrane surface can block the membrane surface charge, thus decreasing the repulsive electrostatic forces and therefore enhancing virus adsorption. In the case of hydrophobic foulants (i.e. humic substances), adsorption to the surface might enhance the hydrophobic attractive forces. This effect of adsorption is complicated due the nature and characteristics of different fractions of NOM and their role in membrane fouling. Fouling can also affect the surface charge and consequently the removal by electrostatic repulsion between the virus and the pore walls. For example, the adsorption of charged macromolecules (i.e. humic substances) to membranes may enhance the removal of viruses by electrostatic repulsion due to the increased negative surface charge of the membrane. In combination, the effects of membrane fouling on virus removal mechanisms could result in a

considerable increase in virus removal. Each type of membrane foulant will interact with the viruses in different way and have a varying effect on virus removal based on the type of the virus as well.

2.5.1.1 Impact of reversible hydraulic fouling (short term fouling)

Reversible hydraulic fouling, or fouling that can be removed by membrane backwashing procedures, can include particle depositions that form a porous cake layer on the membrane surface. Reversible hydraulic fouling has typically resulted in an increase in virus removal by MF membranes. Using kaolinite as a model for particles, the formed cake layer could improve the removal of MS2 bacteriophage using different types of MF membranes (Jacangelo *et al.* 1995). Similar results showing improved phage removals were obtained in the same study by running a pilot scale MF membrane with surface water for approximately 5 h, and this effect was lost after membrane backwashing. When the cycles were reduced to 30 min (e.g. full scale membrane filtration practice) no effect on virus removal was observed. A similar effect of cake layer formation on virus removal was observed for MF membranes using natural turbidity from wastewater sediments (Madaeni *et al.* 1995). Urase *et al.* (1994) used latex particles to simulate cake layer fouling and concluded that improved Qβ phage removal was due to the pore blockage by the latex particles and not due to the adsorption properties for the Qβ bacteriophage.

The increase in phage removal due to particle deposition and cake layer formation was further investigated by Jacangelo *et al.* (2006), who used increasing TMP values and bentonite loading to study cake layer formation and compression on MS2 bacteriophage removal by a 0.1 μm MF membrane pilot unit. They found that improvements in MS2 removal were primarily due to either pore blockage or virus adsorption to the cake layer, and not due to sieving by the cake layer. Both pore blocking and cake adsorption depended on size and hydrophobicity of the colloidal particles. In the same study Jacangelo *et al.* (2006) also tested MF pilot units with 0.1 μm pore size, and found that reversible fouling could improve the removal of MS2 bacteriophage by 1 to 1.6 logs after the unit was operated using raw water for 4 h without backwashing. When filtered water from the same unit was used as feed water, this effect was minimal. This shows that the nature of the formed cake layer and the size of particles and colloids in the raw water could affect virus removal.

Although cake layer formation on MF membranes can result in increased virus removal, this effect may not occur in UF membranes. In addition to their work with MF membranes discussed above, Jacangelo *et al.* (2006) also tested the effect of cake layer formation on MS2 removal by UF membrane pilot units of similar pore size (35 nm and 23-30 nm). For these UF membranes, no

significant or consistent increase in removal was observed for the 4 h operation using either raw water or filtered water through the same UF membrane unit. One possible explanation for difference in cake layer effect between MF and UF membranes may relate to the difference in pore size range of the membranes. For UF membranes, pore sizes maybe be smaller than the size of the particles in the cake layer, and therefore a cake layer would not provide additional benefits to improve virus sieving. This may also depend on the difference in morphological structure of the membrane, as UF membranes usually have an asymmetric structure with a dense skin layer that will be responsible for rejection characteristics making it less prone for pore blockage.

2.5.1.2 Impact of hydraulically irreversible fouling (long term fouling)

Another important type of membrane fouling is the irreversible fouling of membrane units. This develops after long term membrane operations including filtration cycles with backwashing. In general, irreversible fouling has been found to increase virus removal by both MF and UF membranes. Using a 0.2 μm MF membrane with two different source waters in long term experiments of approximately 45 d, the log removal of MS2 bacteriophage improved by nearly 3 logs when the TMP increased by nearly 300%. For a third type of water which was of lower quality (e.g. high turbidity and high minerals), such high removals were not achieved and the maximum obtained increase was 2 logs (Jacangelo *et al.* 1995). In a different study using two different pressurized MF pilot units, the long term irreversible fouling was found to have a significant effect on removal of MS2 bacteriophage (Jacangelo *et al.* 2006). Removal of MS2 phage increased to 4 or 5 logs after more than 10 d of operation. Chemical cleaning of the membranes decreased this additional removal to nearly 1 log but could not remove it completely. This shows that the foulants remaining after chemical cleaning could still affect virus removal. The main conclusion is that long term irreversible fouling of MF membranes can improve MS2 rejection thus achieving virus removals similar to the ones observed for UF membranes.

In the same study of Jacangelo *et al.* (2006) using two UF pilot units, hydraulically irreversible fouling was found to improve MS2 bacteriophage removal by 0.5 to 1.5 additional log units for both UF pilot units. After 8 d of operation. But unlike MF membranes, when filtered water from the unit (i.e. foulant free water) was used as feed water for the fouled membrane, MS2 removal still increased by 0.1 to 1.3 logs. The specific flux for the foulant free water experiment dropped only to half of that of the raw water value after the 8 d period indicating that removing the fouling material in the feed water in the first filtration step (i.e. larger MW organics and colloids) could not prevent irreversible

fouling and the increase in MS2 bacteriophage rejection. These results raise questions about details of the irreversible fouling mechanisms and support the hypothesis that the adsorption of smaller macromolecules to the inside walls of the UF membrane pores may decrease pore dimension and thus improve virus removal. In general, irreversible fouling was found to be much more effective than reversible fouling in improving the removal of MS2 bacteriophage even when the colloidal fraction of the water was nearly absent.

2.6 Research gaps

After reviewing the current literature, several research gaps were identified and they were the motivation for this study. The purpose of my research was to gain more knowledge about the interactions between the virus surrogates and UF membranes that can affect virus removal. The apparent research gaps are as follows:

2.6.1 Relating virus characteristics to removal by membranes

Most of the previously reported studies were done using one type of virus surrogate, commonly MS2 phage, and sometimes also a larger phage like PRD1 (Hirasaki *et al.* 2002, Hu *et al.* 2003, Jacangelo *et al.* 1995, Jacangelo *et al.* 2006, Urase *et al.* 1996, van Voorthuizen *et al.* 2001, Zodrow *et al.* 2009). Only few studies used two types of bacteriophage of similar size but with different characteristics (Arkhangelsky and Gitis 2008, Herath *et al.* 1999, Langlet *et al.* 2009). Using only one type of virus will not allow investigation of the effect of virus characteristics on the removal by membranes. Testing different viruses of similar size and different surface properties would allow the investigation of removal mechanisms other than size exclusion. Understanding the contributions of different virus removal mechanisms will help in choosing the best virus surrogate to be used to simulate worst case conditions or to investigate the risk associated with the presence of a certain strains of enteric viruses in the feed water of the membrane unit.

2.6.2 Effect of membrane surface characteristics

Generally membranes are characterized by their MWCO or nominal pore size which is not suitable for the interpretation of virus removal results. The reason is the great difference between the viruses and organic macromolecules in terms of rejection mechanisms. Detailed knowledge of membrane morphology, especially the pore size distribution of the membrane, will be essential to get an understanding of the fraction of virus removal that will be due to physical sieving. This will represent the base removal of viruses by the membrane. The pore size distribution still needs to be combined

with data on membrane surface charge at different solution environments and hydrophobicity to investigate the other removal mechanisms such as electrostatic repulsion or adsorption. The removal of a virus by a membrane pore depends on the ratio of virus size to pore diameter. Pores larger than the virus size can also reject viruses due to adsorption or electrostatic repulsion, but as the pore become too large the viruses will break through the membrane.

Only one study has conducted a detailed study of membrane characteristics as they investigated virus rejection, but this study did not use their data to explain the obtained virus removals (Arkhangelsky and Gitis 2008). However, detailed membrane characteristics will be necessary to form the basis for an acceptable mechanistic model and for predicting rejection of a certain virus strain.

2.6.3 Experimental apparatus and conditions

There is debate about the difference between bench and pilot scale membrane units and if the results from both types of units are in agreement. One difference can be the probability of detecting integrity problems within the membrane module that will affect the results. Filtering a limited amount of viral feed solution (in the range of few hundreds of millimeters) will not provide reliable results. This will only provide an approximation of the average total virus removal without any differentiation between the various removal mechanisms since an operational equilibrium has not been established and for example the effect of adsorption may be overestimated. The bench units should be carefully designed in order to make any conclusions derived from it as representative as possible of what would happen for pilot scale units or even full scale treatment plants.

2.6.4 Impact of membrane fouling

Only a few studies have investigated the impact of membrane fouling on virus removal (Jacangelo *et al.* 1995, Jacangelo *et al.* 2006). One important aspect of studying the impact of membrane fouling are the conditions under which a membrane fouling layer is established. In these published studies for reversible fouling, the membrane unit is operated for several hours without backwashing. This has two main problems. The first problem is that this technique is not representative of reversible fouling in actual membrane treatment systems. Membrane filtration cycles are usually much shorter (e.g. less than one hour of operation prior to hydraulic backwashing). If the obtained fouling has an effect on the virus removal, this might be due to the greater accumulation of solid that will not happen in real treatment conditions. The second problem is that this does not completely differentiate between the irreversible and reversible fouling or study the interplay of both types of fouling on the virus removal

by the membrane. A more realistic fouling experiment simulating operational conditions employed in practice can help in explaining how virus removal will vary during unit operation at different fouling stages. Also, studies to date have not investigated the effect of fouling on different types of viruses and how the virus characteristics will affect the improved removal due to fouling.

2.7 Summary

UF membranes can provide high and reliable removal of enteric viruses from surface waters. Different removal mechanisms are believed to be responsible for these high virus removals by UF membranes, however there is no in depth understanding of the extent to which individual mechanisms contribute to virus removal. Investigation of virus and membrane characteristics can be beneficial in gaining a better understanding of these mechanisms. Membrane fouling which is a common problem for membrane operators can enhance the ability of the membrane to remove viruses. Fouling is a complex phenomenon due to different types of fouling (e.g. reversible, irreversible), different foulants and different fouling mechanisms. Understanding its effect on virus removal can raise the trust in UF membranes as an acceptable barrier for viruses during treatment, as fouling will always exist on membranes in drinking water treatment plants.

2.8 Research goals

The experimental work presented in the next chapter had different objectives:

1. Provide detailed characterization of the UF membrane especially the porous structure of the membrane as it will be expected to greatly influence rejection of viruses.
2. Design a UF bench unit to be used in the viruses challenge tests and the membrane fouling experiments and be able to simulate treatment conditions in full scale water treatment plants.
3. Perform virus challenge experiments at clean water conditions using different types of virus surrogates to get their base removal by the UF membrane and compare their characteristics.
4. Using representative surface waters to develop membrane fouling and study the effect of different types of membrane fouling on virus removal at different degrees of fouling within the fouling experiment in addition to the nature of the fouling layer due to the feed water source.
5. Provide a mechanistic model for the rejection of virus surrogates by UF membrane to understand the rejection mechanisms of viruses and the effect of virus and membrane characteristics on the rejection.

Chapter 3

Pore Size Distribution Determination of Ultrafiltration Membranes

3.1 Introduction

Ultrafiltration (UF) membranes are widely used in either industrial applications or drinking water treatment due to their ability to reject large macrosolutes and colloids. Commonly used UF membranes are integrally skinned asymmetric membranes with a dense skin layer. The membranes consist of a thin skin layer that contain the membrane pores overlaying a more open structure as shown in Figure 3-1. The pore size range for UF membranes is from 1 to 100 nm (Matsuura 1994). The major rejection mechanism is sieving also described as size exclusion (Khulbe *et al.* 2008). Another removal mechanism for UF membranes is hydrophobic adsorption to the membrane surface or the open porous structure due to the hydrophobic properties of most polymeric materials used for manufacturing these membranes (Zeman and Zydney 1996). For charged colloids, electrostatic interactions can also play a role in their removal by typically negatively charged membranes (Deen 1987). Because of these different rejection mechanisms, it is therefore of great importance to study membrane surface characteristics in order to be able to predict and interpret the rejection of different contaminants.

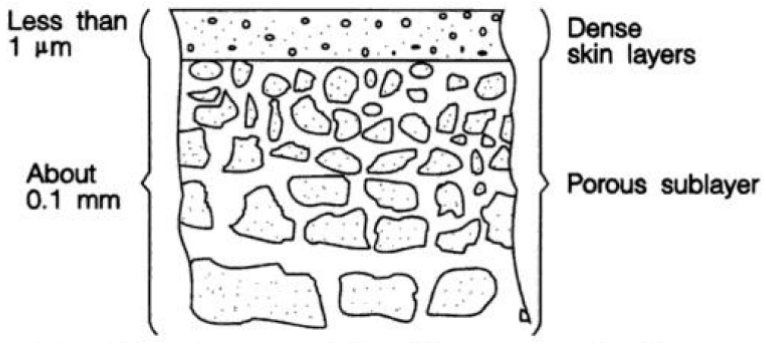

Figure 3-1 Schematic of Asymmetric Structure of UF membranes (Matsuura 1994)

3.1.1 Pore size rating of UF membranes

UF membranes are usually characterized by the molecular weight cut off (MWCO). MWCO is the size of a molecule that will be rejected by the membrane at a certain rate, commonly 90%. This is based on the concept that the spatial dimensions of a molecule will depend on its molar mass. The molecules typically used to determine MWCO include proteins or other organic molecules like

dextran or polyethylene glycols (PEGs) (Zeman and Zydney 1996). MWCO is not applicable for predicting the removal of certain types of contaminants, especially enteric viruses (Langlet *et al.* 2009, Urase *et al.* 1994, 1996) because the MWCO depends also on the shape of the molecule (i.e. either a chain or coiled molecule). In addition, some organic molecules might be adsorbed to the membrane material under specific conditions. Concentration polarization can also affect the rejection. In addition, the MWCO value does not provide information about the pore size distribution or the membrane structure (Hernandez *et al.* 1999). To determine MWCO it is recommended to use a solute that will not adsorb to the membrane (e.g. dextran) and to report the test conditions (e.g. pH, ionic strength, flux, concentration, transmembrane pressure) (Zeman and Zydney 1996). Other alternative membrane characterization techniques (Section 3.1.2) can also be used to evaluate the pore size distribution of a membrane. Obtaining a valid pore size distribution for a UF membrane will be a key step in predicting the UF membrane's ability to reject different types of molecules such as proteins (Mehta and Zydney 2005, 2006, Wickramasinghe *et al.* 2009) and viruses (Urase *et al.* 1994).

3.1.2 Membrane pore size measurement techniques

There are two major types of techniques that can be used to measure the pore size distribution of a membrane. The more common one is the direct measurement of pore sizes using microscopic techniques including atomic force microscopy (AFM), scanning electron microscopy (SEM), and transmission electron microscopy (TEM). The other type is an indirect pore size measurement based on membrane performance using methods such as bubble pressure breakthrough, mercury porosimetry, and solute rejection using a series of solutes with varying molecular mass. The indirect methods can give information about the size of the pores across the membrane depth as it uses the entire area that is open to flow, unlike direct microscopic methods that mainly image the surface or the first few nanometers of the pore. For asymmetric membranes like the UF membranes used in this study, both direct and indirect techniques should yield similar results since the thin skin layer on top of the open support structure will be mainly responsible for rejection and should therefore be characterized adequately with microscopic techniques (Hernandez *et al.* 1999). Based on this, AFM and SEM were used in this study due to their ability to give exact information about pore size distribution and pore shape.

Optical microscopes are not able to obtain images of very small features like the membrane pores due to the light diffraction pattern; therefore electron microscopes such as TEM, SEM and AFM must be used. TEM which was first used by Ernst Ruska in 1937 depends on using a high voltage (100 – 300

KV) electron beam that will penetrate a thin sample of several micrometers so it will exhibit some diffraction across the sample. The diffracted electron beam can then be recorded to provide a high resolution image (Egerton 2005). However, this method can be problematic with polymeric UF membranes. For surface pore visualization, a replica of the surface needs to be prepared by coating the surface using a carbon film, followed by dissolving the membrane polymer and imaging the carbon film. This method can cover up small pores on the surface (Sheldon 1991, Zeman and Zydney 1996).

Another type of microscope that can be used is the scanning electron microscope (SEM) or more recently the field emission scanning electron microscope (FE-SEM). The FE-SEM uses lower electron voltage compared to a standard SEM, resulting in higher resolution and less damage to biological samples. SEM is suitable for thick samples where electrons cannot pass through the sample. The sample is first dried and then coated with a conductive material like gold, chromium or carbon, and then an electron gun focuses an electron beam on the surface while inside the vacuum chamber of the SEM instrument. The scattered electrons from the surface are recorded to generate a raster image of the surface. The same sample preparation and analysis technique is applied for FE-SEM as well. The resolution of FE-SEM can be as low as 0.7 nm depending on the electron voltage used (Kim *et al.* 1990). However several problems are reported for FE-SEM imaging of membranes such as:

- Membrane drying can affect the surface structure, as SEM samples have to be completely dry. Pore dimensions may be altered and may therefore not be representative of true pore dimensions. More advanced drying techniques like critical point drying can be used to avoid this (Kim *et al.* 1990, Zeman and Zydney 1996).
- Sample coating can also affect the pore dimensions, as the nano-gold particles can cover some of the pores or decrease their dimensions (Kim *et al.* 1999).
- The vacuum pressure during operation of the FE-SEM can damage the sample surface.
- The electron beam can also damage the surface.

The images obtained are then analyzed using different image analysis techniques to get the pore shapes and dimensions (Hernandez *et al.* 1999). Traditionally, the grayscale images that result from SEM analysis are converted to a binary image using simple grayscale thresholding to isolate the pores. The grayscale threshold level is usually selected manually or according to various algorithms available in the literature (Hernandez *et al.* 1999, Kim *et al.* 1990). There is a need to optimize this commonly employed grayscale thresholding techniques in order to improve the detection of pore

boundaries (Sun *et al.* 2007). One approach is to apply different filters to remove image artifacts (Zeman and Zydney 1996). Alternatively, a relatively simple method called watershed thresholding can be used. Watershed thresholding detects depressions in the surface by detecting the pore boundaries in a similar manner to a topographic surface. The method predicts the flow of water on a folded surface, and objects (pores) will be the areas where water will collect (Vincent 1991). This method was used for the current study mainly for SEM images, and further details of the method are described later in section3.3.3.

A more recently developed type of microscope is the scanning probe microscope invented by G. Binning and H. Rohrer, which was later developed into the atomic force microscope (AFM) (Binnig *et al.* 1986). AFM utilizes a probe for scanning the surface of the sample, and due to the atomic forces between the sample and the probe the features of the surface can be recorded. Different operational modes can be used such as contact, non-contact and tapping mode. In contact mode, a very sharp tip attached to a cantilever is placed a few angstroms away from the sample surface within the repulsive force region (Figure 3-2). The deflection of the cantilever is then monitored using a laser beam focused on the back of the cantilever to measure its Z position. Moving the tip across the sample surface to predefined X,Y coordinates and obtaining readings for the Z position as described results in a 3D image of the surface. For non-contact mode, the cantilever is oscillated near the surface in the attractive force region as shown in Figure 3-2. When the tip encounters a surface feature, the tip oscillation is affected and the Z position can be measured to obtain the 3D image. The third and more recent mode is the tapping mode, which is an intermediate mode between the contact and non-contact mode. The tip oscillates near the surface and slightly taps the surface during its oscillation to go into the repulsive region (Khulbe *et al.* 2008). This mode is very advantageous as it minimizes the tip to sample forces, eliminating the probability of surface damage and improving the lateral resolution of images (Lee *et al.* 2005, Veeco Instruments Inc. 2004).

AFM has many advantages over other imaging techniques including:

- Provides a reliable 3D image of the sample surface at very high resolution that can be at the sub-nanometer level.
- Does not require any sample preparation or sample coating even for non-conductive samples.
- Ability to image wet samples and conduct tapping mode analysis of surfaces in liquids.

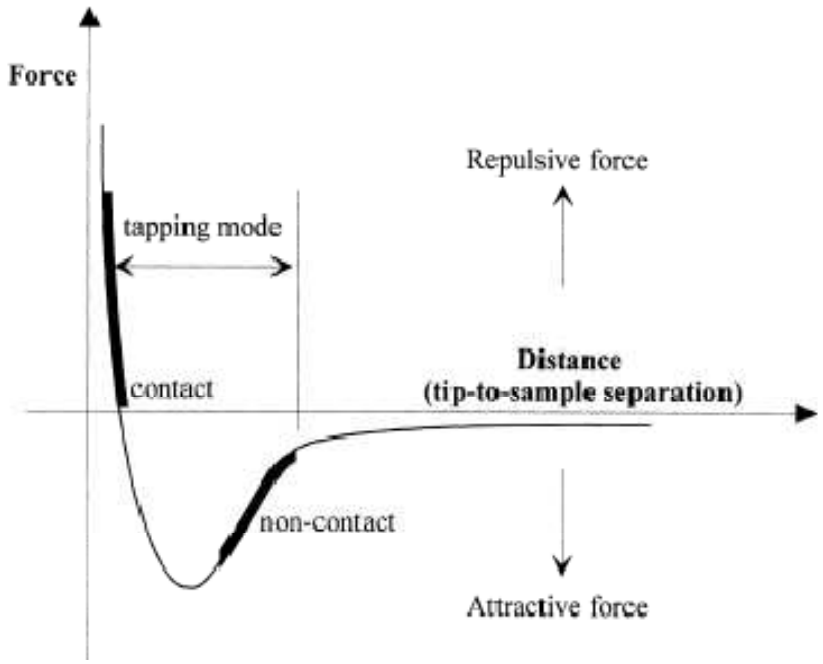

Figure 3-2 Inter atomic forces plotted against the distance between scanning tip and sample surface (Kim *et al.* 1999)

AFM results are usually evaluated using manually drawn cross sections across the image by the instrument software as shown in Figure 3-3. The start and end points of the pore shown by the red markers are placed manually. The result window shows the measured horizontal distance between the two markers. Usually the markers are placed at a preselected reference Z level (Bowen *et al.* 1996, Hayama *et al.* 2002, Khayet and Matsuura 2001, Richard Bowen *et al.* 1996). This method of analysis has substantial drawbacks as it does not provide an automatic measurement of pore density, pore area, or any parameters describing the pore shape. It is also easily affected by any tilt or other image artifacts or surface contamination. Overcoming these drawbacks was the main motive in this current study for developing a new data analysis technique. This new technique called pore construction technique is based on the automatic detection of pores from the image without any segmentation. Instead, each pore is detected and constructed separately from the data set and then analyzed to get its exact shape and dimensions. In other words, each pore will be separated from the image first and then it will be analyzed.

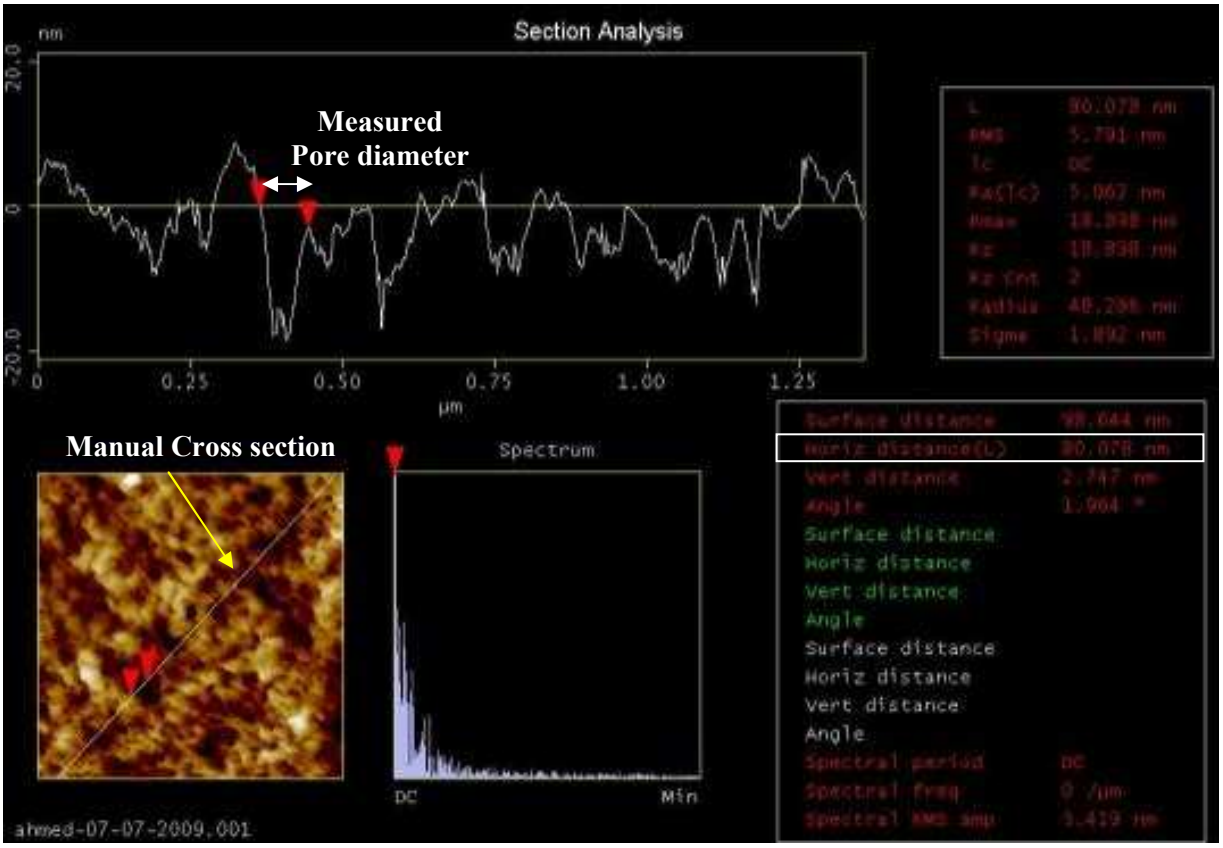

Figure 3-3 Conventional AFM analysis and results using instrument software

One important limitation of AFM measurement is tip convolution. When the size of the scanning tip is comparable to the dimension of the scanned pores, then the tip will not be able to go inside the pore and get the exact dimensions, as shown in Figure 3-4 (Dietz *et al.* 1992, Khulbe *et al.* 2008). Tip convolution will primarily affect the pore dimensions at the pore bottom height which is the maximum penetration of the tip inside the pore.

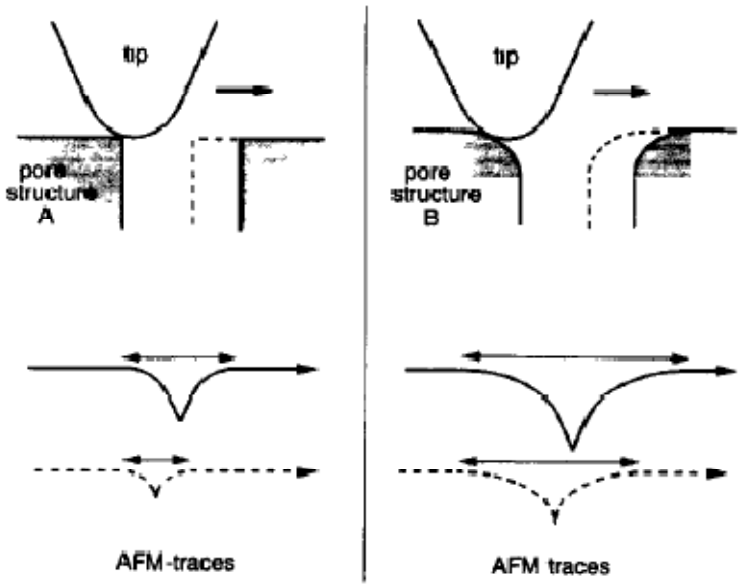

Figure 3-4 Interaction between tip and pore structure and its effect on the resulting trace image (Dietz *et al.* 1992)

Comparing results from the literature SEM usually reports smaller pores compared to AFM using the conventional manually drawn cross sections for data analysis. (Hayama *et al.* 2002) reported that the ratio of the average pore diameter measured using AFM to FE-SEM was 1.1 to 1.2 depending on the sharpness of the scanning tip. (Kim *et al.* 1999) reported that the ratio between the AFM and FE-SEM mean pore radius was 1.3, with a flatter distribution in the case of the AFM. A summary of the advantages and disadvantages of both FE-SEM and AFM are shown in Table 3-1.

Table 3-1 A summary of FE-SEM and AFM advantages and disadvantages

	SEM and FE-SEM	AFM
Advantages	• No need for advanced sample preparation techniques for conducting samples other than drying • Application of electron beam voltage for image generation • Can reach a high magnification (2000 KX) with an image resolution of 0.7 nm which will depend on the used electron voltage	• No drying or coating ever for non-conductive surfaces • Very high spatial and vertical resolution • Can measure wet samples and scan below the liquid surface • Minimal forces prevent sample damage • 3D imaging of the surface • Different imaging modes for specific applications • Can provide additional information (i.e. surface adhesion)
Disadvantages	• Non-conductive samples require metal coating • Samples must be completely dry • High vacuum imaging chamber (except for environmental FE-SEM) • Cannot provide 3D structures directly • Electron beam voltage can affect image quality and damage delicate samples	• Tip shape can affect the dimensions of small features • Result interpretation is more complex than SEM or TEM

3.1.3 Objectives

The main objective of this section was to obtain a complete and detailed description of the pore size characteristics of UF membranes. A reliable method to measure pore size distribution is necessary for studies on membrane performance and membrane rejection of different types of molecules or contaminants. To reach this goal, various available microscopic techniques including FE-SEM and AFM were used, and the data obtained were analyzed using different available image analysis techniques. A new image data analysis technique was developed to 1) overcome the limitations of the other methods 2) handle image artifacts and 3) improve the amount of information obtained from the raw data for both AFM and SEM.

3.2 Materials and Methods:

3.2.1 UF membrane

The membrane used in this study was a commercially available asymmetric polyvinylidene fluoride (PVDF) hollow fiber ultrafiltration membrane with a supporting structure. The outside fiber diameter was 1.95 mm and the inside diameter was 0.8 mm. The membrane fibers used in the characterization study were obtained from a pilot scale module that was provided directly by the manufacturer. The pilot scale module was preserved in glycerin. The module was thoroughly rinsed with deionized (DI) water before four individual fibers were cut from the module. Each fiber was then cut into 2 cm samples and placed into sealed containers in ultrapure water (resistivity 18 MΩ-cm, TOC 0.5 to 50 ppb). Image analysis (FE-SEM or AFM) was performed on individual fibers as shown in Figure 3-5 to investigate the differences in pore size distributions among different fibers within the same module. Further details on the image analysis methods are provided below in sections 3.2.2 and 3.2.3.

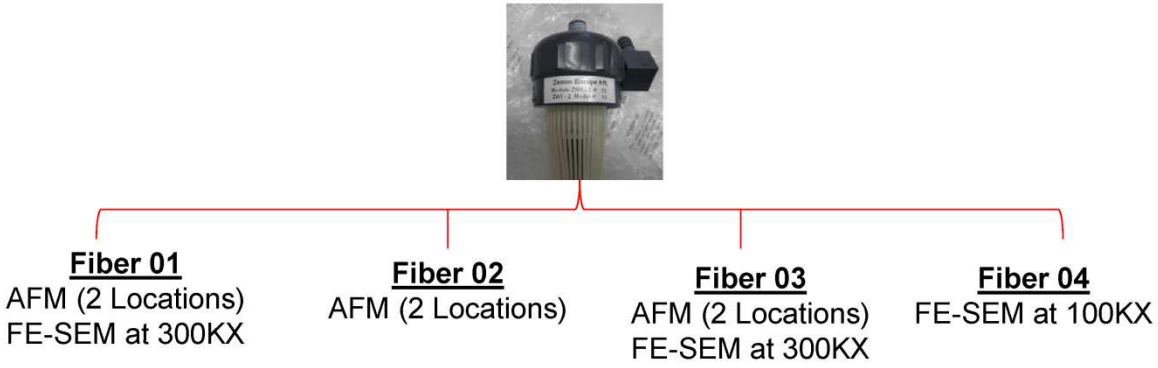

Figure 3-5 Selection scheme for membrane samples to be studied

3.2.2 MF Membranes

A commercially available MF membrane (Millipore MF ™ membrane filter, catalogue number VMWP04700, Millipore, USA) was also characterized using AFM. The membrane is made from mixed cellulose esters with a pore size rating of 0.05 µm according to the manufacturer. The membranes were used dry, without wetting in water.

3.2.3 AFM Measurement

The UF fiber pore structure was characterized by AFM using a Dimension 3100 multimode scanning probe microscope (Digital Instruments, Santa Barbara, CA). The AFM was operated in tapping mode

using a silicon tapping mode probe (Veeco Instruments, part MPP11100, Bruker Corporation, USA). The cantilever had a spring constant at 20-80 N/m, resonant frequency of 257-332 KHz and length of 11.5-13.5 µm. The nominal tip radius of the probe was 8 nm and the maximum tip radius was 12 nm. The tip 3D geometry can be described by the front, back and side angles of the tip which were 15±2º, 25±2º and 17.5±2º, respectively. A 1 µm calibration grid was used to test the accuracy of the instrument. Tapping mode was used instead of contact mode to preserve the pore structure of the polymeric membrane and to overcome drawbacks of the other AFM modes (Khulbe *et al.* 2008). In AFM tapping mode, the tip oscillates at its resonant frequency in air next to the scanned surface so it just taps the surface without any direct contact, to produce high resolution topographic dimensions of the surface (Veeco Instruments Inc. 2004).

All samples were measured within a maximum of 1 h after they were taken out of water. The surface of the fiber was wiped gently using a KimWipe tissue to remove excess water. The fibers remained moist during measurement by AFM. A micro-vise sample holder (Bruker AFM Probes, part PSH-103, Bruker Corporation, USA) was used as shown in Figure 3-6, in order to keep the fiber stable and not to distort the pore structure on the membrane fiber. The fibers were held horizontally within the clamp prior to inserting the sample into the AFM. The laser beam was focused on the apex of the fiber using the optical microscope system provided with the instrument, to minimize the effect of the surface curvature on the resulting image.

Figure 3-6 AFM sample holder used for the membrane fibers (Bruker AFM Probes)

The AFM scan rate was 1.0 Hz with a scan size of 1.5 µm × 1.5 µm and 512 grid points per scan line. After engaging the tip, both the proportional and integral gain were adjusted as described in the instrument manual to match the trace and retrace line in order to get the optimum image. For fiber 1, 2 and 3, two different locations 5 – 10 mm apart were imaged.

For the MF membrane used, AFM images were obtained over 2.0 × 2.0 µm area for 3 different spots on the MF membrane sample. An image of the membrane surface was available from the manufacturer (MF-Millipore™ MF-Millipore Membrane Filter) as shown in Figure 3-7a. It may be

an SEM image but this could not be confirmed. Figure 3-7b shows one of the obtained AFM images of the surface of the MF membrane.

3.2.4 FE-SEM measurements

The fiber samples were dried prior to analysis at room temperature for 24 h, then sputter coated with gold nanoparticles. The samples were examined using a FE-SEM (Zeiss FE-SEM LEO 1530). Fibers 1 and 3 were analyzed using a magnification of 300 KX at 4.0 KV accelerating voltage, and fiber 4 was analyzed using a magnification of 100 KX at 5.0 KV accelerating voltage. Different magnifications were used to determine the effect of magnification and gold particles on the resulting pores size distribution. Energy dispersive x-ray (EDX) analysis was also used to determine the chemical composition of the surface.

To study the structure of the membrane, cross section of the membrane was studied using FE-SEM. The membrane samples were dried in air for 24 h then the skin layer of the dried sample was peeled of the support structure first then it was frozen in liquid nitrogen. The frozen membrane was broken in order to get a sharp cut of the membrane cross section. The frozen sample was fixed a sample holder then gold coated in the same way like regular samples and different images were obtained for the cross section.

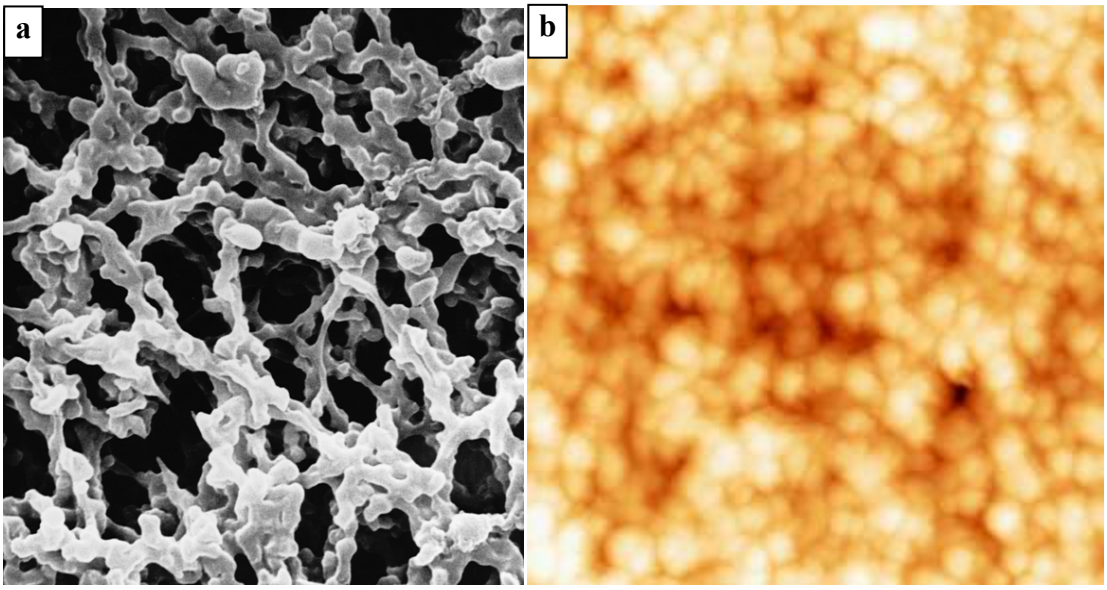

Figure 3-7 a) Image of the MF membrane surface as reported by the manufacturer (Millipore) (http://www.millipore.com/catalogue/item/vmwp04700) , and b) AFM image (2.0 ×2.0 µm) of the MF membrane from this study.

3.3 Data Analysis Techniques for AFM and FE-SEM Results

The images resulting from FE-SEM and AFM analysis appear to have a different format, but actually they are very similar. The FE-SEM result as seen in Figure 3-8 a is in the form of a grayscale image, and the pixels can be described as a 3D matrix with the X and Y coordinates for each point on the surface and the Z coordinate will be the grayscale level that will range from 0 (black) to 256 (white). The AFM result as shown in Figure 3-8b is also a 3D matrix, with X and Y coordinates measured in nanometers and the Z axis is the surface height as measured from the probe signal as explained previously. Because both techniques result in 3D images with X, Y and Z coordinates common image analysis techniques can be used for both AFM and FE-SEM images. The main difference will be in the quality of the image. In the case of FE-SEM, the change in the Z value (i.e. the grayscale level) is large at the pore boundaries, which results in a sharper image and makes it easier to detect pores. AFM images typically do not display sharp boundaries at the pore edge. Instead, the AFM pore boundary will usually have a mild side slope, as side slopes can be more accurately determined by AFM through actual measurement of the Z value (height). This makes detection of pore boundaries during data analysis more difficult though. To resolve this problem, different techniques can be used for analyzing AFM and FE-SEM images, and the choice of the appropriate image analysis technique will depend mainly on the image quality as briefly explained in Table 3-2.

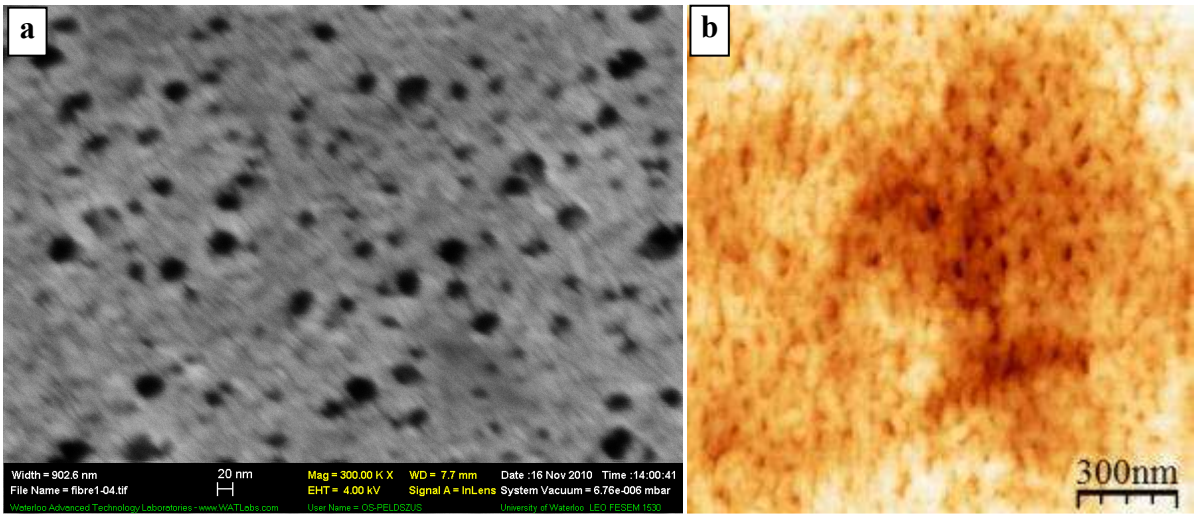

Figure 3-8 Images resulting from (a) FE-SEM and (b) AFM

Table 3-2 Summary of the different available image analysis techniques and their limitations

Image analysis technique	Description	Disadvantages or limitations
1) Manual cross section	Draw a line from A to B. Then draw cross sections across apparent pores in desired direction (usually maximum opening)	• Cannot measure pore shape or area • No automatic counting of pores • Not suitable for large number of pores • Subject to human error • No consistent reading of pore dimensions or depth
2) Grayscale thresholding	Set a specific grayscale level as cut-off. Transform image to binary image to differentiate between membrane surface and pores.	• Cannot detect pore boundaries accurately which affects measured pore area • Easily affected by noise or image artifacts (hence, not suitable for AFM) • Requires advanced image filters to overcome these limitations
3) Watershed thresholding	Detect each pore boundary independently based on the local slope of the surface around the pore.	• Works better for sharp images • Cannot detect pores which have a mild slope at their boundaries (i.e. high magnification FE-SEM or AFM)
4) Pore construction	Detect region where the data points form an apparent pore-like structure of conical shape, then analyze pore applying user selected data filters.	• Familiarity with Matlab • Optimization of analysis parameters is required

Following is a description of the image analysis techniques as they were applied in this research.

3.3.1 Manual Cross Sections

This is the most basic and simplest image analysis technique. This is the method more typically used for AFM image analysis. However, it can be applied to any image by simply placing a cross section across the apparent pore on the surface, and the obtained line profile can be used to measure the pore opening. This technique is time consuming and largely affected by human error when placing the cross section across the pore and when choosing the height at which the measurement will be done. Limited information can be obtained from this technique. No pore area or pore density can be measured. For these reasons, this technique cannot be used to provide a reliable pore size distribution to compare different membranes or fibers.

3.3.2 Grayscale Thresholding

Grayscale thresholding is also a common, simple technique for image analysis. It is typically used for the analysis of FE-SEM images and in this study it's use for AFM images was also explored. For this technique a certain grayscale level (or a certain depth in case of AFM) is selected and any surface below this level is treated as a pore whereas anything above is treated as membrane surface. The main disadvantage of this technique is that it cannot accurately detect pore boundaries. Pores are not simple vertical cylinders but resemble conical shapes with varying side slopes. Hence, the depth/grayscale level chosen will influence pore dimensions. This technique will also be affected negatively by image artifacts such as tilt or curvature of the surface.

3.3.3 Watershed thresholding

Instead of using the regular grayscale thresholding, this more recently developed method by Vincent (1991) can be used to improve the detection of pore boundaries. This analysis technique has only recently been applied to SEM images and was used in this study primarily for SEM images but was also tested on AFM images. The Matlab (Version R2009a; MathWorks) image analysis tool box was used for this purpose. The analysis of each image was performed in the following order:

1. Convert the original grayscale image Figure 2-9a into an average gradient image in both X and Y directions based on the grayscale values, as shown in Figure 3-9b simply by replacing the Z value at each point by the average of both the gradient in X and Y directions. This step will help in detecting the boundaries of the pores, as the boundaries will have a large difference in their color intensities and, hence, a higher gradient unlike flat surfaces which will have a low gradient.
2. Filter the obtained image to suppress the lower intensity points from the gradient map leaving only the detected boundaries which have the highest gradient.
3. Applying the watershed segmentation to detect the pore boundaries as separate objects and measure their different properties as shown in Figure 3-9c.

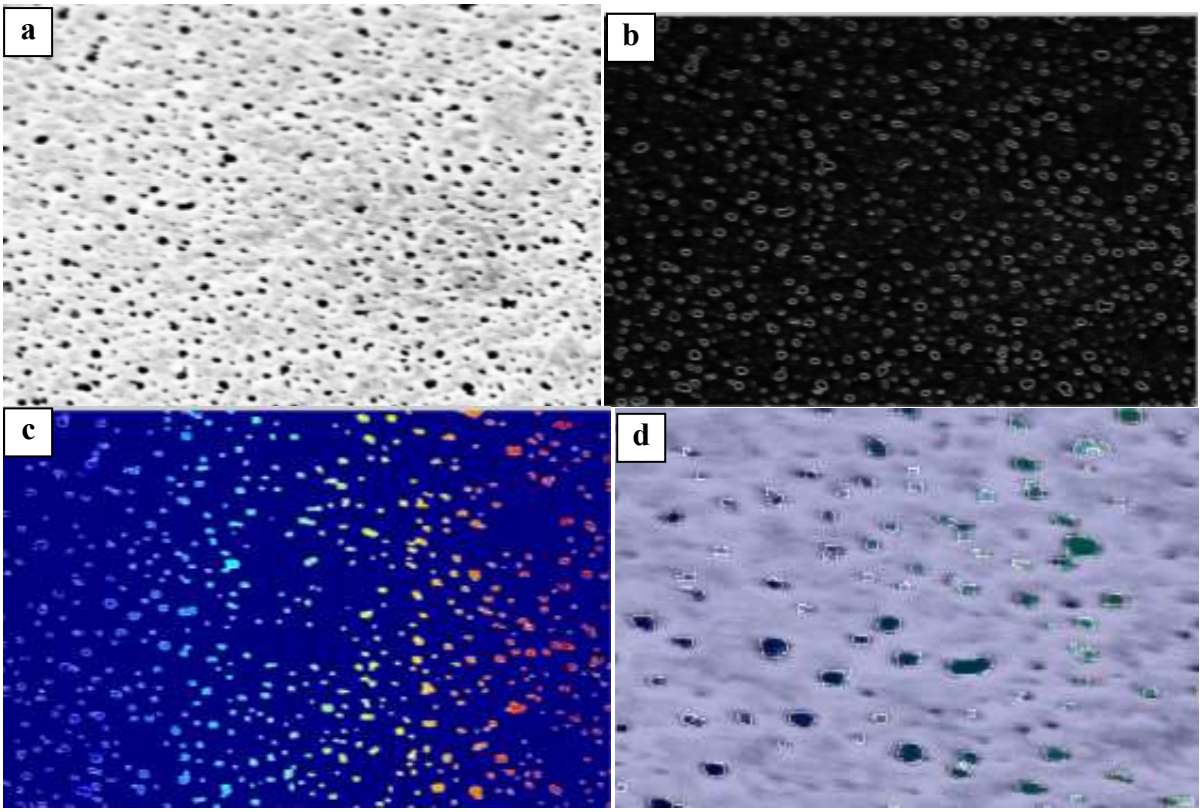

Figure 3-9 Result of FE-SEM image analysis using the watershed thresholding technique. Illustration of individual steps including a) original image, b) gradient image, c) watershed segmented image, d) overlaying detected pores over original image.

As can be seen in the final result shown in Figure 3-9d, this technique allowed better detection of the outer pore boundaries regardless of minor image artifacts. However, this method has some drawbacks. It can easily be disrupted by blurred, non sharp or dark FE-SEM images. This made the technique unsuitable for FE-SEM images that were taken at lower gold coating times or at magnifications higher than 100 KX, conditions which are necessary for a closer study of the pore shape and dimensions. Using watershed thresholding analysis on their AFM images Knoell *et al.* (1999) were able to detect pores on membranes with average equivalent diameters, albeit these were larger than the pores of membranes used in this study. Watershed thresholding was applied to AFM images from this current study but meaningful results could not be obtained.

3.3.4 Pore construction method

This technique was developed by the author to evaluate AFM images that could not be examined by any of the previously mentioned data analysis techniques. Initially, AFM image raw data in numerical form are imported into Matlab prior to processing as described below.

The pore construction method is divided into several different tasks, all performed in Matlab. The first task is to detect regions inside the image where data points will form a structure similar to an apparent pore geometry. This step is repeated for each pore individually instead of treating the entire data set at once. The benefit of this approach was that it is less impacted than other image analysis technique by image artifacts such as surface roughness, contamination or image tilt. As a result of this first step only pore data will remain for further analysis. The pores, as depicted in the AFM image (Figure 3-10), have non-perfect conical shapes. Subsequently, different filters were applied (described below) to trim the detected pores to get a unified, consistent measurement of pores within each image and of pores in different images of the same membrane. The use of filters also eliminated surface notches that can be incorrectly detected as apparent pores. To do this, the pore shape is fitted to a 3 dimensional shape, and the obtained shape is then studied at user defined height steps as depicted by the contour lines in Figure 3-10b.

The first applied filter is the minimum and maximum allowable pore size. Setting of a minimum pore size will delete notches smaller than the resolution of the AFM (i.e. length of scan line/points per scan line). It will also eliminate small pores that would otherwise have large errors associated with their dimensions due to their smaller size. One advantage is that this minimum pore size filter value can be decreased when image resolution increases. Setting a maximum pore size will delete detected valleys on the surface and also trim the pore entrance part that might otherwise be interpreted as part of the pore. The selection of a value for this filter is based on either FE-SEM results or any rejection data available from other studies for the investigated membrane (e.g. MWCO).

The second filter is the minimum pore depth which works along with the minimum pore opening filter to delete shallow notches. The minimum value for this filter should be set in accordance with the expected pore size of the membrane, as it will depend greatly on the tip penetration inside the pores. Tip penetration will depend on the relative size of the tip used, the membrane pore opening and scan resolution. This value should be increased with increasing expected pore size and with decreasing tip dimensions.

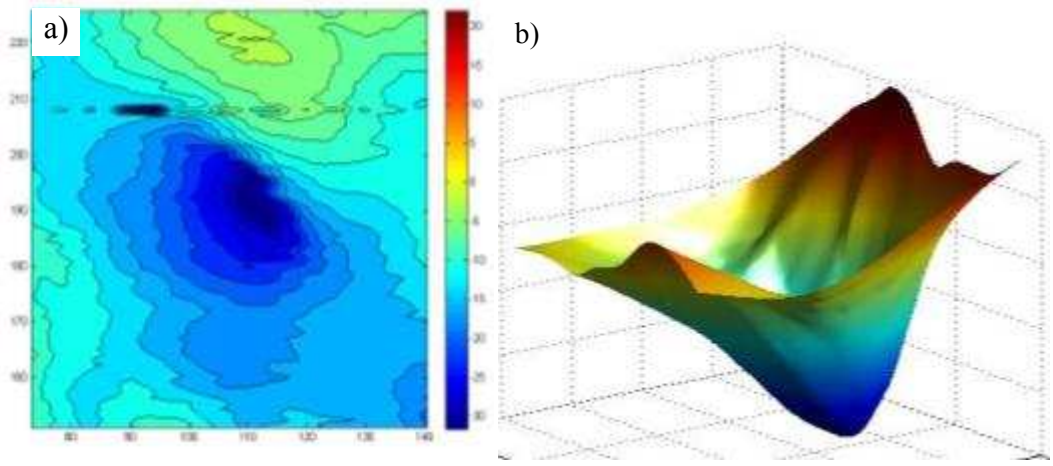

Figure 3-10 Image of an actual detected membrane pore using the AFM pore construction method in (a) 2 dimensions and (b) 3 dimensions

The final filter and the most important one is the area gradient filter which was specifically developed for final pore identification. As explained earlier, the detected pores have a non-uniform conical shape which makes a gradient based on a uniform slope in either X or Y direction unsuitable for pore identification. Hence, an area gradient filter was selected instead. The area gradient was defined as the change in pore cross sectional area over a user defined height step. At pore bottom this parameter will have a higher value as the measured dimensions have a higher error due to tip convolution, as explained in section 3.1.2. Going up along the pore, the gradient value decreases gradually, and as the pore entrance is approached the gradient value will increase again since the slopes tend to become shallower. By setting the gradient filter to a maximum value the measurement of the pore at the top level is defined and unified. Setting this value too low can prevent the detection of pores, leading to a lower pore density. Setting the gradient value too high will give misleading pore dimensions at the top and some surface valleys might be misinterpreted as large pores. A trial and error approach was used for setting this filter to an optimum value.

After the optimal gradient filter is set and applied for the detection of all pores, different geometrical descriptors of the detected pores are calculated at two different Z levels, including the pore top and the pore at mid-height. The pore top measurement is chosen as it represents the maximum dimensions of a pore and can therefore be considered as a detection limit for the pore shape. Pore top measurements can also show if the filters applied could trim all the pores consistently. Pore mid-height is chosen as it will represent the average reading within the detected pore. As already discussed, the pore bottom measurement was not used as its dimensions will have a high uncertainty

associated with it due to tip convolution. Although the pore construction method was mainly developed for AFM data sets, it can also be used successfully on FE-SEM images, with the only difference is that the measurements are done at the pore bottom.

The AFM images obtained for the different membrane samples were analyzed using Matlab and the values for the different filters are shown in Table 3-3. The area gradient filter was determined based on different trials to get the value that will maximize the number of detected pores per image. The original AFM images and the detected pores are shown in Figure 3-11

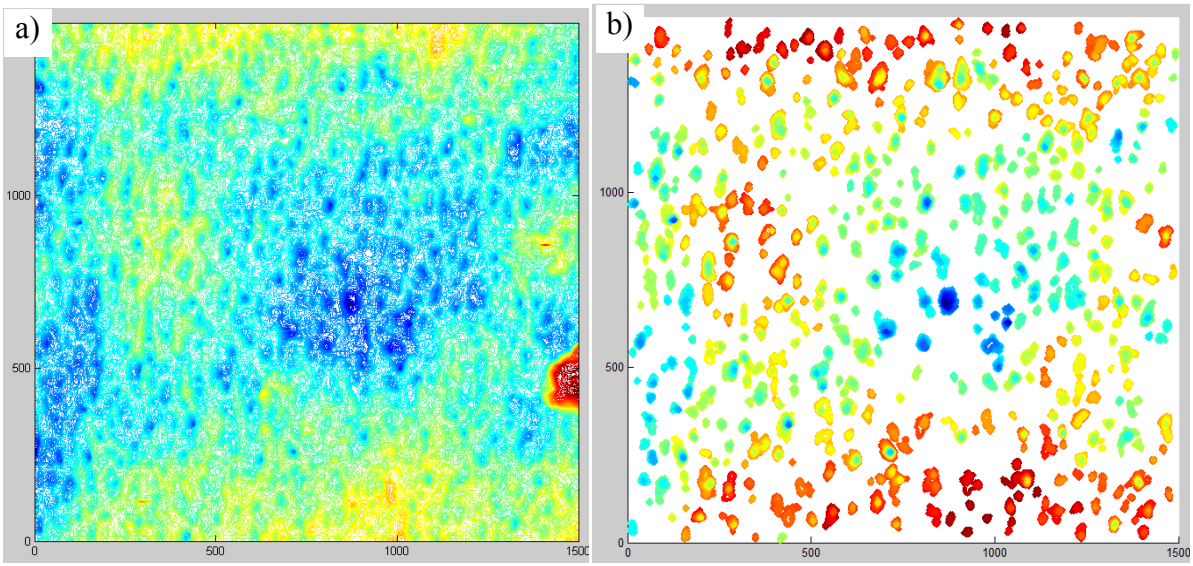

Figure 3-11 original AFM image of fiber 1 (a) the detected pores in the image (b)

Table 3-3 Filter values used for analysis of AFM images using the pore construction method in Matlab

Filter	Value	Additional Notes
User defined height step	1 nm	
Minimum pore size	3 nm	Based on the image resolution for the AFM
Maximum Pore size	90 nm	Based on the maximum pore opening expected for a UF membrane
Maximum area gradient	500%	Set to maximize the number of detected pores
Minimum pore depth	3 nm	Based on three times the height step to ensure pore detection
Neglected data at image borders	3 nm	Neglect the last two data points on each side of the pore border to delete incomplete pores and features

3.3.5 Summary of data analysis techniques

Any of the four available data analysis techniques (manual cross section, grayscale thresholding, watershed thresholding or pore construction) is in principle applicable to images of the membrane surface obtained either with AFM or FE-SEM. The choice of the appropriate data analysis technique will depend on the image quality and the type of features inside the image. Both watershed thresholding and pore construction techniques have major advantages over grayscale thresholding as they can overcome some of the image artifacts and hence, get better detection of pore boundaries. Watershed thresholding was applied to FE-SEM images at lower magnifications. This method will not be suitable if the pores have a mild slope at the pore entrance. This typically occurs at high magnification FE-SEM, and in most AFM images, as the instrument has a high Z resolution which will generally be able to display the mild pore side slopes encountered near the surface. However, the pore construction method is able to overcome these limitations and is therefore applied to AFM and high magnification FE-SEM images throughout this study unless mentioned otherwise.

3.4 Results and Discussion

3.4.1 UF Membrane material and morphology

This study aimed at identifying the morphology of a commercial UF membrane that would be used in further experimental studies. The study of the membrane cross section morphology was necessary to provide the basis for a detailed study of the membrane pores that exist on the skin layer of the membrane facing the feed side and are responsible for most of the rejection. To obtain pore size distribution and porosity are the main objectives of this chapter. Both will be required to get in depth knowledge of membrane rejection characteristics and are used in later chapters in the interpretation of virus rejection results.

The UF membrane fibers used for this study were supported membrane fibers. Figure 3-13 shows FE-SEM images of the membrane cross section. The total thickness of the membrane polymer was nearly 150 µm, however, the skin layer (i.e. the actual separation layer) was only 100 nm in thickness as can be seen from the higher magnification image of the skin layer. The underlying support structure is more porous and it will only contribute minimally to the rejection of particles and enteric viruses.

The polymeric material for the UF membrane was reported to be a PVDF [-$(C_2H_2F_2)_n$-] polymer. The surface chemical structure of the virgin membrane was studied using EDX and the results are shown in Figure 3-12. These results show that the surface is composed of 75% carbon, 5% oxygen and 16%

fluoride. These results point either to a surface modification or the addition of a modifier to the polymer used for manufacturing the membrane since PVDF does not contain any functional groups containing oxygen. The introduction of oxygen into the membrane surface decreased the surface hydrophobicity compared to what would be expected for pure PVDF.

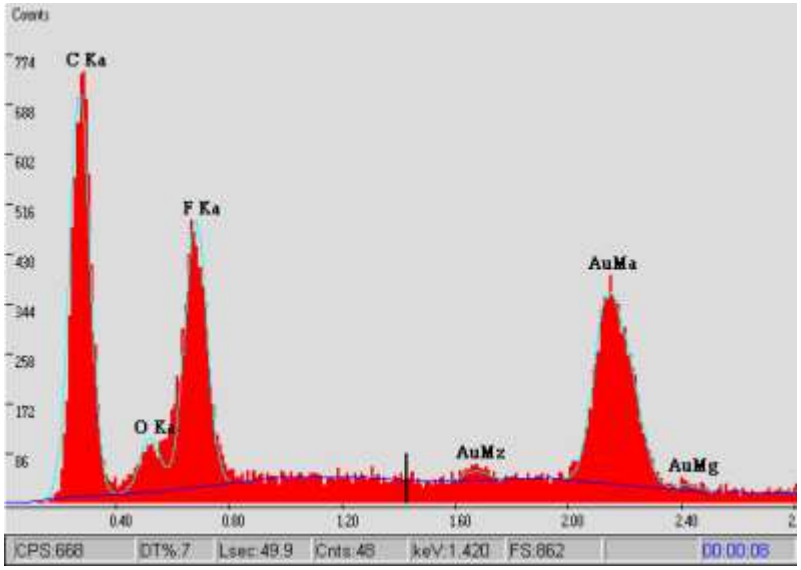

Figure 3-12 Results of EDX analysis of a virgin membrane at 10 KV

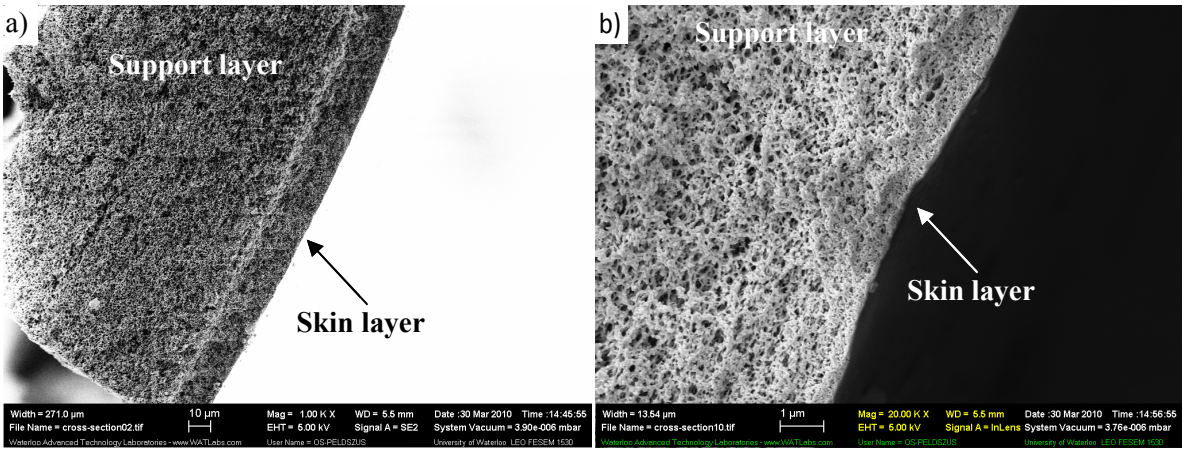

Figure 3-13 FE-SEM images of the UF membrane (a) cross section (1 KX magnification) and (b) the skin layer (20 KX magnification)

3.4.2 AFM analysis of UF membrane

AFM was used to image the skin layer of the UF membrane samples in a top view. Images were analyzed using the new pore construction technique (as described in section 3.3.4) to evaluate pore size distribution and surface porosity. Manual cross sections were also used to analyze one of the images (as described in section 3.3.1 and Figure 3-3) to compare the obtained results of this conventional data analysis method to the new pore construction method. Watershed or grayscale thresholding were not able to detect the pores in the obtained AFM images.

Table 3-4 provides a summary of the different geometric descriptors used for identifying the pore size and shape of the detected membrane pores from the AFM images using the pore construction method. The 'inscribed circle diameter' is a new parameter developed by the author which can be used later for modeling virus removal by membranes. As mentioned previously, membrane pore characteristics were determined at both pore top and pore mid-height. The results are presented as frequency histograms per square micrometer area, instead of relative frequency histograms. If a certain region of the distribution was not detected then the relative frequency histogram will be affected as it presents ratios of detected pores of a certain pore size to total frequency of all pores detected. Using frequency histograms per unit area instead will help to investigate the change in pore density and also to overcome any imaging technique problems that might prevent the detection of smaller pores. The bin size for the histograms was determined using the Freedman rule (Freedman and Diaconis 1981) to get a better view of the trend in the pore size distribution. The same bin size was used for any two curves being compared.

Table 3-4 Different geometrical descriptors for pore size and shape

Parameter	Description
Equivalent Diameter	The diameter of the circle which has the same area as the membrane pore
Pore maximum opening	The maximum distance between two points on the pore border
Pore average opening	The average of the distance between two points on the pore border
Inscribed circle diameter	Diameter of the largest circle that can be drawn within the pore border
Aspect ratio	Ratio of pore maximum opening over pore average opening
Roundness	$\frac{4 * area}{\pi * Pore\ \max opening^2}$
Form Factor	$\frac{4 * \pi * area}{Perimeter^2}$

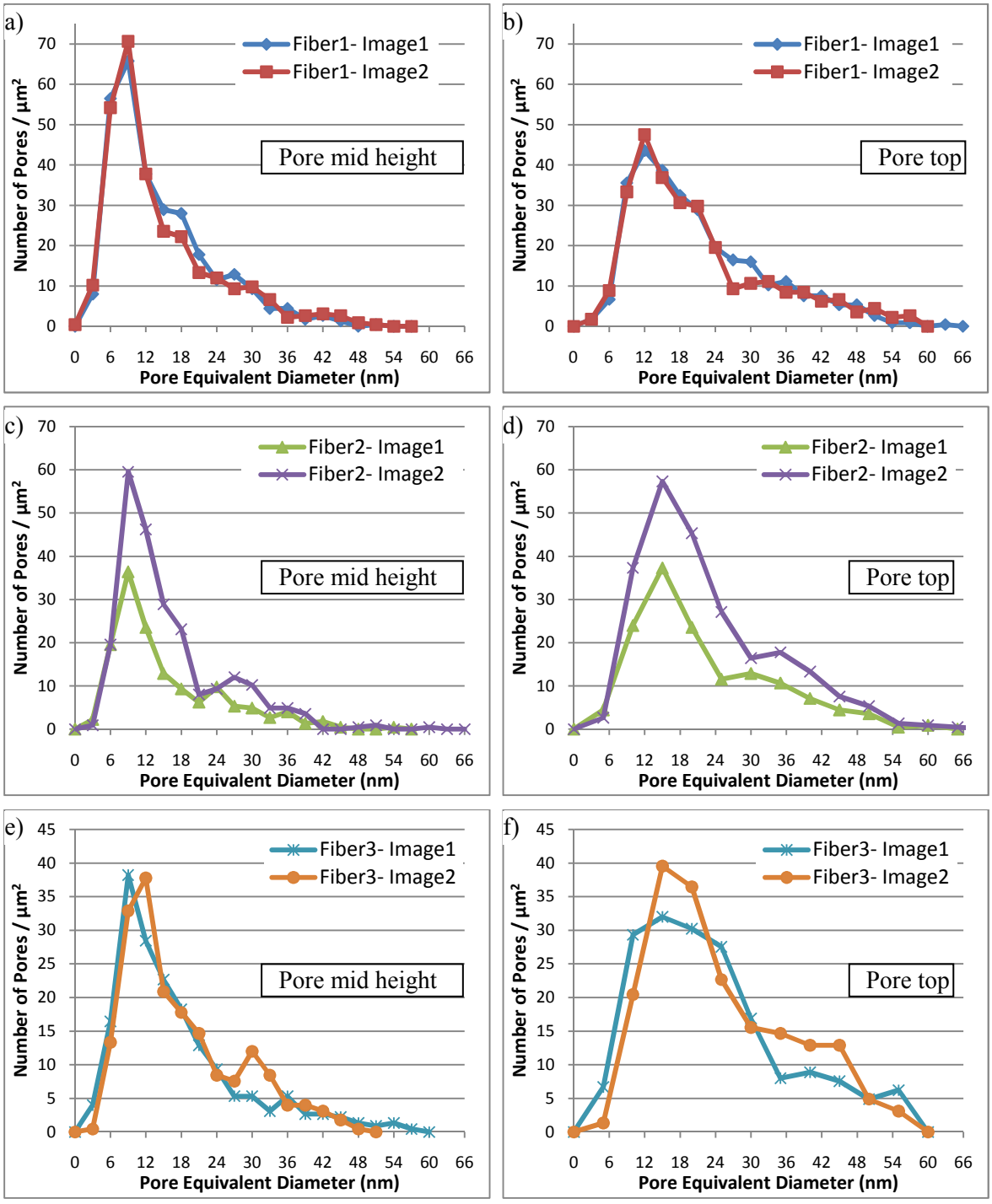

Figure 3-14 Comparison of AFM measured pore equivalent diameter for fiber 1(a,b), fiber2 (c,d), fiber3 (e,f) at pore mid height (a,c,e) and pore top (b,d,f)

For each UF fiber used for testing, two different images are compared to check the reproducibility of the pore construction data analysis technique. As shown in Figure 3-14, the separate images taken for both fiber 1 (Image 1& Image 2) and fiber 3 (Image 1& Image 2) had very similar distributions for pore equivalent diameter, both at pore mid height and at pore top. For both fibers, images 1 and 2 displayed the maximum number of pores at essentially identical pore equivalent diameters. However, for fiber 2 image 2 had a lower number of pores compared with image 1. This can be explained by several factors. In the AFM image 2 for fiber 2, the image upper part was highly tilted. This fiber also showed apparent surface contamination shown as large peaks on the surface, which was also seen in FE-SEM images of this UF fiber. This reduced number of detected pores in image 2 also affected the detected pore density for this image. This same trend was also noticed for other descriptors like pore maximum opening, pore average opening and inscribed circle diameter. Overall though results for fiber 1 to 3 show that the pore construction method for detection and measurement of membrane pores using AFM is a reproducible technique and it can therefore be applied in further studies of membrane pore structures. Furthermore, image artifacts could be isolated and taken into account when using the pore construction technique.

Studying the variability between different membrane fibers was one of the objectives of this study. This will help to understand if different modules of the same membrane would exhibit different removal of viruses, although they might have similar properties such as water permeability. A comparison of the three different fibers used in this study is shown in Figure 3-15 and Figure 3-16. The presented pore frequency histograms are based on the total number of pores of a certain size detected in both images of each fiber divided by the total area of both images of each fiber. All three fibers had similar shapes of log normal distributions as is usually reported for UF membrane pore size distributions (Zeman and Zydney 1996). The maxima of the pore size distributions of fiber 1 seems to be at slightly lower pore size than fiber 2 and fiber 3 which are very similar. The corresponding frequency of these distributions is different due to the difference in pore density. Fiber 2 and fiber 3 look identical. However, fiber 1 had a higher frequency of smaller pores. This would mean that using data from all the three fibers to generate a general distribution for this membrane might not be suitable, as it will neglect the variability between fibers that was found to be important in this case. So for studies that will depend on pore size distributions, it will be advantageous to use samples from various fibers or batches to determine their variability. At the tail of the pore size distribution towards the larger pores, the different fibers were very similar which is of interest when interpreting results for rejection of viruses. Assuming that viruses can be represented by spherical colloids, previous studies

on colloid removal become relevant in this context. Rejection of spherical colloids depends on the part of the pore size distribution larger than the diameter of the colloid (Mehta and Zydney 2005). In this case, these three different distributions would exhibit similar removal of these particles, since fiber to fiber variability at the large pore sizes is very small. Besides spherical colloids this will also apply to larger molecules like the organic macrosolutes used for MWCO determination of UF membranes and also to enteric viruses.

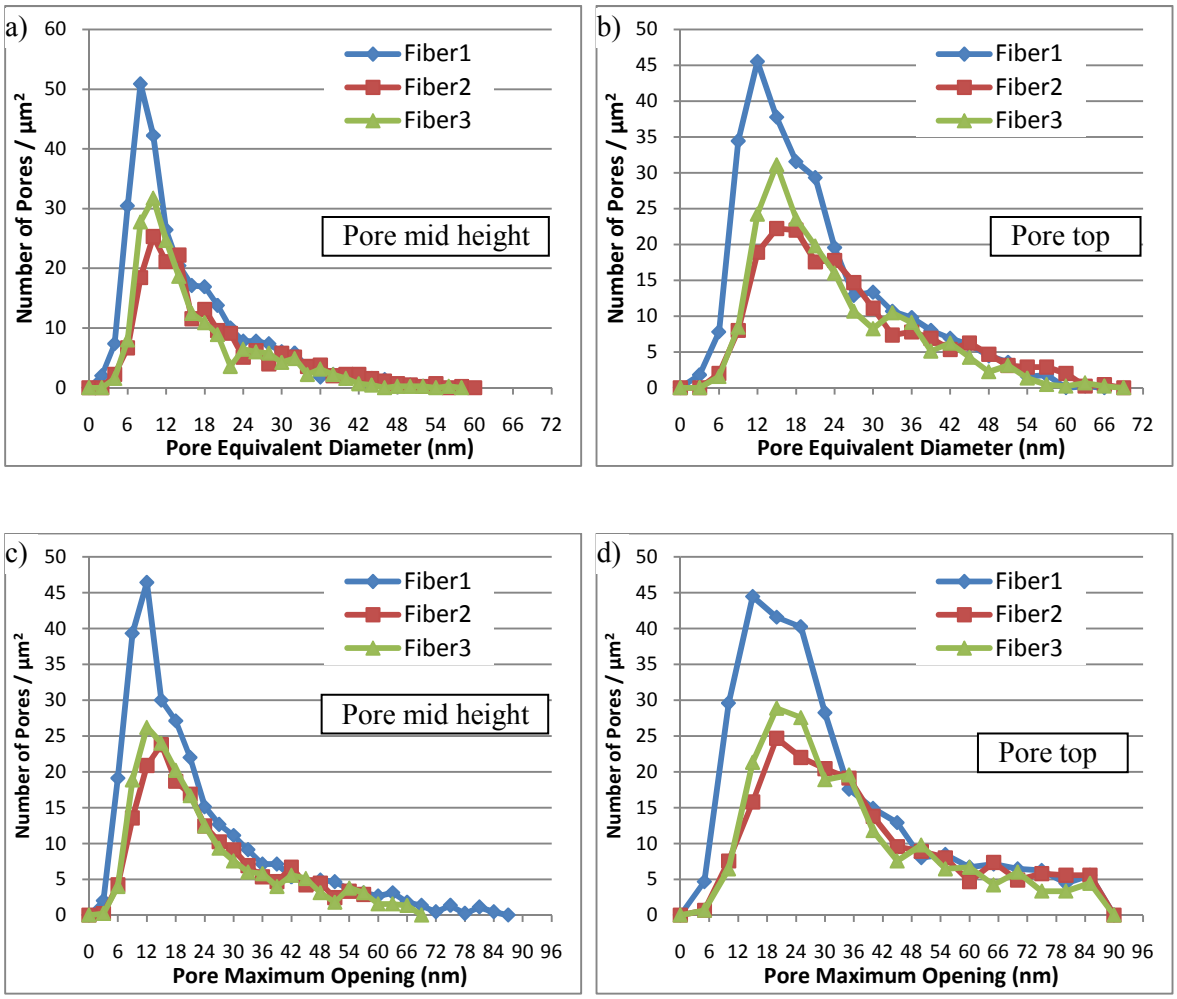

Figure 3-15 Comparison of different fibers tested at pore middle (a,c) and pore top (b,d) for equivalent diameter(a,b) and max pore opening (c,d)

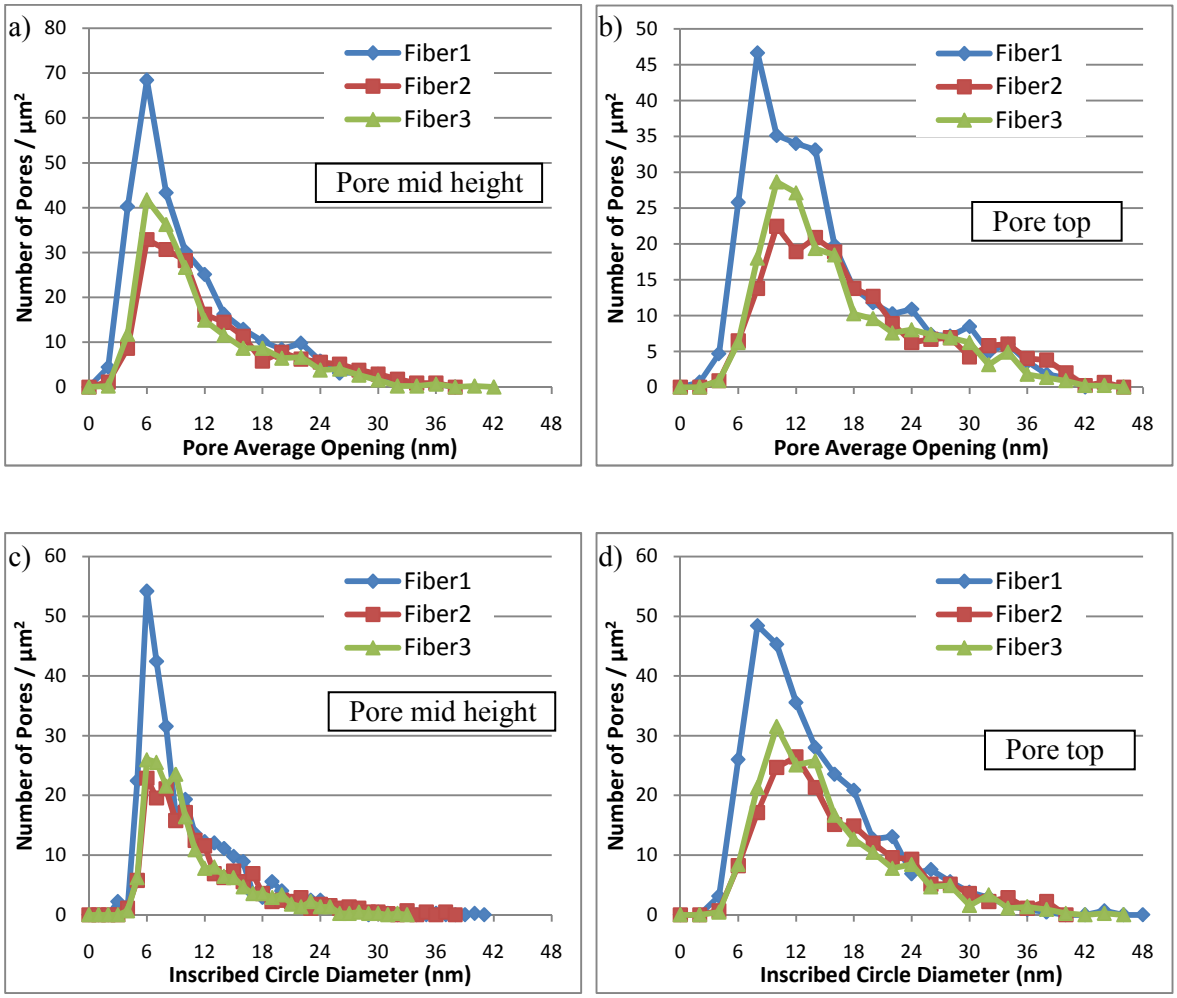

Figure 3-16 Comparison of different fibers tested at pore middle (a,c) and pore top (b,d) for pore average opening (a,b) and inscribed circle diameter (c,d)

The conventional manual cross section technique for AFM data analysis was also used on one of the images (fiber1-image 2) to illustrate the difference in results between the new pore construction method and the conventional technique. Manual cross-section analysis was done on pores that were randomly chosen from the image and the total number of pores measured was 129. To obtain the maximum pore opening the horizontal distance was measured in the direction that appeared to be the maximum pore opening. Results for the manual cross section technique compared to the pore construction technique are shown in Figure 3-17. The y-axes shows relative frequency instead of the frequency per unit area since not all pores within the image could be measured using the manual cross-section technique. The AFM pore size distribution obtained with the conventional technique had its maxima at a larger pore size than both the pore mid-height and pore top distributions obtained

with the new data analysis technique. A possible reason for this is that the manual cross section measurement was done at a pore height that was higher than what is used for pore construction pore top measurement. However, this is unlikely as a mid-height equivalent plane (between membrane surface and pore bottom) was used for the manual cross section measurements. The other possibility is that the choice of the pores for the manual cross section method was biased due to human error as the larger pores are usually picked for measurement, which will affect the distribution and shift it towards the larger pore size as seen in Figure 3-17. This may also be an explanation for the difference that is usually reported between AFM and FE-SEM pore size distributions in the literature.

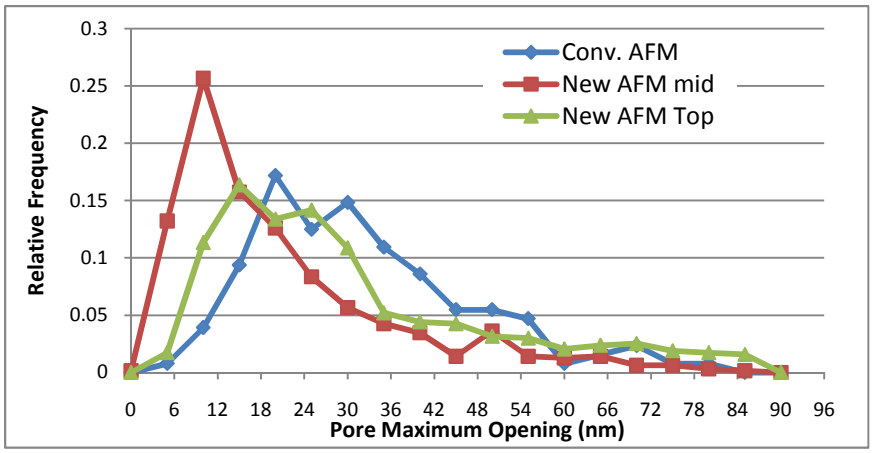

Figure 3-17 Comparison of conventional AFM image analysis (manual cross section analysis) and new AFM data analysis technique (pore construction technique) at different levels within the detected pores

3.4.3 FE-SEM Results

Three different FE-SEM images with a 100 KX magnification taken of UF membrane fiber 4 were characterized using both the watershed and grayscale thresholding techniques. Ideally, similar results should be obtained since the same images were characterized with both methods. But this was not what was observed and may be expected due to the limitations of each method. When comparing both techniques for FE-SEM (Figure 3-18), the grayscale thresholding gives a more flat pore size distribution. The maxima of the pore size distribution for pore maximum opening (Figure 3-187b) and pore equivalent diameter (Figure 3-18a) for FE-SEM grayscale thresholding is at a larger pore size than for watershed thresholding. This was expected since grayscale thresholding will not detect the exact boundaries of the pores and tends to overestimate pore size (see also Figure 3-9). Hence, for

smaller pores where any small error would affect the detected pore shape this could skew the results. For the larger pores, where the error would be less significant, both techniques will yield very similar results as shown in Figure 3-18a and Figure 3-18b. The flat distribution seen in the grayscale thresholding can also be attributed to the inaccurate detection of the pore boundaries and resulting lower pore density compared to the AFM results as will be explained later.

The watershed segmentation distribution results are in agreement with the AFM results, since both display distribution maxima at very similar pore openings (Figure 3-18a,b). It was also observed (Figure 3-18 a,b) that the watershed thresholding method of FE-SEM images obtained a pore density that was lower than that of any of the AFM samples. Hence, it was clear that watershed thresholding of FE-SEM images could not detect all pores, especially the smaller pores which had unclear images at this magnification. The pore construction technique was not used for FE-SEM images at this magnification because the number of pores detected in the FE-SEM images were much larger than for the AFM images due to the larger scan area (5 μm^2 for FE-SEM compared to 2.2 μm^2 for AFM). This will make processing of the FE-SEM data sets with the pore construction technique time consuming and requires high processing power which was beyond the scope of this study.

Although a different fiber (Fiber 4) was used for FE-SEM analysis than for AFM analyses (Fiber 1-3), FE-SEM results indicate that fiber 4 had a similar pore size distribution as that obtained by AFM analysis of fiber 2 and 3 (Figure 3-18 a, b). For pore equivalent diameter (Figure 3-18a), the maxima of the FE-SEM distribution was at the same pore diameter as for both fiber 2 and 3, but with a lower frequency per unit area. This can be due either to FE-SEM sample preparation methods, pore detection technique limitations, or fiber to fiber variability. For the right side of the distribution at larger pore sizes, the FE-SEM distribution was nearly the same as the AFM distributions. This shows that the new AFM pore construction technique was able to detect larger pores similar to FE-SEM using watershed thresholding analysis, which is a significant finding for this study. This clearly shows that the obtained AFM pore size distribution can be trusted and used for interpreting the pore size distributions of the membranes. For Figure 3-18b AFM pore maximum openings are compared to the size of the major axes of the pore in the FE-SEM image. This comparison has to be interpreted with caution as these entities are determined differently and results are therefore slightly different. For the watershed thresholding through Matlab, the major axes is defined as the length of the major axis of the ellipse that has the same normalized second central moments as the pore. Hence, it will be smaller than the maximum pore opening which is defined as the maximum distance between any two points on the actual irregular pore shape.

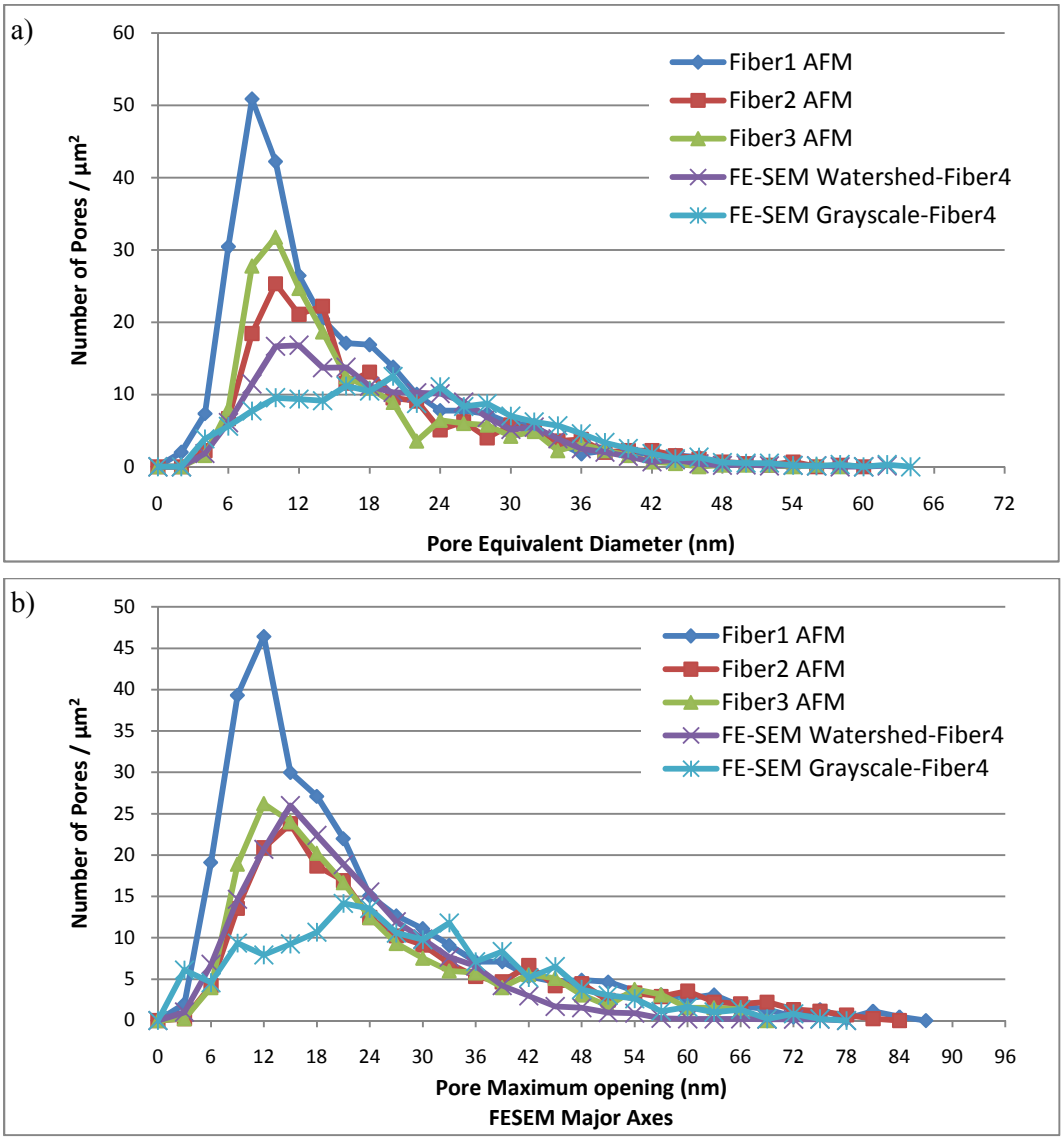

Figure 3-18 a) Pore equivalent diameter and b) pore maximum opening of FE-SEM results of fiber 4 at 100 KX magnification analyzed with watershed segmentation and grayscale thresholding techniques compared to AFM results analyzed with the pore construction method at pore mid height for fibers 1-3 (combined data for both images from each fiber)

To further investigate the fiber to fiber variability observed in Figure 3-15 and Figure 3-16 fiber 1 and fiber 3 were chosen for additional investigation by FE-SEM at higher magnification as shown in Figure 3-19. From the obtained images it can be clearly seen that fiber 2 (Figure 3-19 b,d) has larger pores than fiber 1 (Figure 3-19a,c) and some pores in fiber 3 are even connected to form larger pores. This may explain the slight shift of the maxima of the pore size distribution towards higher values for

fiber 3 compared to fiber 1 (i.e. larger median of the pore size distribution Figure 3-15 and Figure 3-16).

As explained in section 3.3 the nature of both AFM and FE-SEM images are similar as they are a 3D matrices and in principle the pore construction technique and watershed thresholding can be applied to both the FE-SEM and AFM images. For the FE-SEM take at high magnification such as Figure 3-19 watershed thresholding was not useful. The change in Z value between adjacent points becomes quite small which makes the gradient images less sharp and watershed thresholding fails in this case. The pore construction should overcome this problem as it is independent of the gradient. Hence, the pore construction technique was used to evaluate the FE-SEM images of fiber 1. Figure 3-20a shows a magnification of one of the pores from fiber 1 at 300 KX. This figure confirms the above and clearly shows that the side slopes of the pore in this FE-SEM image are similar to those seen in the AFM image of a pore of the same fiber (Figure 3-20b).

Results from the FE-SEM image for fiber 1 at 300KX using the pore construction method for image analysis were compared with the AFM image analysis results also taken from fiber 1 (Figure 3-21). Results for FE-SEM at this high magnification showed lower pore densities as many of the smaller pores are not clearly visible in the image and hence, they were not detected. Measurements for FE-SEM were done at both the bottom and mid height of the pore. Pore bottom was used in FE-SEM analysis which was not done for AFM since pore bottom data for AFM would be affected by tip convolution as explained previously. Pore mid height for the FE-SEM image analysis would be an average value within the detected pore between maximum and minimum value measured at pore top and pore bottom respectively. These two FE-SEM distributions at different pore heights were compared to the pore size distribution of the AFM at pore mid height for fiber 1 as shown in Figure 3-21. The AFM and FE-SEM pore distribution data obtained at mid-height were not very similar. Instead the AFM pore distribution data at mid height was closer to the FE-SEM distribution measured at pore bottom. These two distributions had similar maxima, but AFM had a higher number of large pores and a higher pore density than FE-SEM at pore bottom. For the large pore sizes, the AFM was more similar to the FE-SEM at pore mid height. A possible explanation for these differences is that the height i.e. Z-value at which pore bottom and pore mid height is defined in the AFM and the FE-SEM image differs. In other words, the AFM measurement at mid-height was probably performed at a Z-level which was located between the FE-SEM Z-level at pore bottom and mid height. The underlying reason is that FE-SEM images do not make a physical measurement for the Z position, as only the color scale in the FE-SEM image is an indication of the Z position. This is unlike AFM,

which can accurately measure Z-position because the cantilever physically monitors the surface height of the membrane. A second explanation why AFM and FE-SEM profiles were different is because only 300 pores were measured with FE-SEM compared to 1290 pores for AFM, and therefore the FE-SEM data may not be representative. FE-SEM images at high magnification were able to identify the exact shape of pore unlike the low magnification FE-SEM images but their major problem is that images at these high magnifications are hard to analyze using common images analysis techniques.

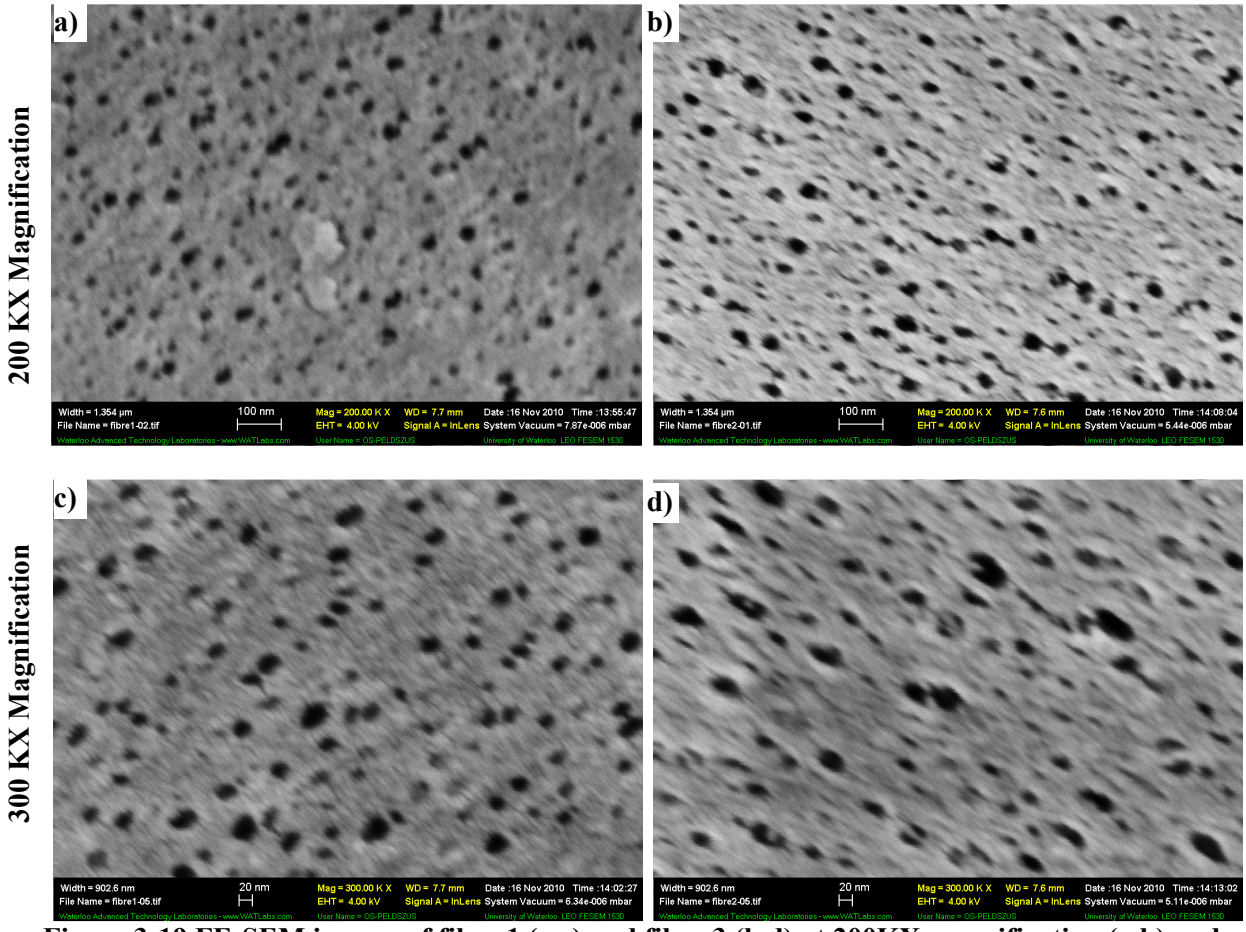

Figure 3-19 FE-SEM images of fiber 1 (a,c) and fiber 3 (b,d) at 200KX magnification (a,b) and 300 KX magnification (c,d)

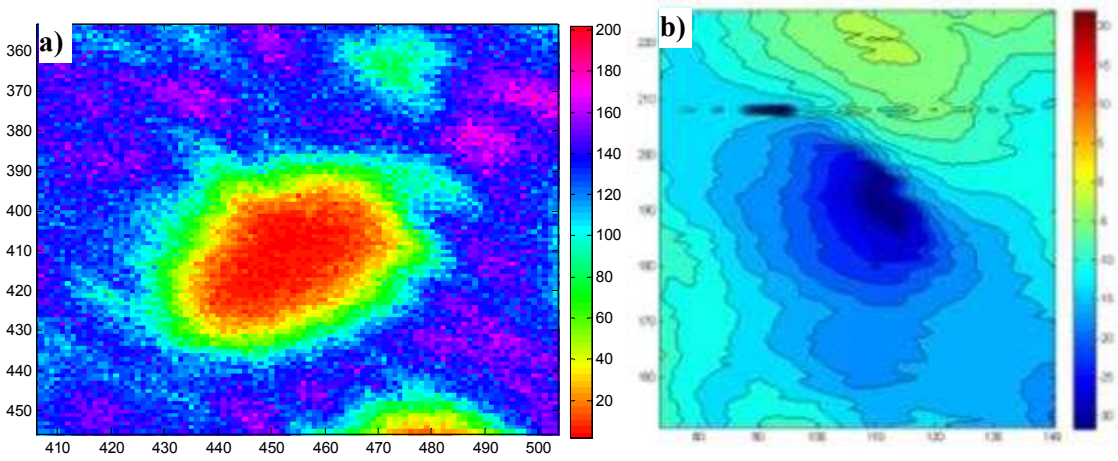

Figure 3-20 Magnification of one of the FE-SEM (300 kX) detected pores showing side slope of pore (a), and AFM detected pore image (b) both from fiber 1

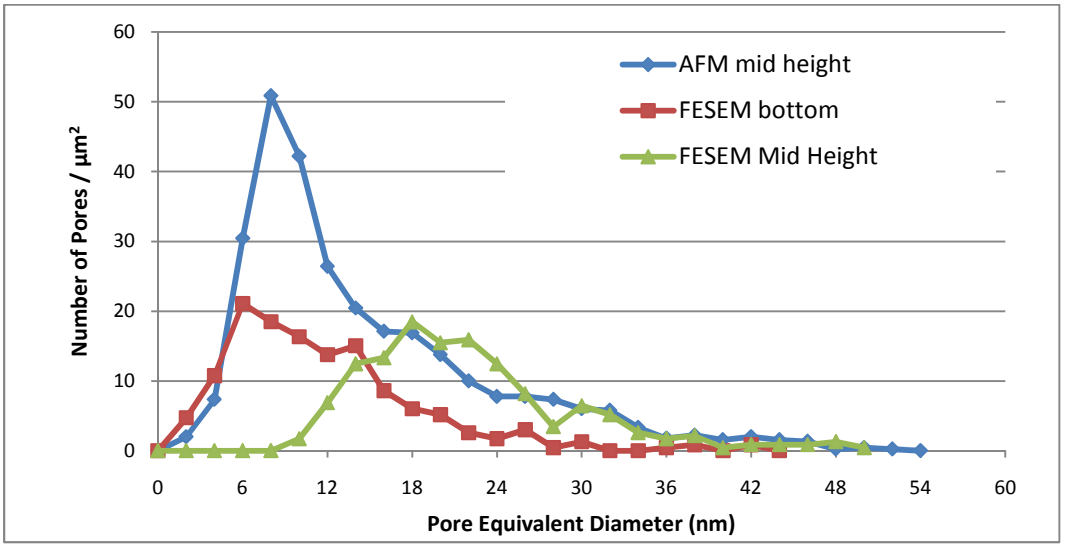

Figure 3-21 FE-SEM results at 300 KX magnification and AFM results at pore mid height; both fiber 1; both images analyzed using the pore construction method.

3.4.4 Surface porosity and pore density

The porosity and pore density of the UF membrane samples using different techniques are shown in Table 3-5. Porosity of each image will equal the ratio of the sum of the cross sectional area of the pores in the image over the image area. Depending on data availability this can be done at different pore heights as AFM analysis for example was done at pore mid height and pore top. For pore density it was measured for each image as the ratio of the number of detected pores in the image over the

total image area. The image analysis techniques provided counts of detected pores, but for FE-SEM images at high magnification, the pores were counted manually as the image analysis techniques employed were not able to detect all pores in the image. For AFM measurements, image 1 of fiber 2 was of lower quality (i.e. tilted image, surface contamination) which led to a reduced number of detected pores as explained in section 3.4.2.Hence, results for image 1 of fiber 2 were not used for the data presented in Table 3-5. As indicated by the lower standard deviation, variability in the porosity data obtained by AFM measurements using the pore construction technique is much lower than those obtained by FE-SEM measurements at 100KX magnification using watershed thresholding. This confirms the earlier observed reproducibility of the AFM results when using the new pore construction method for data analysis. AFM results for porosity are very consistent at each height in that they were very close for all 3 fibers. However, fiber 1 and fiber 3 differed in pore density, whereas their porosities did not differ statistically. Although more pores were detected on fiber 1, similar porosities are likely due to the smaller pores sizes found on fiber 1 compared to fiber 2 and 3 as shown earlier by the shift of the maxima of the pore size distributions of fiber 1 towards the smaller pores (Figure 3-15 and Figure 3-16).

For fiber 2, AFM results showed that one of the two images had a porosity of 0.069 and pore density of 234 pores /μm^2 as listed in Table 3-5. These values are very similar to fiber 1. As mentioned above, the second image for fiber 2 though was influenced by image artifacts and surface contamination and had a porosity of 0.041 and pore density of 142 pores /μm^2.

Overall, for the UF membrane tested, the obtained porosity was consistent for different AFM images taken on each fiber, and between different fibers taken from the same module. This further proves the reproducibility of the pore construction technique in detecting pores and the importance of using the different filters to trim the pores. The consistent porosity results can also explain the consistent clean water permeability of the UF membrane, as porosity is the major factor for determining membrane permeability (Mehta and Zydney 2005).

The porosity obtained from the FE-SEM (100KX magnification) watershed segmentation analysis for fiber 4 is similar to the AFM porosity at pore mid height for fibers 1to 3. A slight drop in pore density for FE-SEM watershed thresholding results (fiber 4) compared to AFM results for fiber 2 and 3 may have resulted from either the limitation inherent to the watershed thresholding method or sample preparation (the gold coating partially obstructing pores). This again confirms that results obtained at

100 KX magnification and analyzed by the watershed thresholding method provide comparable results to AFM with the pore construction technique.

As discussed in the latter part of Section 3.4.3 evaluation of FE-SEM measurement at high magnification (300 KV) encountered some limitations and hence, porosity and density data obtained at this magnification have to be interpreted with caution. Image analysis was performed manually by counting pores since both watershed thresholding and the pore construction method failed to provide reliable data. The porosity for FE-SEM images at 300KV at pore bottom (fiber 1) was much lower than the AFM porosity measured at pore mid height for fiber 1. However, at mid height the FE-SEM porosity for fiber 1 was similar to that of the AFM at mid height for fiber 1. These differences may be explained by the pore size distribution presented in Figure 3-18. The FE-SEM distribution at pore bottom for the larger pores, which have a big impact on porosity, was quite different from the AFM distribution at mid-height. However, for the larger pores, porosity at pore mid height FE-SEM (300KX, fiber 1) was similar to porosity for AFM at mid height (fiber 1).

Pore density for fiber 3 at 300KX magnification FE-SEM images was quite closer to the AFM pore density for fiber 3. This is different than the obtained results for fiber 1 where the pore density obtained with FE-SEM at 300KX was substantially smaller than for AFM results for fiber 1. This may be explained by the observation that fiber 1 has a larger proportion of smaller pores unlike fiber 3 (Figure 3-15 and Figure 3-16) and these smaller pores may be more susceptible to be buried below the gold coating thus leading to a lower number of detected pores.

Table 3-5 Membrane surface porosity and pore density for the different techniques used

Sample		n	Porosity		Pore Density Pore/μm^2		Comments
			μ	σ	μ	σ	
AFM Pore Mid height	Fiber1	2	0.076	0.00047	288.4	6.6	Total scanned area of 2×1.5^2 μm^2 for each fiber, evaluated images with pore construction method
	Fiber2[a]	1	0.0689	NA	234.1	NA	
	Fiber3	2	0.072	0.00525	185.2	4.7	
AFM Pore Top	Fiber1	2	0.148	0.00134	*	*	
	Fiber2 [a]	1	0.142	NA	*	*	
	Fiber3	2	0.142	0.00919	*	*	
SEM 100KX	Fiber4	3	0.060	0.01496	161.8	18.3	Watershed segmentation with a scanned area of 5 μm^2 for each image
SEM 300KX Pore bottom	Fiber1	4	0.022	0.00266	176.3	14.3	Pores are counted manually [b] for pore density with a total surface area of 2.87 μm^2
SEM 300KX mid height	Fiber1	4	0.063	0.00784	*	*	
SEM 300KX mid height	Fiber3	6	NA	NA	168.6	32.5	Pores are counted manually [b] for pore density with a total surface area of 5.33 μm^2

n Number of images analyzed

μ Average

σ Standard deviation

[a] fiber 2 had one image that had lower number of pores due to image artifact and surface contamination and was therefore not included in the calculations

[b] Manual counting of pores was done by user to overcome the inability of the available techniques to detect all the pores in the high magnification FE-SEM images

* Pore density is the same as the pore density measured at pore mid height for the same fiber

NA Not applicable

3.4.5 AFM analysis of MF membranes

The pore construction method was applied to AFM images of other types of membranes to test its applicability. A tight MF membrane was used for this purpose. Three different AFM images were characterized using the pore construction method. The filters used for image analysis had to be changed due to the different nature of the membrane such as pore size and morphology. The following filters were used. Filters for minimum and maximum pore size were 10 nm and 250 nm respectively. The chosen height step was 3 nm as the difference in Z values across the image was higher than the difference for UF membranes where a 1 nm step was used. A minimum pore depth of 10 nm was chosen because the pores are larger than the tip so the tip would be able to penetrate the pore deeper than for the UF membrane. The chosen area gradient was 600% over each 1 nm depth. The obtained pore size distribution for the pore equivalent diameter measured at pore mid height of 146 detected pores is shown in Figure 3-22. The maxima of the pore size distribution is at around 55 nm which corresponds to the manufacturer pore size rating for this membrane of 50 nm.

These results demonstrate the wide applicability of the newly developed pore construction method. This data analysis method can be applied to a wide range of membranes including UF and MF membranes even though they have different morphological and pore size properties.

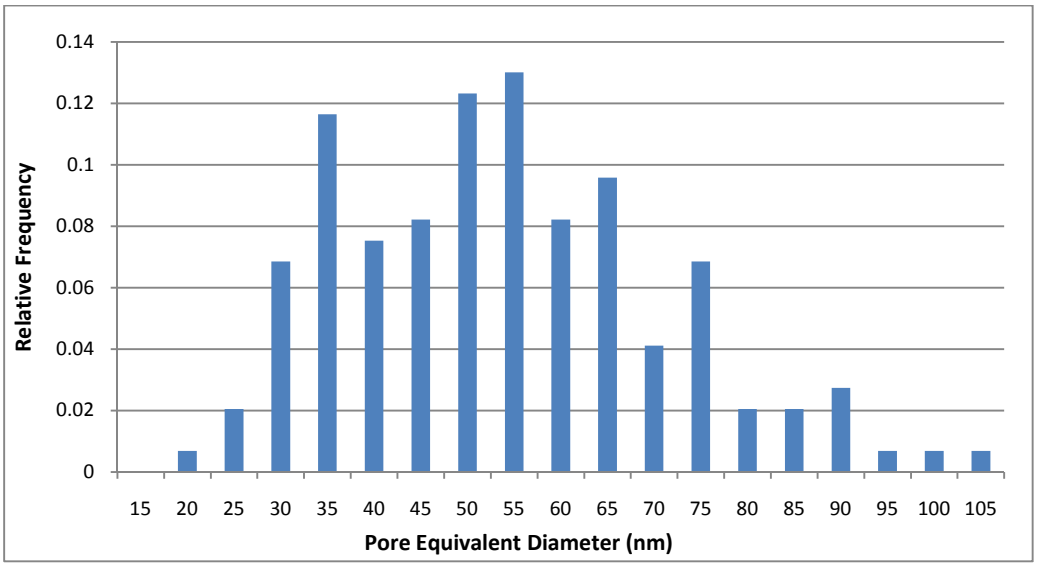

Figure 3-22 Pore size distribution for the MF membrane

3.5 Conclusions

This work aimed at determining reliable pore size distributions of UF membranes in order to gain a more in depth understanding of membrane rejection characteristics. To achieve this goal, different imaging techniques and different image analysis methods were tested to identify the best methodology. A commercial UF membrane, which had an asymmetric structure with a thin skin layer over a thick more porous supporting structure, was used in this study. Different membrane fibers were characterized using AFM and FE-SEM and their images were analyzed using manual cross sections, grayscale thresholding and watershed thresholding. In addition, it was found necessary to develop a novel image analysis technique, the pore construction technique.

The main findings can be summarized as follows:

- The newly developed pore construction technique proved to be a reproducible and informative analytical technique for AFM images which is able to analyze the entire AFM image with minimum input from the user. It was far superior to the manual cross section method which is most commonly employed in AFM image analysis. Other image analysis techniques such as grayscale and watershed thresholding did not achieve satisfactory results for AFM images. AFM combined with the pore construction technique had the ability to study the 3D structure of the pores in detail and provide data on pore dimensions and pore size distributions at different pore heights. Based on these data membrane porosity and pore density can be reliably determined. The pore construction technique can also be applied to membranes far different from the UF membrane used in this study as was proven by the successful analysis of an MF membrane image. In addition, AFM images of varying qualities could be analyzed successfully.
- FE-SEM images were obtained at different levels of magnification. For sharper images obtained at lower magnification (e.g. $\leq$ 100 KX), grayscale and watershed thresholding were applicable. Both are image analysis techniques commonly used for FE-SEM images. However, watershed thresholding was superior since it could better detect the boundaries of the pores and eliminate some image artifacts. For FE-SEM images at larger magnification (e.g. $>$ 200 KX), grayscale and watershed thresholding did not provide meaningful results. The pores did not have sharp boundaries which is a prerequisite for watershed thresholding analysis. The images also had a lot of noise that made grayscale thresholding not applicable as well. The newly developed pore construction was applied to these images and could detect pores but experienced some limitations.

- When comparing results obtained using AFM images with the pore construction technique and FE-SEM (100 KX) with watershed thresholding, it was found that their results are similar thus confirming the validity of the new pore construction technique. However, overall pore size distribution measured at pore mid height were essentially lower than results of traditional FE-SEM (i.e. evaluated with gray-scale thresholding) unlike what is reported in the literature when comparing traditional FE-SEM with AFM results obtained using the conventional manual cross section method. AFM analysis resulted in higher pore densities than FE-SEM which can be attributed to FE-SEM sample preparation (i.e. gold coating). For the larger pores, both FE-SEM and AFM could get very similar results as these pores are large enough to be detected accurately using different techniques.
- AFM imaging combined with the pore construction analysis of different fibers gave insight into fiber to fiber variability. For three different fibers, the fibers had similar occurrence of the larger pores whereas there were some differences for the smaller pores. This difference in distribution of pore sizes caused a difference in pore density between different fibers. However, the porosity was similar which was consistent with the permeability of the different fibers. The similarity for the larger pores implies a consistent rejection of larger molecules using different fibers.

Overall, AFM along with the new pore construction data analysis technique provided a powerful tool to detect membrane pore size distribution without extensive sample preparation, sophisticated data filters to improve image quality or advanced image analysis methods. With the recent advances in the field of atomic force microscopy the pore construction method can be further developed to be a standard way for detecting membrane pore structure more reliably.

Chapter 4
Removal of Enteric Virus Surrogates by Clean Ultrafiltration Membranes

4.1 Introduction

Drinking water pathogens of concern to human health include different microorganism groups such as bacteria, protozoa and enteric viruses. Different sources of contamination can introduce waterborne pathogens into the water body such as storm water runoff, wastewater treatment plant effluents or even untreated sewage (Health Canada 2004). Although enteric viruses are unable to replicate outside the cells of its host, they can remain viable in the environment under common conditions (Fong and Lipp 2005). This makes the removal of enteric viruses by drinking water treatment processes a necessity. Viruses have a simple structure of nucleic acid (either DNA or RNA) surrounded by a protein capsid, with an additional protein envelope for some viruses. Based on the virus strain, the protein capsid usually has some chemical groups that can possess a charge at different pH values, to give the virus a surface charge that is usually negative at neutral pH (Schijven and Hassanizadeh 2000). Enteric viruses are small compared with bacteria and protozoa, and have a size range from 20 to 160 nm (Health Canada 2004).

Health Canada requires a 4 log removal of enteric viruses for municipal drinking water treatment (Health Canada 2004, 2010). UF membranes are an increasingly used drinking water treatment technology worldwide. Since late 1980s, UF membrane installation in drinking water treatment plants have seen a considerable increase (USEPA 2001a). A total of 37 low pressure membrane filtration drinking water treatment plants are found in the province of Ontario in Canada, including the Raymond A. Barker Water Filtration Plant in Collingwood and the Lakeview water treatment plant in Peel (Sahely 2005). Polymeric UF membranes have a pore size of 1 to 100 nm, which is similar to the size of enteric viruses, so they are capable of removing viruses from water (Jacangelo *et al.* 2006). Current drinking water treatment regulations in Canada give no credit for UF membranes in removing enteric viruses, and require free chlorine disinfection following UF membranes to achieve the 4-log virus removal requirement (Health Canada 2004). In February 2010, a new proposed Guideline for Canadian Drinking Water Quality was made available by Health Canada for public comment and suggested granting UF membranes a removal credit based on challenge testing and continuous membrane integrity monitoring to verify unit performance (Health Canada 2010).

Bacterial viruses, also called bacteriophage, are often used as surrogates for enteric viruses in drinking water treatment challenge tests. Bacteriophage have a similar size and structure to the smaller enteric viruses. In addition, bacteriophage are easy and inexpensive to enumerate and detect with no considerable health effect. Most of the virus removal tests for either granular media filtration or membrane filtration are done using different strains of bacteriophage (Jacangelo *et al.* 1995, Jacangelo *et al.* 2006, Schijven and Hassanizadeh 2000). Different strains of bacteriophage have been used as enteric virus surrogates in membrane filtration virus challenge experiments, including MS2 (Jacangelo *et al.* 1995, Jacangelo *et al.* 2006, Langlet *et al.* 2009, Madaeni *et al.* 1995), Qβ (Langlet *et al.* 2008, Otaki *et al.* 1998, Urase *et al.* 1996) and φX174 (Arkhangelsky and Gitis 2008, Hirasaki *et al.* 2002). It can be seen that MS2 is commonly used in membrane filtration research.

4.1.1 Removal mechanisms of viruses by UF membranes

The comparable size of enteric viruses and the UF membrane pore size show that UF membranes have a potential for the removal of enteric viruses. Each part of the membrane pore size distribution or range will exhibit different removal mechanisms. For pores smaller than or equal to the size of the virus, size exclusion (e.g. physical straining) will be the removal mechanism (Jacangelo *et al.* 1995). For pores larger than the virus size, hydrophobic or electrostatic adsorption of the viruses to the membrane material can contribute to the membrane rejection (Fiksdal and Leiknes 2006). Hydrophobic properties depend on the amino acid groups in the viral protein capsid (Schijven and Hassanizadeh 2000). Membrane surface charge can play different roles in the rejection of viruses by membranes. Most of the polymeric membranes are negatively charged due to the surface chemical groups at the membrane surface (Zeman and Zydney 1996) such as carboxyl groups. Viruses with neutral or opposite surface charge will exhibit better adsorption to the membrane surface or membrane material (Schijven and Hassanizadeh 2000), whereas viruses of similar surface charge can be rejected due to electrostatic repulsion during transport across the membrane pores (Fiksdal and Leiknes 2006) in similar manner to what is seen for charged proteins (Mehta and Zydney 2006). The final removal will be the sum of all these different components.

4.1.2 Characteristics of Virus Surrogates

Two bacteriophage commonly used in filter performance studies are MS2 and φX174, and these were the surrogates selected to be used in this study. MS2 is the most commonly used surrogate for enteric viruses in UF membrane testing. MS2 is a single stranded RNA virus from the *Levivridae* virus

group. The particle has a molecular weight of 3.6×10^6 Dalton (Da). MS2 is a non-enveloped virus with a 2 nm thick icosahedral protein capsid consisting of 60 equal triangular units (Valegard *et al.* 1990). The capsid has a triangulation number of 3, giving more complexity to the protein structure of the capsid as each triangular unit will consist of three different polypeptide chains (Figure 4-1; Carrillo-Tripp *et al.* 2009). The outer capsid diameter is 27.4 nm, measured using X-ray diffraction data (Kuzmanovic *et al.* 2003, Valegard *et al.* 1990), which is larger than reported values of 24-26 nm (ICTVdB Management 2006b). As shown in Table 3-1, the size of MS2 bacteriophage is usually slightly different among different studies and by changing the method used. The isolectric point of MS2 is 3.5 (Penrod *et al.* 1996), so it will be negatively charged at neutral pH and in most surface waters. Also, MS2 is known to exhibit more hydrophobic properties than other bacteriophage including φX174 or Qβ (Schijven and Hassanizadeh 2000).

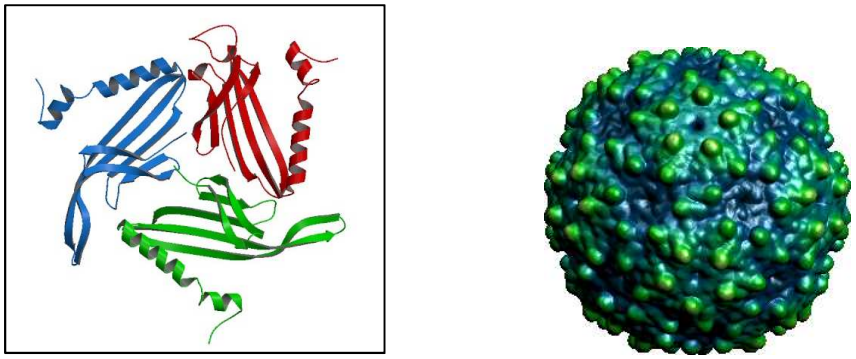

Figure 4-1 Triangular sub-unit of the T=3 protein capsid of MS2 bacteriophage (left) and overall 3D geometry of the virus (right) (Carrillo-Tripp *et al.* 2009)

Table 4-1 Size of MS2 bacteriophage reported in the literature

Size (nm)	Method	Reference
30	TEM	(Arkhangelsky and Gitis 2008)
25.42±0.93	TEM	(Gutierrez *et al.* 2009)
30.83±0.31	Hydrodynamic diameter	(Gutierrez *et al.* 2009)
31	Hydrodynamic diameter	(Pham *et al.* 2009)
30	TEM	(Pierre *et al.* 2010)
26	Hydrodynamic diameter	(Pierre *et al.* 2010)
23±1	Hydrodynamic diameter	(Langlet *et al.* 2008)

φX174 is a single stranded DNA virus from the *Microviridae* virus group. The particle has a molecular weight of $6.2X10^6$ Dalton (Da). φX174 is also a non-enveloped virus with a 3 nm thick icosahedral protein capsid consisting of 20 equal triangular units. The capsid has a triangulation number of 1, so it consists mainly of one type of protein, making it simpler than the MS2 capsid. The capsid has a maximum outer diameter of 27.6 nm at the 3 fold axes and a minimum of 22.2 nm at the 2 fold axes. φX174 has 12 protein spikes extruding from the 5 fold axes of the capsid for an additional 3.2 nm, to give the particle a total outer diameter of 33 nm (McKenna *et al.* 1992). A size of 25 – 27 nm for φX174 is also reported (ICTVdB Management 2006a). φX174 has been found to be less hydrophobic than MS2, with an isoelectric point of 6.6 to 6.8 (Schijven and Hassanizadeh 2000). This will make it neutral at neutral pH and slightly negative at the pH of most surface waters.

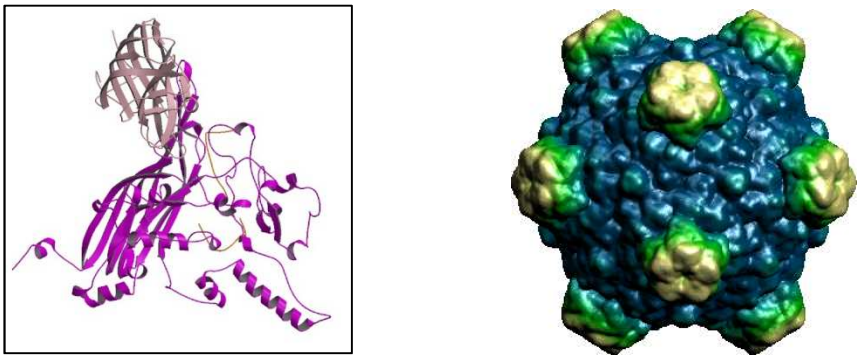

Figure 4-2 Triangular sub unit of the T=1 protein capsid of φX174 bacteriophage (left) and overall 3D geometry of the virus (right) (Carrillo-Tripp *et al.* 2009)

According to this, we can see that both MS2 and φX174 have different characteristics that can be compared and used to explain removal mechanisms of viruses by UF membranes. Both MS2 and φX174 have a similar size range close to the smaller enteric viruses. φX174 is slightly larger than MS2; this will enhance the removal by size exclusion. Also, φX174 has a more complicated shape with the additional spikes on the capsid. The shape of φX174 will affect the charge distribution on the surface. The outer spikes will further separate the charged capsid from the charged membrane surface to reduce the probability of electrostatic repulsion between φX174 and the pore side walls. MS2 is more negatively charged than φX174 due to its low isoelectric point; this improves the removal of MS2 by electrostatic repulsion. MS2 is also believed to be more hydrophobic than φX174 from soil adsorption studies (Schijven and Hassanizadeh 2000). This may also enhance the hydrophobic adsorption of MS2 over φX174, although this mechanism is not completely understood because of the differences between soil media and membranes. The last mechanism to consider is

electrostatic adsorption between the virus and the membrane surface. MS2 negative surface charge will probably prevent electrostatic adsorption, unlike φX174 which would be able to adsorb to the negatively charged surface of the membrane as the phage will be less charged or even neutral. Both hydrophobic and electrostatic adsorption mechanisms will depend on the available adsorption sites on the membrane surface, so it should have a declining rate over time as the available adsorption sites will be exhausted. The extent of each of these mechanisms for both MS2 and φX174 bacteriophage can be expressed qualitatively as presented in Figure 4-3, which was developed in this thesis and based on known properties of the phage. By comparing the removal of both types of viruses we can provide a reasonable explanation for the removal of viruses by the UF membrane used. Finally, size exclusion seems to be the main removal mechanism for both viruses, however other mechanisms will be contributing to the removal as well in varying extents (Jacangelo *et al.* 1995, Urase *et al.* 1996).

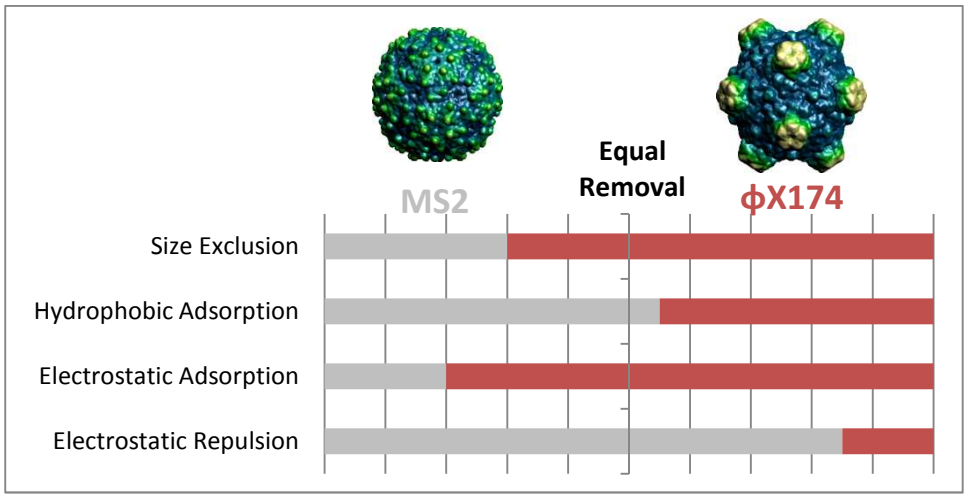

Figure 4-3 Schematic for the different removal mechanism of both φX174 and MS2

4.1.3 Membrane Surface Characteristics

Along with the membrane pore size distribution presented in Chapter 3, other membrane surface characteristics will influence the removal of enteric viruses. One of these characteristics is the contact angle of the surface which is a measure of the surface hydrophobicity. Surfaces with a contact angle close to zero degree are known to be hydrophilic (i.e. water loving) and surfaces with contact angle close to or larger than 90 are known to be hydrophobic. The majority of the polymeric membrane surfaces are hydrophobic due to aliphatic or aromatic chemical group composition, but surface modification or additives to the base polymer (the addition of hydroxyl, ether, or carboxyl

groups) is usually done to make them more hydrophilic. Hydrophobicity is linked to higher fouling rates of membranes due to the higher ability of organic molecules and proteins to adsorb to the membrane surface (Zeman and Zydney 1996). This can also be the case for enteric viruses as they have adsorption sites on their protein capsid so they will be adsorbed and removed by the membrane.

Another important characteristic is the surface charge of the membrane will which will largely affect the transport of charged molecules towards the membrane surface and within the pores of the membrane (Deen 1987, Mehta and Zydney 2006). UF polymeric membranes are usually negatively charged at neutral pH due to the ionization of surface functional groups or adsorption of specific ions. Surface charge is usually calculated by measuring the streaming potential of the surface (Crittenden and Montgomery Watson 2005, Zeman and Zydney 1996). This is done using an electrolyte solution such as potassium chloride that flows along the fixed membrane sample, moves the charges close to the membrane and generates an electric streaming potential that can be used to interpret the surface charge of the membrane (Saksena and Zydney 1995).

4.1.4 Effect of membrane operational parameters

Operational parameters of the membrane units include permeate flux, transmembrane pressure (TMP) and virus feed concentration. If any of these parameters have an effect on the removal of viruses, it needs to be taken into account while performing the virus challenge experiments to be able to compare the results of different experiments. Membrane operation under no fouling conditions is believed not to have an effect on the removal of viruses by the membranes. Studies have shown that membrane TMP did not have any effect on the removal of different types of viruses both in bench and pilot scale testing (Jacangelo *et al.* 1995, Jacangelo *et al.* 2006, Urase *et al.* 1996). However, some references reported that increasing TMP caused a decrease in the removal of viruses due to pore enlargement (Arkhangelsky and Gitis 2008). Madaeni *et al.* (1995) found that the effect of increasing the TMP was similar to the absence of cross flow conditions, as it will favor concentration polarization of viruses at the membrane surface. Virus influent concentrations are typically measured in the bulk solution, but a higher concentration of viruses at the membrane surface will raise the permeate concentration and result in a lower apparent removal.

In addition to membrane TMP, the concentration of the viral feed solution is also an important factor in membrane challenge experiments. In most challenge experiments, higher concentrations of viruses than are usually found in water are employed. The effect of virus feed concentration was investigated in a study by Jacangelo *et al.* (1995). Using a PVDF UF membrane with a 35 nm nominal pore size,

the removal of MS2 decreased by nearly 1 log as the virus loading went above 1.6×10^7 pfu/cm^2 (Jacangelo et al. 2006). Similar observations were also reported in another study (Jacangelo *et al.* 1995). These studies show that it is essential to use the same range of virus feed concentrations when conducting membrane challenge tests, in order to obtain comparable virus removal results. However it is also important to note that the virus concentrations that are typically used in challenge tests are much higher than what would be experienced in surface waters.

4.1.5 Objectives

There are two main objectives for the work presented in this chapter. The first objective is to compare two different bacteriophages of similar size to study the effect of bacteriophage characteristics such as surface charge and hydrophobicity on removal by UF membranes at different operational pHs. These results can be studied in relation to the membrane surface characteristics described in Chapter 3. The other objective is to build a base removal value for each type of phage with clean water conditions and clean membranes. This will aid in the second phase of the project, to investigate the impact of different types of membrane fouling on virus removal.

4.2 Materials and Methods

4.2.1 Preparation of Host Cultures

Escherichia coli Hfr C-3000 (American Type Culture Collection [ATCC] 15597) was used as the host culture for MS2. *E. coli* C (ATCC 13706) was used as a host culture for φX174. Host cultures were stored at -80ºC in 20% (v/v) glycerol. A small amount of the host bacterium was streaked on a nutrient agar (BD) plate and then incubated for 24 h at 37ºC. *E. coli* was transferred to nutrient agar plates at least twice before using it in any of the following steps. The *E. coli* cultures were stored on nutrient agar plates at 4ºC for a maximum period of 14 d.

4.2.2 Preparation of High Titer Bacteriophage Solution

4.2.2.1 MS2

The growth of MS2 bacteriophage was based on the International Organization for Standardization (ISO) method 10705-1 (International Organization for Standardization 1995). The day prior to phage inoculation, a 125 mL Erlenmeyer flask containing a 50 mL of sterile Tryptone Yeast Glucose Broth (TYGB; Appendix C) was inoculated with *E. coli* ATCC 15597 from the nutrient agar plate. The

TYGB was incubated for 24 h at 37ºC without shaking. The overnight *E. coli* broth culture was used to inoculate two 1000 mL flasks each containing 500 mL of sterile TYGB, by adding 5 ml of inoculum (1% by volume) to each flask. The inoculated TYGB was incubated at 37ºC with shaking at 150 rpm. The absorbance of the broth was monitored using a spectrophotometer (UV-Vis model 8453, Hewlett-Packard, Palo Alto, CA) at a wavelength of 600 nm until it reached an absorbance of 0.3, which is equivalent to an *E. coli* concentration of 3×10^8 cells mL^{-1}. MS2 phage stock was then added to each flask. MS2 stock culture (ATCC 15597-B1) was previously prepared in our laboratory at the University of Waterloo and stored at -80ºC. The MS2 stock had a concentration of approximately 10^{11} plaque forming units $pfu.mL^{-1}$. One mL of MS2 stock was added to each flask containing 500 mL of *E. coli* culture, to get a ratio of one *E. coli* cell to each MS2 phage virion. The broth was then incubated for 24 h at 37ºC and 150 rpm.

Following incubation, the *E. coli* cells and cell debris were removed from the final solution by centrifugation at 10,000 ×g for 20 min The supernatant was then decanted in a sterile bottle and then passed through a 0.45 µm filter (PALL Supor®-450 PES) by vacuum filtration. MS2 concentration of the final solution was enumerated as described in section 4.2.3 below, and resulted in a concentration of 3×10^9 $pfu.mL^{-1}$. The high titer phage solution was stored at 4°C for use in the UF bench scale experiments.

4.2.2.2 φX174

φX174 was prepared using a method similar to MS2 (based on ISO method 10705-1), except that super broth was used to increased the *E. coli* growth yield and result in a high bacteriophage concentration. A 125 mL Erlenmeyer flask containing 50 mL TYGB was inoculated with *E. coli* ATCC 13706 and incubated for 24 hrs at 37ºC. The overnight culture of *E. coli* was used to inoculate 250 mL Erlenmeyer flasks containing 125 mL of sterile Super Broth (SB; Appendix C). SB inoculated flasks were then incubated at 37ºC with shaking at 150 rpm until the UV absorbance reached 0.3. Then 13 mL of φX174 frozen stock (3×10^9 $pfu.mL^{-1}$) was added to each flask containing SB to achieve the ratio of one *E. coli* cell to each φX174 phage viron. The SB was incubated at 37ºC and 150 rpm for 36 h. The *E. coli* cells and cell debris were removed from the final solution by centrifugation vacuum filtration as described for MS2. Two different batches of φX174 were made. The first batch, which was used in the neutral pH membrane challenge experiment, had a φX174 concentration of 5×10^9 $pfu.mL^{-1}$. The second batch, that was used in the high pH membrane challenge

experiment, had a φX174 concentration of 1×10^{11} pfu.mL^{-1}. The reason for the difference in phage concentration between the two batches was likely due to the longer incubation time.

4.2.3 Single Layer Agar (SLA) Bacteriophage Enumeration Method

For enumeration of both MS2 and φX174, a single layer agar method was used as described in Standard Methods for the Examination of Water and Wastewater (American Public Health Assosciation 1998), and is based on the method described by Isbister *et al.* (1983). These publications showed that the single layer method was equivalent or gave increased plaque detection over the double layer method. Similarly, the US EPA method 1602 (USEPA 2001b) uses a single layer agar method for the enumeration of male-specific and somatic coliphage. This method uses TYG broth (TYGB) and TYG agar (TYGA) as recommended in the ISO 10705-1 standard "Detection and enumeration of bacteriophages – enumeration of F-specific RNA bacteriophages" (International Organization for Standardization 1995).

Sterile tryptone yeast agar (TYGA) tubes and phosphate buffered water (PBW) dilution blanks were prepared as described in Appendix C and stored at 4ºC. Prior to analysis, the TYGA tubes were boiled to melt the agar, then cooled and held at 52ºC using a water bath. The day prior to analysis, the appropriate *E. coli* host culture was inoculated into 125 mL flasks containing 50 mL of TYGB, and incubated at 37°C for 24 h. For each phage sample to be enumerated, a series of 10-fold serial dilutions was prepared in PBW to reach the required concentration that will results in the countable region for the method. To conduct the phage enumeration, 1 mL of required sample dilution and 1 mL of the *E. coli* host culture were added to a melted and cooled TYGA tube. The tube was mixed by inversion then poured in a 15 cm diameter sterile Petri plate. For each sample, at least two different dilutions were processed to get a reliable count. The Petri plates were left to solidify and then incubated in an inverted position at 37°C for 24 h. After incubation, the plaques (clear zones) on each plate were counted. The countable range of MS2 and φX174 were 5 to 300 and 5 to 100 plaques per plate, respectively. The samples collected on a certain day were identified as a sample set and analyzed the next day. For each sample set, two quality control standards were analyzed. A negative quality control was done using sterile PBW to check for contamination. A positive quality control was done using a known concentration of phage to ensure that the enumeration was successful.

4.2.4 Purification of High Titer Bacteriophage solution

The high titer bacteriophage solutions prepared in section 4.2.2 had a very high organic content from the nutrients that were used to grow the *E. coli* host culture, and also from the extra polymeric substances produced by the bacteria. This organic material had to be removed from the phage stock solutions before they could be used in the bench scale experiments to limit membrane fouling. To do this, an Amicon 8400 stirred cell unit UF bench unit was used as shown in Figure 4-4. A UF cellulose acetate flat sheet membrane (Diaflo YM30) was used, which had a 30 KDa MWCO. The membrane was expected to reject all the viruses found in the solution and allow the organics less than the MWCO of the membrane to pass through the permeate line to the waste container. The UF unit was sterilized prior to the purification by autoclaving. A new membrane sheet was rinsed in ultrapure water for 2 h and replacing the water every 30 min to remove all the preservation chemicals and wet the membrane. The membrane was then submerged in ultrapure water and autoclaved at 121ºC for 20 min. After aseptically placing the membrane in the stirred cell unit, 250 mL of high titer bacteriophage solution was filtered under cross flow conditions at 18 psi nitrogen pressure. The pressure chosen was at the low operational range of the membrane to improve the purification, as described in the stirred cell unit manual. When the volume inside the unit dropped to 50 mL, the nitrogen cylinder was closed and the pressure inside the unit was relieved. Then sterile PBW was added to the remaining liquid inside the unit to a total volume of 250 mL. The filtration was then resumed as in the first cycle. This was repeated several times until the required purification was achieved. The final filter retentate inside the unit at the end was moved to a sterile glass bottle and this purified solution was used in the spiking experiments. The organics content of the final solution was measured as TOC, and this was done as described in section 4.2.8. The phage concentration of the final solution was measured using the SLA method as described in section 4.2.3.

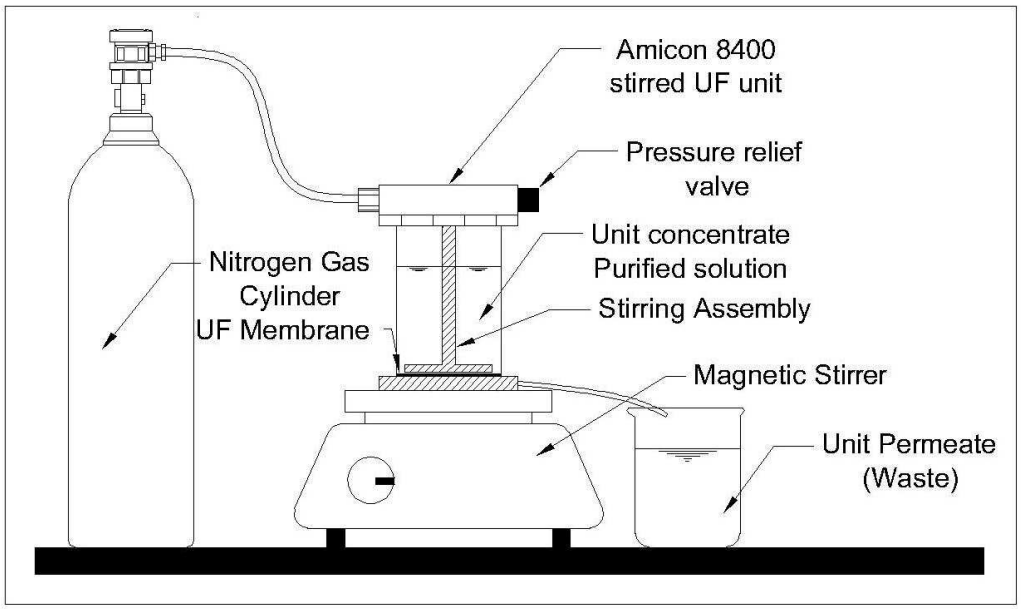

Figure 4-4 UF bench unit used for the purification of both types of high titer bacteriophage solutions

4.2.5 UF Bench Scale Unit

The UF bench scale unit used in this study is a submerged system that operates on an "outside-in" mode of permeation. The feed water continuously flows into the module container while the permeate is obtained using vacuum. At the same time, another waste stream from the container known as the bleed is used to limit the solids concentration in the unit (AWWA 2005). This results in a constant water level in the membrane tank to ensure stable TMP profiles and maximize the recovery ratio. In practice, the above described bleed is minimized or even completely absent. In latter case, the tank of the submerged membrane is drained at the end of the backwashing cycle to minimize solids on the feed side. This configuration is difficult to reproduce in bench scale systems, due to problems caused by backwash regimes, unit control and operation.

In the design phase of the bench unit employed in this study we were able to overcome these problems. A schematic of the unit and its different components is shown in Figure 4-5 and a picture of the unit is shown in Figure 4-6. Using solenoid valves (V1, V2 and V4 in Figure 4-5) and a digitally controlled peristaltic permeate pump drive (E5 in Figure 4-5; Masterflex L/S drive model number 07550-50; Cole-Parmer Canada) full automation of the unit was achieved. All solenoid valves were controlled by a programmable logic controller (Rockwell automation Inc.; model number

Allen Bradley PICO-1760-L 12AWA-NC) to define the time for each step and to completely automate the unit operation. A stainless steel feed tank of 1,300 liters capacity was used to store feed water for the entire experiment. A peristaltic feed pump (Masterflex L/S drive model number 07520-00) was used to fill a 25 L overhead tank that provided a static head of 1.5 meters to feed the UF module container. Using an overhead tank with sufficient hydraulic head allowed the fast refilling of the membrane container to keep the membrane wet and provided also the continuous supply of feed water during filtration to maintain a stable water level in the membrane container. Two different feed lines came out from the overhead tank. The first one was the refilling line that was controlled by a solenoid valve which is able to quickly refill the membrane module container at the start of each filtration cycle due to the head on the line. A flow control valve (V5 in Figure 4-5) was used to feed the unit with a continuous refilling flow to compensate for the permeate flow. This also ensured a high recovery, since the overflow in the module container was minimized during the entire experiment. The membrane container was completely drained and then refilled with fresh feed water at the end of each filtration cycle to prevent any carryover of viruses between cycles during the spiking experiments. At the end of each filtration cycle, the module was sparged with compressed air at 60 psi, and the permeation pump flow direction was reversed to backwash the module and dislodge any fouling layer. The air line was controlled by another solenoid valve. After air sparging and backwashing, the membrane module container was completely drained to the waste tank using a solenoid valve. The module container is then refilled from the overhead tank. The unit was operated in a constant flux mode and the obtained transmembrane pressure was recorded using a pressure transducer and a data logger (Lakewood Systems, model number: CPXA). The permeate flow rate was measured manually. A summary of the different steps during a fully automated filtration cycle are shown in Figure 4-7.

The UF membrane module was housed in a 2.5 liter module container (E-3 in Figure 4-5) that was manufactured at the University of Waterloo. Bench scale hollow fiber UF membrane modules which are commercially available were used in this study. It is a submerged modified PVDF membrane with outside-in configuration. The fibers were supported UF membranes. The operational parameters of the module are shown in Table 4-2 according to information provided by the manufacturer. A detailed study of the membrane surface characteristics and pore size distribution was provided in Chapter 3. The module has a surface area of 470 cm^2. New modules were preserved in glycerin and they were first thoroughly rinsed with deionized (DI) water to remove any apparent glycerin. The clean module was kept in ultrapure water at 4ºC. The day prior to an experiment the module was

chemically cleaned to remove any fouling. First, the module was kept in 200 ppm sodium hypochlorite solution for a minimum of 5 h, and then it was rinsed with DI and moved to a 5 g/L citric acid solution for a minimum of 5 h and then rinsed again thoroughly with DI.

Table 4-2 Operational Parameters of UF bench modules

Parameter	Range
Maximum Transmembrane Pressure	62 kPa (9.0 psig)
Maximum Operating Temperature	40°C (104°F)
Operating pH range	5-9
Cleaning pH Range	2-10.5
Maximum OCl^- Exposure	1000 mg/L

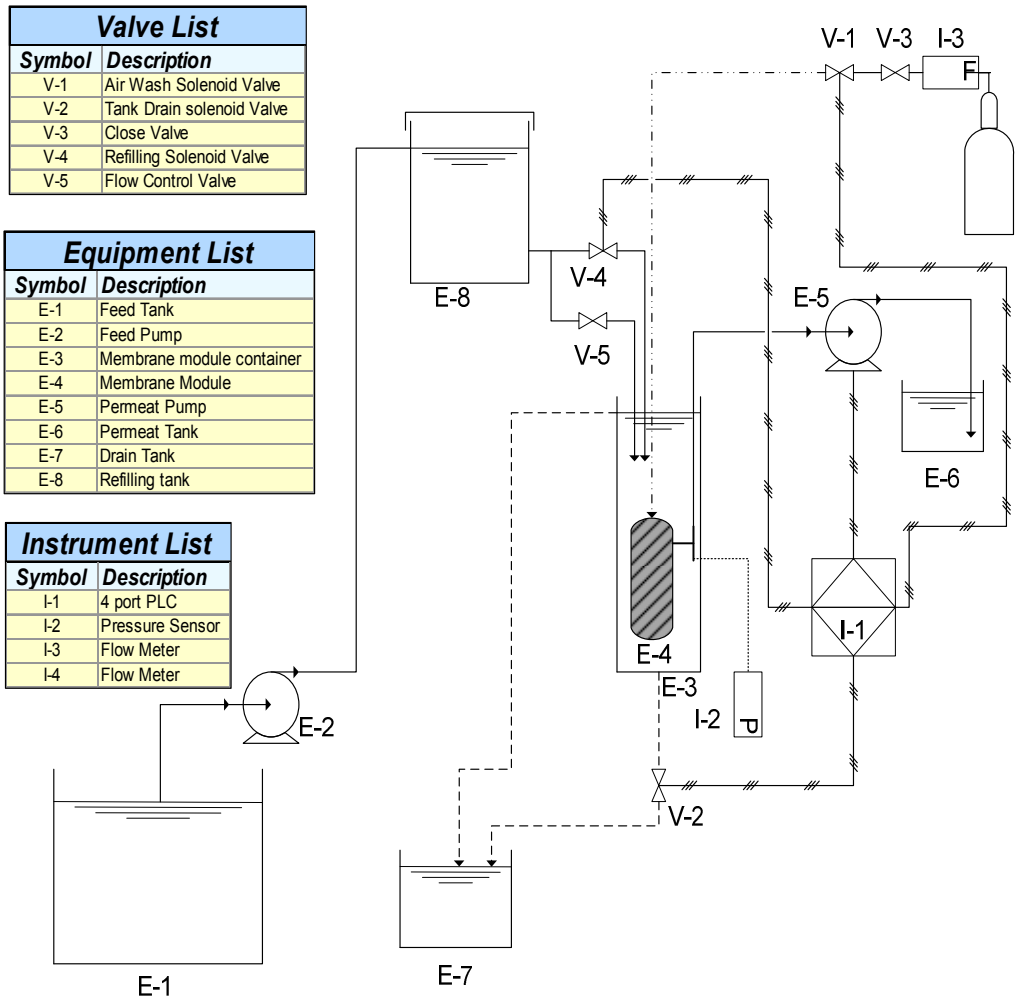

Figure 4-5 Flowchart for the UF bench unit used

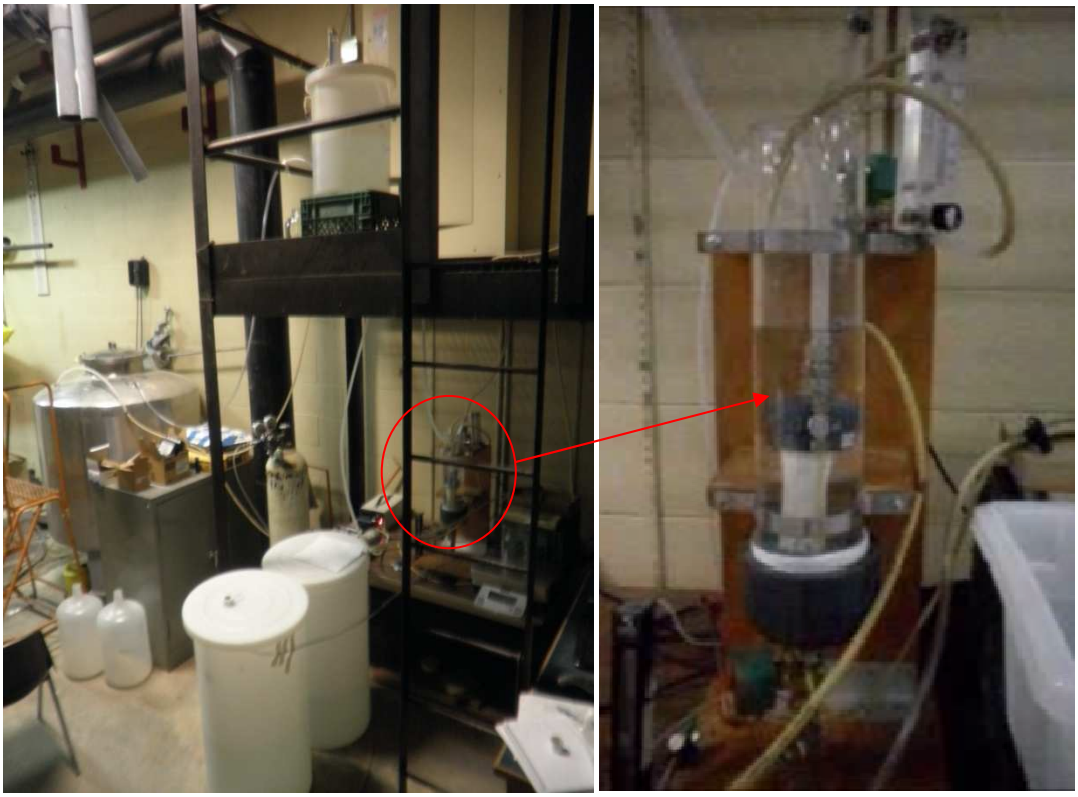

Figure 4-6 Photo of the UF bench unit and the used modules

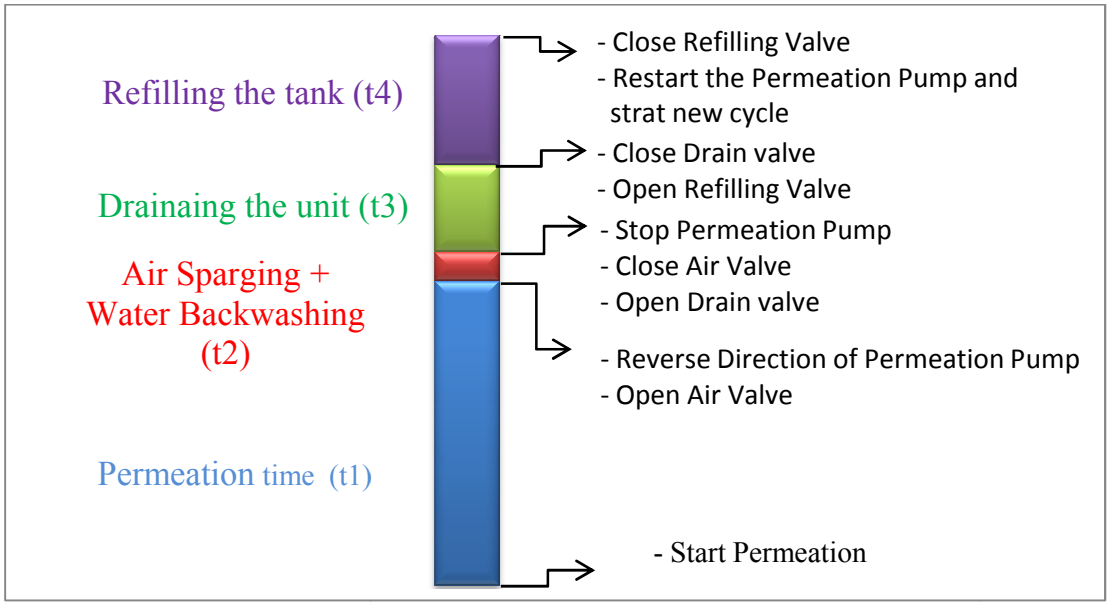

Figure 4-7 Different tasks comprising one fully automated filtration cycle (t_1=30min, t_2=20sec, t_3=40sec and t_4=40sec)

4.2.6 Module Pretesting

Before each experiment, the membrane module was tested to check for integrity problems and to confirm the membrane cleaning efficiency. The pressure decay test was used for integrity testing based on the recommendation of the manufacturer, and is described as follows

- The cleaned module was submerged into a DI water bath.
- The air outlet port was blocked by a stainless steel pipe end cap.
- The permeate port was used to pressurize the inside part of the fiber lumens above 10 psi using air from a gas tank.
- The pressure was maintained above 10 psi for 2 min to remove any air bubbles.
- The gas tank manifold was closed and the pressure drop in the module was monitored using a digital pressure calibrator (Meriam DP2000I Digital Manometer / Pressure Calibrator) over the next 2 min
- A pressure drop above 0.3 psi over 2 min or apparent air bubbles would indicate an integrity problem.

To test the module cleaning efficiency, a clean water permeability test was employed. The UF module was installed in the bench unit. The module container was filled with DI water. The permeate pump was primed to ensure that all lines were full with water and no air bubbles were present. The unit was then operated for 5 min at 4 different fluxes. The transmembrane pressure (TMP) was recorded. The average TMP for each flux over each 5 min interval was temperature corrected to 20ºC according to equation (4-1). The temperature corrected average TMP was plotted against the flow rate and the clean water permeability was defined as the slope of the line.

$$\mathbf{TMPcorrected\ @\ 20^\circ C} = \mathbf{TMP} * \mathbf{1.025\hat{}(T - 20^\circ C)} \quad \text{Equation (4-1)}$$

4.2.7 Phage removal Experiments and Sampling Scheme

Three different bacteriophage challenge experiments were done. The first experiment was done using MS2 bacteriophage in DI water at pH 7.6. The DI water, which had an initial pH of 5.5, was left to equilibrate with air before virus addition, so the pH increased to 7.6 as atmospheric CO_2 dissolved into the water. The second experiment was done using φX174 bacteriophage in DI water at pH 6.8

(again after equilibration with air). A third experiment was done using φX174 in DI water at a higher pH of 9.4. A 33% (w/v) NaOH solution was used to raise the pH of DI water prior to adding the bacteriophage.

The day prior to an experiment, the unit with no membrane module installed was flushed for 30 min with a sodium hypochlorite solution of 100 mg/L free chlorine to disinfect the unit. The unit was then flushed with a 1 g/L $Na_2S_2O_3$ solution for another 30 min to quench the residual chlorine. As a last step, the unit was flushed with DI water for 30 min to remove any remaining chemicals. All tanks were cleaned with the same procedure. The unit was dried until the experiment on the next day. After this the membrane was installed into the cleaned UF bench unit. Module pretesting was done as described in the previous section.

For these clean water virus challenge experiments, only less than 20 liters were required for the whole experiment as each cycle needs approximately 2 liters of water. Therefore, the overhead tank was used as the feed tank instead of the large 1300 liter stainless steel tank. DI water was used to fill the over head tank before the start of the experiment. During each experiment, enough feed water was kept in the overhead tank to run twice the number of cycles required for the experiment. Each experiment was done for a minimum of 3 cycles (a cycle is defined in Figure 3-7). The unit was run first for 4 cycles for MS2 experiment and 3 cycles for both φX174 experiments using the DI feed water without the viruses to condition the membrane. Conditioning the membrane will ensure proper operation of the unit before testing virus removal. After the conditioning cycles, DI water containing either MS2 or φX174 was added to the overhead tank at feed concentrations that ranged from 10^6 to 10^7 pfu.mL^{-1} (resulting in a virus loading of 3.5×10^6 to 3.5×10^7 pfu/cm^2). The virus feed solution was added to the membrane module container from the overhead tank, and then the unit was operated for one cycle, and refilled again with fresh virus feed solution.

The feed solution was sampled at the start of the cycle from the filled membrane module container. Module permeate was then sampled 5 min after the start of the filtration cycle to ensure that the sample was representative of the actual membrane permeate. The t = 5 min permeate sample was used together with the t = 0 min feed sample to determine phage removal at the beginning of a filtration cycle. Due to the dead end operation and rejection of the viruses by the membrane, the concentration of the viruses inside the membrane module container was expected to increase during the filtration cycle. For this reason, a sample was taken from the membrane module container at t = 25 min and this was initially used to measure the feed concentration at the end of the cycle. However, due to the

improper mixing inside the membrane module container, the container drain (described below) was subsequently found to provide a better measure of the feed concentration at the end of the cycle. The permeate at the end of the cycle was sampled at t = 28 min. Following air sparging and backwash, the membrane module container was drained to a separate waste container where it was stirred manually and sampled to represent the average feed concentration at the end of the cycle. The drain concentration was used together with the second (28 min) permeate sample to determine phage removal at the end of a cycle. All samples were collected in sterile 60-mL polypropylene tubes (VWR Cat. Num. 80939-662), and each sample was collected in triplicate. All the samples were immediately placed in coolers on ice, and then stored at 4ºC. All samples were enumerated as described in section 4.2.3. Each triplicate sample was diluted and analyzed separately. Each sample was processed on the next day after 18-24 h except for those from the 2nd and 3rd cycle in the MS2 experiment, which were stored at -20°C and analyzed after 48 h.

Both mean and standard deviation phage concentration was determined for each set of triplicate samples. For the log removal of the bacteriophage, the mean value was calculated as shown in equation (4-2). The standard deviation of the log removal as a dependent variable is calculated according to the delta method (Casella and Berger 2002) based on the mean and the standard deviation of the independent variables as shown in equation (4-3).

For a function g(x,y)

$$mean\ g(x,y) = g(\mu_x, \mu_y)$$

$$Log\ Removal = -1 * \log\left(\frac{\mu_{permeate}}{\mu_{feed}}\right) \quad \text{Equation (4-2)}$$

$$variance\ g(x,y) = \left(\frac{\partial g}{\partial x}\right)^2 * {\sigma_x}^2 + \left(\frac{\partial g}{\partial y}\right)^2 * {\sigma_y}^2 + 2 * \frac{\partial g}{\partial x} * \frac{\partial g}{\partial y} * Cov(x,y)$$

As the cov (x,y) is assumed to be zero

$$variance\ g(x,y) = \left(\frac{\partial g}{\partial x}\right)^2 * {\sigma_x}^2 + \left(\frac{\partial g}{\partial y}\right)^2 * {\sigma_y}^2$$

$$\sigma_{\log removal} = \sqrt{\left(\frac{-1}{\mu_{\text{permeate}} * \ln(10)}\right)^2 * {\sigma_{permeate}}^2 + \left(\frac{1}{\mu_{\text{feed}} * \ln(10)}\right)^2 * {\sigma_{feed}}^2} \quad \text{Equation (4-3)}$$

4.2.8 Water Quality Parameters

. Total organic carbon (TOC) was used to measure the organic content of the sterile TYGB and SB nutrient solutions and the purified high titre bacteriophage solutions. The feed water (after phage addition) in the challenge tests was also measured for TOC content. Samples for total organic carbon were measured using a wet oxidation TOC analyzer (OI Analytical Model 1010 TIC-TOC analyzer). The oxidizing agent was 100 g/L $Na_2S_2O_8$. The samples were initially preserved by lowering the pH to 2-3 using 1N H_3PO_4. The samples were then stored at 4ºC for a maximum of 3 weeks in 45 mL glass vials. The instrument was calibrated using standard solutions of potassium biphthalate ($C_8H_5KO_4$) at concentrations of 0, 2, 4, 6 and 8 mg/L of carbon. The injection volume was 5 mL and 3 replicates of each sample were processed.

A portable pH meter (Mini Lab IQ125) was used for pH measurement and calibrated using a 3 point calibration curve (pH 4, 7, 10). A HACH CO150 conductivity meter (Model 50150) was used for measuring conductivity.

A Liquid Chromatography Organic Carbon Detector (LC-OCD) (DOC-LABOR, Karlsruhe, Germany) at the University of Waterloo was also used to evaluate the different fractions of the organics in water samples and nutrient solutions. This will help in identifying any possible fouling potential in the water or from the phage solutions. The LC-OCD involves a size exclusion column followed by a continuous carbon detector to measure the different fraction of the organics in the sample (Huber *et al.* 2011). The samples were pre-filtered using a 0.45 μm PVDF membrane filter by vacuum filtration, then stored at 4ºC in 45 mL glass vials. The glass vials were heated at 300° for 30 min to remove any trace organics and eliminate carbon contamination prior to use.

4.2.9 UF Membrane Surface Characterization

4.2.9.1 Contact angle measurement

Contact angle was measured according to the sessile drop method. A drop shape analysis system (Kruss Model DSA 100, Germany) was used. A needle with 0.5 mm diameter (Kruss, catalogue number NE44) was used for depositing ultrapure water drops on the top of the fixed virgin membrane fiber. Video clips of the drop deposition on the fiber were recorded, and then still images were extracted at the moment the water drop was deposited on the fiber and the needle was not in contact with the drop. Because the baseline had a very high curvature in this case, the instrument software was not suitable. AutoCAD software (Autodesk, Inc.) was used to approximate both the drop and the

fiber to circular curves. These were used to determine the contact angle on both sides of the drop, and get the average value as shown in Figure 4-8. A single membrane fiber was tested using this method.

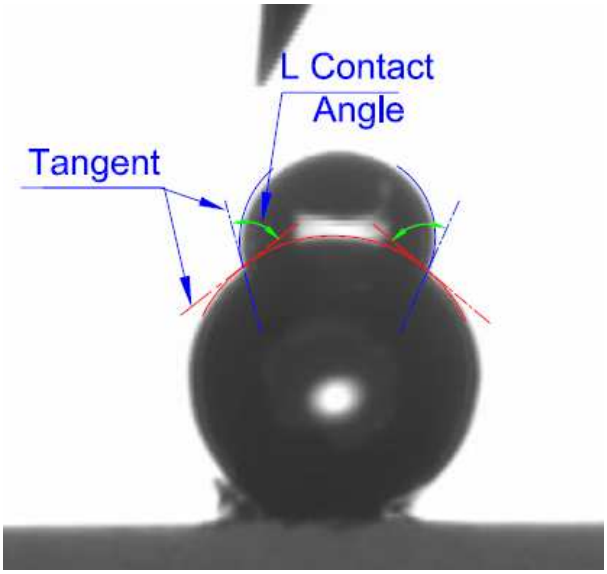

Figure 4-8 Sessile drop over a membrane fiber and contact angle measurement

4.2.9.2 Membrane Pore Size Distribution

The pore size distribution of the UF membrane used in this study was extensively investigated in Chapter 3. The atomic force microscope was chosen as the best technique for imaging the membrane surface to avoid surface damage. The measurement of the pore dimensions was done using the newly developed pore construction technique at the middle of the pore depth to be as close as possible to the minimum dimension of the pore that will be responsible for rejecting the viruses. Modeling rejection of the viruses was performed using the maximum inscribed circle measurement, which represents the diameter of the largest sphere that can pass the pore with only physical straining as a removal mechanism.

4.3 Results and Discussion

Three different virus challenge experiment were done in this study. MS2 bacteriophage was spiked into DI water for the first experiment at pH of 7.6. This was done to compare the performance of the UF membrane used in the study with results from the literature, as MS2 bacteriophage is a common virus surrogate in virus challenge experiments. At neutral pH, MS2 will be negatively charged as its isoelectric point is 3.5. For the second experiment, φX174 bacteriophage removal was also tested in

DI water at neutral pH. Unlike MS2, φX174 bacteriophage is expected to be neutral or slightly negatively charged at this pH as its isoelectric point is 6.6. This will allow a comparison of two viruses of similar size, 27.4 nm outer diameter for MS2 compared to 33 nm for φX174. A third challenge experiment was done using φX174 at a pH of 9.4, as the phage will be negatively charged at this pH, to see the impact of pH on the removal of viruses. The charge on MS2 is not affected by pH values in the range of 7 to 10 (Herath *et al.* 1999, Jacangelo *et al.* 2006). Comparing the removal of both viruses will allow further investigation of the impact of virus characteristics on virus removal by UF membranes.

4.3.1 Purification of bacteriophage high titer solutions

The two types of nutrient solutions used for the growth of MS2 or φX174 had very high TOC values of 5,400 mg/L and 20,600 mg/L for TYGB and SB, respectively. Even though the phage stocks will be diluted by 10^{-4} when added to the feed water during the challenge experiments, this will add a lot of organics to the feed water in our experiment, which would compromise our major objective of getting a base removal without any interference from membrane fouling. Using LC-OCD analysis, the nature of these organics was determined as shown in Figure 4-9 after including the dilution factor. The samples analyzed by LC-OCD were first diluted by 1:10,000 for SB and 1:3000 for TYGB, as the maximum allowed DOC for this equipment is 5 mg/L. It is clear that a small fraction of both samples is composed of biopolymers (1.75% for TYGB and 2.90% for SB). Biopolymers will have a MW larger than 150 KDa according to the instrument manufacturer specifications (Huber *et al*., 2011). Biopolymers are believed to be the major fouling component for UF membranes (Halle *et al*., 2009) such as the one used for phage removal experiments in this study. The rest of the organics are mostly humic substances, building blocks and low molecular weight organics as defined by Huber *et al.* (2011). These organics do not seem to contribute substantially to membrane fouling of UF membranes (Halle *et al*., 2009) but they can alter membrane surface characteristics such as hydrophobicity.

The possibility that the phage solutions could cause membrane fouling was the motive for performing a purification step to remove organic material from the phage stocks. For MS2, purification using a small-scale flat sheet UF membrane was an effective method for separating the phage particles from the organic material and salts present in the nutrient solution. The chosen membrane had a MWCO of 30 KDa that will allow a big fraction of organics to be removed and at the same time retain the bacteriophage. The UF membrane could retain all the MS2 phage in the

retentate, resulting in a greater than 8 log recovery, while all the material below the MWCO was passed through the membrane. The virus particles were then resuspended in PBW and the final concentration of the purified phage solution was 8×10^{8}pfu.mL^{-1}. The purified high titer stock had a final TOC of 2.5 mg/L, which is less than 0.1% of the original TOC value. By using a 10^{-2} dilution of the purified high titer stock for the feed to the UF bench unit, this adds only 0.025 mg/L of TOC to the feed water, and a low fouling potential is expected.

Two different batches of φX174 were prepared. The first batch (used for the neutral pH experiment) had a lower phage concentration, and the second batch (used for the high pH experiment) had a higher phage concentration. Both φX174 preparations were purified using the same method described above for MS2. However, unlike MS2, the 30 KDa MWCO membrane did not result in complete recovery of φX174, although a 7 to 8 log recovery of the phage was obtained. The final φX174 concentration of the first purified solution was 5×10^{8} pfu.mL^{-1}, and the final concentration of the second purified batch was 1×10^{10} pfu.mL^{-1} in both purified batches and the final TOC was 68 mg/L, which was only 0.3% of the original TOC value. The reason for higher TOC values of the purified φX174 solutions, compared with MS2, is because the nutrient medium used to growth the φX174 had a much higher concentration of organics. In the neutral pH experiment, the first purified φX174 batch was diluted by 10^{-2} dilution into the feed water. This resulted in additional TOC value of 0.64mg/L in the feed water for the virus challenge experiments compared with MS2. For the high pH experiment, a higher titer φX174 bacteriophage solution (batch 2) was used in a lower TOC addition to the feed water of 0.064 mg/L. Even with this increase in TOC for the first φX174 experiment, no significant fouling happened during the challenge test as will be shown later in section 4.3.5. The obtained results should be representative of the clean water test conditions for φX174 bacteriophage experiment.

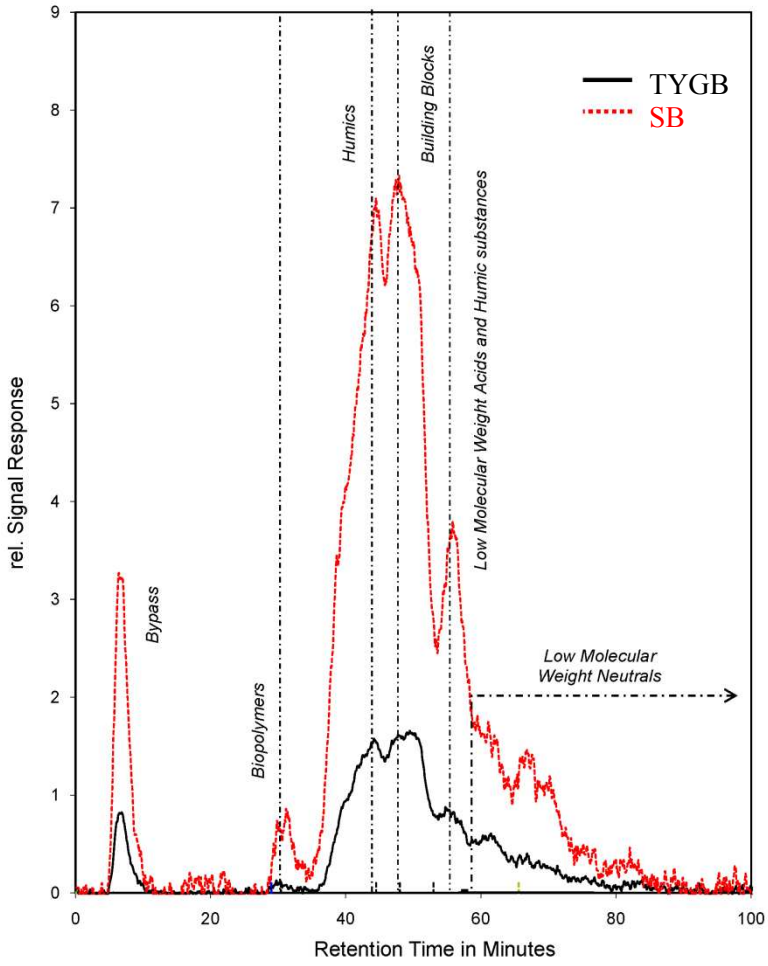

Figure 4-9 LCOCD chromatograms for TYGB and SB nutrient solutions

4.3.2 Membrane Surface Characterization

The polymeric material for the UF membrane was reported to be a PVDF [-$(C_2H_2F_2)_n$-] polymer. PVDF is considered to be a piezoelectric polymer with considerably higher piezoelectric or dielectric constant than other polymers. The surface charge was previously reported for this membrane in 1 mM KCl background solution (Hallé 2010) as shown in Figure 4-10. The isoelectric point of the membrane material is at pH of 2.5 and the zeta potential of the membrane ranges from 52 mV at pH 7 to 56 mV at pH 9. The measured contact angle of the membrane fiber was found to be 62±3.1º based on eight different measurements, and shows that the membrane hydrophobicity is lower than expected for the normally very hydrophobic PVDF. This confirms that either the bulk PVDF polymer or the membrane surface itself have been modified to reduce hydrophobicity. This is also supported by the

fact that oxygen, which is absent in pure PVDF, was present in the surface functional groups of the investigated membranes as was shown in the EDAX analysis in Chapter 3. The obtained pore size distribution of the membrane is described in Chapter 3. The membrane pore equivalent diameter ranged from 2 to 56 nm with a median value of 9 nm as shown in the AFM measurements at pore mid height. On the other hand, only 1 to 4 pores per μm^2 will physically allow a 27 nm sphere to pass through the membrane, based on the inscribed circle within pore boundaries.

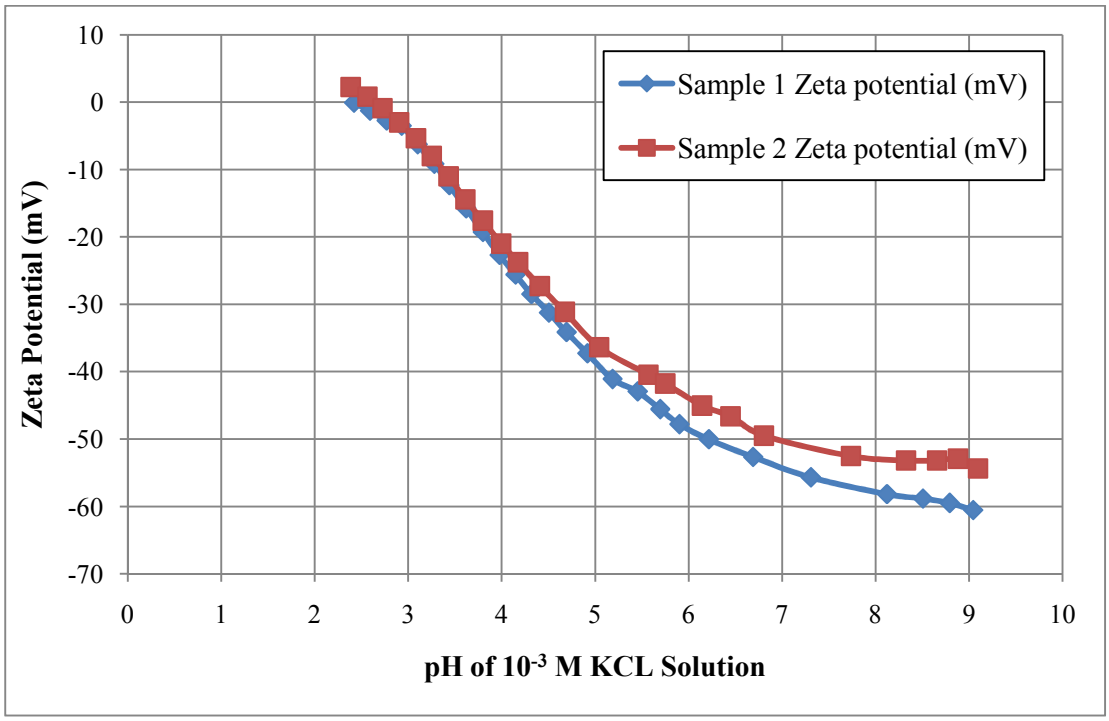

Figure 4-10 Zeta potential of two different membrane samples at different pHs (Hallé 2010)

4.3.3 Membrane Pretesting

Before each experiment was conducted, the UF membrane module was chemically cleaned. After the chemical cleaning, both integrity and clean water permeability were tested. The details of the membrane chemical cleaning and integrity test procedure are described in section 4.2.6 and appendix B. The integrity test was done before each of the three virus challenge experiments. The clean water permeability test was done for the MS2 experiment at pH 7.6 and the φX174 experiment at pH of 6.8, but not for the φX174 experiment at pH of 9.4 because these results would be affected by the high pH value, and results will not be comparable.

The manufacturer defines the acceptable limit for the pressure decay integrity test as 0.3 psi of static pressure drop across the submerged membrane fibers over a period of two minutes. A higher drop would indicate a pin hole in the membrane fiber or a problem with the fibers seal within the module that would allow air leakage and cause a drop in the pressure. For all experiments, the module pressure decay was below the defect limit as shown in Figure 4-11, so no integrity problems were detected.

Clean water permeability tests are a good tool for investigating the presence of fouling material on the membrane or any leaking connection. Membrane fouling will increase the TMP at a certain flux compared to the regular values for the clean membrane. Any leaking connection or even integrity problem in the module will cause a significant drop in the TMP at a certain flux value compared to the proper operation conditions. The clean water permeability test results for the MS2 experiment at pH 7.6 and the φX174 experiment at pH of 6.8 are shown in Figure 4-12. Significant changes in the y values or the slope of the regression line would indicate that the test conditions are not the same due to residual fouling. The permeability value, which is the slope of the two lines, was 0.0483 psi.m^2.hr/L for the MS2 experiment and 0.0439 psi.m^2.hr/L for the φX174 experiment (neutral pH). This can indicate that no significant difference in the fouling condition of the membrane in both experiments was observed. The vertical shift between the two lines may be attributable to the change of pressure transducer between the two experiments. According to this, all three experiments should represent the base removal of both types of phage by the UF membrane with no impact of remaining fouling or integrity problems.

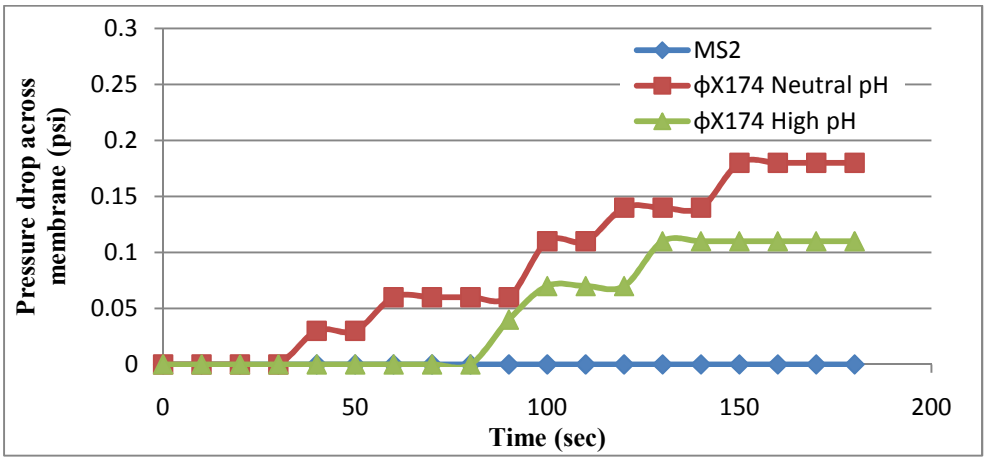

Figure 4-11 Integrity test results for used UF membrane module with a manufacturer limit of 0.3 psi / 2min

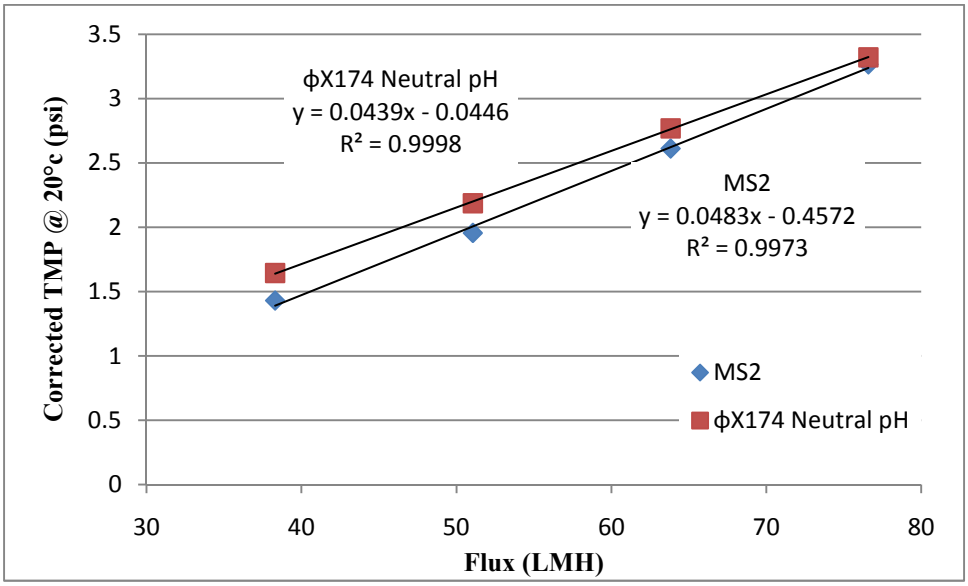

Figure 4-12 Clean water permeability test for the UF membrane module used for the MS2 and the φX174 (neutral pH) experiments

4.3.4 Water Quality Parameters

The water quality parameters for the three challenge experiments conducted in DI water are listed in Table 4-3. Both MS2 and φX174 tests done at neutral pH were done using DI water without any pH adjustments but for the second φX174 experiment, sodium hydroxide was used to raise the pH to 9.4. In experiments conducted at neutral pH, the MS2 feed water had a slightly higher conductivity and slightly higher pH than the feed water for φX174, as it was allowed to equilibrate with air for a longer time. The feed concentration range of phage for all the experiments was 10^6 to 10^7 pfu.mL^{-1}. The addition of phage spiking solutions had a slight influence on DI water quality. Based on the concentration of the final purified high titer bacteriophage solutions, the dilution added to the feed water for each experiment was 1:100 for MS2 and φX174 (neutral pH) and 1:1000 for φX174 at high pH (Table 4-3). Nutrient solutions used to grow φX174 had a much higher TOC, therefore based on the dilution required for the φX174 stocks, the TOC value of the feed water in the neutral pH experiment was just over 2× higher than that of the high pH experiment.

Table 4-3 Water quality parameters for all DI water experiments

Parameter	Unit	MS2	φX174 Neutral pH	φX174 High pH
pH		7.6	6.5	9.4
Temperature	°C	22.8	23.5	22
Conductivity	µS/cm	28	9.1	Not available
TOC of membrane feed	Mg C/L	0.56	1.13	0.53
Approx. dilution of purified phage stock to the feed water		1:100	1:100	1:1000

4.3.5 Transmembrane Pressure Profile for Challenge Experiments

All experiments were performed at a constant flux of 57 LMH, which corresponded to a permeate flow rate of 45 mL/min. This value was verified by measuring the permeate flux at regular intervals throughout the experiment. Throughout each experiment TMP was monitored to assess the fouling behavior the membrane unit. The slope of the TMP within one cycle was indicative of hydraulically reversible fouling and TMP readings at the beginning of each cycle were used to asses hydraulically irreversible fouling. An increasing trend in the latter is a measure of the degree of irreversible fouling. The first part of each TMP profile was the conditioning part of the membrane using DI water without bacteriophage (as seen in Figures 4-13, 4-14 and 4-15), and the second half of the TMP profile (150 to 300 min) was acquired when DI water spiked with bacteriophage was used.

For the MS2 experiment at pH 7.6 shown in Figure 4-13, clearly no apparent fouling was observed. The TMP increase within the four phage challenge cycles was 8%, 2%, 2% and 4%, respectively, compared to 6%, 4%, 4% and 3% for the four conditioning cycles. This shows that no apparent reversible fouling occurred during all cycles, and that the value decreases with increased running time during the challenge experiment, as the membrane becomes conditioned following the change in feed solution after spiking. For the starting pressure of each cycle, the value is the same for the four cycles at 2.02 psi compared to 1.96 psi for the conditioning cycles. No irreversible fouling can be noticed, however, the pressure is slightly higher for the virus spiking cycles due to the addition of viruses. This experiment did not show any contribution of fouling to the obtained removal.

For φX174 experiment at pH of 6.5, a higher a TMP increase was expected due to the higher TOC value in the feed water (as shown in Table 4-3) due to the lower concentration of phage in the used purified stock as explained in section 4.3.1. The TMP increase within the three phage challenge cycles was 6%, 8% and 7% compared to 0%, 0% and 2% for the three conditioning cycles. This was

likely due to the increased TOC value in the virus feed solution of 1.13 mg/L. However this increase in TMP is lower than the regular TMP increase that is typically observed for surface waters, and is believed to be caused by reversible fouling. The starting TMP of each cycle increased slightly by 0.01 psi per 30 min of the filtration cycle.

For φX174 experiment done at pH of 9.4, the first cycle in the conditioning cycles initially had high TMP values that went to the normal TMP of 1.85 psi by the end of the first cycle, and this initial higher TMP value was not observed in the second and third conditioning cycles. This was either caused by introducing a high pH feed water to a module that had been stored in a neutral pH DI water, or some problem with the permeate pump. This problem was not observed for the 3 cycles after spiking the φX174 bacteriophage. For this experiment, the feed water containing phage had a lower TOC value because the higher titer phage purified stock was used. As a result, the TMP increase within the three phage challenge cycles was 4%, 5% and 4% compared to 0%, 0% and 0% for the three conditioning cycles. These values were lower than the values from the φX174 at pH 6.5 experiment as the same TMP value of 1.86 psi was found for the three cycles unlike the φX174 at pH 6.5. For the φX174 experiments the slight irreversible fouling can be due to the very low biopolymer concentration in the nutrient solution. The effect of this increase was investigated as well in the removal experiments in section 4.3.7.

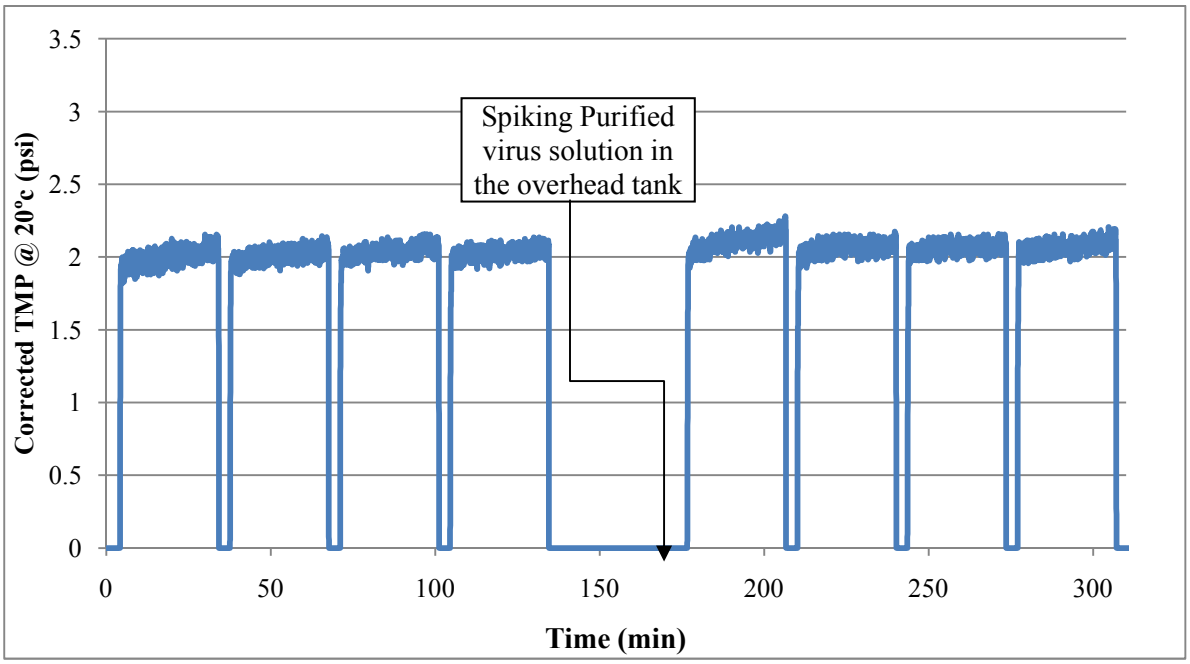

Figure 4-13 TMP profile for MS2 Experiment in DI water at pH 7.6

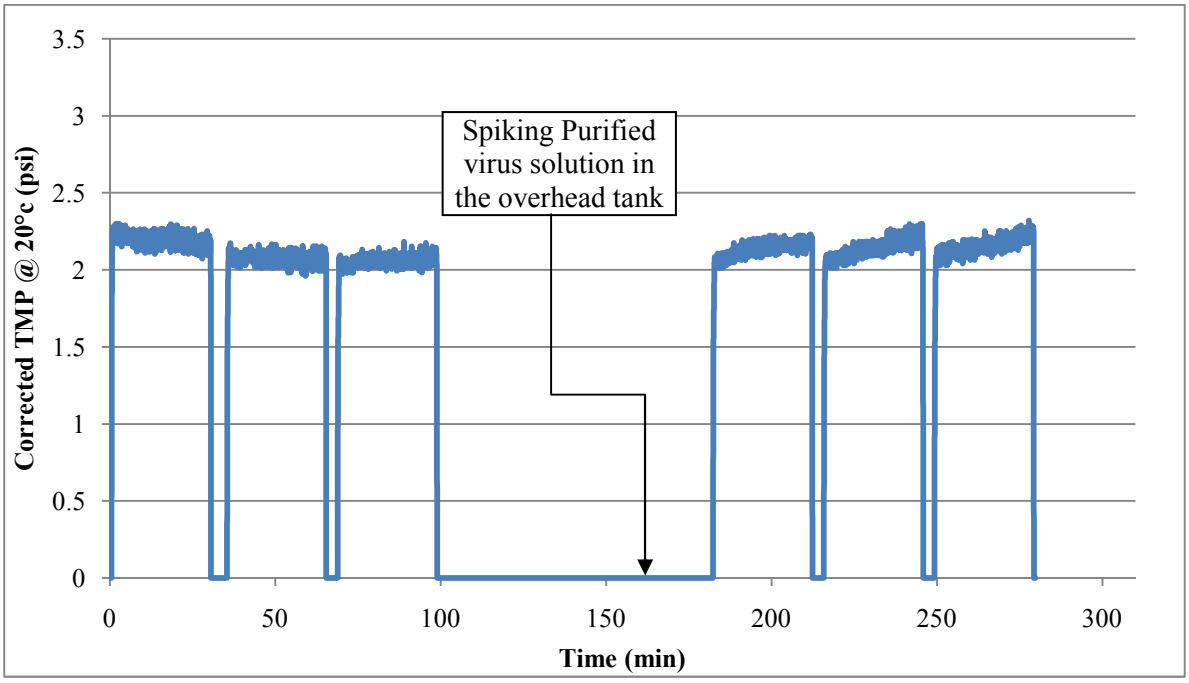

Figure 4-14 TMP profile for φX174 experiment in DI water at pH of 6.8

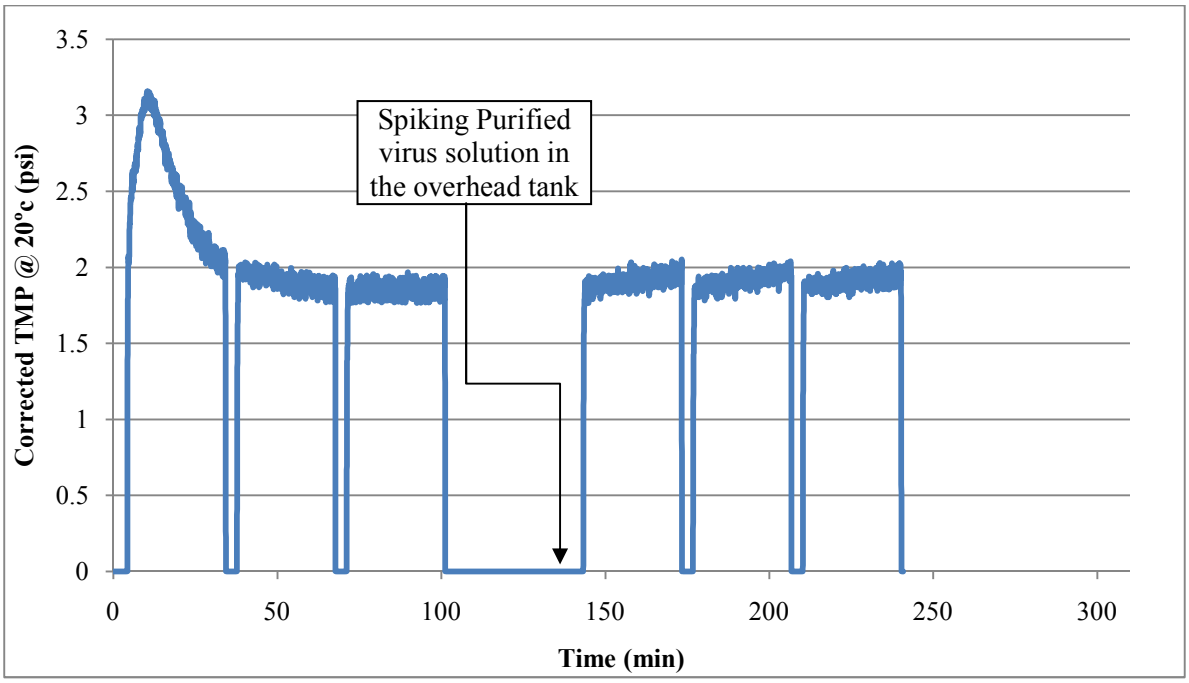

Figure 4-15 TMP profile for φX174 experiment in DI water at pH of 9.4

4.3.6 Mass Balance Model

During the filtration of the virus feed solution, there will be a considerable difference in the phage concentration in unit feed and permeate as more than 99% of the viruses are rejected by the membrane as shown in Figure 4-16. As the filtration cycle continues, the rejected viruses start to accumulate near the membrane surface due to the hydrodynamic conditions in the membrane container in a dead end submerged UF membrane system like the one employed in the design of our unit. This will decrease the apparent rejection of viruses as it will be hard to sample the actual feed at the end of the cycle as the membrane tank is lacking proper mixing conditions. These results can be misleading as it can be misinterpreted as a reversible fouling effect. It became necessary to investigate these conditions to overcome this effect. The following mass balance was developed to serve as a prediction tool for the effect of phage concentration in the unit and get a better interpretation of the membrane rejection over cycle length.

Initially, the unit is filled from the feed tank at a concentration of C_{feed}. During the 30 min of the filtration cycle, the tank will be continuously fed with a similar flow rate to the permeate flow rate to keep a constant water level inside the membrane container with volume ($V_{container}$.) The actual phage concentration inside the membrane container ($C_{container}$) will start to increase with time as shown in equation (4-4). The membrane should have a constant rejection (R_{actual}) of viruses with time in case of no fouling effect. By applying a mass balance on the viruses through the process under certain assumptions including:

- No aggregation of viruses
- No irreversible adsorption of viruses to the membrane surface
- Constant rejection of viruses along the whole cycle
- Accumulated viruses inside the container are completely mixed
- The concentration in membrane container increases linearly with time

$$inflow - outflow = accumulation$$

$$Q_{permeate} * C_{feed} * t - Q_{permeate} * C_{permeate}@t * t = V_{container} * (C_{container}@t - C_{feed})$$

$$Q_{permeate} * C_{feed} * t - Q_{permeate} * (1 - R_{actual}) * C_{container}@t * t = V_{container} * (C_{container}@t - C_{feed})$$

$$C_{container}@t = \left(\frac{Q_{permeate}*C_{feed}*t+V_{container}*C_{feed}}{Q_{permeate}*(1-R_{actual})*t+V_{container}}\right) \quad \text{Equation (4-4)}$$

At time t=0 min (cycle start)

$$C_{cotainer}@0 = C_{feed} \quad \& \quad R_{actual} = \frac{C_{Permeate}@0}{C_{feed}} \quad \text{Equation (4-5)}$$

At time t =30 min (cycle end)

$$C_{cotainer}@30 = \left(\frac{Q_{permeate}*C_{feed}*30+V_{container}*C_{feed}}{Q_{Permeate}*(1-R_{actual})*30+V_{container}}\right) \quad \text{Equation (4-6)}$$

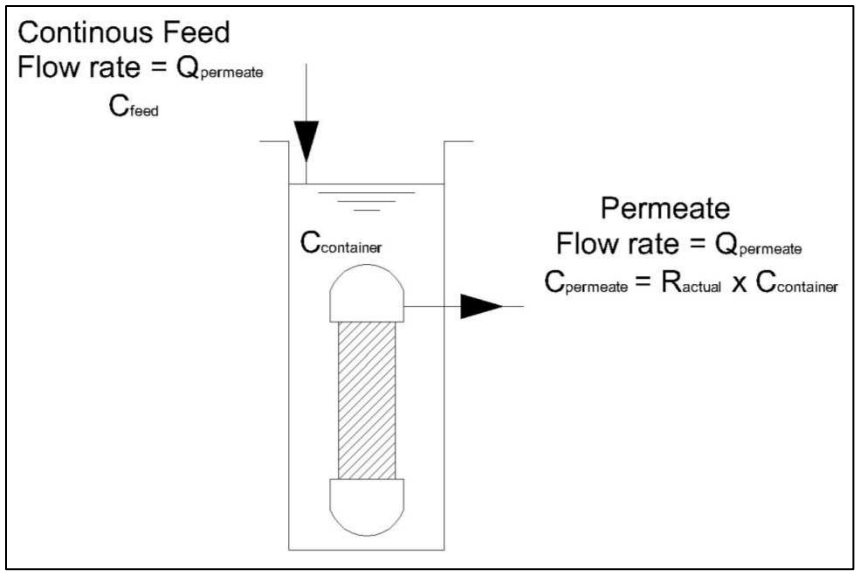

Figure 4-16 Flow diagram of the bench unit for mass balance model

The measured rejection for each cycle at the start based on feed and permeate samples can be considered as the actual rejection of the membrane unit (R_{actual}) as shown in Equation (4-5). The permeate flow rate ($Q_{permeate}$), container volume ($V_{container}$) and initial virus feed solution concentration (C_{feed}) are known, so the average concentration within the membrane container ($C_{container}$) can be measured using Equation (4-6).

Based on the experimental conditions used for the membrane pilot unit, the expected rejection of viruses will be 3 to 4 logs based on the type of membrane used, the module container volume (1800 mL) and the permeate flow rate (45mL/min). From these data it was estimated that the phage concentration in the module container at the end of the cycle would be 175% the initial feed solution (i.e. phage concentration in the overhead tank). Therefore, using the initial feed concentration to

measure the virus removal at the end of the cycle will be inappropriate. One alternative is to get a representative sample from the membrane module container at the end of the cycle. A grab sample from the module container itself will be problematic as the hydraulic conditions inside the membrane container will not allow proper mixing, and regions close to the membrane will have higher phage concentrations than the rest of the membrane container. Another option will be measuring the average drain concentration after emptying the unit at the end of the cycle. Mixing of this drain sample can be done effectively, and can be used to represent the feed concentration at the end of the cycle. Although the phage concentration in the drain sample will be a slight underestimation of actual phage concentration on the membrane surface, it will be more representative than the overhead tank feed value. For all of the virus challenge experiments (Section 4.3.7, Figure 4-17 to Figure 4-19), the drain concentration was in agreement with this mass balance model as it was nearly 150% to 200% of the initial feed concentration. For this reason, the drain concentration was used to measure the virus removal at the end of the virus filtration cycle in this study.

4.3.7 Virus Challenge Experiments

Three different experiments were done using DI water to get the basic removal of phage by the UF membrane with no effect of membrane fouling. MS2 was tested at pH 7.6 (Figure 4-17) while φX174 was tested at pH of 6.5 (Figure 4-18) and pH of 9.4 (Figure 4-19).

For the different virus challenge experiments, virus concentrations in both the membrane feed and permeate samples were analyzed to get the virus removal by the membrane at both the start and the end of each cycle as shown in Figure 4-17 to Figure 4-19. In each figure, (a) shows the phage concentration in the feed sample at the start of each cycle, and (b) shows the phage concentration in the drain tank at the end of the cycle, and measure the membrane feed at the end of the cycle. The permeate samples at cycle start and end are shown in (c) of each figure. The error bars in these figures are based on the values of the three replicate samples taken from each location. Feed samples and permeate samples at cycle start are used to measure virus log removal at cycle start while drain and permeate samples at the end of the cycle are used to measure virus log removal at cycle end as shown in figure (d). The error bars in figure (d) are calculated based on the delta method as explained in equation (4-3).

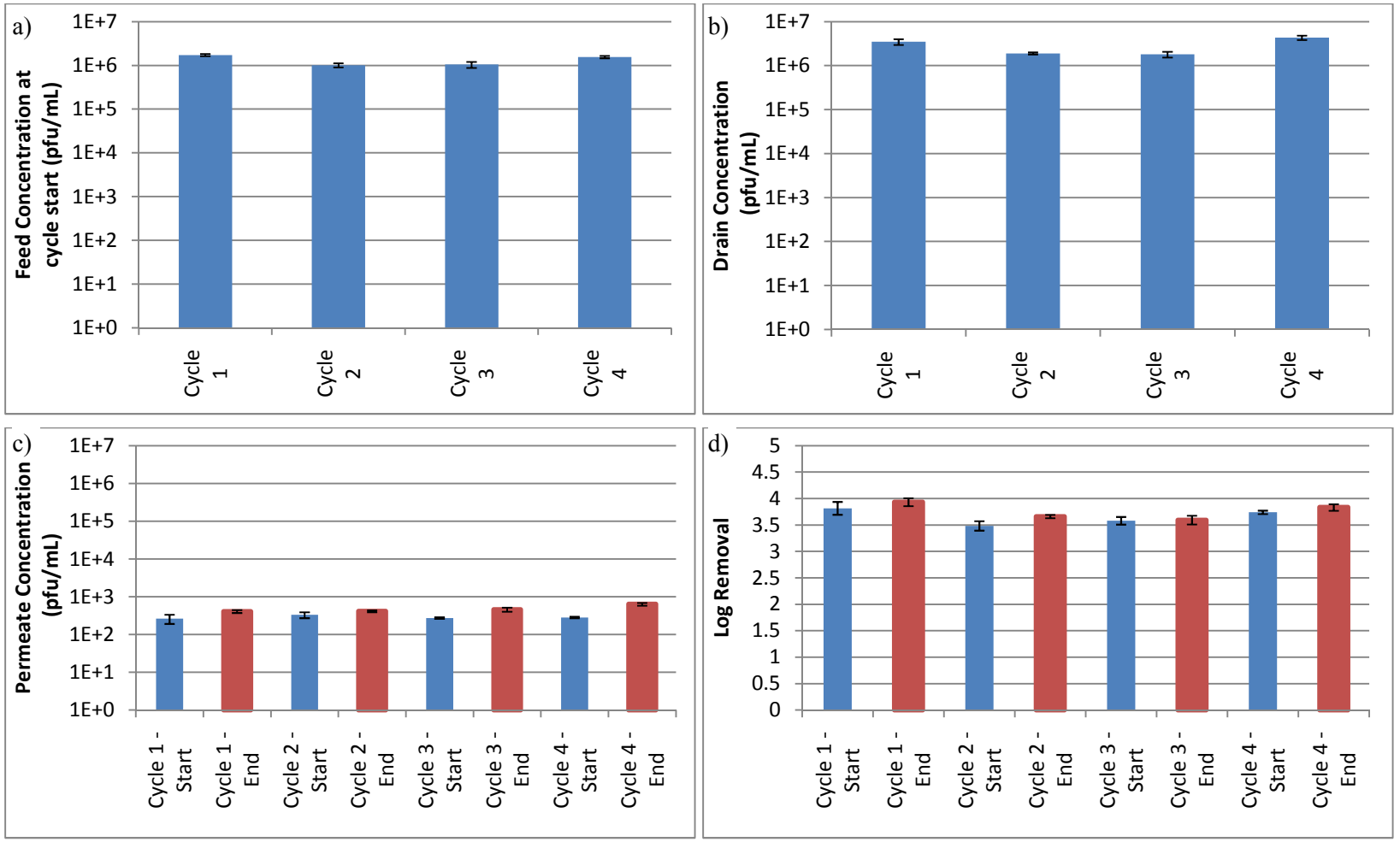

Figure 4-17 MS2 removal by UF membranes using DI feed water at pH=7.6. Phage concentrations were measured for membrane feed (cycle start)(a), drain tank (cycle end) (b), permeate line (cycle start and end) (c). Log removal (d) values were determined at both cycle start and end.

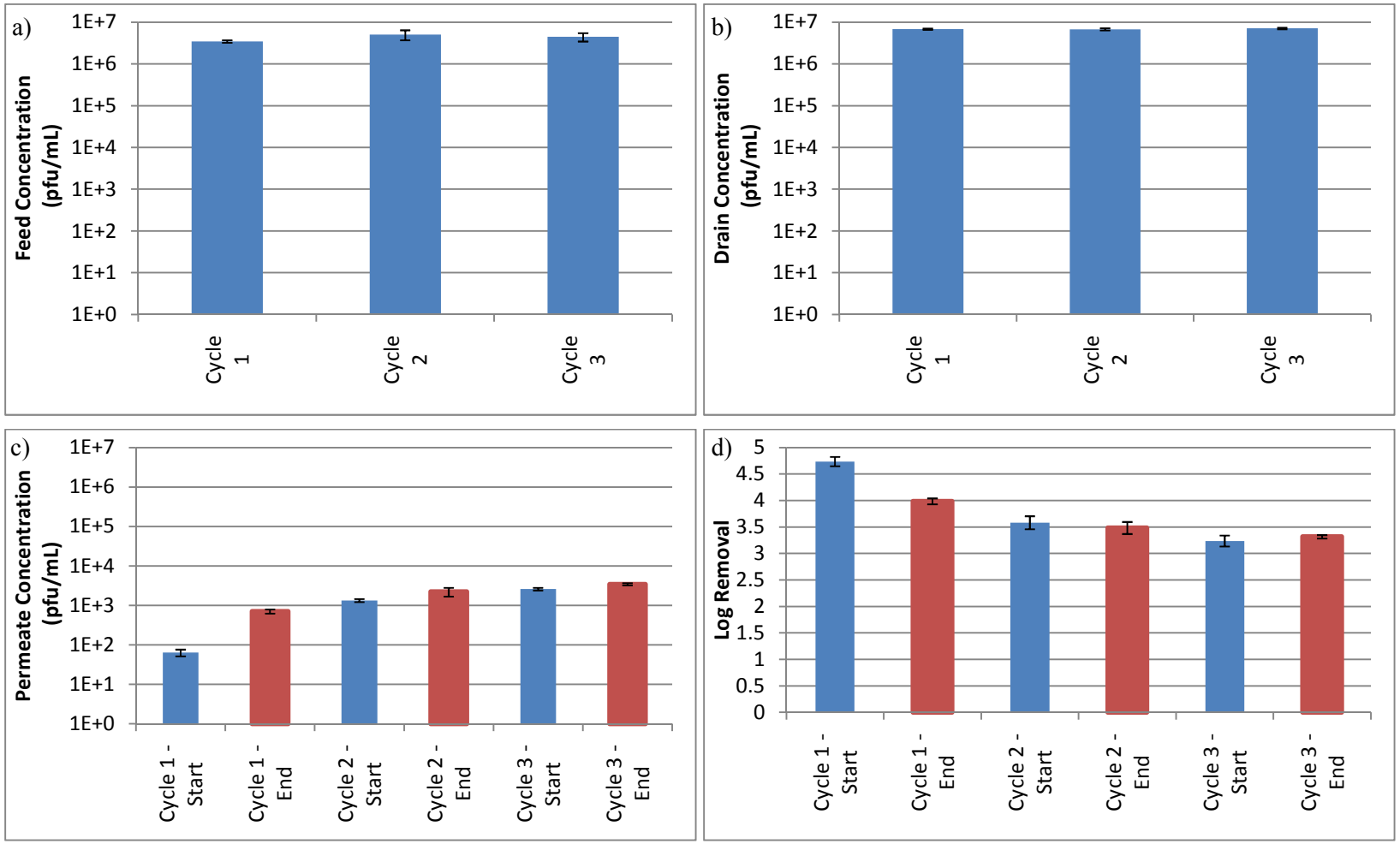

Figure 4-18 φX174 removal by UF membranes using DI feed water at pH=6.8. Phage concentrations were measured for membrane feed (cycle start)(a), drain tank (cycle end) (b), permeate line (cycle start and end) (c). Log removal (d) values were determined at both cycle start and end.

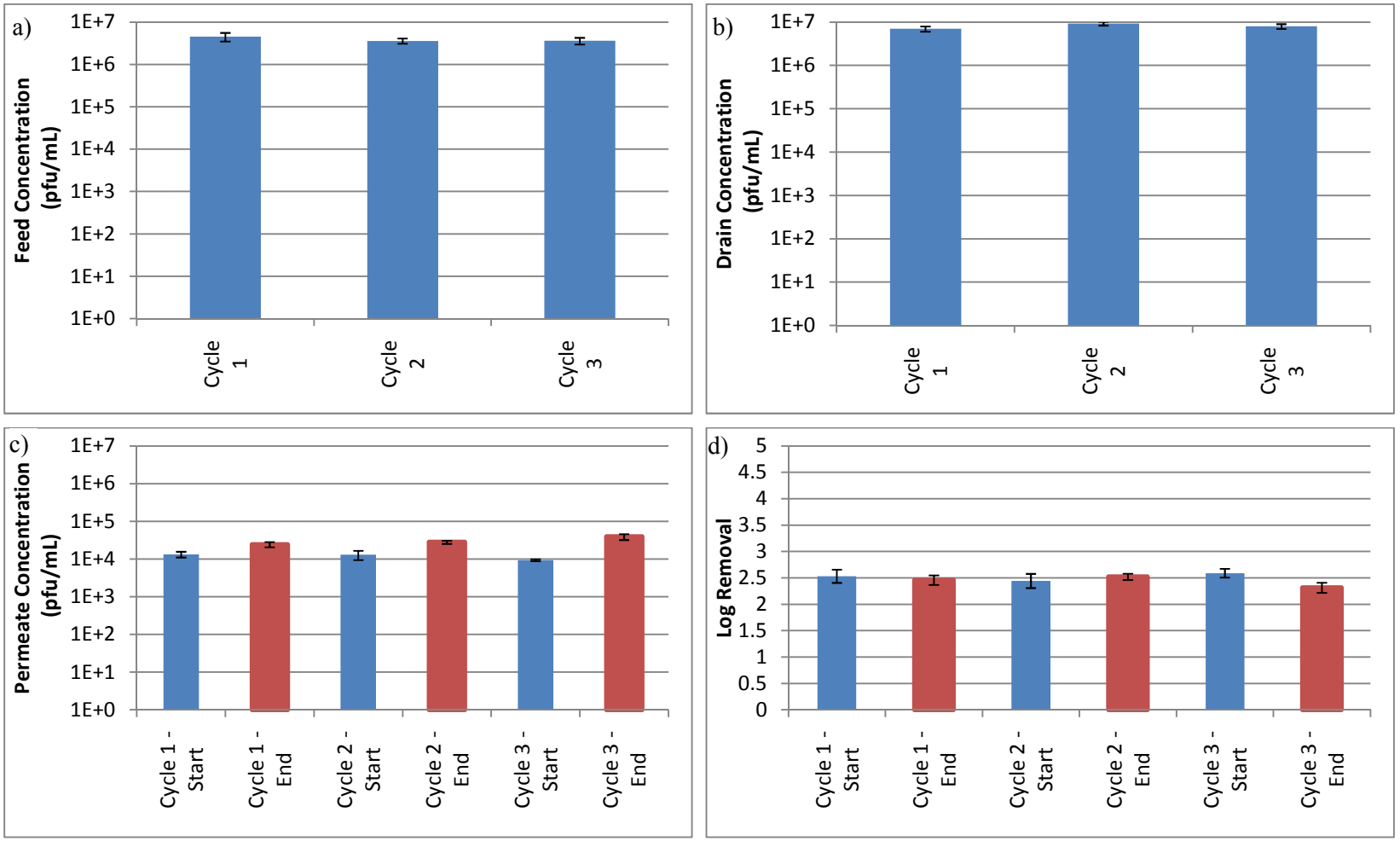

Figure 4-19 φX174 removal by UF membranes using DI feed water at pH=9.4. Phage concentrations were measured for membrane feed (cycle start)(a), drain tank (cycle end) (b), permeate line (cycle start and end) (c). Log removal (d) values were determined at both cycle start and end.

4.3.7.1 MS2 Bacteriophage at pH 7.6

Both membrane influent (feed and drain) and effluent (permeate) samples from cycle one and four were processed 1 d after the samples were taken. Samples from cycle 2 and 3 were processed 2 d after the samples were taken. Samples from cycles 2 and 3 were kept frozen prior to analysis. The concentration of the bacteriophage in the different samples is shown in Figure 4-17. It was clear that the feed and drain samples analyzed after 48 h had a lower concentration than those analyzed on the next day probably due to freezing. The sample hold time and freezing before analysis did not affect enumeration results in the permeate samples which were at a lower concentration. This slightly affected the removal of cycle 2 and 3 and caused it to be lower than cycle 1 and 4. Because of this problem, for later experiments all samples are processed after 24 h and samples were stored at 4°C to decrease the variability in the obtained removal results.

The obtained log removals for the start of the four cycles were 3.8, 3.5, 3.6 and 3.7, respectively, while the removals at the end of all the cycles were 3.9, 3.7, 3.6 and 3.8, respectively. For cycles 1, 3 and 4, no significant difference was observed between the start and the end of the cycle. The difference between the obtained log removal values over the different cycles was 0.4 logs for the four cycles while only a difference of 0.2 logs was shown on cycles 1 and 4 or cycles 2 and 3 which were analyzed on the same day. This low variability in the results proved that the experimental protocol for our virus challenge experiments was valid and able to detect small changes in the log removal of MS2 phage. The UF membrane was able to provide a consistent removal of MS2 bacteriophage over 4 different filtration cycles with no obvious trends. This indicates that virus aggregation was not happening as this would increase the variability in the obtained removal. The average MS2 removal based on these results was 3.7 logs (i.e. 99.98%) which nearly meets the total required log removal of enteric viruses according to the Canadian Drinking Water Guidelines (Health Canada 2004).

The expected removal mechanisms for MS2 bacteriophage at pH of 7.6 would be mainly size exclusion and electrostatic repulsion due to the negative charge on both the membrane surface and the bacteriophage protein capsid. The hydrophobic adsorption will be less suspected, as the negative surface charge on the phage would cause the electrostatic repulsive force to prevent virus adsorption. This MS2 removal value represents the base value for MS2 with the UF membrane used in this study. It can be used to compare MS2 to other types of viruses or to study the impact of operational conditions on virus removal.

4.3.7.2 φX174 experiment at pH of 6.5

Compared with MS2, φX174 has a slightly larger size of 33 nm with a different capsid structure. Another major difference is that φX174 has a higher isolectric point (i.e. pH where the virus will be neutral) of 6.6 (compared with 3.9 for MS2) which will make φX174 nearly neutral in feed water with a pH of 6.5. Comparing the removal of MS2 and φX174 can explain how these differences in virus properties affected the virus removal. The same spiking and sample analysis protocols used for the MS2 challenge experiment were used in this experiment as well. The results of this experiment are shown in Figure 4-18.

The feed virus concentration from the overhead tank over the three cycles seems stable (Figure 4-18a). The drain concentration is also stable over the three cycles (Figure 4-18b) in a similar manner to the MS2 experiment. The main difference is the permeate concentration, which increased over the three cycles both at the start and the end of the cycle (Figure 4-18c). At the start of the first cycle, the membrane was able to achieve a 4.7 log removal of φX174 bacteriophage and this dropped to 4.0 logs at the end of the cycle. A difference of 0.7 logs within a 30 min filtration cycle shows a rapid decrease in the ability of the membrane to remove the viruses. In the second cycle, the removal dropped from 3.6 at the start to 3.5 at the end, so the membrane removal of viruses was nearly stable within this cycle. Similarly, the third cycle had a removal of 3.2 at the start and 3.3 at the end. This removal pattern was attributed to a contribution by adsorption of φX174 bacteriophage to the membrane that caused the declining removal. Only first cycle had a large drop in removal as the adsorption rate was much higher than the other two cycles, likely because the available adsorption sites were occupied by the adsorbed phage from the previous cycles. Over time it is expected that φX174 will occupy all of the adsorption sites, and phage removal will drop to its lowest value as adsorption will diminish eventually. The obtained removal in this case would be mainly due to size exclusion as no electrostatic repulsion is expected for this neutral virus at pH of 6.5.

Our results show that the major removal mechanisms for φX174 would be size exclusion, followed by both reversible and irreversible adsorption in the first cycles of operation. After all the irreversible adsorption sites are occupied, only size exclusion followed by reversible adsorption would be dominant. Since φX174 bacteriophage (33 nm outer diameter) is larger than the MS2 bacteriophage (27.4 nm outer diameter), it is expected that φX174 would be better removed by size exclusion. Except for the first cycle, φX174 removal ranged from 3.2 to 3.6 log removal, which is lower than that obtained for MS2 (3.5 to 3.9 log). This indicates the great importance of the higher surface

charge on the MS2 phage compared to φX174 phage due to its lower isoelectric point. The higher negative surface charge on the MS2 virus would increase the electrostatic repulsion with the membrane pores and enhance the virus removal by the negatively charged UF membrane.

4.3.7.3 φX174 experiment at pH=9.4

Based on the difference in removal values between MS2 and φX174 in the neutral pH experiments, it was predicted that the surface charge of the virus (based on its isoelectric point) may play a role in virus removal by a UF membrane. To further test this theory, a further experiment was conducted to test φX174 removal at a higher pH to confirm these findings. By increasing the pH of the feed solution, the φX174 bacteriophage will have a negative charge similar to MS2 at pH 7.6. In this experiment, φX174 was tested using DI water in which the pH of the feed solution was increased to 9.4 using sodium hydroxide. The results of this experiment are shown in Figure 4-19.

Phage concentrations in both the feed and drain samples were both stable over the three cycles with no significant changes (Figure 4-19a-b). Unlike the experiment conducted at pH 6.5 where the virus removal declined over the three cycles, the removal of φX174 bacteriophage was nearly the same over the three cycles at pH 9.4 (Figure 4-19d). In the first cycle the removal was 2.5 logs both at the start and the end of the cycle. For cycle two the removal was 2.5 logs at the start and 2.4 at the end of the cycle. The third cycle had a slight difference in removal as it dropped from 2.6 at the start to 2.3 at the end. The removal of φX174 at pH 9.4 was lower than its removal at pH 6.5 for all of the cycles. φX174 will be negatively charged at pH 9.4 and the negative charge of the membrane will increase as well. It seems that this disturbed the adsorption of the phage to the membrane and prevented the adsorption effect.

Compared to MS2 phage, even with the slight larger size of φX174 bacteriophage (33nm) compared to MS bacteriophage (27.4nm), φX174 average log removal of 2.5 logs at pH 9.4 was lower than MS2 average removal of 3.7 logs at pH 7.6. It is possible that this can be attributed to the difference in the characteristics of both viruses such as the negative surface charge on their capsid, but this was not further evaluated in this study and no information is available in literature regarding this. An important difference may be due to the 3D geometry of both viruses. φX174 capsid has 12 extruding spikes from the icosahedral capsid unlike MS2 which does not have these spikes. The length of each spike is 3.2 nm, so the spikes will distance the inner protein capsid from the membrane pore wall, minimizing their electrical interaction and decreasing electrostatic repulsion. Since these spikes are also made from proteins, they will also possess a negative charge but these point charges will be

different than a charged MS2 sphere surface, and may exhibit electrostatic repulsion in a different way. The difference in removal between MS2 and φX174 can be attributed to the improved electrostatic repulsion of MS2 phage compared to φX174 phage. φX174 seems to be a good model for removal of viruses by membranes as it can explain the effect of membrane surface charge, hydrophobicity and solution conditions.

4.3.8 Modeling of the bacteriophage removal

Different mass transport models are available in the literature to model the rejection of spherical colloids by UF membranes, and they have been employed in modeling protein transport through UF membranes (Deen 1987, Mehta and Zydney 2005). By employing a model to predict the removal of both MS2 and φX174 phage using the known pore size distribution of our membrane, the contribution of each type of removal mechanisms in our experiments can be investigated.

The pore size distribution of the UF membrane that was used in the phage challenge experiments was characterized in Chapter 3. The obtained measurements of the inscribed circle within each pore were obtained using 3 different fibers from the same UF membrane used in our experiments. The data were fitted according to the log normal distribution in equation (4-7) as shown in Figure 4-20, where x is the radius of the inscribed circle and f(x) is the probability of its occurrence on the membrane surface. The obtained log normal distribution descriptors are also reported in Table 4-4. The log likelihood value for each fiber can be used to study how well the log normal probability distribution fits the experimentally obtained pore size distribution. The better the log normal distribution fits the data, the lower the log likelihood will be. Results in Table 4-4 show that fiber 3 had the best fit among all fibers. Also the full data set from all the three fibers was fitted with lognormal distribution to get an idea about the total pore size distribution of the whole module

The sieving coefficient (Sa) was derived according to (Deen 1987) as shown in equation (4-7) and the expressions for K_s and K_t are available elsewhere (Bungay and Brenner 1973). The obtained asymptotic sieving coefficient for a porous UF membrane with a pore size distribution following a continuous probability distribution f(r) can be computed as shown in equation (4-9) (Mehta and Zydney 2005). Where (r) is the radius of the inscribed circle inside the membrane pore and λ is the dimensionless radius of the virus (i.e. ratio of the virus outer diameter to the diameter of the inscribed circle within pore). The obtained sieving coefficient from equation (4-9) will be used to predict the log removal of the viruses as shown in equation (4-10). The main assumptions for this model are:

- Transport of viruses inside the membrane will be dominated by convection only due to the larger size of the viruses and high filtration velocity.
- No concentration polarization will happen near the membrane surface.
- No short range intermolecular forces exist between the membrane pore and the virus such as van der Waals forces or electrostatic repulsion forces.
- The concentration inside the pore is equal to the permeate concentration.
- The ratio of the pore radius to the pore length is large.

$$f_x(x;\mu,\sigma) = \frac{1}{x.\sigma.\sqrt{2\pi}} e^{-\frac{(lnx-\mu)^2}{2\sigma^2}} \ , \ x > 0 \qquad \text{Equation (4-7)}$$

$$S_a(r) = \begin{cases} 0 & 0 < r \le a \\ (1-\lambda) * [2-(1-\lambda)^2] * \frac{K_s}{2K_t} & a < r < \infty \\ 1 & r = \infty \end{cases} \qquad \text{Equation (4-8)}$$

$$S_0 = \frac{C_{filterate}}{C_{feed}} = \frac{\int_0^\infty S_a(r) * f(r) * r^4 \, dr}{\int_0^\infty f(r) * r^4 \, dr} \qquad \text{Equation (4-9)}$$

$$\log \text{removal} = -\log_{10}(S_0) \qquad \text{Equation (4-10)}$$

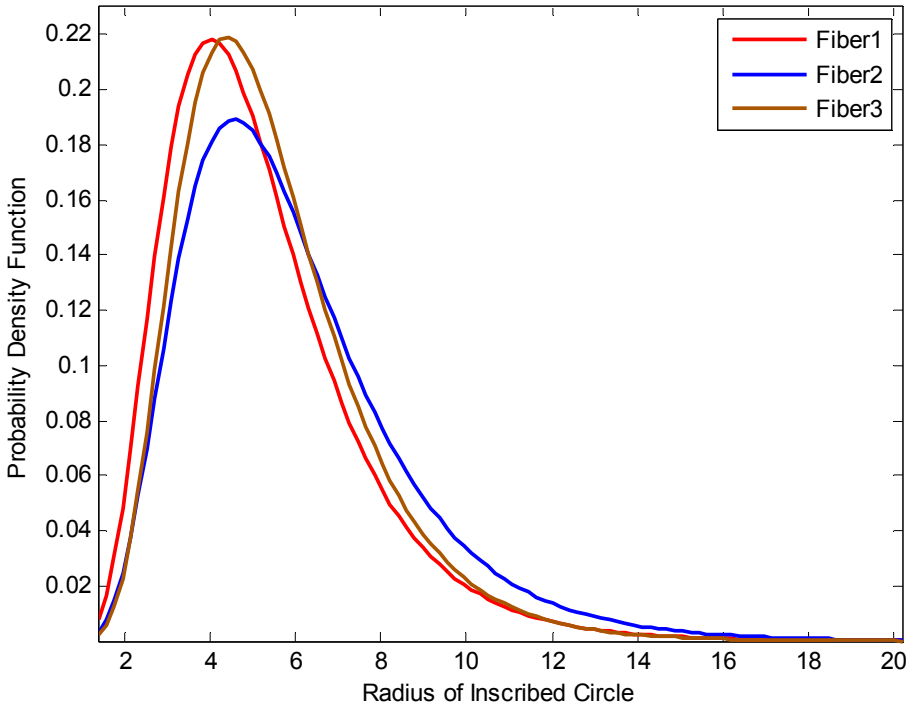

Figure 4-20 Log normal probability distribution fit for the radius of the inscribed circle in nm for membrane pores in different fibers that were taken from the same type of UF membrane module used in this study.

Table 4-4 Log Normal probability distribution fitting for different UF fibers used in this study, and the log removal values obtained from mass transport modeling

	Radius of inscribed circle log normal fit			MS2 log removal	φX174 log removal
	μ	σ	Log Likelihood	27.4 nm capsid	33 nm capsid
Fiber1	1.56131	0.418658	-2722.93	1.80	2.23
Fiber2	1.69441	0.423694	-1868.57	1.50	1.86
Fiber3	1.62714	0.385435	-1759.46	2.03	2.52
Total	1.61727	0.414514	-6382.12	1.73	2.15

The log removal values obtained for both MS2 and φX174 using the mass transport model is consistent with the experimentally obtained values. For φX174, the log removal is very similar to the obtained removal at pH 9.4 where size exclusion was believed to be the dominant mechanism with minimal contribution of surface charge electrostatic repulsion (due to the virus geometry). This also supports the theory that at the pH 6.5 experiment, adsorption has a significant role in the removal of φX174. For MS2, the removal determined using the mass transport model is only half of the experimentally obtained log removal. This shows the big contribution of electrostatic repulsion to the rejection of MS2 bacteriophage.

4.4 Conclusion

UF membranes are one of the promising drinking water treatment technologies for removing enteric viruses from drinking water because the size of the viruses is similar to the pore size range of the UF membranes. A commercial UF membrane was used along with two different types of enteric virus surrogates with different characteristics and similar size to the smaller enteric viruses. The major objectives were to study the removal of both viruses under clean water conditions, to determine base removal values without the influence of membrane fouling. The experiments also investigated the effect of virus characteristics on the removal and reach a better understanding of the virus removal mechanism.

By applying a purification step of the bacteriophage stock solution, more than 99% of the organics in the solution were removed, and this was reflected on the low fouling potential of the virus feed solution in the virus challenge experiments. The design of the membrane bench scale unit and the protocol used for the virus challenge experiments was successful and could provide consistent results and stable performance of the UF bench unit. The operation of the bench scale unit was representative of that used in full-scale systems, and therefore the results will have application for the drinking water industry. This protocol will be further applied for the fouling experiments to investigate the impact of membrane fouling.

For both types of bacteriophage, the UF membrane tested in this study achieved high removals (above 2 log). The more negatively charged MS2 bacteriophage was better removed than φX174 bacteriophage, even though φX174 is larger in size. Size exclusion is the main removal mechanism for enteric viruses, but the effect of the electrostatic interactions could greatly increase the removal of viruses. The importance of electrostatic interactions was especially important for MS2 bacteriophage,

and may explain the higher removal of this phage type compared with φX174. φX174 bacteriophage was affected by the pH of water, and the increase in pH decreased the removal of φX174 bacteriophage. Adsorption of φX174 bacteriophage obviously occurred at pH of 6.5 as the removal dropped from 4.7 to 3.2 logs over time during the virus challenge experiment, however this adsorption effect was not seen at pH 9.4. φX174 removal trends at pH 9.4 were similar to MS2 bacteriophage tested at pH 7.6, but φX174 had a lower rejection.

According to these results, the geometry of the virus capsid and its net surface charge will greatly influence the removal by UF membranes. For viruses with a high isoelectric point like φX174, the conditions of the experiment such as the solution pH and the filtration time needs to be controlled as they can greatly influence the rejection of the viruses.

The UF membrane pore size distribution was useful in predicting the rejection of both types of viruses; however the electrostatic interactions could not be accurately predicted. Modeling the rejection of the viruses can help in more understanding of the rejection mechanism of viruses. This can be a useful tool to predict the minimum removal of a certain virus by UF membranes due to the pore size distribution of the membrane and the virus size. This would be a conservative tool to predict the removal of viruses by UF membranes.

In summary, a better idea about the removal mechanism of enteric viruses by a UF membrane was obtained by using two different types of bacteriophage together with a study of the membrane surface characteristics. Both types of bacteriophage provided useful information than can be used to predict enteric virus removal by UF membranes.

Chapter 5
The Impact of Fouling of Ultrafiltration Membranes on the Removal of Enteric Virus Surrogates

5.1 Introduction

UF membranes are now widely used for the treatment of surface waters to provide safe drinking water. Membrane fouling is a major problem for municipalities and producers that use membrane filtration. Fouling can be defined as a decline in productivity of the membrane unit either by a decline in permeate flux when operating at a constant transmembrane pressure or by an increase in transmembrane pressure when operating at constant permeate flux. Reversible and irreversible fouling can be responsible for this, as will be explained. As a result of fouling, membranes require cleaning to retain their original performance. Hydraulically reversible fouling effects can be reversed by mechanical means (i.e. backflushing/backpulsing of the membrane), whereas hydraulically irreversible fouling requires the use of chemical cleaning agents. Maintenance cleaning using only chlorine is usually employed in full scale membrane filtration plants where chlorine is used for a short period of time usually few minutes to remove organic fouling and retain most of the membrane permeability. Maintenance cleaning can be done daily based on the rate of fouling but full chemical cleaning will be required on longer time periods usually every few months to retain the original permeability of the membrane unit.

As discussed in Chapter 4, UF membranes have a good potential for removal of enteric viruses by different removal mechanisms. The effect of fouling on this base removal will likely be an important factor in a full scale water treatment plant. The interactions between membrane surface characteristics and viruses are believed to play an important role in the removal of viruses. As a result, any changes in membrane surface characteristics due to fouling could have an effect on virus removal.

5.1.1 UF membrane fouling

The different types of fouling that can occur on UF membranes include organic, inorganic and biological fouling. A major type of fouling for UF membranes, especially in drinking water treatment, is organic fouling which is very complex in nature. Natural organic matter (NOM) and also effluent organic matter (EfOM) found in surface waters are believed to be a common cause of UF membrane fouling as numerous studies sometimes with conflicting results can attest (de la Rubia *et al.* 2008,

Jarusutthirak *et al.* 2007, Lee *et al.* 2004, Lee *et al.* 2006, Makdissy *et al.* 2002, Verliefde *et al.* 2009, Zularisam *et al.* 2006). NOM is a mixture of organic molecules, varying in molecular weight, composition and properties, and can be found in nearly all water sources. A major component of NOM is humic substances. Reports on the fouling potential of humic substances are varied and it seems to depend among other factors on the properties (esp.MWCO) of the membrane. Humic substances show less fouling than for example biopolymers due to their lower molecular weight (MW), and thus have lower hydrophobic interactions. Humic substances also contain a large number of carboxylic acid functional groups so they experience more repulsion with a negatively charged membrane surface (Hong and Elimelech 1997). Humic substances main fouling mechanism will be adsorption to a hydrophobic membrane surface or aggregation due to the presence of inorganic ions such as calcium (Yuan and Zydney 1999). Adsorption of humic substances to polymeric membranes made the membrane more negatively charged and increased surface hydrophobicity and this effect increases as humic substances continue to adsorb to the membrane surface and inside the pores as well (Jucker and Clark 1994).

An important fraction of the effluent organic matter, polysaccharides and proteins are considered to be the major fouling agents for UF membranes due to their higher MW (Hallé *et al.* 2009, Lee *et al.* 2004, Zheng 2010, Zheng *et al.* 2010). Using alginate as a model for polysaccharides, Jermann *et al.* (2007) found that it can cause more severe fouling to the UF membrane compared with humic acids. He also concluded that alginate and humic acid react with membranes in a different way, as alginate causes more reversible fouling than humic acid. Alginate will mainly block smaller membrane pores or aid in the formation of a cake layer due to its larger MW while the humic acid will be removed by different mechanisms due to its smaller MW. Another explanation is that alginate is able to form a gel layer on the membrane surface (Li and Elimelech 2004). Similar findings were reported for Bovine Serum Albumin (BSA) as a model for protein. Large BSA molecules compared to the UF membrane pores were believed to form a gel layer on the membrane surface which cause membrane fouling (Haberkamp *et al.* 2008). Lee and co-authors (2004) suggest that the larger MW hydrophilic fraction of the NOM in water, the more fouling will happen even if the DOC level was lower. This is based on their contact angle measurement for the surface of clean and fouled membranes and they concluded also that the fouling layer viewed in their AFM images was more hydrophilic than the original clean membrane surface(Lee *et al.* 2004).

Other types of fouling include inorganic fouling and biofouling. Inorganic fouling and scaling is controllable for UF membranes in surface water applications as the concentrations of rejected ions will not be high enough to cause severe salt precipitation. Any scaling can be reversed through suitable chemical cleaning employing acids such as citric acid. For biofouling, it can affect the UF membranes in the long run as deposited bacteria on the membrane surface can form a biofilm, resulting in a flux decline or an increase in transmembrane pressure (Flemming 1997, Vrouwenvelder *et al.* 1998). Bacteria deposited on the membrane can produce extracellular polymeric substances (EPS) such as polysaccharides and proteins that fix the biofilm and form the biofouling layer (Flemming *et al.* 1997). Operationally biofouling of UF membranes is controlled through regular chemical cleaning with disinfectant - most commonly chlorine.

5.1.2 Fouling mechanism and impact on virus removal

Membrane fouling mechanisms are not fully understood. Fouling is known to have an effect on membrane surface charge, hydrophobicity and porosity which can interfere with virus removal. One of the common theoretical membrane fouling models is the pore blockage model developed by Hermia (1982) depicting foulants as particles. It involves four different fouling mechanisms for membranes which can be described by simple mathematical formulas. The four fouling modes are shown in Figure 5-1 and are described as follows:

- Complete blockage: each particle similar in size to the pore deposited on the surface blocks a membrane pore preventing water from passing through it. These particles form a monolayer over the surface.
- Intermediate blockage: particles block the membrane pore in the same manner as in complete blockage; but particles can be adsorbed in multilayers thus reducing the number of particles available to block individual pores.
- Standard blocking: particles smaller than the pores deposit within the membrane pores and adsorb to the pore walls causing a restriction of the pore and a reduction in overall pore area.
- Cake layer formation: for larger particles that are too big to enter the pores, they will form a porous cake layer on the membrane surface.

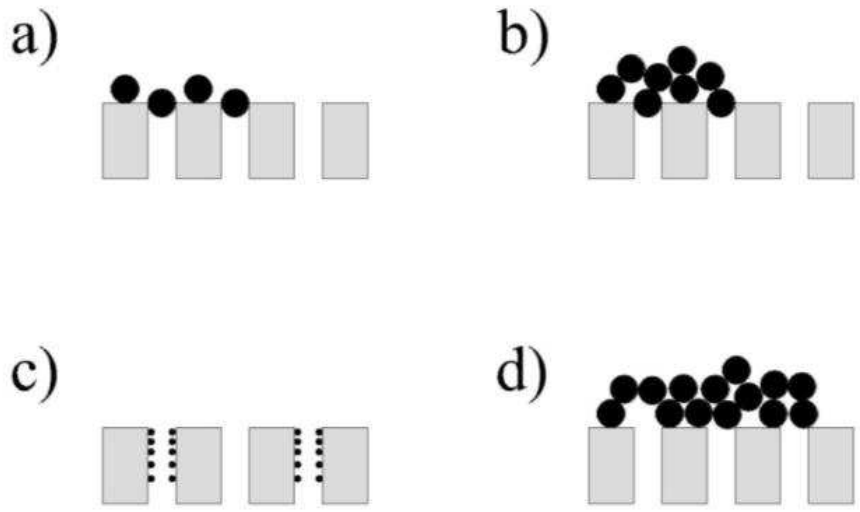

Figure 5-1 Fouling modes according to the Hermia model (Hermia 1982): a) complete blocking, b) intermediate blocking, c) standard blocking, and d) cake layer formation.

Hermia's model was developed for dead end filtration with a constant transmembrane pressure which is different than the constant flux filtration used for the UF system in this study. A modification to this model was done to account for the constant flow rate filtration (Hlavacek and Bouchet 1993, Huang *et al.* 2007) and was used for analysis of fouling mechanisms in this study. The general model given by Huang *et al.* (2007) is as follows:

$$\frac{dP'}{dV_s} = k_v * P^n$$

$$P' = \frac{P}{P_0}$$

Where:

P	Transmembrane pressure at time (t)
P_0	Transmembrane pressure at time zero
Vs	Cumulative permeate volume per membrane surface area
n	Constant depending on the filtration mode
k_v	Fouling parameter

The value of the fouling mode constant (n) describes the final relationship between the TMP (P') values and the cumulative permeate volume (V_s) as shown in Table 4-1. The n value is indicative of the fouling mode. The final relationship is found using integration of the general expression represented above. This is similar to the relationships represented by Hlavacek and Bouchet (1993) for all the four fouling modes.

Table 5-1 Linearized form for the different fouling models under constant flow rate conditions (Kang *et al.* 2007)

Fouling Mode	n	Relationship
Complete blockage	2	$\frac{1}{P'} = -k_v * V_s + Constant$
Intermediate blockage	1	$\ln(P') = k_v * V_s + Constant$
Standard blockage	3/2	$\frac{1}{\sqrt{P'}} = \frac{-k_v * V_s}{2} + Constant$
Cake Layer formation	0	$P' = k_v * V_s + Constant$

Evolution of membrane fouling for MF membranes were predicted by (Bowen et al. 1995) using Hermia's model for constant pressure filtration For MF membranes, they found that the first step was complete blockage of the larger pores followed by covering the inner surface of larger pores. Later the particles will start to adsorb over each other as intermediate blockage, and finally cake layer formation starts to occur. For UF membranes with a smaller pore size than MF membranes and a broad pore size distribution, like the one used in this study, it is hypothesized that standard blocking will happen first as smaller protein molecules or humic substances will adsorb to the membrane pores to decrease their dimensions, then complete blockage or intermediate blockage may occur due to larger molecules such as biopolymers followed by cake formation.

The three blocking mechanisms (complete, intermediate and standard) are expected to affect virus removal by either blocking the larger pores or narrowing them. This will enhance the size exclusion removal mechanism as it will block larger pores that can pass the viruses. Cake layer formation will affect both hydrophobic and electrostatic adsorption of viruses to the cake layer or to the modified surface. In addition, the fouling material can alter the membrane surface charge which will affect the electrostatic repulsion between the viruses and the membrane surface.

Reversible fouling which can be removed by backwashing is not believed to have a substantial effect on virus removal under backwashing conditions employed in practice. Jacangelo *et al.*

(2006) used a UF pilot plant with a submerged membrane unit (35 nm pore size) and during a 4 h filtration cycle, the increase in the removal of MS2 bacteriophage was not significant. The maximum increase was 0.9 logs but this was observed for a single sample. Unlike reversible fouling, irreversible fouling was able to improve virus removal for the same pilot UF membrane unit as it achieved a constant and stable increase in the removal of MS2 bacteriophage by 0.5-1.5 logs in 8 d long experiments. These findings were confirmed on a different UF pilot unit as well (Jacangelo *et al.* 2006).

Elements of the surface water matrix are not believed to have an effect on the virus removal by membranes. For four different types of tested membranes, adding NOM in the form of Suwannee River fulvic acid did not affect the removal of MS2 bacteriophage by any of the tested membranes in the bench scale experiments (Jacangelo *et al.* 2006). However viruses may adsorb to or aggregate with particles or organic foulants prior to membrane filtration and which can enhance virus removal. This can be reflected on the membrane performance as increased fouling rate either due to adsorption or pore blockage (Urase *et al.* 1994, van Voorthuizen *et al.* 2001). This can be viewed as an effect of fouling on virus removal.

5.1.3 Objectives

The major objective of this study was to evaluate the impact of both reversible and irreversible fouling on the removal of both MS2 and φX174 bacteriophage. The experiments were designed in a way that would simulate the real conditions in a full scale water treatment plant employing UF membranes. Also the effect of maintenance cleaning of the UF membrane using sodium hypochlorite only (i.e. the partial removal of the foulant layer) on virus removal was evaluated. Two different types of surface waters, including river water and lake water, were used to evaluate if the type of surface water would affect the nature of the fouling layer and also virus removal. A better insight of how fouling affects the removal of viruses can help in understanding the interactions between viruses and UF membranes. This information will be beneficial for plant operators and regulators, as fouling is expected to improve the efficiency of UF membranes as a barrier for waterborne pathogens.

5.2 Materials and methods

5.2.1 Surface waters

Two different types of surface waters were used as feed water in this experiment. The first surface water was the Grand River in Kitchener, Ontario, Canada. This river is highly impacted by agricultural activities and treated municipal wastewater effluents. The water was taken from a biofiltration pilot plant which was located at the full-scale Mannheim Water Treatment Plant. The full scale plant employs coagulation/sedimentation then ozonation prior to biological filtration. Disinfection is done using UV disinfection followed by chloramination. Both plants used the same Grand River water influent. The pilot biofilter had an empty bed contact time of 15 min and the filter media consisted of gravel, sand and anthracite. Biofiltered water was used instead of the raw water as the raw water without a proper pretreatment was known to cause very high fouling rates of the membrane unit which were not representative of the degree of fouling aimed for in this investigation. The biofilter has been shown to lower the biopolymer concentration in the feed water which is known to be a major fouling component of UF membranes (Hallé *et al.* 2009). For each fouling experiment performed using Grand River water, 800 liters were collected in four 250 liters tanks at the treatment plant. These were then transported to the University of Waterloo and the collected water was pumped into the feed tank for the bench scale unit using a submersible pump. This amount of feed water was sufficient to provide the influent for each long term experiment (1 week experiment). A 1,200 L open stainless steel container was used for storing the feed water without any mixing.

The second source of surface water was Lake Huron water from the Georgian Bay, Collingwood, Ontario, Canada. The water was taken from the feed of the Raymond A. Barker UF Water Treatment Plant which has a treatment train of pre chlorination of raw water prior to UF membrane filtration then post chlorination. The water was subjected to low level pre-chlorination to limit the bacterial growth and organic fouling of the UF units. A batch of 2000 L was collected from the intake to the full scale UF membrane system after pre chlorination in a tanker truck, and then transported to the University of Waterloo the same day it was collected, and pumped into the feed tank for the bench scale set-up as described for the Grand River water. Residual chlorine was still present in the feed water in such low concentration that it was below the detection limit of the free chlorine test of the HACH spectrophotometer test (i.e. less than 0.02 mg/L). Using a simple 24 hrs incubation test it was found to cause approximately 1 log reduction in φX174 phage concentration.

Hence, the chlorine residual was quenched using sodium thiosulfate at a final solution concentration of 2.25 mg/L $Na_2S_2O_3$ in the overhead tank. For the first spiking experiment at the start of the membrane fouling a 1000-fold higher thiosulfate concentration was added by mistake to a final concentration of 2.25 g/L $Na_2S_2O_3$ which raised the conductivity from 195.9 µs/cm to 3000 µs/cm. For all the other experiments the regular thiosulfate concentration was used (2.25 mg/L $Na_2S_2O_3$). Regular operation of the unit without viruses to develop fouling was done without any chlorine quenching.

5.2.2 Fouling experiments

The long term fouling experiments were operated continuously till the required degree of fouling was reached. The intention in this study was to simulate fouling close to what may be experienced at a full-scale plant and the operating flux was therefore chosen to achieve moderate levels of fouling. This was confirmed using a simple sustainable flux experiment for the Grand River water by running the membrane at different fluxes for 3 cycles to evaluate the fouling rate at this flux. Following this, all experiments were done at a flux of 51 LMH. A similar flux was employed in a previous study using the same source water and UF membrane (Hallé *et al.* 2009). A higher permeate flux was not used as it might compact the cake layer formed on the membrane surface and result in increased irreversible fouling. The chosen flux was fixed for the different experiments to be able to compare them.

The unit was operated continuously using the control system. For each spiking event automated operation was stopped until the spiking event was completed and then the regular automated operation was resumed. TMP was monitored every 15 secs during the whole experiment and water temperature was measured daily. The other water quality parameters including LC-OCD and Fluorescence EEM samples were sampled prior to each spiking event. The chemically cleaned UF membrane module was used in each experiment. The experiment was done indoors, and temperatures fluctuated only slightly as shown in Table 5-2. These fluctuations were accounted for by correcting TMP profiles shown in Figure 5-6 to 4-7 to 20°C as described in Chapter 4. The unit operated under the same protocol as described in Chapter 4 which simulated operating conditions at full-scale membrane plants. Integrity and clean water permeability tests were performed on the chemically cleaned and fouled modules to check the cleaning efficiency and to evaluate the extent of fouling as described in Appendix B. For safety reasons both filtrate and waste were collected and first bleached before being discharged into the sewer.

5.2.3 Virus Challenge experiments

Within each fouling experiment, four challenge tests for bacteriophage removal by the UF membrane were done. The first challenge test was done at the start of the experiment after conditioning the membrane by running it for 3 filtration cycles using the surface water. No irreversible fouling layer had been formed on the membrane, and this challenge test was done to show baseline virus removal rates in natural water, and to assess the effect of reversible fouling of the UF membrane on virus removal. The second spiking event was done at approximately 50% increase in TMP to evaluate the impact of moderate irreversible fouling. The third challenge test was performed at approximately 100% increase in TMP to evaluate the impact of severe irreversible fouling on virus removal. After the third challenge test, the membrane module went through a maintenance cleaning which is performed daily at most full-scale membrane plants. To conduct the maintenance cleaning, the UF module was soaked in 500 mg/L free chlorine solution (prepared using commercial bleach) for 5 min to oxidize the fouling layer. The module was then rinsed with deionized water to remove the remaining chlorine, and then operated using the feed water for 2 cycles to flush the residual chlorine. TMP readings after maintenance cleaning provided an indication of cleaning effectiveness where a decrease in TMP readings indicated increased permeability and therefore a change in fouling layer on the membrane. The fourth spiking test was done after maintenance cleaning to evaluate changes in membrane fouling layer on the removal of the enteric viruses.

All virus challenge experiments were done using the same protocol previously described in Chapter 4 section 4.2.6. Samples for bacteriophage enumeration were collected and analyzed in triplicate within 24 h.

5.2.4 Analytical methods

Analytical methods for TOC, LC-OCD, conductivity, UV absorbance and pH, were performed as described in Chapter 4. The levels of protein and humic like substances in the water samples were measured by fluorescence excitation emission (EEM) spectroscopy done at the University of Waterloo using a Varian Cary Eclipse Fluorescence Spectrophotometer (Palo Alto, CA), collecting 301 individual emission intensity values (within the 300 – 600 nm emission range) at sequential 10 nm increments at excitation wavelengths between 250 nm and 380 nm. A detailed description of the technique is available elsewhere (Peiris *et al.* 2010).

5.3 Results and Discussion

5.3.1 Water quality

Both experiments using the Grand River water were done at the end of the summer season (late August and late September 2010). Heavy rainfall during that period may have affected the water quality as an increase in the TOC levels (Table 5-3) and turbidity (Table 5-2) which are fairly high for the pilot biofilter effluent used as feed in these experiments. The Georgian Bay experiment was done early November at the start of the winter season but before the water temperature dropped. The pH during the two Grand River water experiments was 8.3, and that of the Georgian Bay water was also 8.3 but with a slightly declining trend throughout the experiment. Thus the impact of pH on the removal results was assumed to be very similar in both types of water. A drop in the turbidity of the feed water was observed over time during the experiment, as measured during each the challenge tests in all three experiments. This likely indicated some settling of particles in the feed tank. The Grand River water had higher conductivity than the Georgian Bay water but both were well below conductivity values of approximately 37000 which have had a significant effect on the rejection of viruses by a 0.1 μm MF membrane according to (Jacangelo *et al.* 2006).

Table 5-2 Water quality parameters for the different fouling experiments.

	Grand River MS2 August 17, 2010			Grand River φX174 September 28, 2010			Georgian Bay φX174 November 4, 2010		
Spiking event	1st	2nd	3rd	1st	2nd	3rd	1st	2nd	3rd
Temperature °C	22.6	22.2	21.7	20.1	21	20.3	19.2	19.8	19.6
pH	8.3	8.3	8.3	8.3	8.3	8.3	8.3	8.2	8.1
Conductivity μs/cm	NA	NA	540	541	530	518	3000*	198	198
Turbidity NTU	1.4	0.61	0.47	1.1	0.74	0.52	0.97	0.93	0.56

* Due to experimental error, higher amounts of sodium thiosulfate was added and raised conductivity to 3000 μs/cm. The conductivity of water without sodium thiosulfate addition was 196 us/cm.

The NOM of the feed water was quantified as TOC and DOC as shown in Table 5-3.. TOC is the total amount of organic carbon found in particulate and dissolved fractions of NOM while DOC is the amount of organic carbon found in the dissolved fraction that will pass a 0.45 µm filter. The difference between TOC and DOC for the feed can show the amount of particulate organic matter in the unit feed water. But for the permeate the DOC should be the same as the TOC as the used membrane pore size is less than 0.45 µm. The organic carbon rejection through the unit will be the difference between the TOC of the feed and the DOC of the permeate as this fraction was retained by the membrane and can cause fouling. The Grand River water for the first MS2 experiment had the highest TOC of 10 mg/L and this may have been due to seasonal impact on the water source as explained earlier. In the second Grand River experiment, the TOC was much lower. No obvious differences were noted between the TOC or DOC values among the three days of each experiment. The OC rejection for the first Grand River experiment was higher than the other two experiments which had a similar OC rejection. The Nature of the organic constituents in the Georgian Bay water can be also affected by the pre chlorination step as some of the organics could have been oxidized.

Table 5-3 TOC/DOC values of feed and permeate samples for the UF unit for the three experiments.

		Grand River MS2 August 17, 2010			Grand River φX174 September 28, 2010			Georgian Bay φX174 November 4, 2010		
	Spiking event	1st	2nd	3rd	1st	2nd	3rd	1st	2nd	3rd
Feed	TOC mg/L	10.5	10.9	10.8	6.85	6.92	7.07	2.02	2.02	2.13
	DOC mg/L	NA	NA	NA	6.71	6.79	6.89	1.79	1.98	2.00
Permeate	DOC mg/L	9.59	9.43	9.83	6.50	6.59	6.44	1.80	1.71	1.81
Overall OC rejection	mg/L	0.93	1.51	0.98	0.35	0.33	0.63	0.22	0.31	0.32
Overall DOC rejection	mg/L	NA	NA	NA	0.21	0.2	0.45	-0.01	0.17	0.19

5.3.2 NOM characterization in the feed water

The different fractions of the NOM in the feed water were characterized by both LC-OCD and fluorescence EEM. LC-OCD fractionates the DOM found in the sample using a size exclusion column into four different fractions as shown in Figure 5-2. The biopolymer fraction of the NOM is characterized by the peak around an elution time of about 33 min for the LC-OCD chromatographs, denoted (A), as shown in Figure 5-2. This fraction will have a MW of more than 10 KDa and is thought to contain both proteins and polysaccharides (Huber *et al.* 2011). Proteins contain nitrogen and they should therefore be detected by the organic nitrogen detector (OND). But since neither proteins nor polysaccharides contain any UV absorbing moieties this fraction will not have a UV absorbance signal as indicated by the UV detector (UVD). The OCD signal for fraction A was integrated manually to find the area below this peak which is an indication of the biopolymer concentration in the feed sample and the permeate sample of the UF unit. The second and largest Peak (B) is humic substances and since they have a smaller MW they will be less affected by the UF membrane. Peak (C) represents building blocks which sometimes appear as a shoulder of the humic peak. Peak (D) represents low MW acids and (E) represents low MW neutrals. LC-OCD chromatographs of samples of all experiments are shown in Appendix D. The biopolymer concentrations for the three spiking events in the different experiments are shown in Table 5-4.

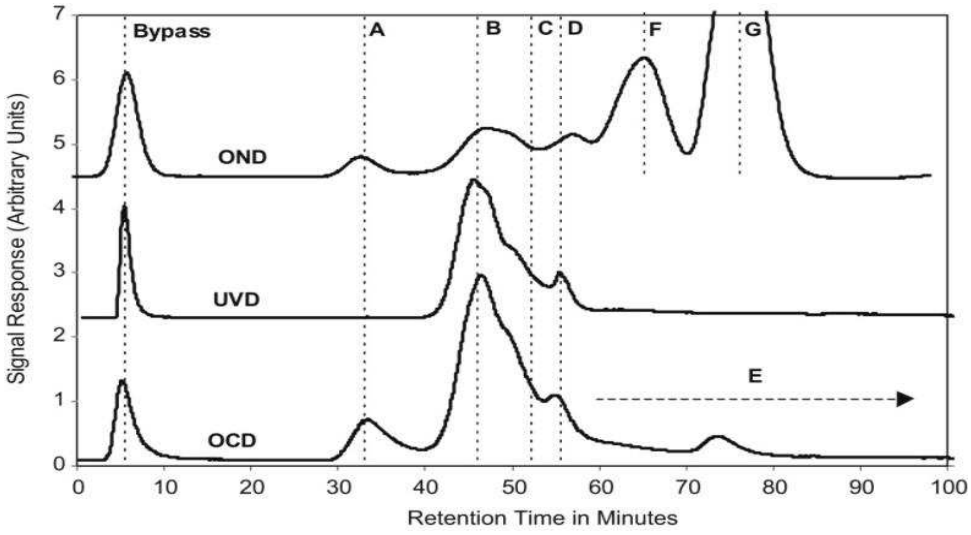

Figure 5-2 Typical LC-OCD results (Huber *et al.* 2011).

The first experiment of the Grand River showed a decline in the biopolymer concentration over time. This was confirmed later using fluorescence EEM. This was possibly due to either aggregation that

was removed by the 0.45 µm pre filtration during sample preparation for LC-OCD measurement or due to settling in the feed tank during the fouling experiment. The other possibility was degradation of this fraction by bacteria found in the feed water tank during the fouling experiment. However, the percent rejection of the biopolymers by the UF membrane in this first GR experiment dropped only a slightly during the 3 different spiking events. This indicates that the nature of the biopolymers nearly remained the same although its concentration was changing. This discounts the theory that aggregation caused a decrease in the biopolymer concentration. However, it is possible that degradation of the biopolymer fraction was taking place. For the second experiment with Grand River water, the TOC and DOC levels were similar over time and the biopolymers concentration and rejection remained also stable. This may be due to the nature of the organics found in the water in this second Grand River water experiment compared to the first one which had a significant higher TOC level.

For the Georgian Bay water, the biopolymer levels in the feed water were lower than in the second Grand River water experiment but showed a similar percent rejection of biopolymers by the membrane. Also, similar DOC rejection values (Table 5-3) were obtained except for the third spiking in the second Grand River water experiment and the first spiking of the Georgian Bay water experiment which can in part be due the TOC instrument sensitivity at this low OC levels. Biopolymers formed a fairly large fraction of the NOM of the Georgian Bay water compared to the Grand River water as shown by comparing the Biopolymers concentration from Table 4-4 to the DOC values of the samples in Table 5-3.

Table 5-4 Biopolymer concentrations and removals for the three fouling experiments

	Grand River MS2 August 17, 2010			Grand River φX174 September 28, 2010			Georgian Bay φX174 November 4, 2010		
Spiking event	1st	2nd	3rd	1st	2nd	3rd	1st	2nd	3rd
Feed (µg/L C)	382	189	181	527	534	514	408	402	400
Permeate (µg/L C)	91	49	52	159	157	146	133	146	152
Removal (µg/L C)	291	140	129	368	377	368	275	265	248
Removal %	76	74	71	70	71	72	67	64	62

The fluorescence EEM results can give more insight to the nature of the NOM. Usually; the result matrix of surface water has three apparent peaks. As discussed by Peiris *et al.* (2010) the first peak is around excitation/emission of 320/415 nm which corresponds to fulvic acid and a shoulder at 270/460 nm which belongs to the remaining humic-like substances. The second peak is at excitation/emission of 280/330 nm which corresponds to proteins-like matter. The last series of peaks in the excitation range of 260 to 300 nm and emission of 500 to 600 are caused by second order Raleigh scattering and they correspond to the colloidal and/or particulate matter (Peiris *et al.* 2010). The NOM fractions (i.e. peak 1 with shoulder) are usually not affected by the UF membrane since their MW is expected to be lower than the MWCO of most UF membranes. Thus there should be no difference between feed and permeate unless adsorption to the membrane plays a role. However, protein-like material (i.e. peak 2) is removed by UF membranes as seen in this study and by Peiris *et al.* (2010) and will contribute to fouling. Polysaccharides which together with the proteins comprise the biopolymers cannot be detected directly by fluorescence EEM as they do not have any fluorescent functional groups. In our analysis of fluorescence EEM data, examination of single peaks (i.e. fluorescence intensity at the coordinates defined above) is used instead of full spectra analysis to simplify analysis. Although this does not allow for quantitative analysis is sufficient to show trends. The measured peak heights for feed and permeate samples from different experiments are shown in Table 5-5.

Table 5-5 Peak height of the fluorescence excitation emission matrix for both humic substances and protein peaks for the different fouling experiments

		Grand River MS2 August 17, 2010	Grand River φX174 September 28, 2010	Georg. Bay φX174 November 4, 2010
Feed	Humics Peaks (Exc/Em=320/415)	831	631	38
	Protein like matter peak (Exc/Em=280/330)	118	101	39
Permeate	Humics Peaks (Exc/Em=320/415)	806	640	33
	Protein like matter peak (Exc/Em=280/330)	69	78	27

Fluorescence EEM of the first Grand River water experiment (August 2010) (Figure 5-3), resulted in a drop of the protein-like matter peak from a maxima of 117 in the feed at the first day of the fouling

experiment to 82 on the remaining days similar to the drop in the biopolymer peak in the LC-OCD results. For the second fouling experiment of the Grand River water, the maxima of the protein peak was stable at 101 throughout the entire experiment with more than 50% reduction in the permeate for all samples. This indicates that this fraction was partially retained by the membrane and likely contributed to membrane fouling. For the Georgian Bay water, the protein peaks were nearly the same for the feed at 39 compared to the permeate at 27. This showed that the proteins were passing through the UF membranes and did likely not contribute to membrane fouling. The removal of the biopolymer peak observed in the LC-OCD results for this water (Table 5-4) is therefore probably due to biopolymer constituents other than protein-like matter e.g. polysaccharides or organic colloids.

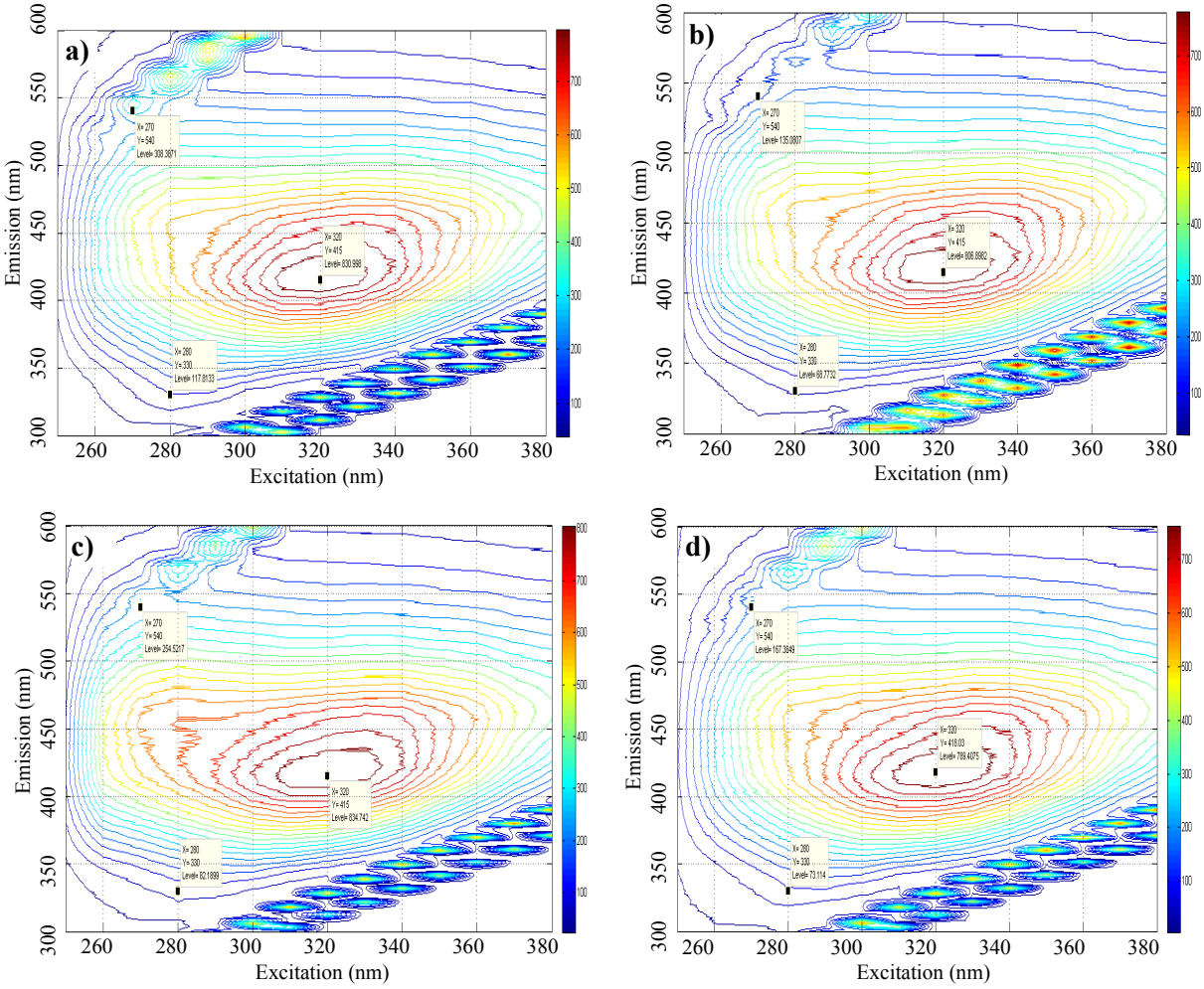

Figure 5-3 Fluorescence EEM of the first Grand River fouling experiment (August 2010) for (a) the feed of 1st spiking event, (b) permeate, (c) feed of 3rd spiking event, and (d) permeate.

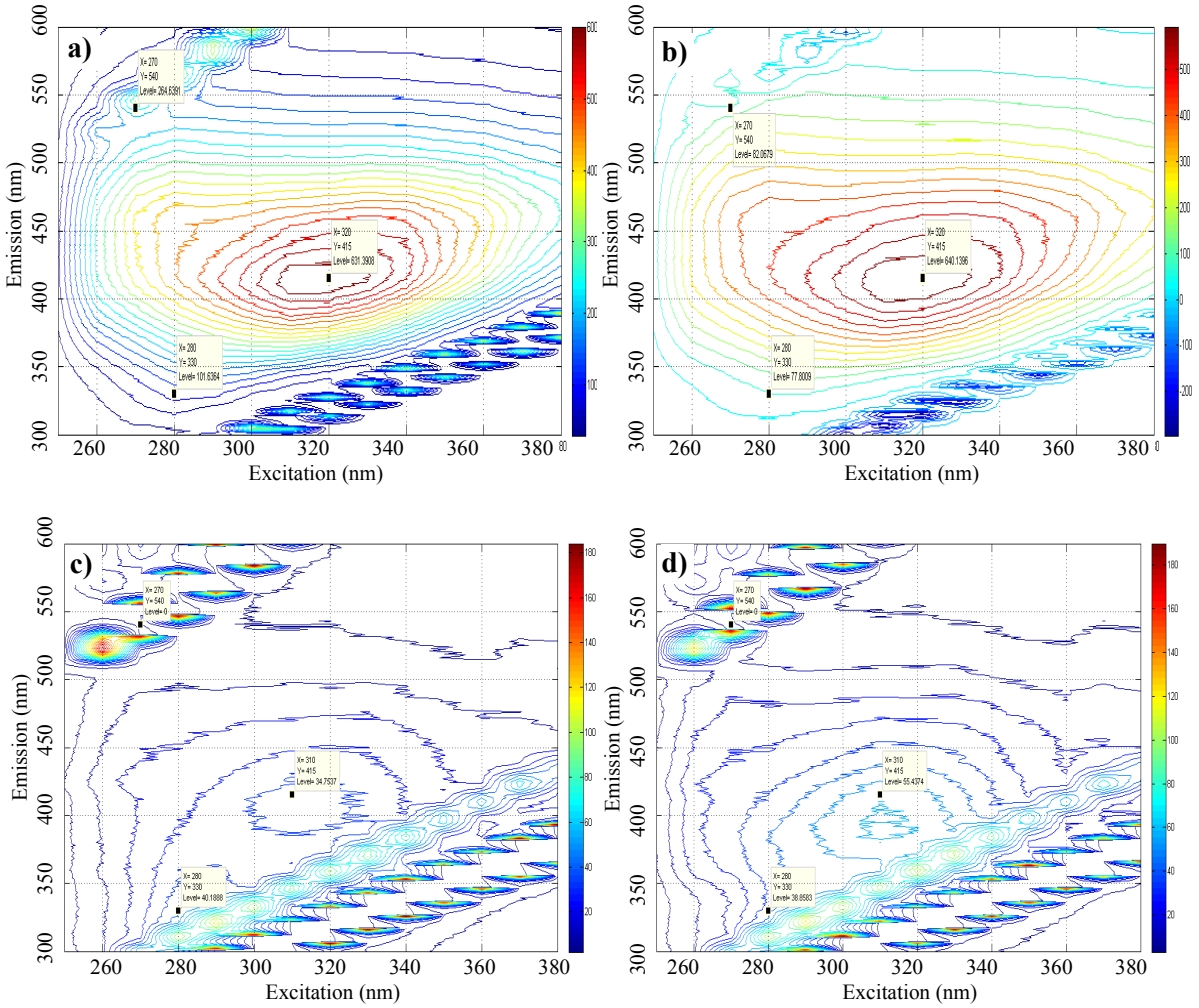

Figure 5-4 Fluorescence EEM of the second Grand River fouling experiment (September 2010) for (a) the feed of experiment 1, (b) permeate, (c) Georgian Bay fouling experiment of feed for experiment 1, and (d) permeate.

5.3.3 TMP profiles

For each fouling experiments, the unit was operated at constant flux over longer time periods (app. 5 d) using surface water and the TMP was monitored as an indication of the degree of fouling. MS2 or φX174 bacteriophage were spiked to assess virus removal at different degrees of fouling by spiking at 50% and 100% increase in TMP over the initial TMP. At the end of the experiment membrane maintenance cleaning was done prior to a last virus spiking to assess the impact of a partial removal of the foulant layer due to cleaning on virus removal. A sample of the recorded TMP is shown in

Figure 5-5**.** During each filtration cycle, both reversible and irreversible fouling start to develop at a rate which is the total fouling rate as indicated by the slope of the solid arrows. After backwash at the end of each cycle which is shown as the gap between the cycles, the reversible fouling is removed and only irreversible fouling remains. By monitoring the pressure increase at the start of cycles, the irreversible fouling rate can be measured as indicated by the dashed arrow.

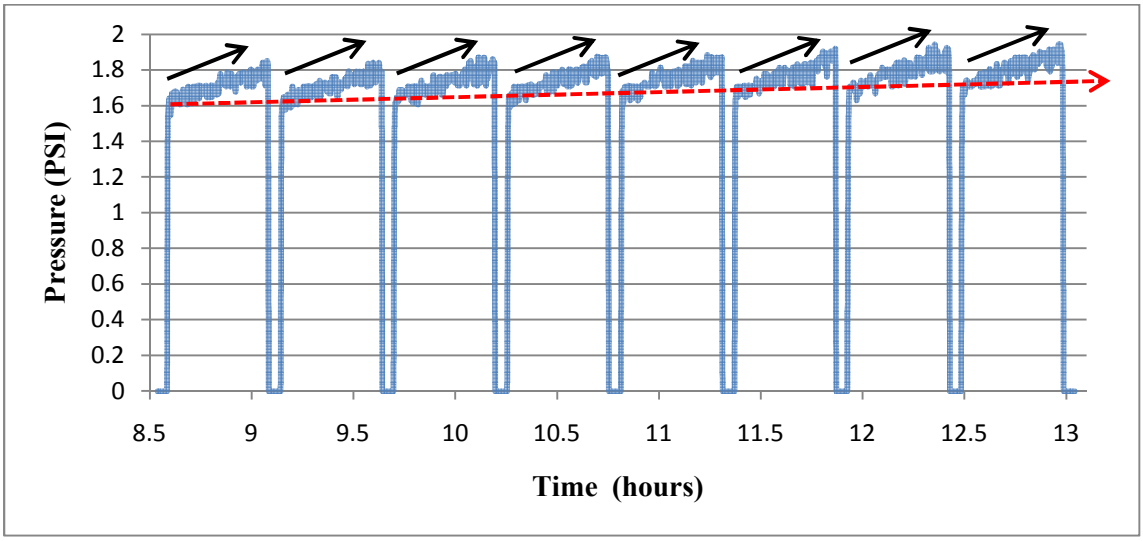

Figure 5-5 Sample data (8 filtration cycles) from the first Grand River water experiment showing the developing irreversible fouling as a dashed arrow and total fouling rate during each cycle as solid arrows.

The recorded TMP during the Grand River first fouling experiment is shown in Figure 5-6. A gradual increase in the TMP can be observed which is indicative for irreversible fouling. The first spiking event was done at the start of the experiment. Then the unit was operated for another 47 h, at which time the pressure increased to around 50% of the original TMP and the second phage spiking event was done . After the second spiking, the compressed air supply cylinder for the module was empty and needed to be replaced. The unit was turned off for 10 h for the replacement of the cylinder. This explains the drop in the TMP curve at the 50 h mark. The unit was operated again continuously until the third spiking. An obvious dip in the pressure can be seen around the 80 h of operation up to 85 h. No clear reason could be identified, but at about 90 h the pressure started to increase again but at a lower rate. The third phage spiking event was done at 105 h after a nearly 110% increase in TMP. After this third spiking event, the module underwent maintenance cleaning which partially removed the fouling layer. This is supported by the observation that the TMP was lowered by nearly 1 psi, however the TMP remained 33% higher than the original TMP. This shows that some of the fouling

layer still existed on the membrane. The last spiking was done after maintenance cleaning to evaluate the impact of the remaining membrane fouling layer on virus removal. The observed drop in the biopolymer concentration from the first to the second phage spiking as indicated by LC-OCD data (Table 5-4) did not have a clear effect on the apparent irreversible fouling rates.

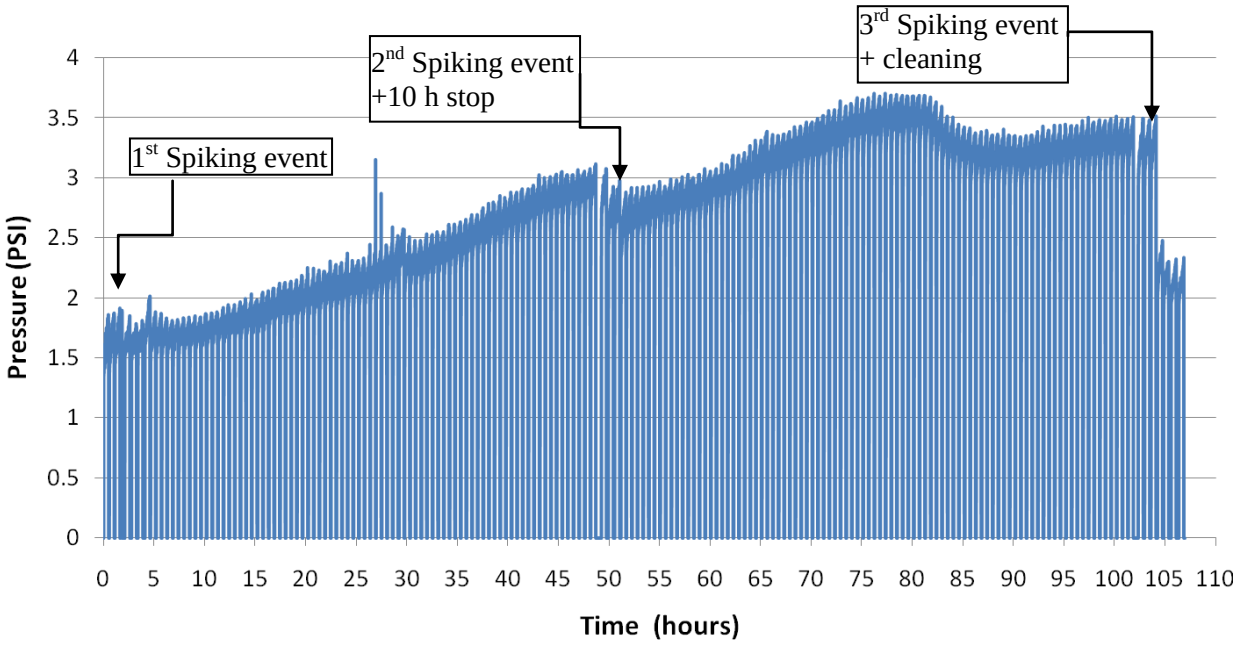

Figure 5-6 Recorded TMP for the first Grand River fouling experiment (August 2010).

The second Grand River fouling experiment (September 2010), was done to compare removal of MS2 and φX174 using a similar water and a similar testing procedure. The TMP profile is shown in Figure 5-7. The first spiking event was done at the start of the experiment and the second one was done after 57 h when the TMP increased by nearly 50%. The TMP continued to increase until 97 h of operation, then a power shutdown occurred resulting in a drop in TMP. The operation of the unit was then resumed and the last spiking was performed at 120 h of operation (150 % increase in TMP). After that the module had a maintenance cleaning that recovered most of the membrane performance, however the original pressure could not be recovered as the TMP was 0.2 psi higher than the original TMP so some fouling remained on the membrane. After maintenance cleaning the final spiking was done.

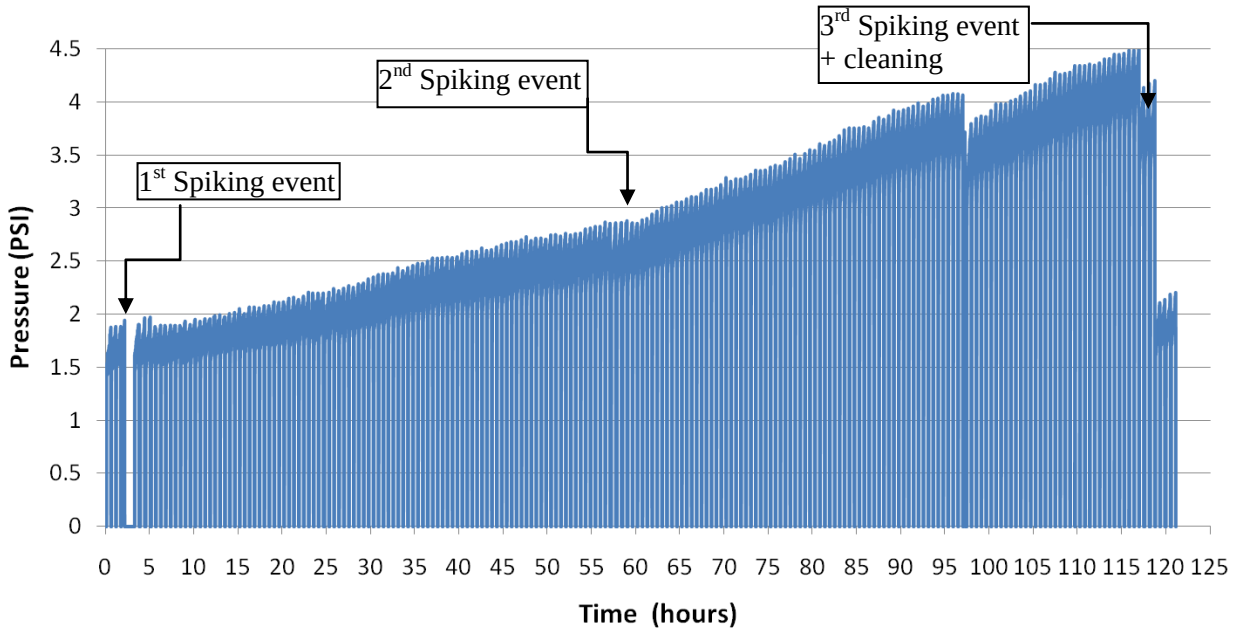

Figure 5-7 Recorded TMP for the second Grand River fouling experiment (September 2010).

The third experiment used Georgian Bay water and spiking of φX174 bacteriophage which proved to be more sensitive to pH than MS2 as explained in Chapter 4. The TMP profile for the Georgian Bay fouling experiment is shown in Figure 5-8. The fouling rate is clearly lower than the fouling rate obtained from the Grand River experiment. This can likely be attributed to a difference in water quality but the exact cause is difficult to determine. As shown in Table 5-4 biopolymer concentrations for the Georgian Bay water experiment were in between the concentrations observed for the Grand River water experiments. However, the composition of the biopolymers was likely different as the fluorescence EEMs indicated smaller protein-like matter peaks in he Georgian Bay water. This is consistent with Halle *et al.* (2009) who reported that biopolymer composition is likely to play an important role in irreversible fouling. In addition, pre chlorination of Georgian Bay raw water for zebra mussel control may have altered the composition of the NOM in the water by oxidizing some of the organic molecules. However, this change would have been reflected in the fluorescence and LC/OCD results as they have been obtained after prechlorination. The remaining trace amount of chlorine in the Georgian Bay feed water (less than 0.1 mg/L free Cl_2) at the start of the fouling experiment might have influenced fouling rates slightly. Note that chlorine residuals were quenched before phage spiking in the overhead tank (see Section 5.2.1 for further details). The first spiking was done at the beginning of the experiment and for the 3 cycles of this phage spiking the sodium thiosulfate concentration was higher than planned (see Section 5.2.1). The second spiking was done

after 95 h of operation after a 50% increase in TMP (similar to the Grand River experiments). After that the unit operation was resumed, but at 110 h of operation the unit experienced a decrease in TMP. This continued until 150 h, and was attributed to a slight integrity problem of the membrane. This was confirmed by conducting an integrity test at the very end of the experiment following intense chemical membrane cleaning. The pressure decay integrity test (Appendix B) showed that there was a pressure drop of 0.18 psi/3 min compared with 0.11 psi/3 min which was measured in all the previous integrity test on the same module. At 150 h, the pressure started to increase at a lower rate, and resumed to the previous value (about 3 psi) after 170 h. It is possible that membrane fouling was able to 'fix' the integrity problem, which would explain the drop and then the increase in pressure. The final spiking was done at 218 h of operation, at a TMP increase of 76% of the original values. It was not feasible to wait until 100% increase in TMP as in previous experiments since the feed water supply was running low. Finally a maintenance cleaning of the membrane was done followed by the fourth spiking. After maintenance cleaning, the TMP was slightly higher than the initial TMP by 0.1 psi. The membrane was chemically cleaned after that and a fifth spiking event was performed to see if the integrity problem affected the base removal or not.

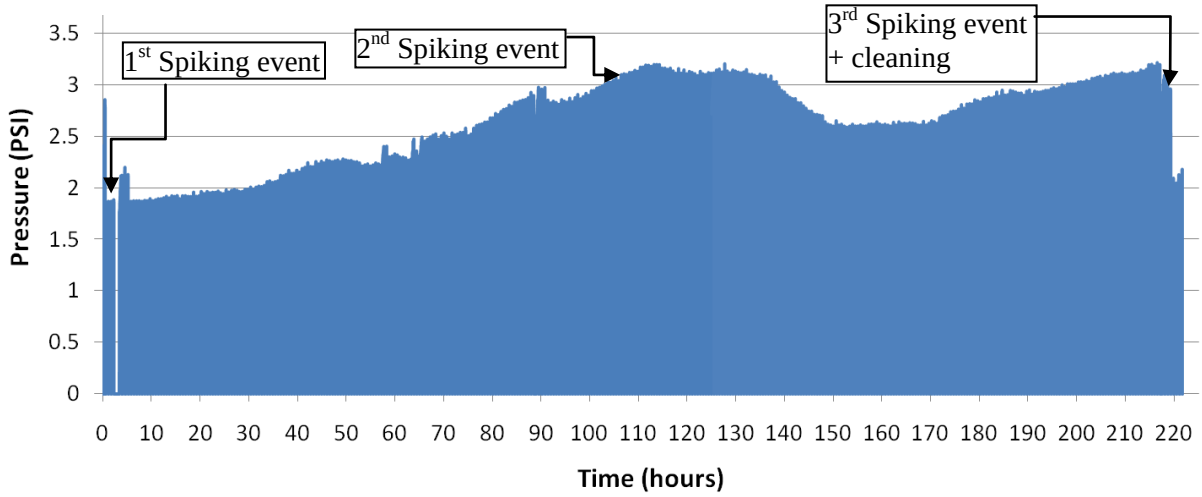

Figure 5-8 Recorded TMP for the Georgian Bay fouling experiment (November 2010).

5.3.4 Virus removal

For each fouling experiment, three different spiking events were done using either MS2 or φX174 bacteriophage. Spiking events were done at different degrees of fouling to evaluate the impact of fouling on virus removal. Three conditioning cycles without viruses preceded the spiking which was done over three filtration cycles. Samples were collected from the feed and the permeate at the start of

each cycle to measure virus removal at cycle start. At the end of the cycle a sample was collected from the permeate and then after the end of the cycle the unit was drained to a separate container to obtain the drain sample. The drain sample and the permeate sample at the end of the cycle were used to calculate the virus removal at the end of the cycle. The difference in removal between cycle start and the end of the cycle can show the effect of reversible fouling on virus removal. The virus concentrations of all the samples from each spiking event are shown in Appendix D. The virus removal results are shown in Figure 5-9 to 5-11.

The MS2 bacteriophage removal results of the different spiking events for the first Grand River water fouling experiment (August 2010) are shown in Figure 5-9. For the first spiking event (Figure 5-9a), the membrane had only been operated for 3 cycles and hence, there was not sufficient time for any substantial irreversible fouling to occur and the UF membrane was still clean at the time. Hence, any effect on the removal of MS2 bacteriophage can be attributed to any surface water matrix effects, if present, and/or any differences between the start and the end of the cycle would be caused by reversible fouling. The removal of MS2 bacteriophage was very consistent and stable for the three cycles. In addition, there was no difference in virus removal between the start and the end of each cycle. This shows that reversible fouling at these early stages of the membrane fouling experiment did not affect the removal of viruses. The average removal was 3.5 LRV which was comparable to the base value with deionized water that ranged from 3.5 to 3.9 (as shown in Chapter 4). This indicates that there is no significant difference between the removal of MS2 bacteriophage at pH 8.3 (Grand River water experiment 1st spiking) and at pH 7 (deionized water experiment). After the end of the first spiking event, the unit was operated using the surface water without viruses for one day then one sample was collected from the permeate and analyzed to ensure that no MS2 bacteriophage remained in the bench unit that would affect the second spiking experiment. The sample was negative as no viruses were detected.

For the second spiking event (Figure 5-9b), the TMP of the UF membrane increased by 50% allowing the evaluation of the impact of moderate levels of irreversible fouling and also the effect of reversible fouling. The removal of MS2 bacteriophage was up to the sensitivity limit (i.e. all of the spiked phage were essentially removed) at the start and the end of the first cycle with giving an increase of 2.5 LRV compared to the first spiking event. This increase can be attributed to the irreversible membrane fouling that developed on the membrane. Irreversible fouling may have blocked some of the larger pores or even made them narrower. It may have also masked or altered the surface charge of the membrane thus leading to some adsorption of the phage to the membrane surface or to the cake layer

which had been formed by then through irreversible and reversible fouling. For the second and third filtration cycle, the removal of the bacteriophage was lower than in the first cycle –especially at the cycle start. This may be explained by adsorption. In the first cycle adsorption of viruses was believed to be quite high and then as the adsorption sites were occupied less adsorption happened for the following two cycles. The removal at the start of cycle 2 and cycle 3 were very similar with LRVs of 5.1 and 4.9 respectively and there was a difference of 0.25 and 0.8 LRV between the start and end of cycles 2 and cycle 3, respectively. This indicates that reversible fouling started to have some effect on the removal of bacteriophage in this second spiking event whereas it did not for the first spiking event. This means that reversible fouling only had a positive impact on virus removal after irreversible fouling had occurred i.e. an irreversible fouling layer had been established. One interpretation may be that the porosity or the compressibility of the reversible cake layer may have been affected by the increased TMP caused by irreversible fouling.

For the third spiking event (Figure 5-9c), the membrane pressure had increased to 110% of its original value indicating that irreversible membrane fouling was well established. The virus removal results were very consistent, with the same removal at the start of the three cycles of 5.0 LRV. This is in the same range as the LRVs observed for the second spiking and it is higher by 1.5 LRV compared to the first spiking where no irreversible fouling was present. These results confirm the positive effect of irreversible fouling which may be attributed to the effect of fouling on the membrane pore size. Very similar removals in cycle 1-3 suggest that adsorption was likely not contributing to phage removal at this point unlike in the second spiking event that nearly reached similar removal of 5.0 logs at the start of second and third cycle. The removal at the end of all three cycles was also very consistent at 5.6 LRV, and it was higher than the removal at the start of the cycle. This positive effect of reversible fouling on phage removal was more obvious (i.e. a higher increase in LRV within a cycle) than for the second spiking experiment. This may be due to changes in the surface charge of the membrane which might have allowed for adsorption of the MS2 bacteriophage to the formed cake layer on the fouled membrane surface. However, this hypothesis could not be confirmed since zeta potential measurements of virgin and fouled hollow fiber membranes were beyond the scope of this study. Another potential explanation may be reversible pore blockage which would be removed by backwashing.

The results for the fourth spiking show that as soon as the irreversible fouling layer was partially removed by the maintenance cleaning, the removal of the MS2 bacteriophage dropped (Figure 5-9d). For the first cycle, the removal at the start and the end were exactly the same with 4.5 LRV. For cycle

2, the removal at start and end was exactly the same at 4.4 LRV. These results show that the removal of the membrane foulants resulted in a decrease in MS2 removal, but the removal was higher than that of the initial value of the clean unfouled membrane (first spiking event). The remaining irreversible fouling had an impact on the removal of viruses even after maintenance cleaning of the unit which included the use of a high free chlorine concentration. The stable removal within each cycle showed that reversible fouling did not affect MS2 removal as soon as the irreversible fouling layer was partially removed. This may be attributed to a potential change in the nature and porosity of the formed cake layer at these lower TMP values.

The results of the second fouling experiment using the Grand River water (September 2010) and spiking φX174 bacteriophage are shown in Figure 5-10. The pH of the river water was 8.3 which was the same as in the previous spiking experiment with MS2. However, the pH of 8.3 was an intermediate value between the previously tested pH values of 6.8 and 9.4 that were used in the clean water experiments in Chapter 4. Therefore, the expected removal of φX174 would be between 3.3 and 2.4 LRV that were measured at pH 7 and 9.9, respectively. For the first spiking event with the clean membrane (Figure 5-10a), the removal in the first cycle was 3.25 LRV both at the start and the end of the cycle. At the start of the second and third cycles, the removal was nearly the same with 3.0 and 3.1 LRV, respectively. The similarity of these results to the clean water experiments at pH 6.8 which had a minimum LRV of 3.2 indicate that there was no impact of the water matrix on the φX174 removal in Grand River water. This also shows that φX174 seems to behave similar at pH 7 and at pH 8.3. At the end of both cycles in the φX174 Grand River water experiments, the removal was 3.4 and 3.6, respectively, showing an increase in removal from the start of the cycle of 0.4 and 0.5 LRV, respectively due to reversible fouling. This is different from the MS2 experiment where no effect of reversible fouling was observed in the first spiking event. This difference between φX174 andMS2 may be attributed to the lower surface charge of φX174 thus allowing for easier association with the reversible fouling layer. Generally, MS2 removal was also confirmed to be higher than φX174 with an average log removal of 3.5 compared to average of 3.2 logs for φX174 at cycle start.

For the second spiking event shown in (Figure 5-10b) (at 50% TMP increase at 57 h), the removal at the start of first, second and third cycles ranged from 4.8, 4.5, and 4.4 LRV, respectively. Irreversible fouling substantially improved the removal of φX174 by more than 1.3 logs compared to the removal at the first spiking where no irreversible fouling existed. This effect is less pronounced than that observed in the case of MS2 Grand River water experiment where irreversible fouling increased LRVs by 2.5 logs. The removal at the end of the three cycles remained stable at 4.7 LRV but the

removals at cycle start, where no reversible fouling existed, dropped slightly from cycle to cycle. A possible explanation for this is adsorption of the phage to the membrane (i.e. higher adsorption was observed in the first cycle and due to exhaustion of adsorption sites removals dropped). This is similar to the observed drop in removal at cycle start in the MS2 Grand River experiment of 1.1 logs between cycle 1 and 3 in the second spiking event however this was much higher than the observed value in this second Grand River experiment. Also reversible fouling effect on virus removal was seen in the second and third cycle by having an increase in removal of 0.17 and 0.25 LRV, respectively similar to MS2 experiment as well. These effects were all similar between the two experiments albeit lower values were observed for φX174 than for MS2 in Grand River water. This may be attributed to differences in the nature of the membrane fouling as the water quality in the river changed between the two experiments. Another explanation would be the difference in size and surface charge between MS2 and φX174 bacteriophage which influenced the results in the clean water experiments as shown in Chapter 4. MS2 is smaller in size than φX174 bacteriophage so increased MS2 removals compared to φX174 can only be attributed to increased electrostatic repulsion or improved MS2 adsorption to the membrane. MS2 is more hydrophobic than φX174 phage with a lower isoelectric point which makes it more negatively charged than φX174 (Schijven and Hassanizadeh 2000). In addition, the surface charge on the membrane may have become more negative due to fouling/adsorption of humic substances (Jucker and Clark 1994). It follows that MS2 may have experienced more electrostatic repulsion which would explain the increased effect of irreversible fouling for MS2. For φX174 though adsorption onto the fouling layer may have taken place since it carries a low negative surface charge at pH 8.3 than MS2 bacteriophage. For the effect of reversible fouling or the drop in removal between cycles, MS2 higher hydrophobicity may have made it more amenable to adsorb to the fouling layer in the first cycle that will be missed in the other two cycles.

For the third spiking event (Figure 5-10c) (TMP increase of 150% at 97 h of operation), the φX174 removal was higher than the obtained removal in the second spiking event. The removal was 5.4 LRV at the first cycle then dropped to 5.2 in both cycle 2 and 3. This indicates that further irreversible fouling (i.e. 100% increase in TMP compared to the second spiking) increased the removal by 0.6 to 1.0 LRV. This was not observed in the MS2 experiment where removals remained at 5 LRV for the second (50% TMP increase) and the third spiking event (100% TMP increase). This showed that irreversible fouling further improved only φX174 bacteriophage removal. The reversible fouling effect on the φX174 removal was more pronounced in the third than in the second spiking event, as the LRV increased within each of the three cycles by 0.4, 0.7 and 0.6 LRV, respectively. This effect

is similar to that shown in the MS2 experiment. At more severe fouling conditions (i.e. 100% TMP increase due to irreversible fouling), both viruses behaved in a similar manner with regard to the effect of reversible fouling on virus removal.

For the fourth spiking event after the maintenance cleaning (Figure 5-10d), the removal decreased significantly as was expected since the fouling layer had been partially removed. The virus removal at the start of cycle 1 was 3.6 and slightly dropped to 3.5 LRV for cycle 2, which is similar in behavior to MS2 experiment. The removal at the end of both cycles increased slightly to 3.8 LRV. This means that reversible fouling was still showing an effect for φX174 phage removal even after the removal of organic fouling from the membrane but to a lesser degree than when a pronounced irreversible fouling layer was present.

To summarize results from experiments using Grand River water once with MS2 and once with φX174, removals of both viruses were substantially increased by the presence of irreversible fouling on the membrane at moderate and severe irreversible fouling conditions. But φX174 showed an additional increase in removal under more severe fouling conditions (i.e. increase in TMP from second to third spiking event) whereas removals of MS2 bacteriophage remained unchanged. As explained earlier, irreversible fouling is believed to be due to pore narrowing or due to adsorption of proteins or humic substances. This will make φX174 bacteriophage which is larger in size than MS2 bacteriophage more affected by the irreversible fouling. The increase in MS2 removal due to irreversible fouling will be more affected by its negative charge and the increased negative charge on the membrane due to irreversible fouling. The major difference between MS2 and φX174 bacteriophage were observed with regard to reversible fouling. Removal of φX174 bacteriophage was positively affected by reversible fouling in all four spiking events - even at the first spiking event and after maintenance cleaning where no or only little irreversible membrane fouling existed. MS2 removals were positively affected by the reversible fouling only after the development of an irreversible fouling layer but not with the clean membrane or after maintenance cleaning. These differences may probably be due to the virus surface charge. Under more severe irreversible fouling conditions (i.e. TMP increase of at least 100%) reversible fouling had similar positive effect on both viruses with an approximately additional 0.5 LRV increase within a filtration cycle.

Results of the Georgian Bay water fouling experiment are shown in Figure 5-11. The pH of this water was only slightly lower (pH 8.1) than in both Grand River water experiments and pH effects should therefore be comparable in all 3 experiments. The Georgian Bay water had a very low chlorine residual of less than 0.1 mg/L that was quenched only in the feed water used for the different spiking

events as explained in detail in section 5.2.1. Long term operation i.e. fouling was done with the original water without chlorine quenching. For Georgian Bay water only φX174 and not MS2 was used to assess virus removal in this surface water. MS2 has already been studied in detail by others. Also, both viruses showed similar behavior in the two experiments done with the Grand River water. For these reasons and also due to limited resources, only φX174 was examined in Georgian Bay water. For the first spiking event (Figure 5-11a), a very high amount of sodium thiosulfate was mistakenly added to the surface water, which raised the conductivity to 3000µs/cm and had the potential to influence/increase virus removal (Jacangelo *et al.* 2006). All subsequent spiking events had the appropriate dosing of quenching agent and conductivities were much lower (i.e. 195 µS/cm). In this first spiking event, the removal of the φX174 using Georgian Bay water was similar to that achieved in the Grand River water experiment. The φX174 removal was nearly 3 LRV in all three cycles, and there was no difference in removal between the start and end of the cycle. φX174 bacteriophage had nearly the same removal for both Georgian Bay and Grand River feed waters in the fouling experiments regardless of the nature of the water, its fouling potential or the large difference in conductivity. This indicates that the effects reported by Jacangelo *et al.* (2006) were not observed here. However, in this first spiking in the Georgian Bay experiment with its higher ionic strength no increase in removals due to reversible fouling was observed, whereas this was experienced at the first spiking in the second Grand River experiment with φX174. These removals were also very similar to the ones observed in DI water at pH 6.8 (Chapter 4) at the third cycle after the end of high adsorption rate for the first cycle (Figure 3-18). It may be concluded that baseline removals established at clean water conditions on clean membranes are representative for phage removals in any type of water before the onset of irreversible or reversible fouling. Hence, phage removal studies under clean water conditions are capable of establishing the minimum log removals. This is a result which regulators may be able to use for setting procedures and regulations for giving removal credits in full-scale plants.

The second spiking event (Figure 5-11b) was done at 50% increase in TMP after running the unit for 95 h which took double the filtration time of Grand River water due to the lower fouling potential of the Georgian Bay water. LRV for φX174 was 4, which was higher than in the first spiking event due to irreversible fouling. A drop in the removal of φX174 bacteriophage of only 0.2 LRV happened between the first and third cycle. The developed irreversible fouling improved the removal by 0.9 to 1.2 LRV over the obtained removal at the first spiking. Irreversible fouling did increase the removal of φX174 bacteriophage by nearly 1 log removal but this is still lower than the increase in removal at

similar increase in TMP due to irreversible fouling in the second Grand River water experiment which showed an increased removal by 1.3 to 1.6 LRV (between first and second spiking event). These results show that the nature of the irreversible fouling due to the difference in the feed water quality had an impact on the increase in the removal of viruses. This water was lower in total organic content than the Grand River water and had a lower concentration of humic substances as well. But it did seem to have a higher content of protein-like matter whereas the biopolymer concentrations lay between concentrations observed in the two Grand River water experiments (Table 5-4). It is hypothesized that all these fraction may have contributed to the formation of a fouling layer but a detailed analyses of the fouling layer was beyond the scope of this study. Note that reversible fouling did not have a significant effect in this second spiking event as the removal at the start and at the end of the three cycles were identical for each cycle.

After the second spiking, the membrane unit had a problem that was seen in the TMP profile (Figure 5-8) and the module was suspected to have a slight integrity problem. The TMP started to drop between 110 and 150 h of operation and then started to increase again until the third spiking at 218 h of operation. This shows that irreversible fouling was able to 'fix' the problem that happened to the membrane prior to the third spiking. The φX174 removal results of the third spiking event (Figure 5-11c) were very similar to the removals obtained in the second spiking event. The removal at the start of cycle 1 and 2 was stable at 4 LRV, which then decreased to 3.8 LRV on the third cycle. These values were essentially the same as in the second spiking event and were about 1 log higher than in the first spiking event indicating that irreversible fouling was still effective. However, the more severe irreversible fouling in this third spiking event did not increase φX174 removal which is similar to the first Grand River experiment with MS2 bacteriophage, but different from the second Grand River experiment with φX174 where an increase was observed. There are two possible explanations for this: 1) the fouling layer of Georgian Bay water was different and hence, did not increase LRVs similar to the MS2 GR water experiment or 2) when the integrity problem occurred it caused the removal of φX174 bacteriophage to drop. But then irreversible fouling could 'fix' the problem and retain the removal at the same level as the second spiking experiment. This hypothesis is supported by the lower final TMP increase of 76% at the third spiking which is similar to the TMP value at 110 h before the integrity problem. A slight reversible fouling effect was seen as the removal at the end of the cycles was higher than at the start by 0.31, 0.16 and 0.48 LRV, respectively.

After the maintenance cleaning of the module and the fourth spiking event (Figure 5-11d), reversible fouling remained effective and it could improve the removal by 0.3 LRV which was similar to the

results obtained in the fourth spiking event in the second Grand River fouling experiment with φX174 bacteriophage. Even after maintenance cleaning, the remaining fouling material was able to support additional removal due to reversible fouling. However, in the fourth spiking event (Figure 5-11d) removals dropped significantly to 2.6 LRV which was lower by 0.4 LRVs than in the first spiking event. This drop in LRV is consistent with the previously suspected membrane integrity problem as indicated by the TMP profile.

To verify this, the module was chemically cleaned (as outlined in Appendix B) and a fifth spiking event was performed with the same feed water on the now clean membrane (Figure 5-12). The φX174 removal dropped to 2.1 LRV which, compared to the 3 log removal for the first challenge test with the clean membrane, resulted in a decrease of 1 LRV most likely due to the suspected integrity problem with the UF membrane. However, the membrane was still able to provide more than 2 log removal of φX174 bacteriophage even with the suspected integrity problem. Moreover, irreversible fouling was able to increase the removal to 4 LRV under more severe fouling conditions as observed in the third spiking and 2.5 LRV were obtained after maintenance cleaning in the fourth spiking. This shows that the UF membrane remained a good barrier for enteric viruses under all test conditions - even in the presence of integrity problems.

Interestingly, a 0.5 LRV increase due to reversible fouling was observed in the fifth spiking of the chemically cleaned membrane where no or only little fouling remained on the module. This reversible fouling effect was not observed in the first spiking event with the same water with the clean membrane. However, these results are similar to the first spiking event in the second Grand River experiment where φX174 bacteriophage removal was affected by reversible fouling. One interpretation may be that some fouling material remained on the membrane surface even after chemical cleaning which was then supporting the reversible fouling effect as has been observed in the third spiking event.

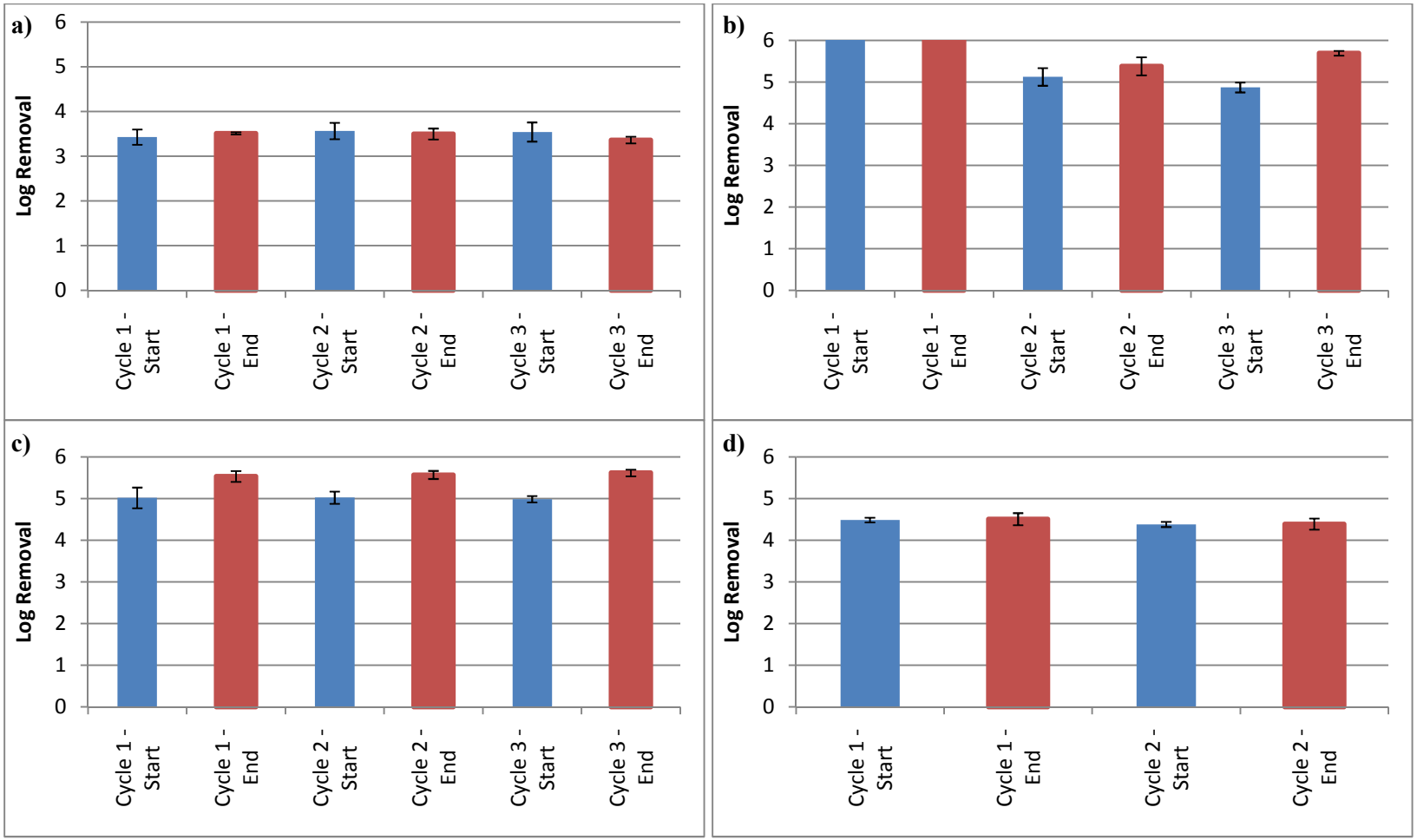

Figure 5-9. Removal of MS2 bacteriophage during the first Grand River water fouling experiment (August 2010) at (a) the start of the experiment (0 h), (b) at 50% increase in TMP (47 h), (c) at 100% increase in TMP (105 h), and (d) after maintainance cleaning.

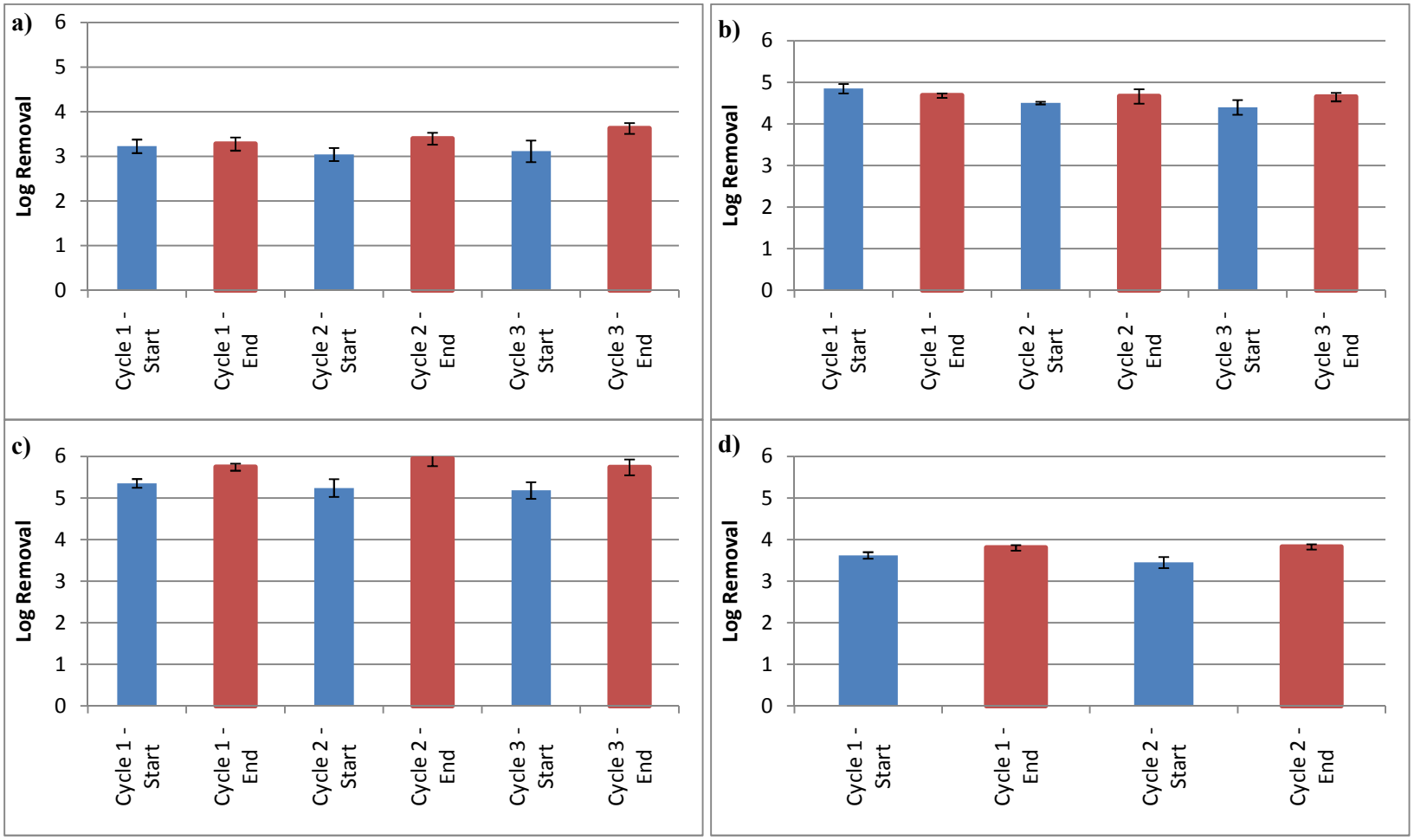

Figure 5-10 Removal of φX174 bacteriophage during the second Grand River water fouling experiment (September 2010) at (a) the start of the experiment (0 h), (b) at 50% increase in TMP (57 h), (c) at 100% increase in TMP (120 h), and (d) after maintenance cleaning.

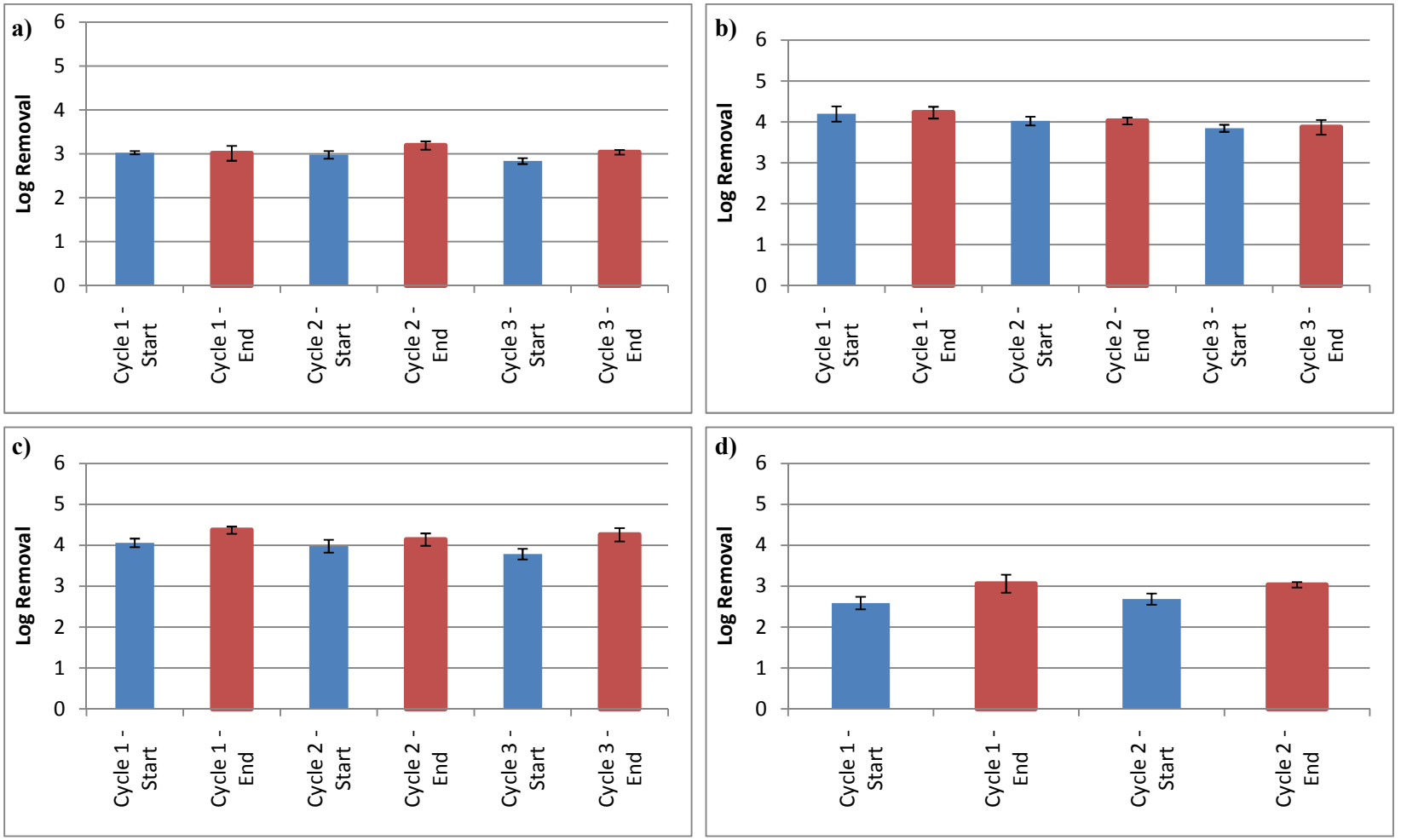

Figure 5-11 Removal of φX174 bacteriophage during the Georgian Bay water fouling experiment (November 2010) at (a) the start of the experiment (0 h), (b) at 50% increase in TMP (95 h), (c) at 76% increase in TMP (218 h), and (d) after maintenance cleaning.

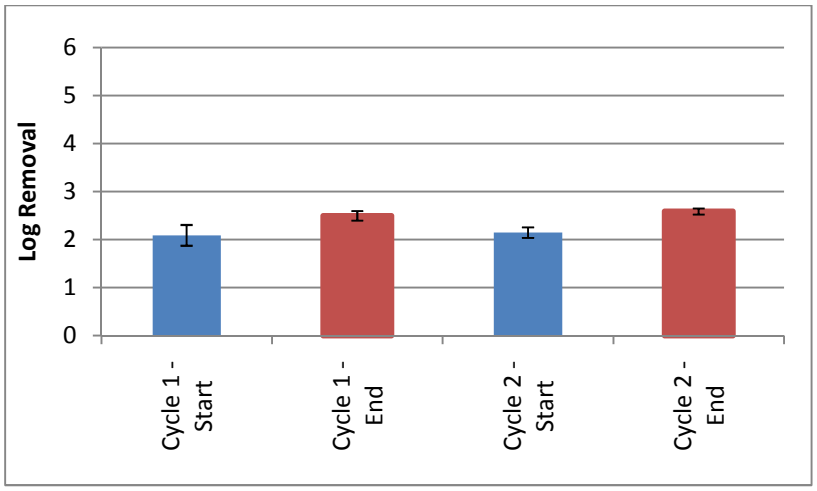

Figure 5-12. Removal of φX174 bacteriophage in the fifth spiking event after chemical cleaning of the membrane after the Georgian Bay water fouling experiment using the same feed water.

5.3.5 Clean water permeability results

The clean water permeability test results for the three different fouling experiments are shown in Figure 5-13. This test can show if the membrane permeability has changed due to fouling and also assess the cleaning efficiency of maintenance and recovery cleaning. Any decrease in permeability can likely be attributed to the impact of the irreversible fouling on the hydraulic resistance of the membrane. Membrane permeability can either be shown by the slope of the regression line for permeability values at different fluxes (i.e. overall permeability) or by a single permeability value at a fixed permeate flux which was chosen to be 51 LMH - the flux used in the fouling experiment. Both values are presented in Table 5-6.

For the first Grand River water experiment, both values of the membrane permeability decreased which can be explained by the increase in membrane fouling. A drop of 44% was observed for the overall permeability whereas permeability at 51 LMH resulted in a smaller decrease. After maintenance cleaning the permeability at 51 LMH was nearly back to its original value whereas the overall permeability was still 23% lower than the initial permeability. The latter though is consistent with the increased MS2 removal observed after maintenance cleaning of the membrane (Figure 5-**9**d).

For the second Grand River water experiment, a slightly more pronounced drop in both permeability values was observed when compared to the first Grand River experiment. This is likely due to the higher increase in TMP at the end of this second experiment. After maintenance cleaning, the permeability at 51 LMH was higher than the initial value which would indicate that no fouling remains. The overall permeability value was still slightly lower than the initial value of the clean

membrane which indicates that some fouling remained on the membrane. In this experiment though φX174 removal after maintenance cleaning (Figure 5-10d) was still elevated and is therefore consistent with the overall permeability values .It seems that overall permeability were better able to reflect the degrees of fouling than permeability values obtained at one fixed flux.

For the Georgian Bay experiment, the drop in permeability for the fouled membrane was substantially less than in the other two experiments with Grand River water. Reasons are a lesser degree of fouling (i.e. TMP increase of only 75% at the end of the experiment) and the slight integrity problem after 110 h of operation. The latter was likely the main reason that a higher TMP increase could not be achieved despite the long filter run time. After the maintenance cleaning, permeability values behaved in the same manner as in both Grand River water experiments. The slightly lower overall permeability after maintenance cleaning in addition to the increase in virus removal that was lost after the chemical cleaning of the membrane (i.e. 2.6 LRV compared to 2.0 LRV after chemical cleaning) showed that some fouling was not removed. However permeability at 51 LMH could not detect this. After chemical cleaning, both permeability values were higher than the initial values which confirmed the expected integrity problem and were already known from the 5th virus spiking (Figure 5-11 and Figure 5-12). Generally, the overall permeability test seems to be a much better tool to predict the degree of fouling than the permeability determined at one certain flux value.

Table 5-6 Measured permeability at different degrees of membrane fouling for different fouling experiments

Experiment	Membrane Condition	Permeability over range of permeate fluxes	Permeability at 51LMH
		LMH/bar @ 20°C	LMH/bar @ 20°C
Grand River first experiment (MS2 phage)	Clean Membrane	382.7	375.9
	Fouled Membrane	213.6	283.8
	After Maintenance cleaning	296.6	370.3
Grand River second experiment (φX174 phage)	Clean Membrane	415.6	402.0
	Fouled Membrane	199.0	298.2
	After Maintenance cleaning	409.7	430.1
Georgian Bay experiment (φX174 phage)	Clean Membrane	410.1	405.3
	Fouled Membrane	297.6	359.9
	After Maintenance cleaning	395.6	436.7
	After Chemical cleaning	447.8	494.3

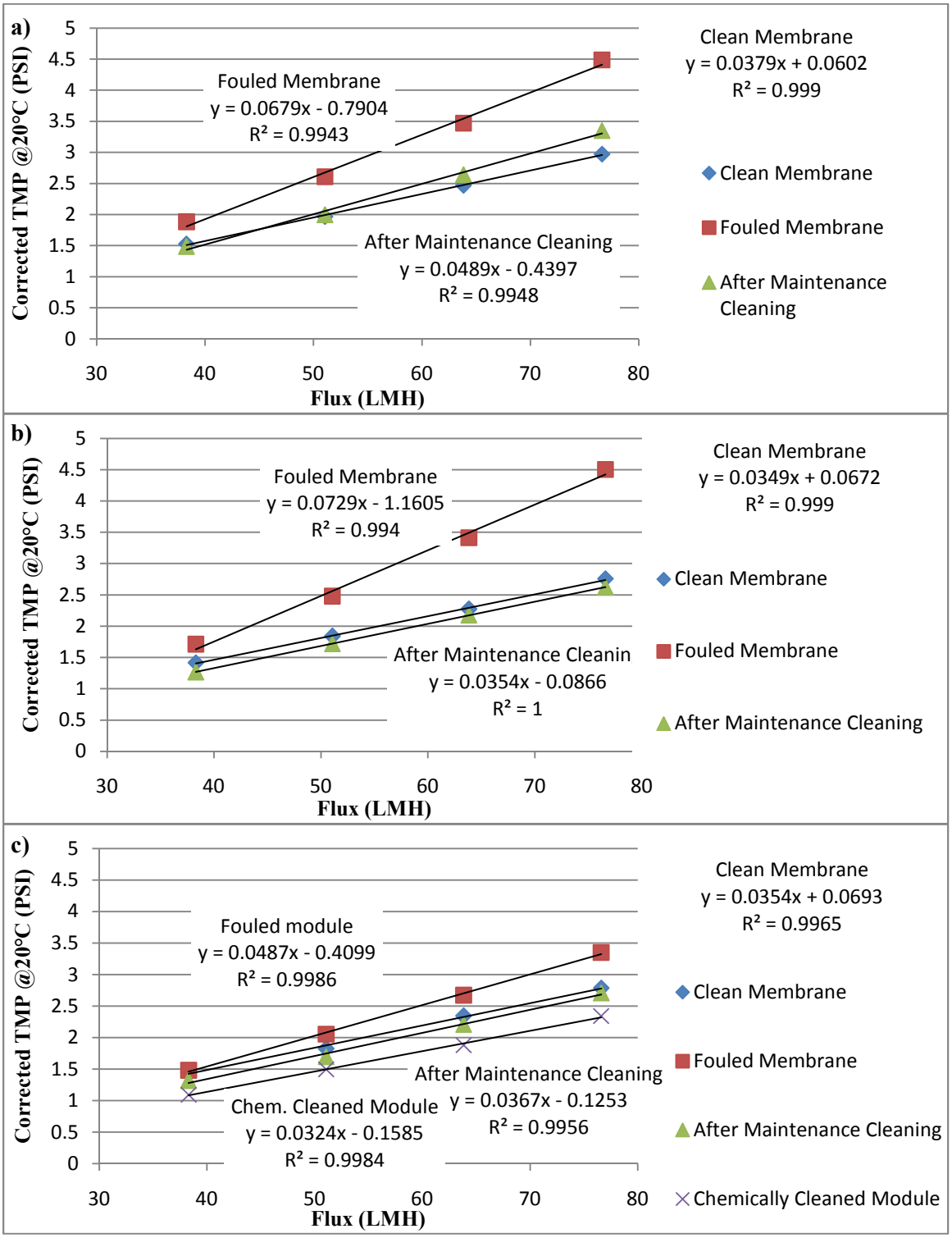

Figure 5-13 Clean water permeability using DI water for the (a) first Grand River fouling experiment, (b) the second experiment, and (c) the Gorgian Bay water fouling experiment.

5.3.6 Fouling mechanism

To further analyze the fouling data, Hermia's model was applied to the TMP curves of individual filtration cycles which will provide a characterization of the type of fouling within each cycle. This analysis pertains to total fouling which includes reversible and irreversible fouling. However, fouling is largely dominated by reversible fouling over the short duration of a filtration cycle with only small contributions from irreversible fouling. The traditional approach for using Hermia model for constant pressure filtration is done by plotting the first and second derivative of total permeate volume over time (dV/dt and dV^2/d^2t) against each other and comparing the obtained slope to certain value for each fouling mode (Bowen *et al.* 1995). In the following analysis a different approach was used as described by Kang *et al.* (2007). The different mathematical relationships developed for the different fouling mechanisms as shown in Table 5-1 were employed for the constant flux filtration data obtained in the fouling experiments. The actual pressure readings were used to fit the different relationships.

Randomly selected filtration cycles were fitted to the four different relationships of fouling modes shown in Table 5-1. The better the fit as indicated by a high correlation coefficient i.e. R^2 value, the more likely this mode was dominating fouling in this particular cycle. The R^2 values of the different models are very close to each other which make it hard to definitely determine a certain fouling mode (i.e. no statistically significant difference) but they can be used as an indicator for the major fouling mechanism and to qualitatively compare different experiments. Results for the first Grand River water experiment with MS2 spiking are shown in Table 5-7 and results for the other two fouling experiments are shown in the Appendix D. Cake filtration was the dominant mechanism for the listed cycles as shown by the highest R^2 value, but cycles 5 and 15 (at the start of the experiment) were dominated by standard and complete blockage, respectively. The same trend was observed for the other two fouling experiments as shown in Appendix D. Also R^2 tends to increase with increasing fouling rates for later cycles. The cake filtration fouling mechanism may be able to explain the small positive effect of reversible fouling on removal even though the observed increase in TMP ranged from 0.44 to 0.67 PSI (e.g. 35% to 50% of initial TMP) within each cycle. It may postulated that mainly a porous cake is formed during reversible fouling that cannot sieve the viruses but may be hydrophobic enough to remove viruses by adsorption which is likely less efficient than a sieving effect. The low R^2 values in the first cycles can be attributed to the low fouling rates in these cycles (i.e. increase in TMO values) which is close to the resolution of the TMP monitoring system. This caused more variability to the data due to the noise and lowered the R^2 for all four fouling models.

Table 5-7. R^2 values for fitting TMP data for random filtration cycles within the first fouling experiment of the Grand River water (August 2010) to the different fouling mechanisms models.

Cycle Number	Standard blockage (n=1.5)	Intermediate Blockage (n=1)	Complete blockage (n=2)	Cake Layer formation (n=0)
5	0.58884	0.588832	0.588833	0.588774
15	0.640848	0.640787	0.640852	0.640493
29	0.697785	0.698495	0.697	0.699686
45	0.727573	0.730424	0.724672	0.735971
80	0.822331	0.824525	0.820095	0.828778
115	0.783986	0.785805	0.782154	0.789399
140	0.82904	0.831656	0.826393	0.836794
180	0.902798	0.905013	0.900523	0.909254
200	0.760244	0.76121	0.759255	0.763073

Data in each filtration cycle were then fitted to the cake filtration model (i.e. $y = ax + b$). The TMP value at the start for each filtration cycle was then extrapolated using this fitted curve rather than taking the actual reading and plotted in Figure 5-14a. This figure will indicate how irreversible fouling developed over the whole fouling experiment. The total fouling rate of each cycle was also calculated using the fitted curve and as mentioned earlier this fouling rate is largely dominated by reversible fouling with small contributions of irreversible fouling in each cycle. These data are shown in Figure 5-14 b and would indicate the reversible fouling rate over each cycle.

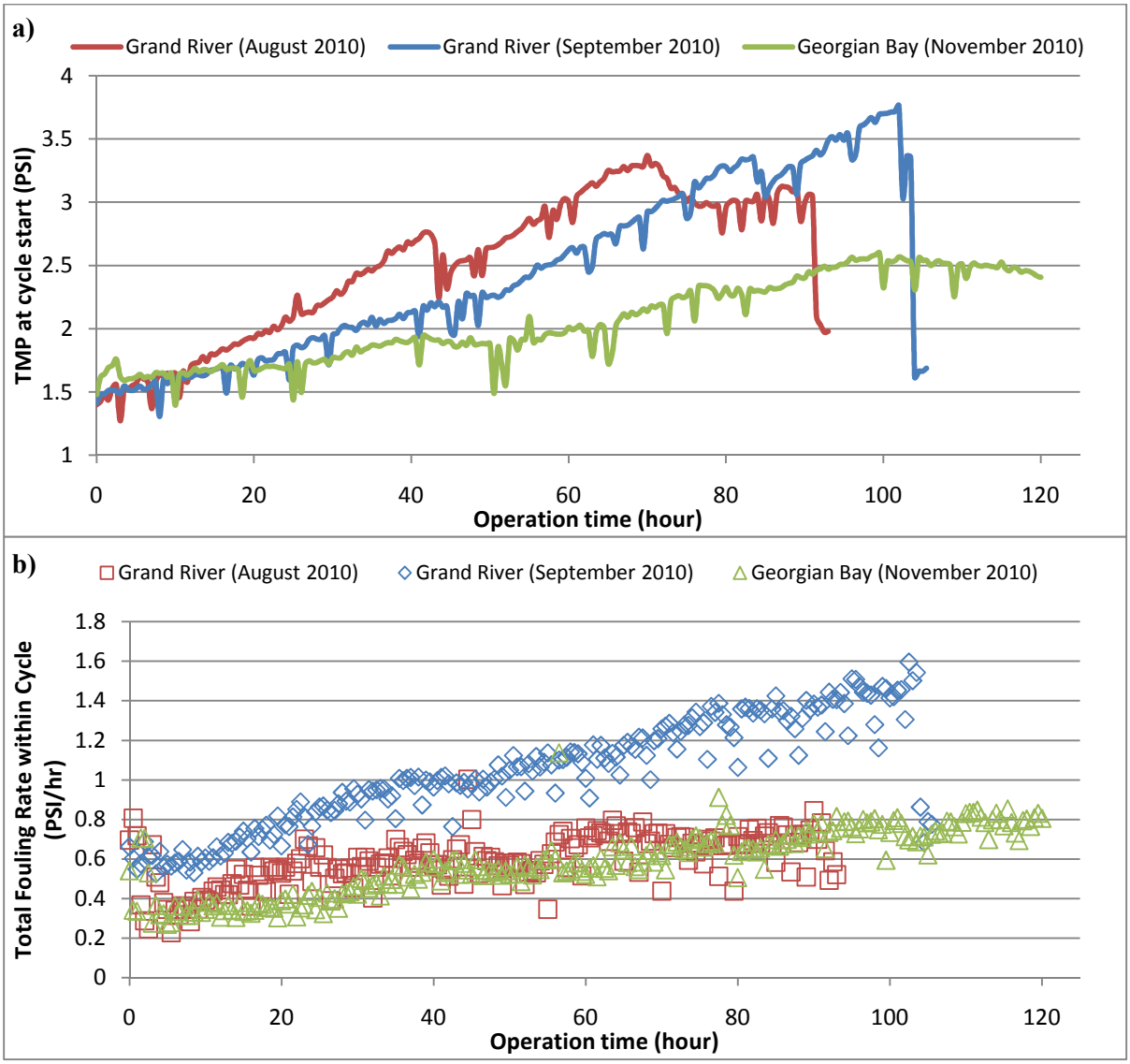

Figure 5-14 Recorded TMP (a) extrapolated value at the start of each filtration cycle, and (b) the total fouling rate within the cycle, for the two fouling experiments for the Grand River water and the first half of the Georgian Bay water according to cake filtration model.

As shown in Figure 5-14b, the second Grand River experiment had the highest reversible fouling rates for all cycles compared to the other two experiments. According to the LC-OCD data shown in Fluorescence EEM of the first Grand River water experiment (August 2010) (Figure 5-3), resulted in a drop of the protein-like matter peak from a maxima of 117 in the feed at the first day of the fouling experiment to 82 on the remaining days similar to the drop in the biopolymer peak in the LC-OCD

results. For the second fouling experiment of the Grand River water, the maxima of the protein peak was stable at 101 throughout the entire experiment with more than 50% reduction in the permeate for all samples. This indicates that this fraction was partially retained by the membrane and likely contributed to membrane fouling. For the Georgian Bay water, the protein peaks were nearly the same for the feed and permeate at 40. This showed that the proteins were passing through the UF membranes and did likely not contribute to membrane fouling. The removal of the biopolymer peak observed in the LC-OCD results for this water (Table 5-4) is therefore probably due to biopolymer constituents other than protein-like matter e.g. polysaccharides or organic colloids.

For irreversible fouling of the membrane as shown in Figure 5-14a, the water in the first Grand River water experiment had the highest irreversible fouling rate (i.e. shown by the higher increase in TMP values over time) followed by the second Grand River experiment and finally the Georgian Bay experiment Although biopolymers have been reported to play a role in irreversible fouling, biopolymer concentrations do not decrease in this same order. Georgian Bay water with its much lower irreversible fouling rate does have an intermediate biopolymer concentration. One explanation consistent with Hallé *et al.* (2009) may be that biopolymer composition is important in irreversible fouling and that protein-like material, one of the constituents of biopolymers, may be directly related to irreversible fouling. This is also supported by results from the fluorescence EEM analysis where it was found that the Georgian Bay water protein-like matter peak had a much lower intensity of 40 compared to the first and second Grand River water experiments with intensities of 117 and 110, respectively. Another interesting finding is that the first Grand River water had a higher content of humic substances shown using both LC-OCD and fluorescence EEM. Smaller molecules of humic substances are reported to adsorb to the membrane by hydrophobic interactions to cause irreversible fouling (Hong and Elimelech 1997, Jermann *et al.* 2007, Jucker and Clark 1994, Yamamura *et al.* 2007).

Irreversible fouling was shown to be more effective in increasing virus removal than reversible fouling and irreversible fouling was therefore further investigated. By fitting the predicted TMP at the start of each filtration cycle (Figure 5-14a) to the different fouling models in Table 5-1, more information can be found about the irreversible fouling mechanism in the experiments. Even though the R^2 of the four models were very close which does not make conclusions from these values definitive, standard blocking had the highest R^2 for all three experiments as shown in Table 5-8. This supports the hypothesis that adsorption of smaller molecules to the membrane pore inner surface thus decreasing pore dimensions and causing standard blocking, may be the major irreversible fouling

mechanism. This would explain the impact of irreversible fouling as it will make the pores of the membrane narrower so more viruses are blocked by the membrane. Yet it does not block the pores completely which explains why we still detect viruses in the permeate of the membrane at the end of the experiment as not all the pore of the membrane that can pass the viruses became smaller than the virus. By further fouling the membrane, more pores will be narrow enough to block the viruses and further improve the rejection.

Table 5-8. R^2 values for fitting irreversible fouling data for the different experiments to the different fouling mechanisms models.

Experiment	Standard blockage (n=1.5)	Intermediate Blockage (n=1)	Complete blockage (n=2)	Cake Layer formation (n=0)
Grand River first experiment Cycles 1 to 86	0.993846	0.992597	0.980786	0.991678
Grand River second experiment Cycles 1 to 168	0.99555	0.993634	0.97534	0.992092
Georgian Bay experiment Cycles 1 to 200	0.971667	0.966056	0.913375	0.950134

5.4 Conclusion

UF membranes are able to remove enteric viruses but there is limited information about the impact of membrane fouling and the constituents of the surface water matrix on virus removal. Using two types of surface water (river and lake) with different pre-treatment conditions, the removal of both MS2 and φX174 bacteriophage was investigated. The impact of both reversible and irreversible fouling was evaluated during these experiments.

- The obtained removal of MS2 and φX174 bacteriophage using surface waters and a clean membrane without fouling were not significantly different than the results obtained with deionized water (Chapter 4). The removal under clean water conditions can then be considered as a base removal for a certain type of bacteriophage using the UF membrane.
- Membrane fouling experiments showed substantial contributions of membrane fouling on virus removal. Irreversible fouling had the biggest impact on the removal of both MS2 and φX174. It could improve the removal of MS2 bacteriophage by up to 2.5 LRV and of φX174 bacteriophage by up to 2.2 LRV depending on the degree of irreversible fouling. At similar

degrees of fouling, as indicated by the increase in the TMP of the membrane, the type of surface water slightly affected phage removal, probably due to the nature of the developed membrane fouling. Severe fouling conditions (i.e. ≥100% increase in TMP) did not substantially improve the removal of viruses compared to removal at moderate fouling conditions (i.e. ≈50% increase in TMP).

- Maintenance cleaning of the membrane is often employed daily in full scale membrane filtration treatment plants to maintain membrane performance by removing some of the developed fouling layer. The effect of maintenance cleaning using sodium hypochlorite on phage removal and TMP recovery was tested at the end of each surface water experiment. In all three surface water experiments TMP was recovered albeit not to its initial value. This caused the phage removal to drop substantially but it remained above the initial removal for the clean membranes in all three experiments.
- Reversible fouling was less effective in improving virus removal than irreversible fouling. MS2 bacteriophage was only affected by reversible fouling after irreversible fouling started to form on the membrane surface as the unit was operated but no effect was observed for the clean membrane. Increased removal of MS2 due to reversible fouling can be attributed mainly to hydrophobic or specific interactions, as MS2 can adsorb to the highly fouled membrane, and this effect became more obvious as irreversible fouling of the membrane developed. φX174 also showed increased removal due to reversible fouling in both types of surface waters, but this effect was less pronounced than that of MS2. Also, the removal of φX174 bacteriophage was slightly affected by reversible fouling even with the clean membrane.
- The biopolymer fraction of the NOM in the water was a major contributor in the membrane fouling along with the hydrophobic humic substances. Measured biopolymer concentration was related to the reversible fouling rates of the different water sources. There was also some indication through fluorescence measurements that proteins contributed to irreversible fouling. Even with an apparent integrity problem encountered in the final Georgian Bay water experiment, the membrane fouling layer could partially fix this problem, even after maintenance cleaning. But as soon as a thorough chemical cleaning was performed, the removal dropped by 1 LRV below the base removal of φX174 bacteriophage of the membrane.

- Fouling mechanisms in natural water are not well understood and it is complicated to determine these mechanisms. Using a simple fouling model from the literature (Huang *et al.* 2007, Kang *et al.* 2007), the best model to fit reversible fouling was cake layer formation and was in agreement with the lesser effects of reversible fouling on phage removal. Irreversible fouling best fit the pore narrowing model which would also explain the increase in removal of viruses due to improved size exclusion by the membrane.

These findings are of great importance to municipalities employing UF membrane filtration for drinking water treatment and legislators drafting and implementing drinking water regulations. These implications include:

- UF membrane filtration was proven to be an excellent technology for removing enteric viruses in drinking water treatment from different types of surface water. Stable removal of viruses was achieved at different stages during week long filtration experiments.
- The removal of viruses achieved in clean water conditions was similar to the removal achieved with surface waters without membrane fouling. These clean water conditions should be used for membrane challenge testing with enteric viruses to provide baseline removals and grant UF membrane virus removal credits representing a worst case scenario.
- Removals of φX174 bacteriophage were always lower than those of MS2 bacteriophage, in both clean and surface water experiments even though φX174 is larger in size than MS2. Hence, φX174 could be used as a surrogate for enteric viruses in membrane challenge testing as a worst case scenario. Test conditions especially pH and should be well monitored as φX174 removal was largely affected by them.
- Irreversible membrane fouling was able to improve UF membrane virus removal substantially depending on the extent of fouling up to 2 logs. Even with low degrees of irreversible fouling as would be expected after maintenance cleaning, the removal of viruses increased by at least 0.5 LRV over the base removal of the membrane. In full scale treatment plants, most of the time there will be some irreversible fouling on the membranes unless a full chemical cleaning was performed. This can add more trust in UF membranes as a technology for removing enteric viruses and providing safe drinking water.
- Membrane maintenance cleaning removed the additional removal due to fouling but not completely. Membrane cleaning should be carefully scheduled in order to maintain the additional removal performance due to fouling which is especially important for example in cases of pathogenic outbreaks.

- Membrane fouling can partially fix slight integrity problem that can occur during surface water filtration and it also help to maintain a high removal of enteric viruses.

Appendix A

Additional results for UF membrane pore size distribution

Comparison of AFM measured pore maximum opening for different images of each fiber

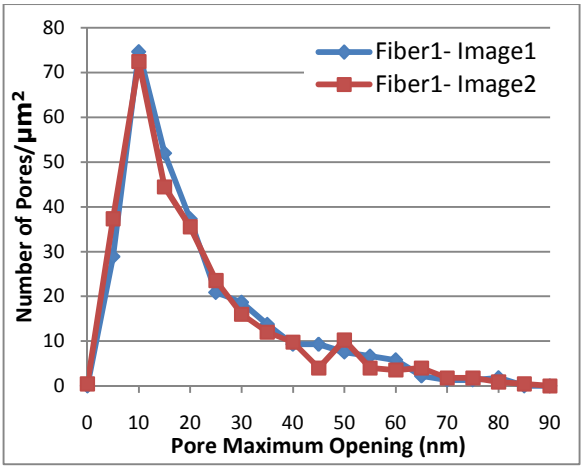

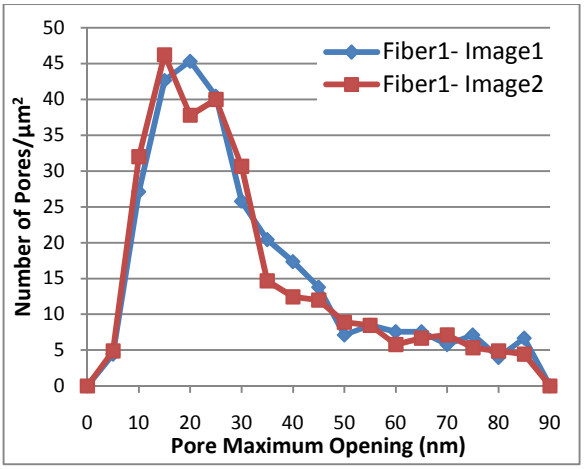

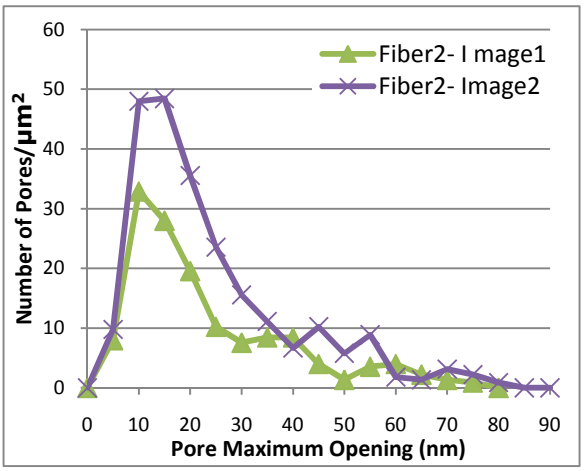

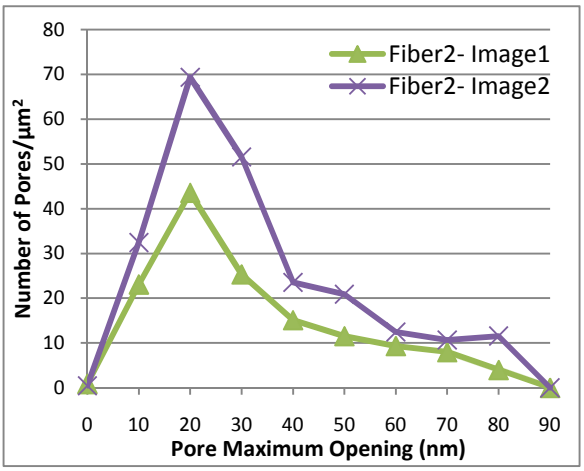

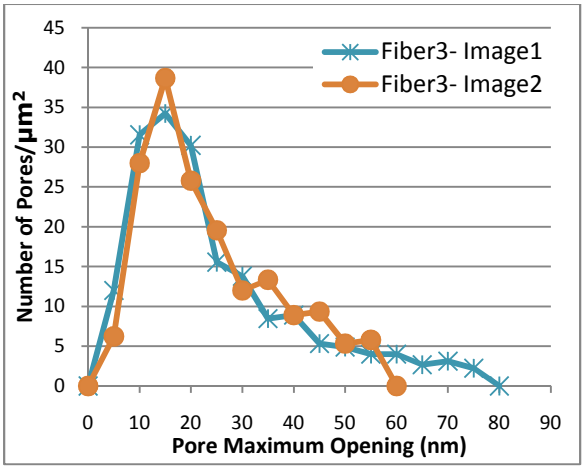

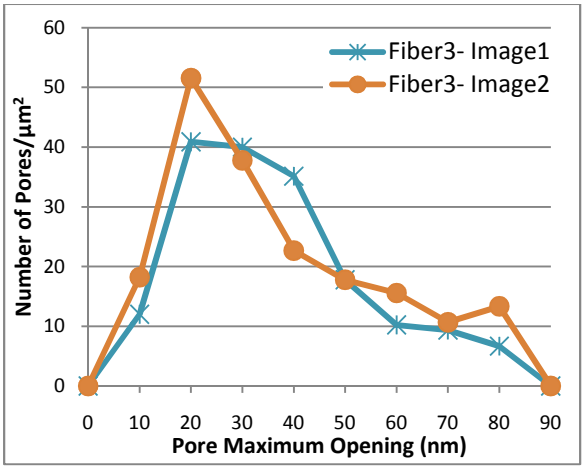

Comparison of AFM measured pore average opening for different images of each fiber

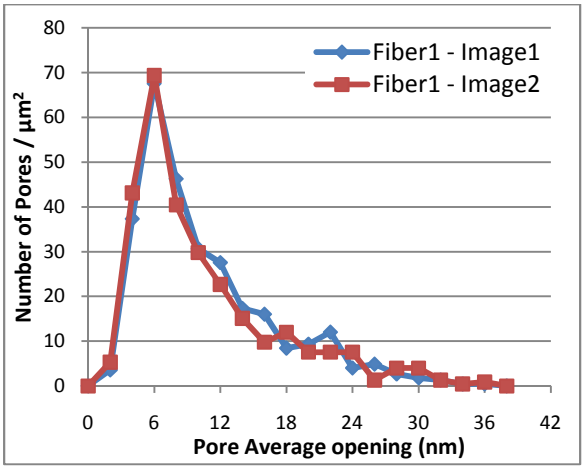

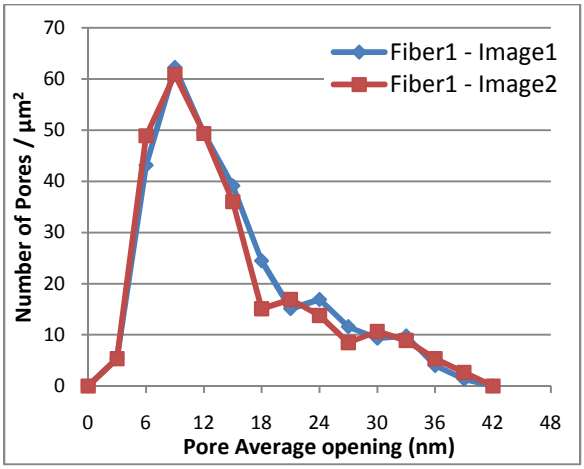

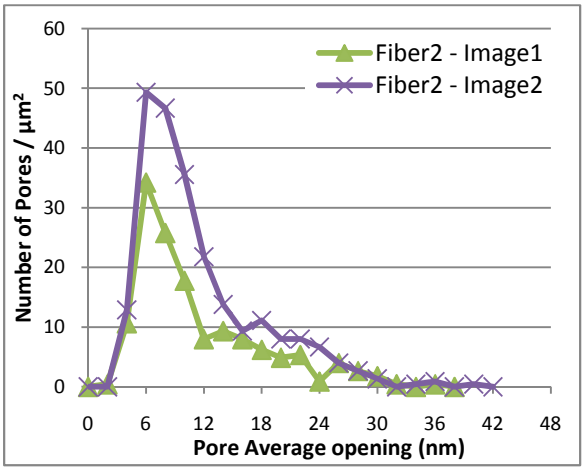

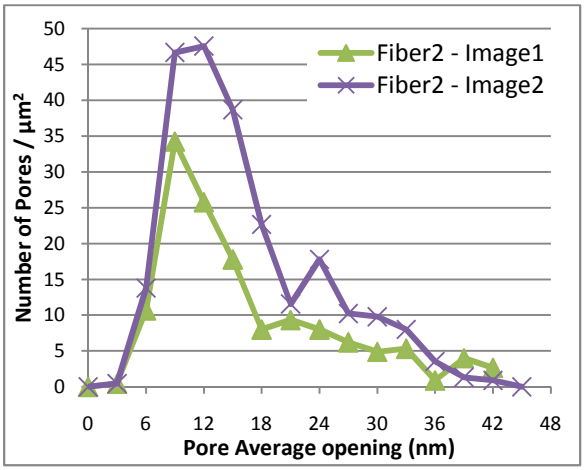

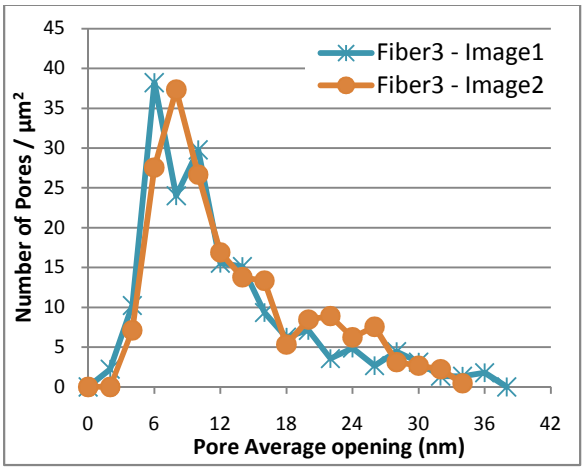

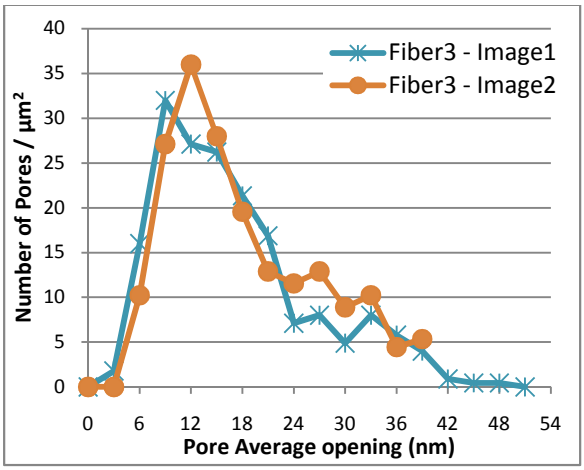

Comparison of AFM measured inscribed circle diameter for different images of each fiber

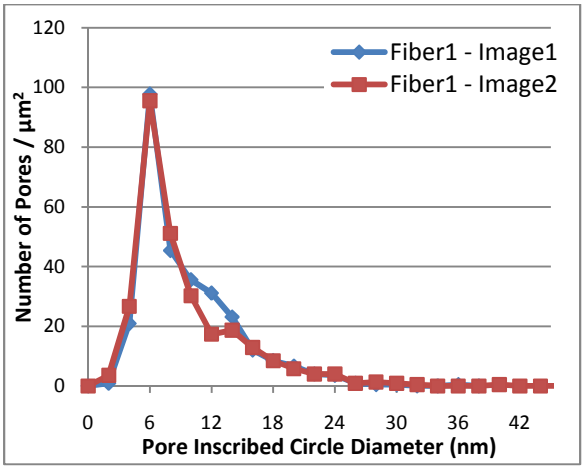

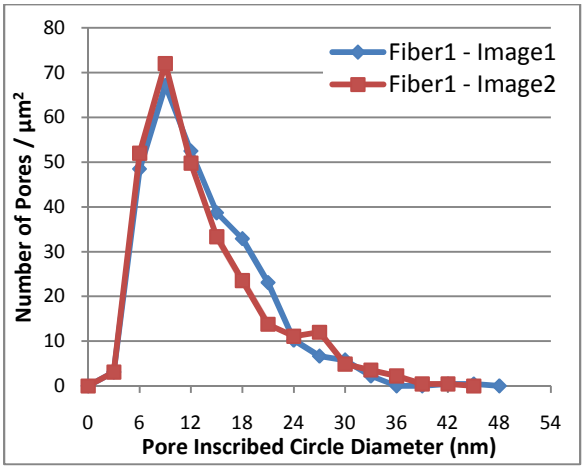

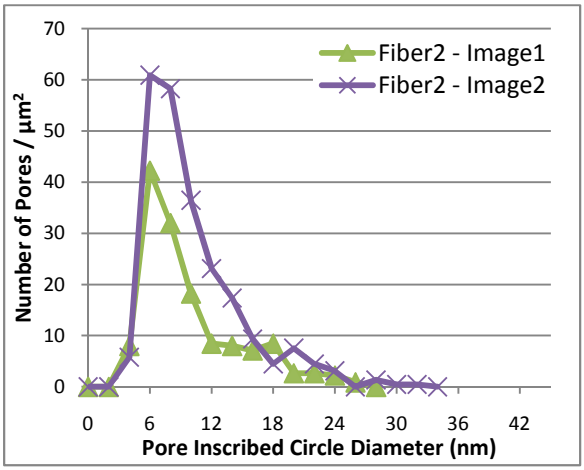

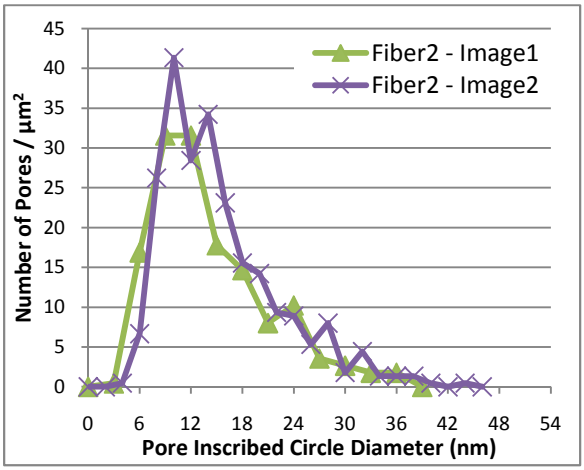

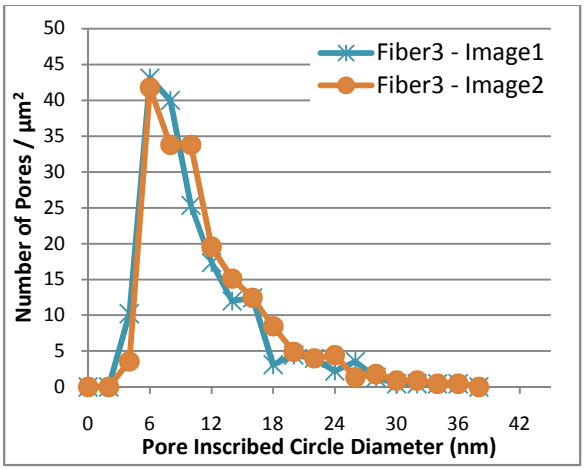

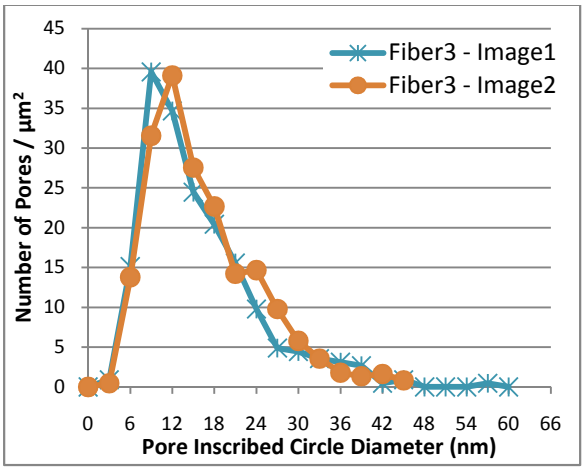

Appendix B
Membrane Cleaning and Integrity Testing

The new UF membrane modules were shipped to the University of Waterloo in sealed bags and preserved in glycerin. The procedures for suing a new module:

1. Rinse new module with warm deionized water.
2. Run the unit at 15mL/min for 5 min and direct to waste.
3. Soak the module in 200ppm sodium hypochlorite solution for a minimum of 5 h.
4. Rinse the module with warm deionized water.
5. Run clean water permeability test

Pressure decay integrity test of the UF module

1. Plug the air supply port of the membrane module.
2. Connect the permeate port of the module to a hand pump.
3. Pressurize the permeate side of the membrane to retain a pressure above 10 PSI for at least two minutes to purge the module and remove any air bubbles.
4. Stop supplying pressure and determine the pressure drop over time.
5. The allowable pressure drop is 0.3 PSI/2 min.

Membrane chemical cleaning:

1. Perform a hydraulic backwash to the membrane module to remove any hydraulically reversible backwashing.
2. Soak the membrane in 200 ppm sodium hypochlorite solution for a minimum of 5 hs.
3. Rinse the membrane with deionized water to remove any remaining sodium hypochlorite.
4. Soak the membrane in 3gm/L acetic acid solution with a pH of nearly 2 for at least 5 h.
5. Rinse the membrane with deionized water to remove any remaining acetic acid.
6. Perform a pressure decay integrity test for the membrane.

Membrane maintenance cleaning:

1. Perform hydraulic backwashing for the fouled membrane to remove hydraulic reversible fouling.
2. Remove the membrane module from the bench unit.
3. Rinse the membrane with deionized water to removed attached materials.
4. Soak the membrane in 500 ppm free chlorine solution of commercial bleach for a period of 5 min to oxidize organic foulants.
5. Rinse the membrane with deionized water to remove remaining bleach solution.
6. Perform a pressure decay integrity test for the membrane.
7. Load the membrane module in the bench unit.
8. Permeate deionized water through the unit for 5 min.
9. Perform clean water permeability test for the membrane.

Clean water permeability test:

1. Filter deionized water through the unit at four different permeate flow rates (30, 40, 50, 60 mL/min) and monitor the TMP.
2. Find the average TMP value for each flux.
3. Perform a temperature correction for the TMP values.
4. Find the linear relationship between the TMP and the flux to find the clean water permeability (PSI/LMH).

Appendix C
Microbiological Media

Tryptone Yeast Glucose Broth (TYGB)

1. Add the following ingredients to a glass container

Tryptone	10.0 g
Yeast Extract	1.0 g
NaCl	8.0 g
Deionized water	1000 mL

2. Mix using a magnetic stirrer till all the components dissolves
3. The final pH should be 7±0.2
4. Autoclave at 121°c for 15 min
5. Add 20 mL of sterile Glucose\ Calcium Chloride solution
6. Dispense 50mL in sterile glass flasks and store for a maximum of 4 months at 4°c
7. For negative quality control incubate a sterile flask of TYGB at 37°c for 24 h and monitor if any bacterial growth happened.
8. For positive quality control, inoculate a 50 mL sterile TYGB flask with the used host bacteria and incubate at 37°c for 24 h and monitor if any bacterial growth happened.

Glucose\ Calcium Chloride

1. Add the following ingredients to a glass container

D-Glucose	1.0 g
$CaCl_2.2H_2O$	0.3g
Ultrapure water	20 mL

2. Mix using a magnetic stirrer till all the components dissolves
3. Filter using a sterile 0.22µm syringe filter into a sterile glass container
4. Store for a maximum of 4 months at 4°c

Tryptone Yeast Super Broth (TYSB)

1. Add the following ingredients to a glass container

Tryptone	32.0 g
Yeast Extract	20.0 g
NaCl	5.0 g
Deionized water	1000 mL
NaOH (1N solution)	5.0 mL

2. Mix using a magnetic stirrer till all the components dissolves
3. The final pH should be 7±0.2
4. Autoclave at 121°c for 15 min
5. For negative quality control incubate a sterile flask of TYSB at 37°c for 24 h and monitor if any bacterial growth happened.
6. For positive quality control, inoculate a 50 mL sterile TYSB flask with the used host bacteria and incubate at 37°c for 24 h and monitor if any bacterial growth happened.

Tryptone Yeast Glucose Agar (TYGA)

1. Add the following ingredients to a glass container

Tryptone	10.0 g
Yeast Extract	1.0 g
NaCl	8.0 g
Granulated Agar	10.0 g
Deionized water	1000 mL

2. Mix using a magnetic stirrer with heating till all the components dissolves
3. The final pH should be 7±0.2
4. Autoclave at 121°c for 15 min
5. Cool down the autoclaved agar into a 55°c water bath
6. Add 20 mL of sterile Glucose\ Calcium Chloride solution
7. Aseptically dispense 20 mL per tube into large, sterile screw cap test tubes and store for a maximum of 4 months at 4°c.

8. For negative quality control, dispense a melted TYGA tube in a Petri dish and incubate at 37°c for 24 h and monitor if any bacterial growth happened.
9. For positive quality control, add 1 mL of host bacteria to a melted agar tube and mix by inversion then dispense into a Petri dish and incubate at 37°c for 24 h and monitor if any bacterial growth happened.

Appendix D

The Impact of Fouling of Ultrafiltration Membranes on the Removal of Enteric Virus Surrogates

Integrity test for the different experiments:

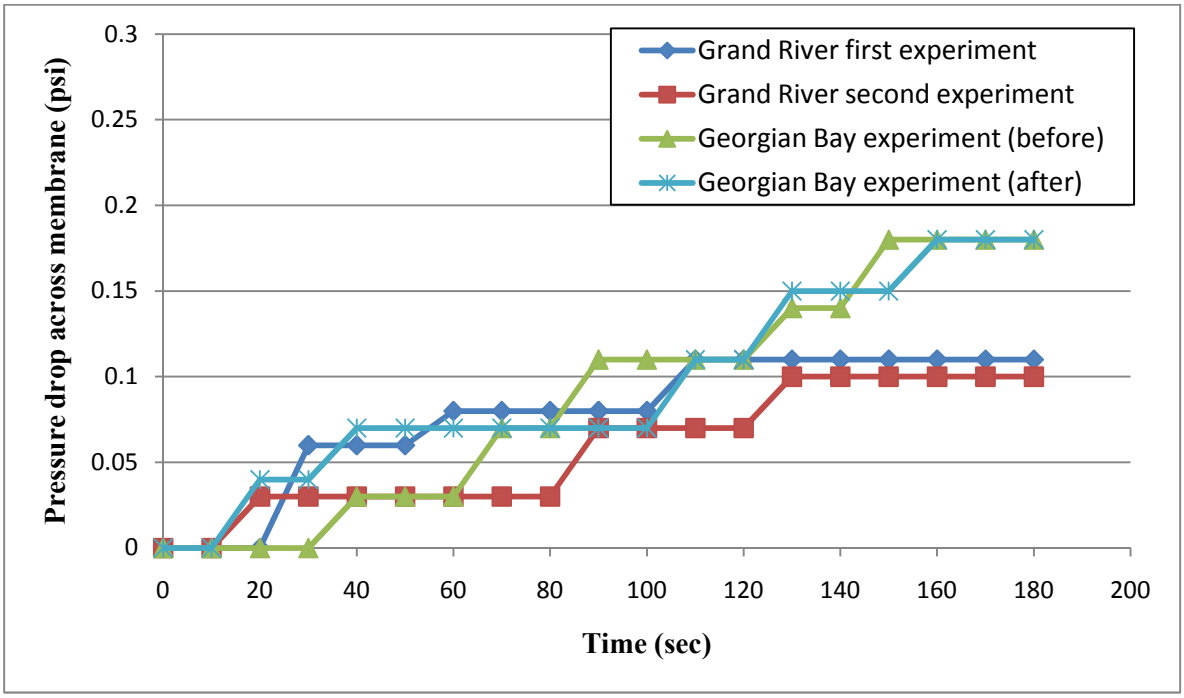

LC-OCD results for feed and permeate of the first Grand River experiment on the first day of the fouling experiment

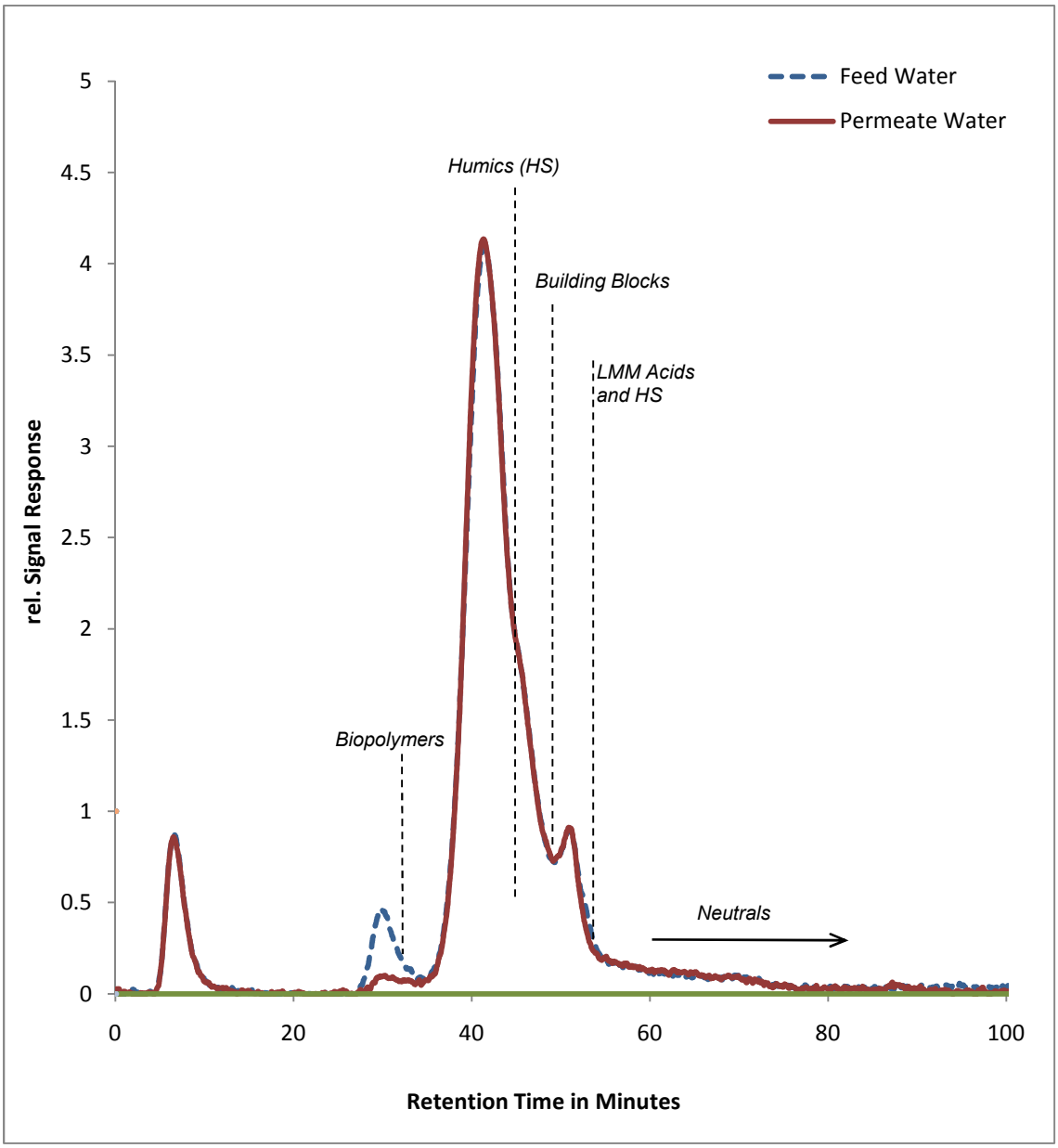

LC-OCD results for feed and permeate of the second Grand River experiment on the first day of the fouling experiment

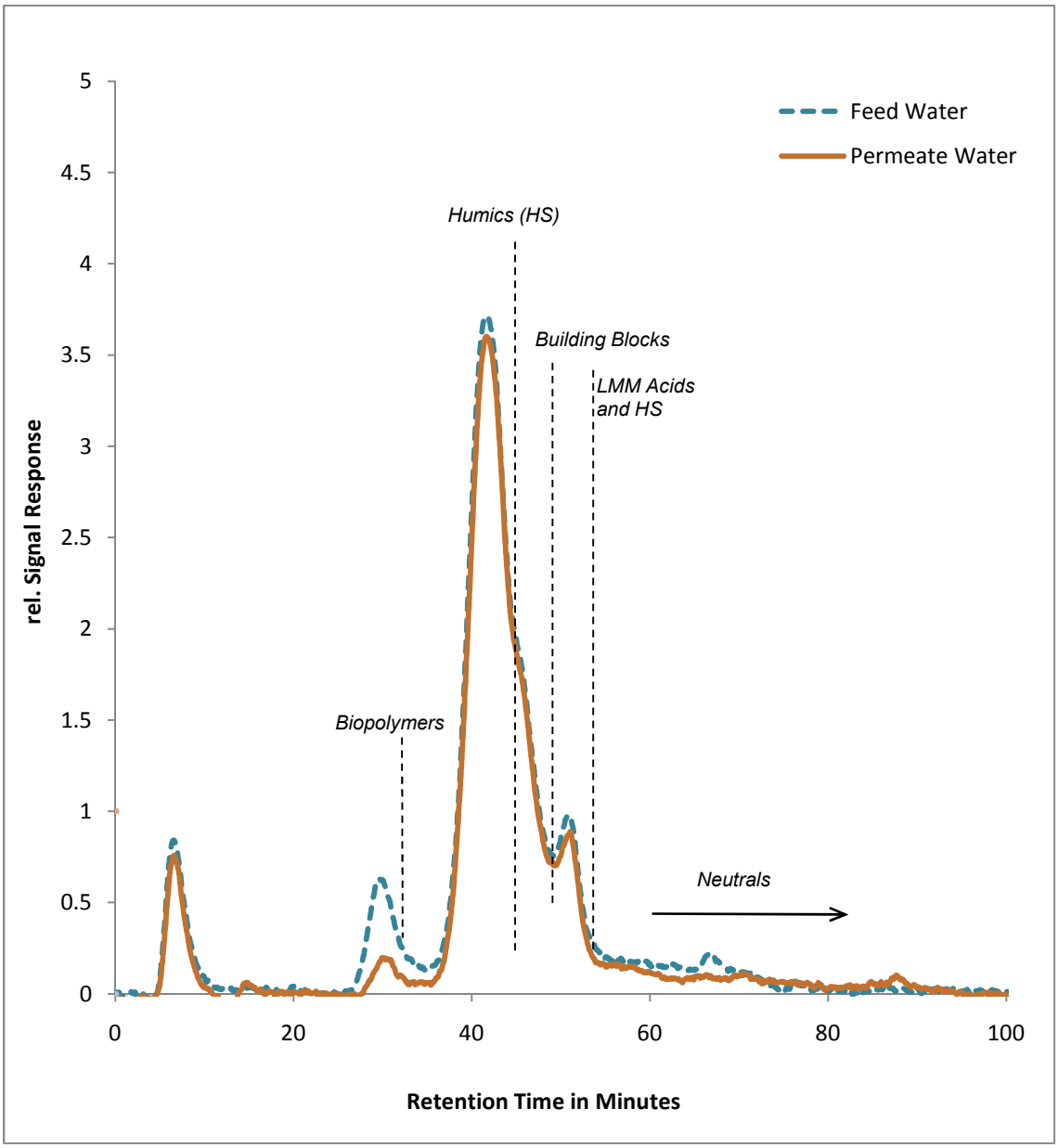

LC-OCD results for feed and permeate of the Georgian Bay experiment on the first day of the fouling experiment

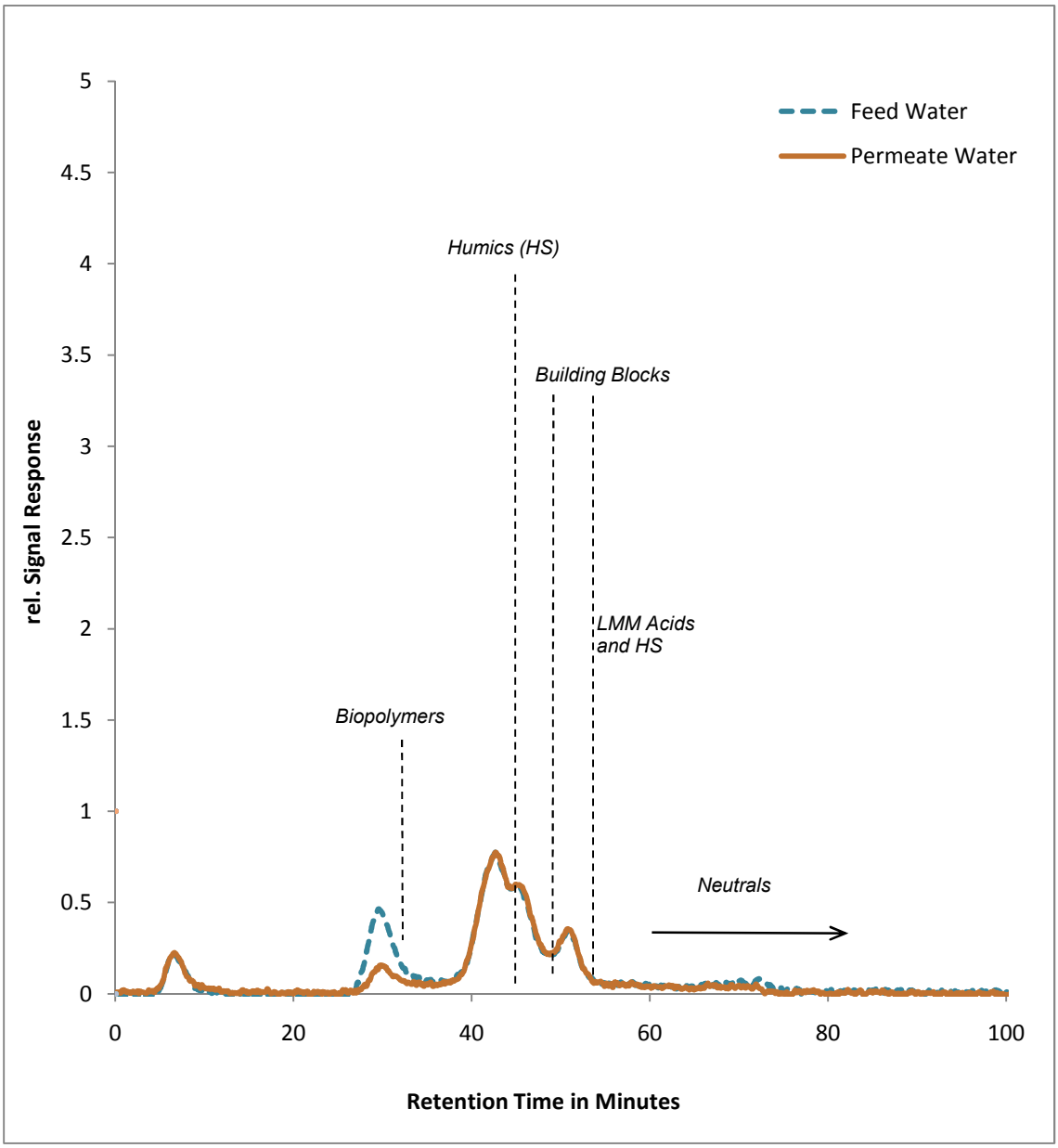

Grand River first experiment (August 2010) first spiking:

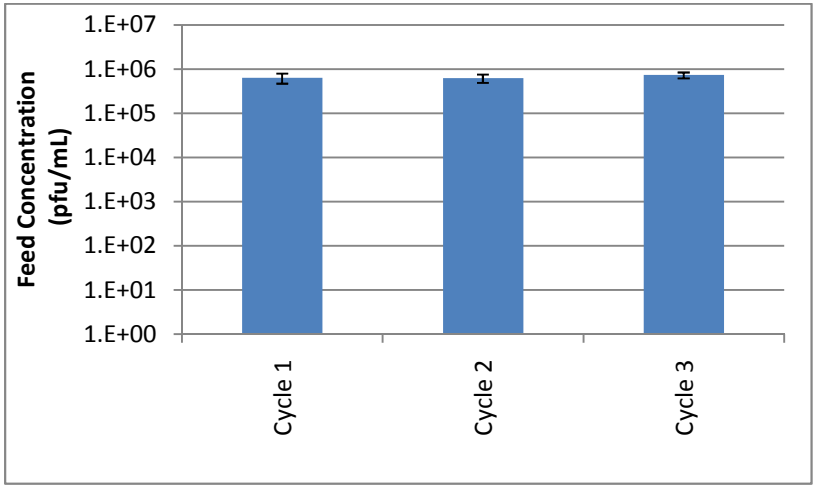

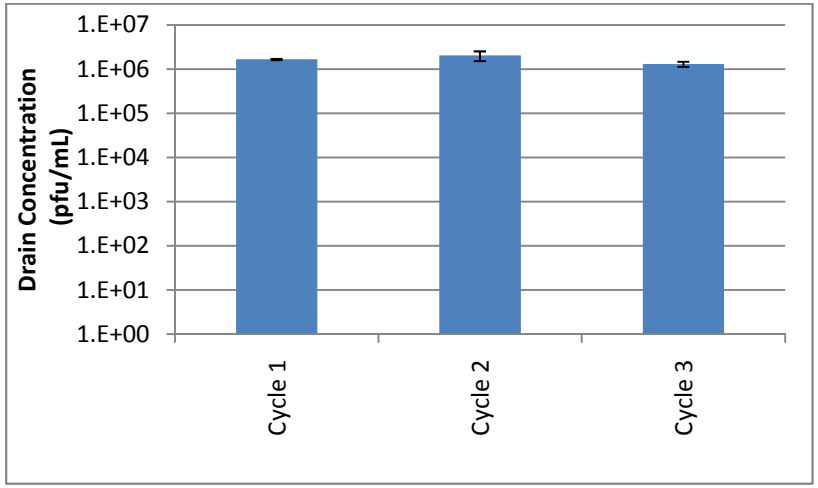

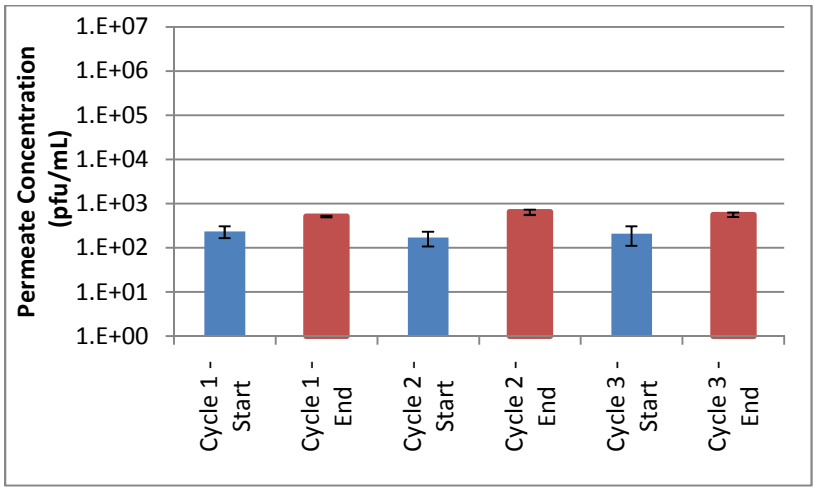

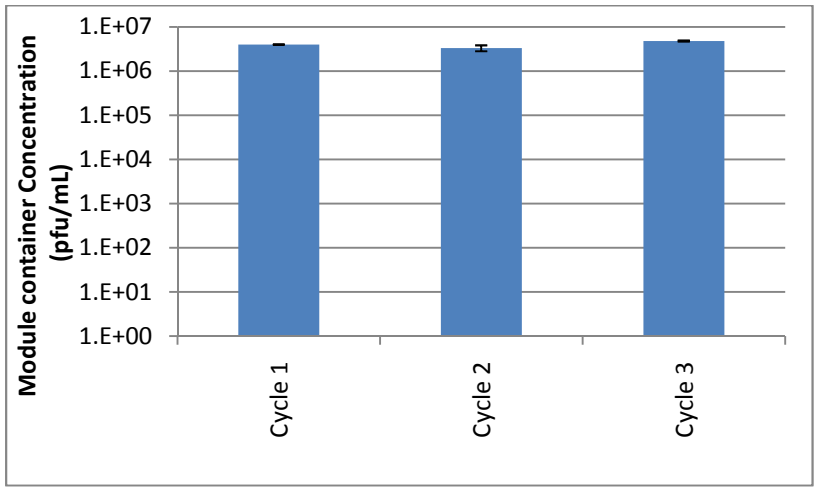

Grand River first experiment (August 2010) second spiking:

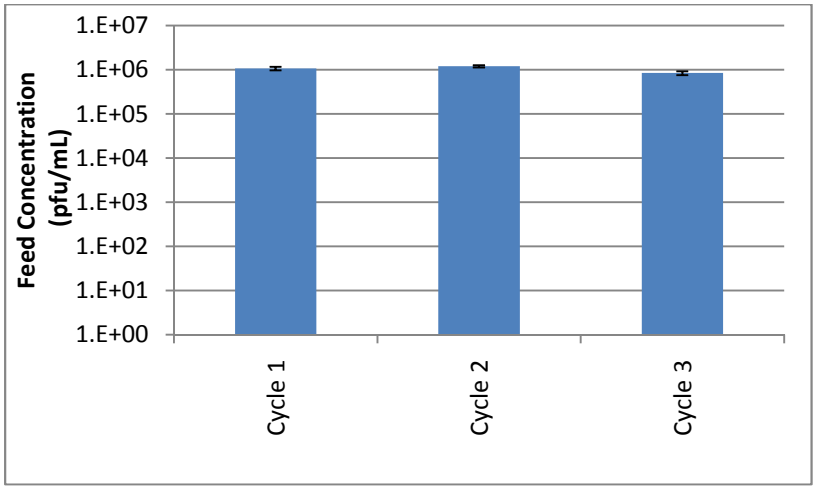

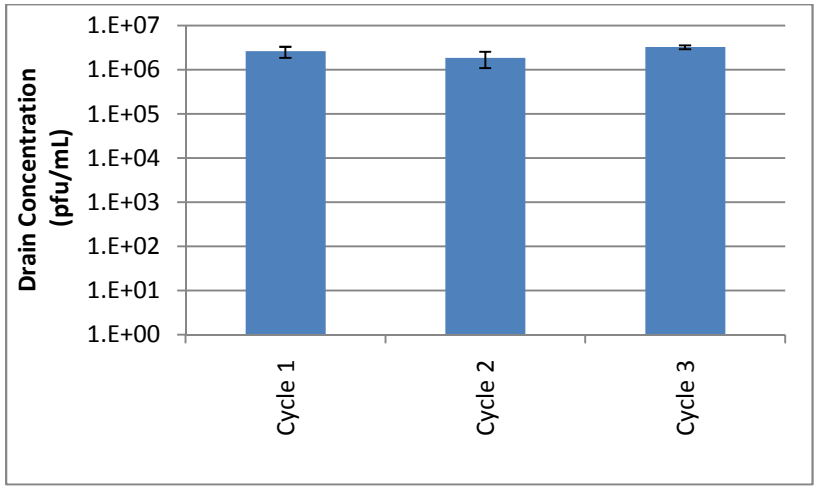

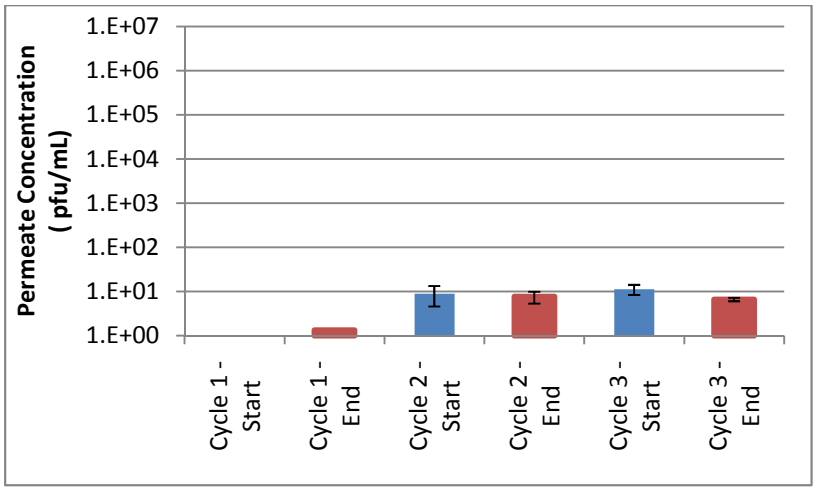

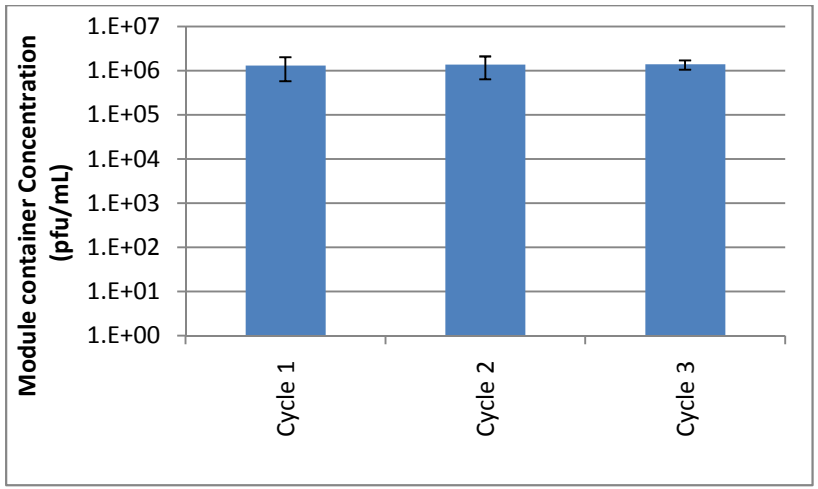

Grand River first experiment (August 2010) third spiking:

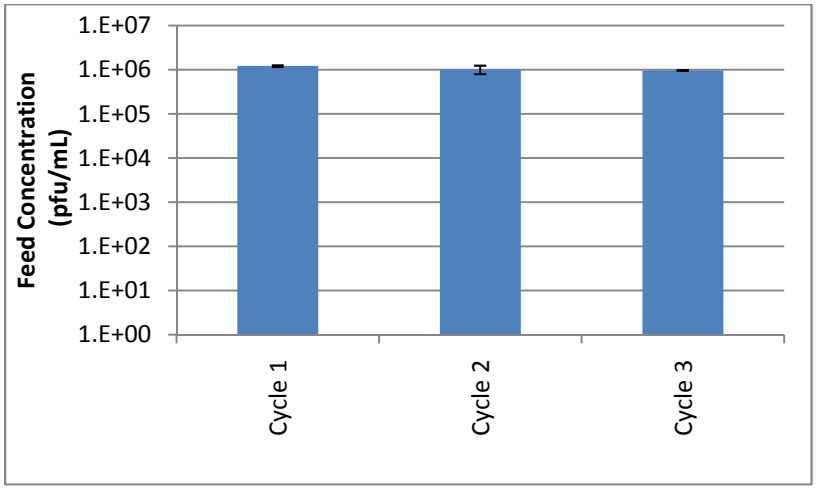

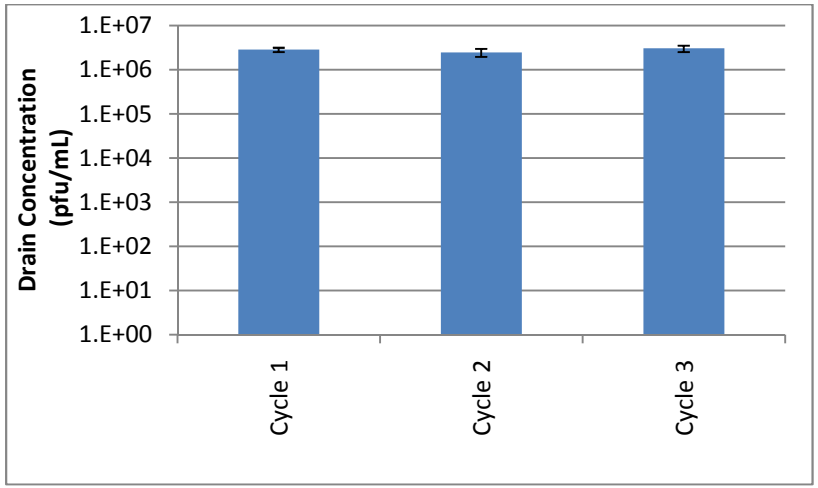

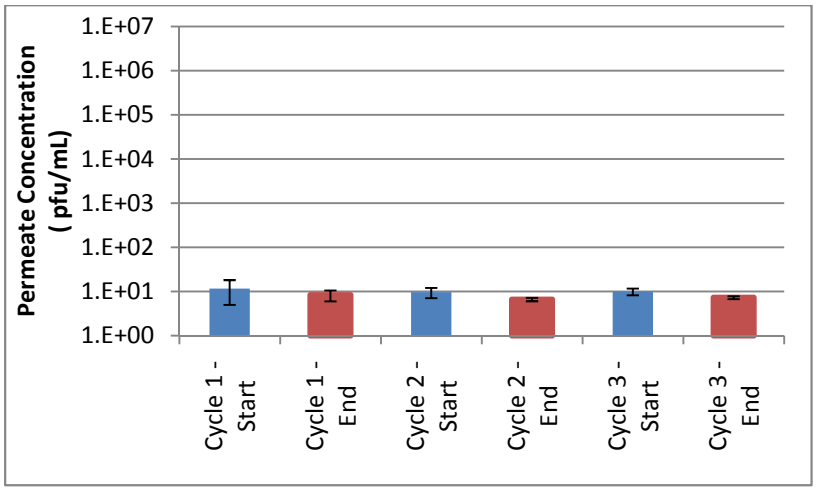

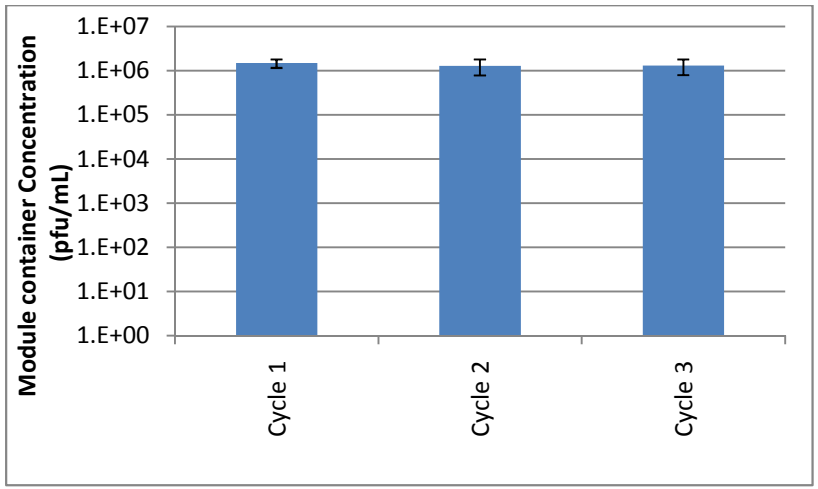

Grand River first experiment (August 2010) fourth spiking:

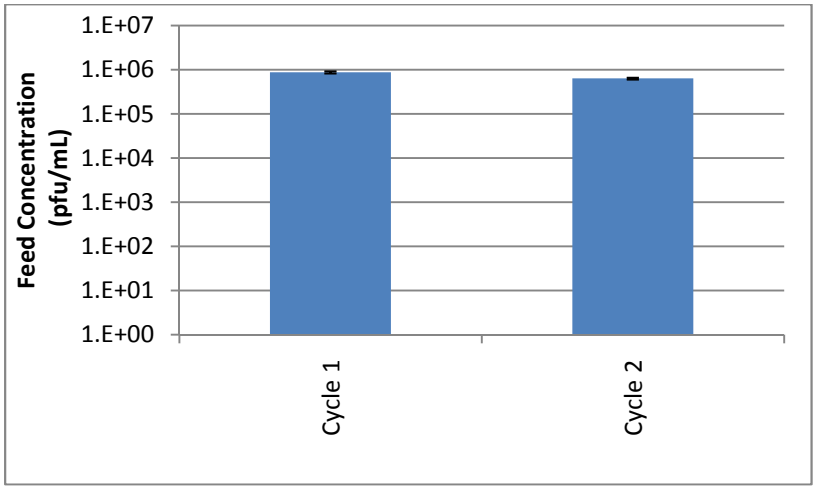

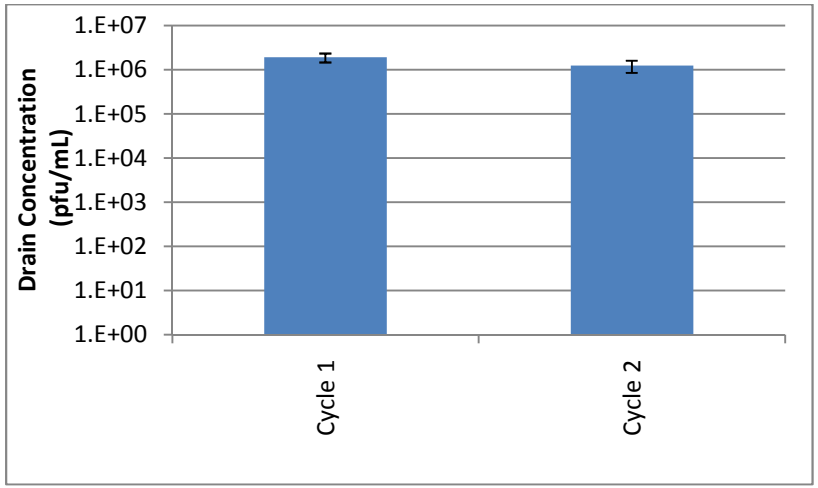

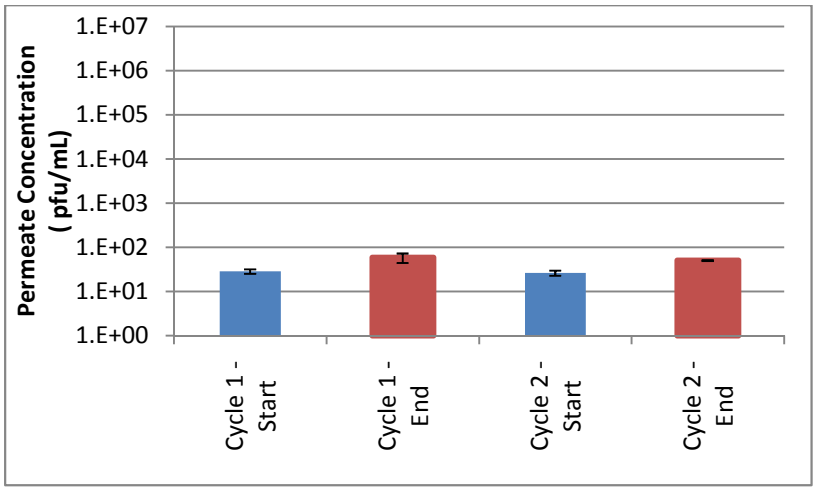

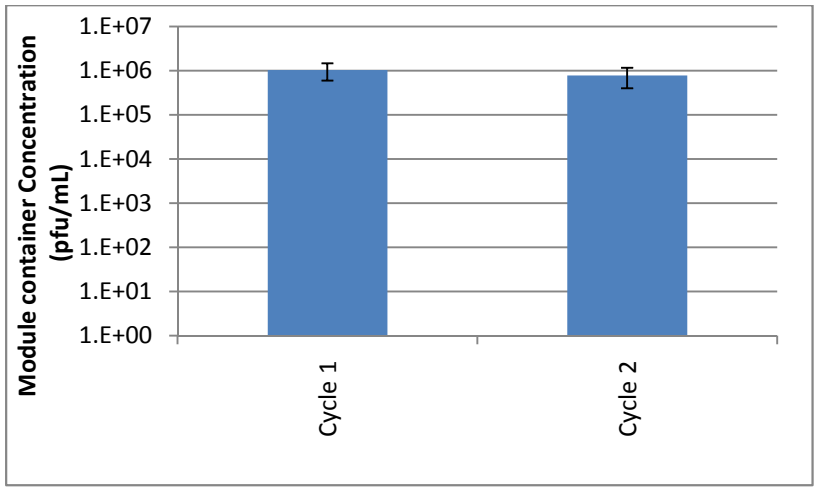

Grand River second experiment (September 2010) first spiking:

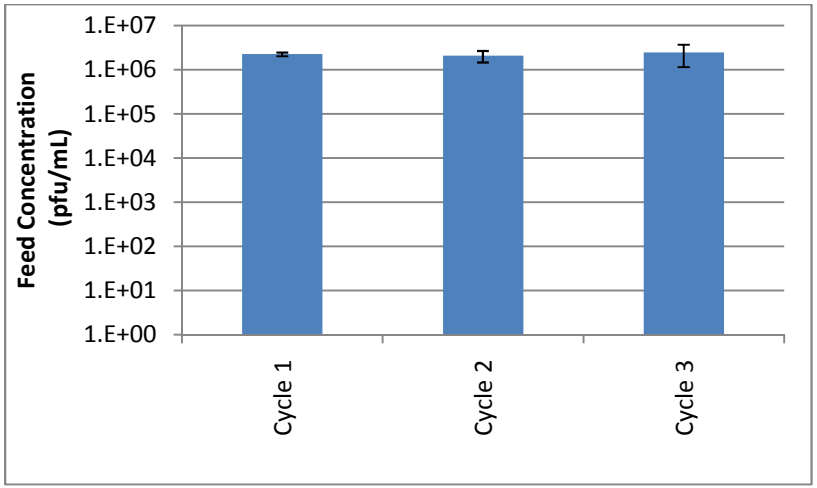

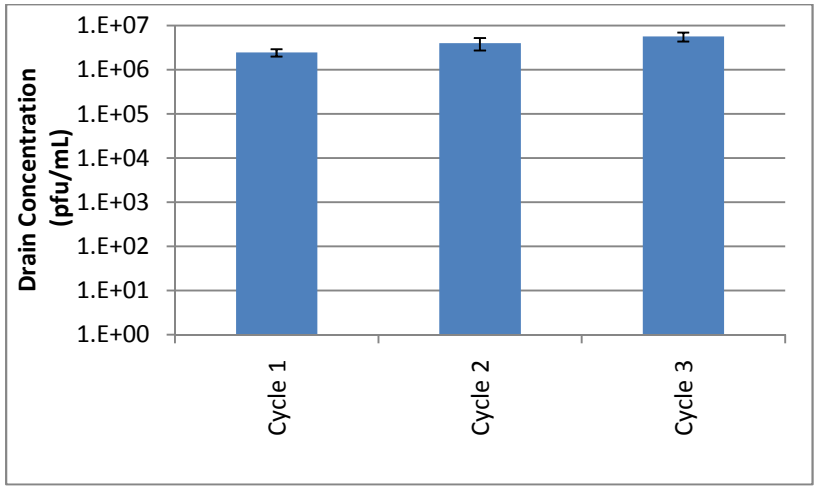

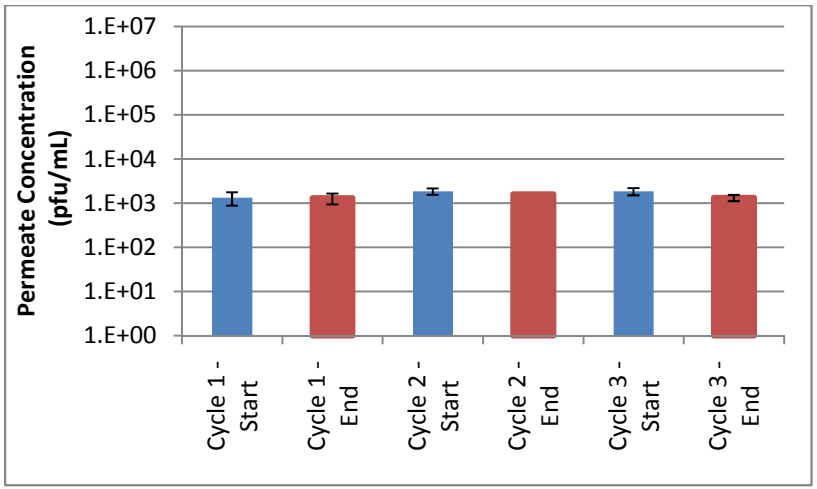

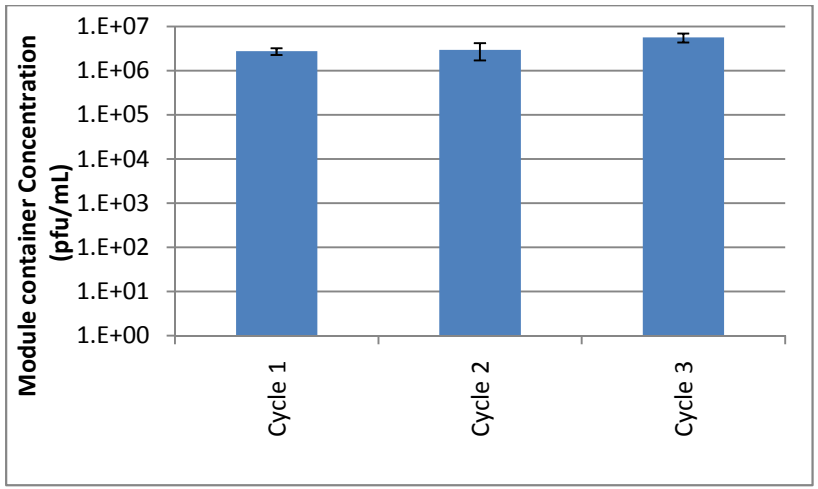

Grand River second experiment (September 2010) Second spiking:

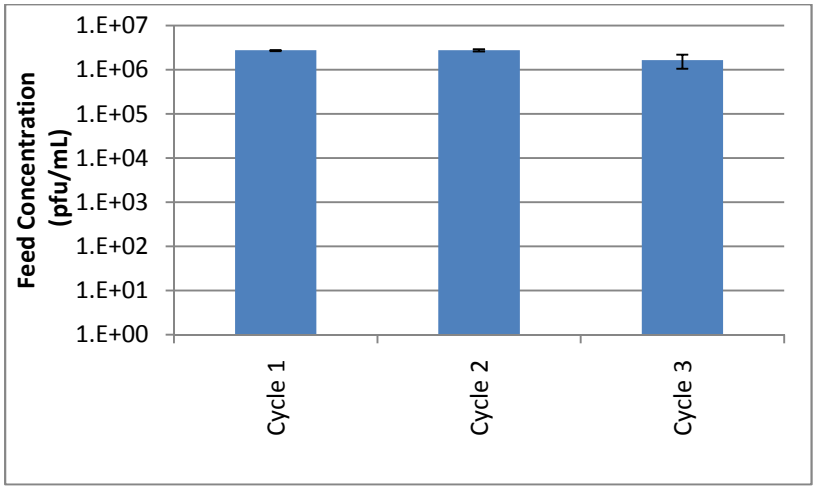

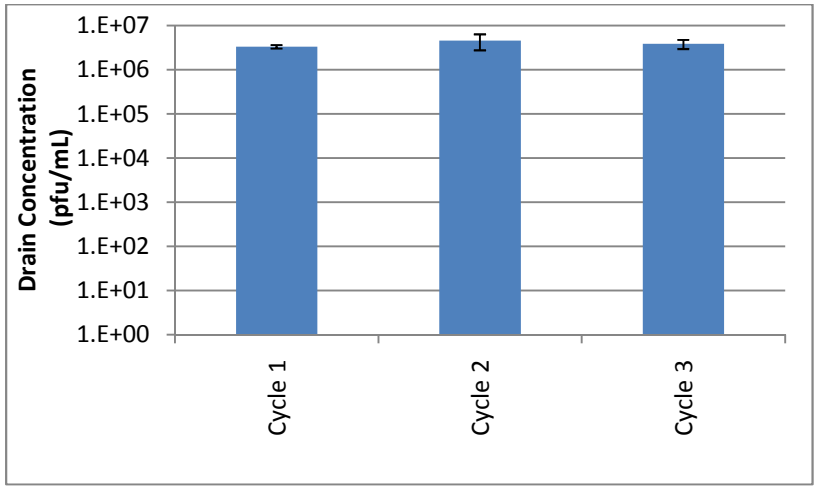

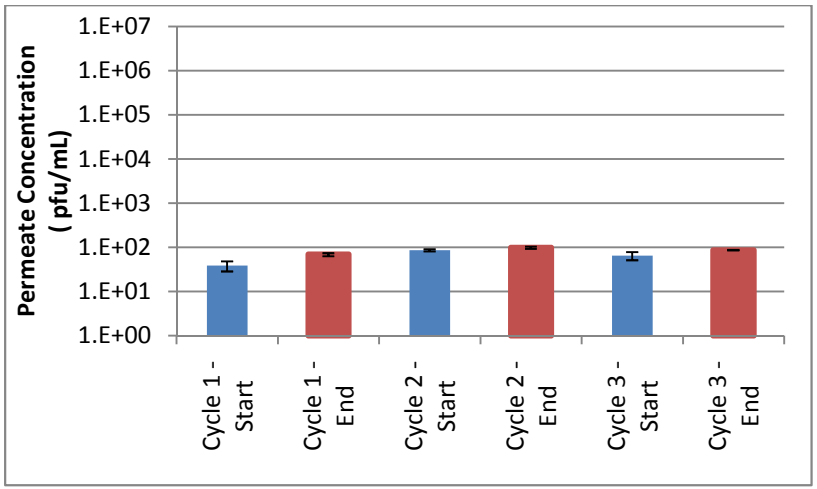

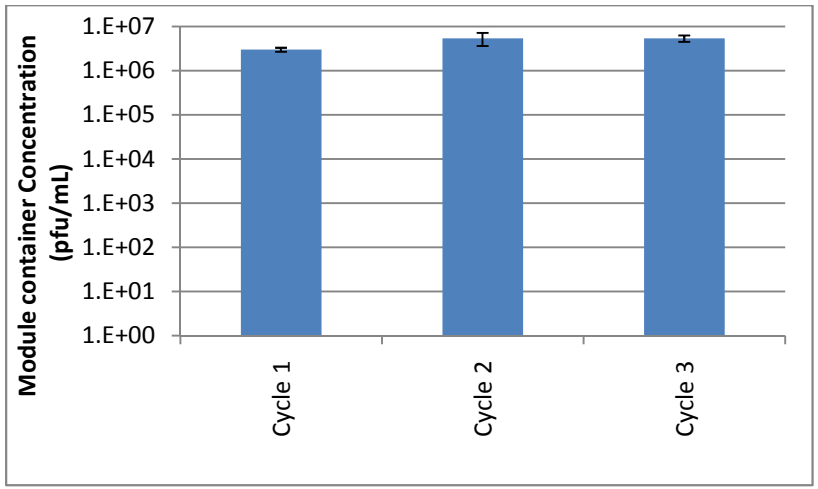

Grand River second experiment (September 2010) third spiking:

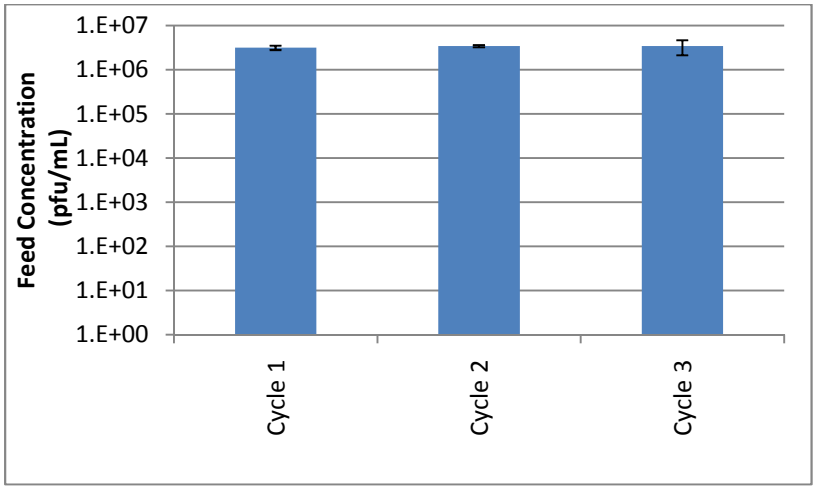

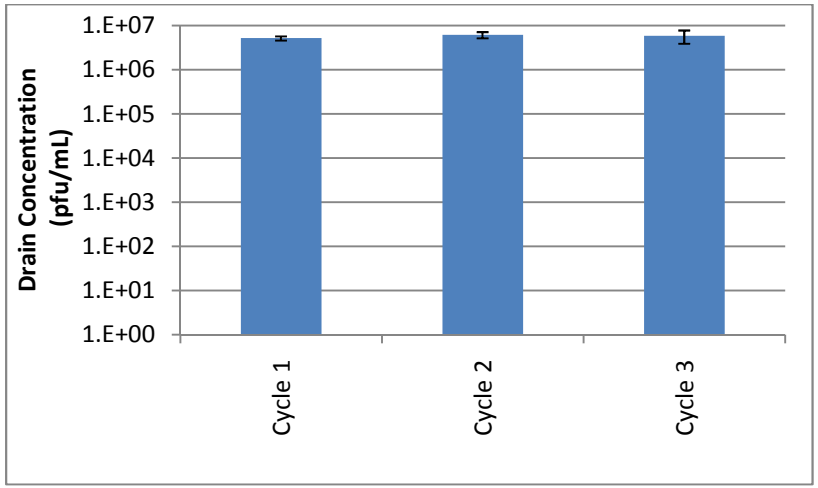

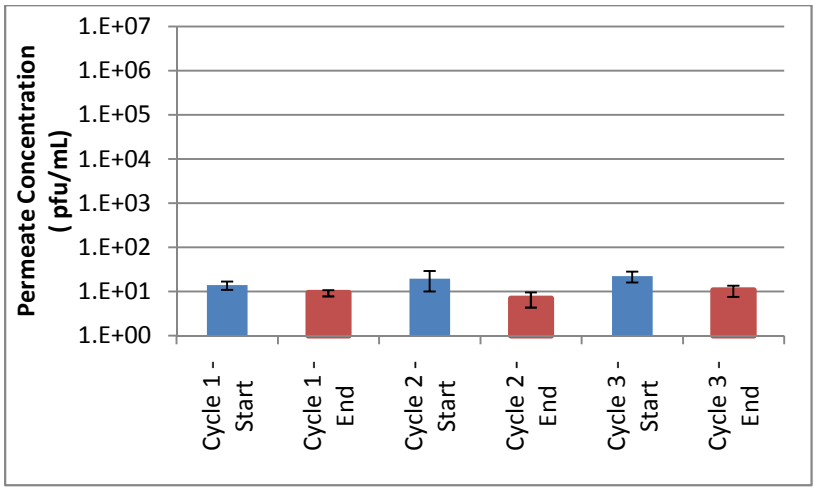

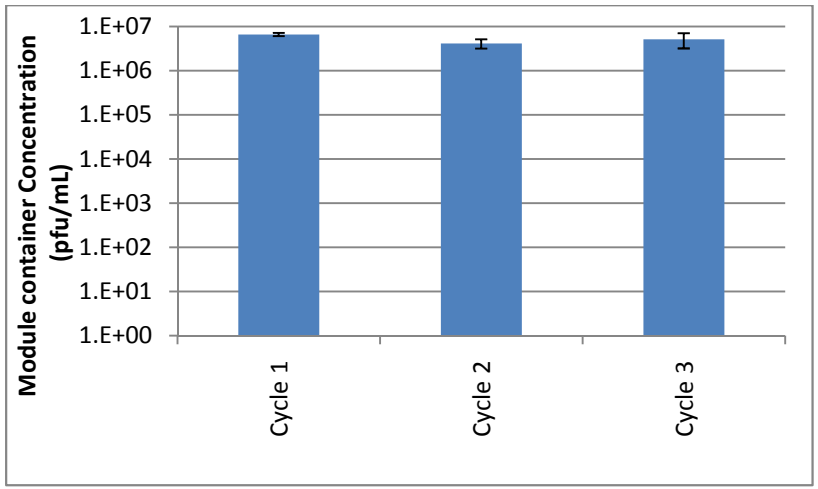

Grand River second experiment (September 2010) fourth spiking:

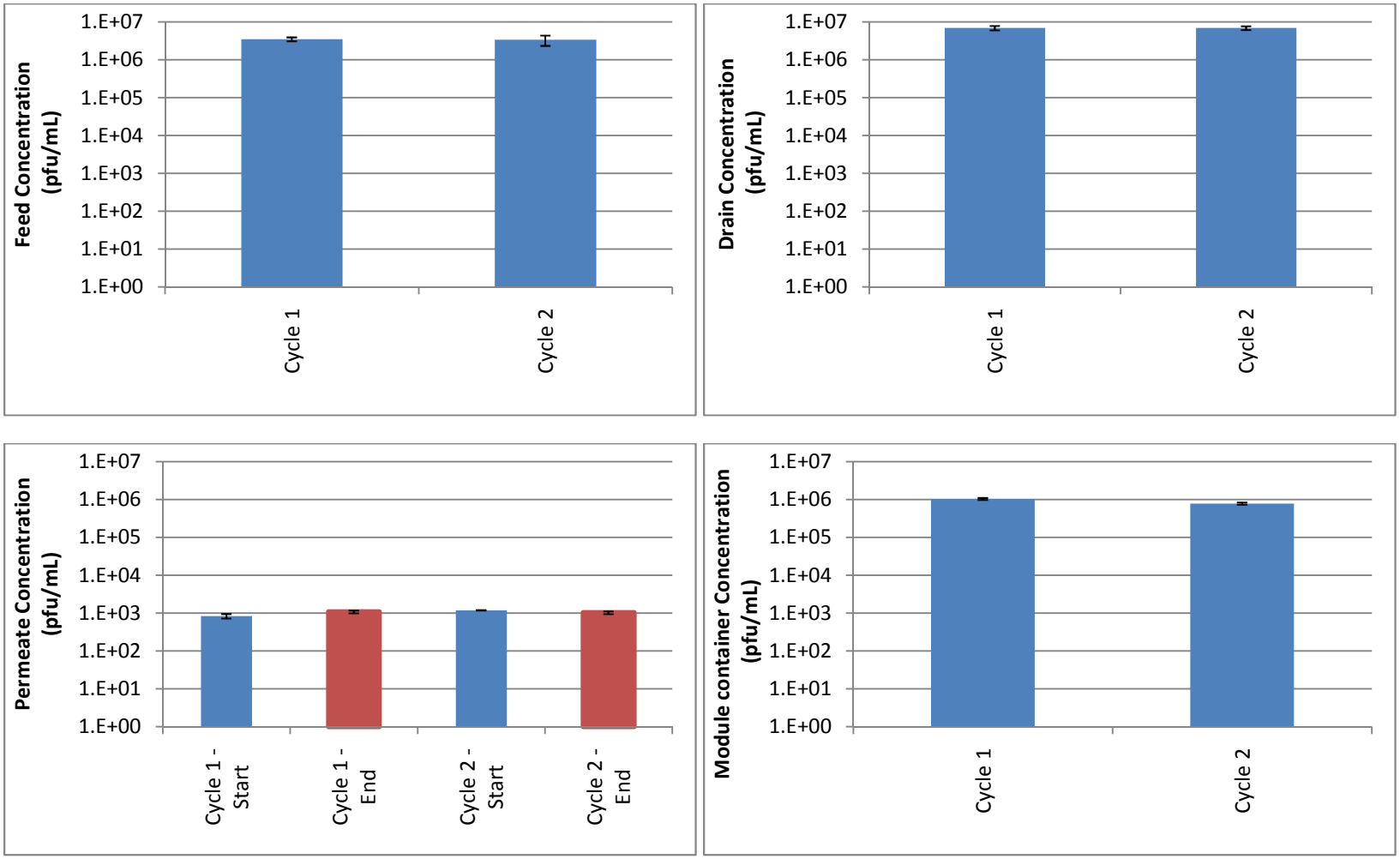

Georgian Bay experiment (November 2010) first spiking:

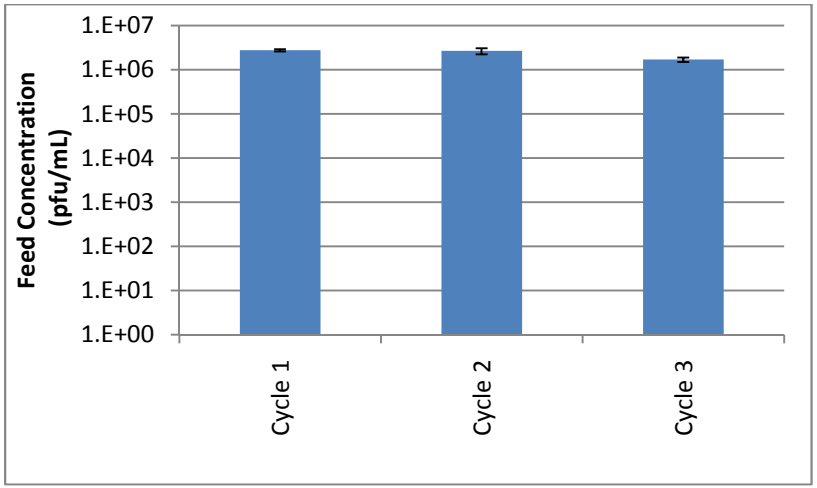

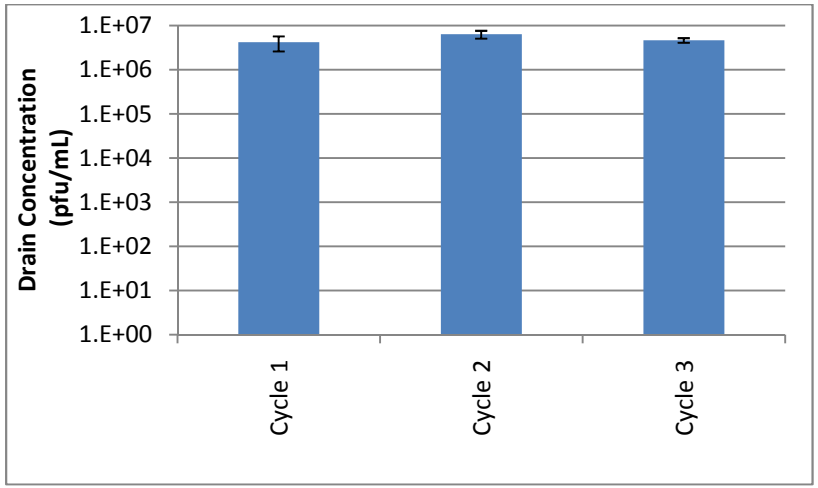

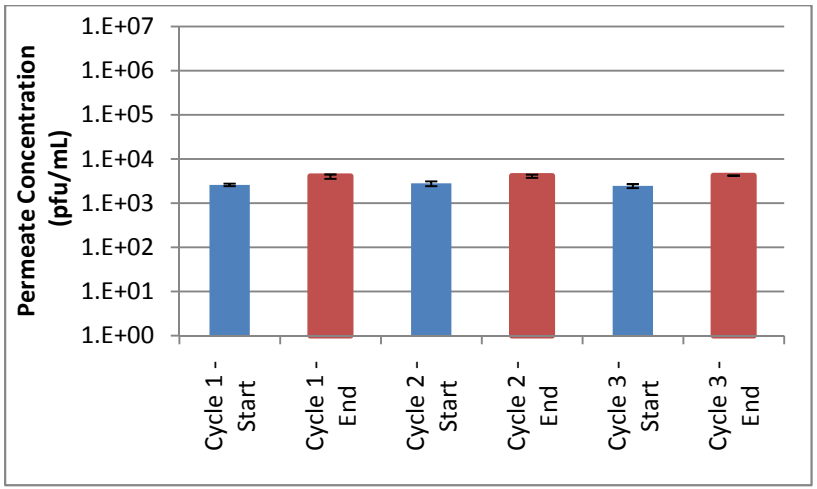

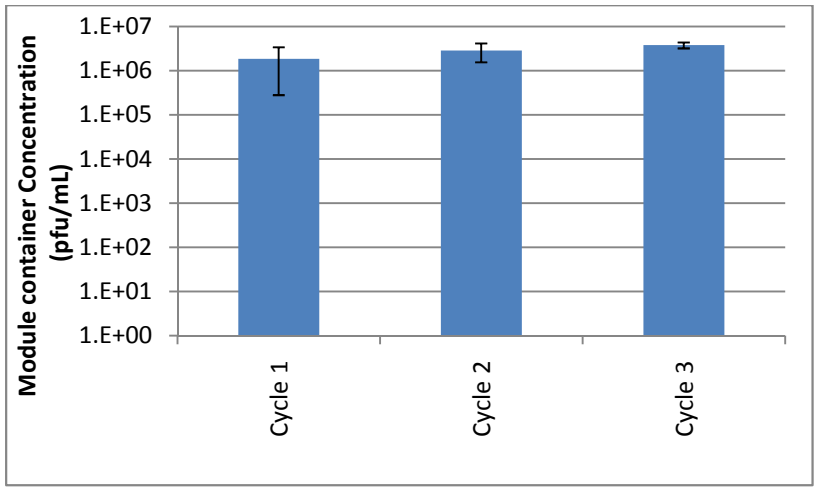

Georgian Bay experiment (November 2010) second spiking:

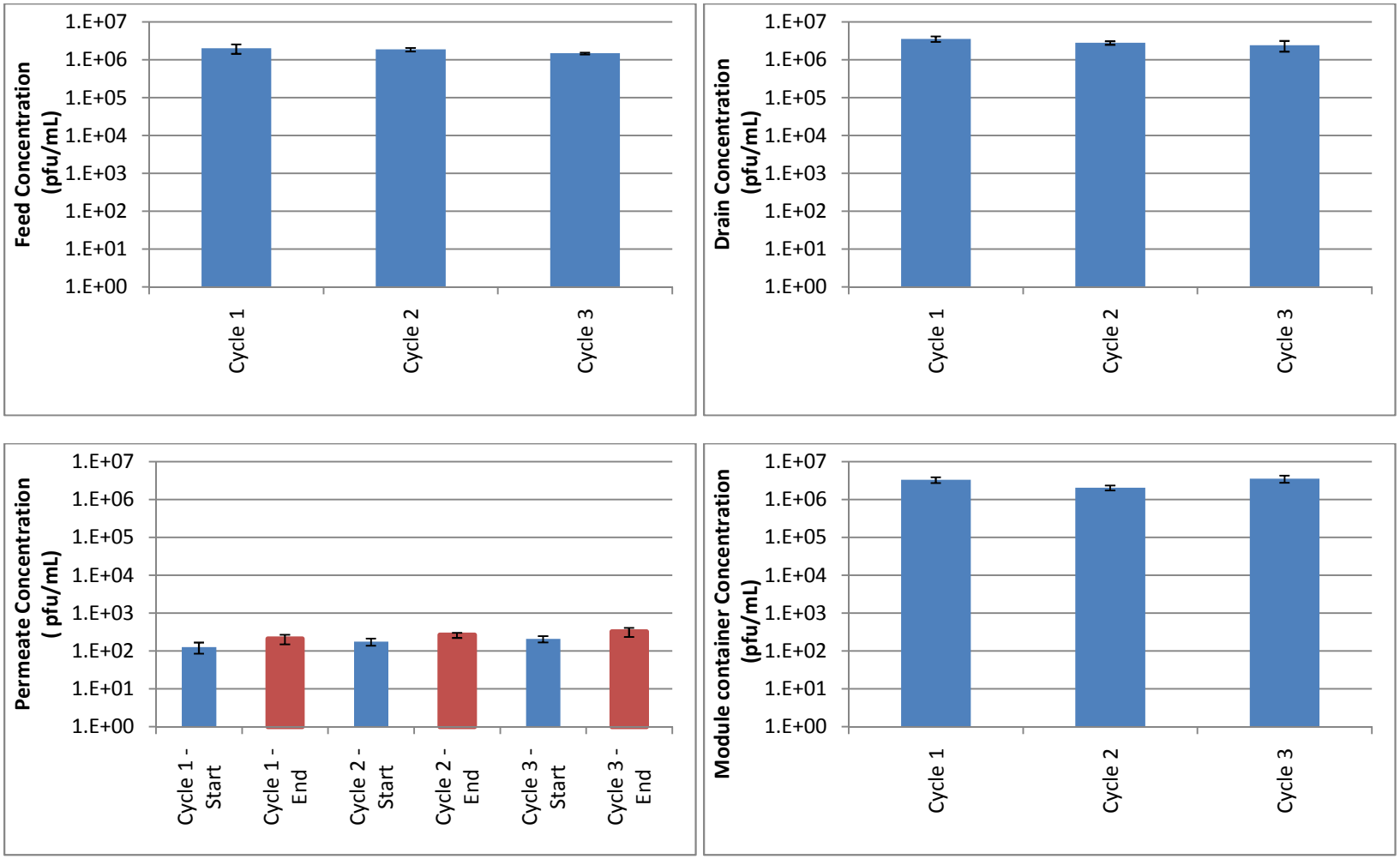

Georgian Bay experiment (November 2010) third spiking:

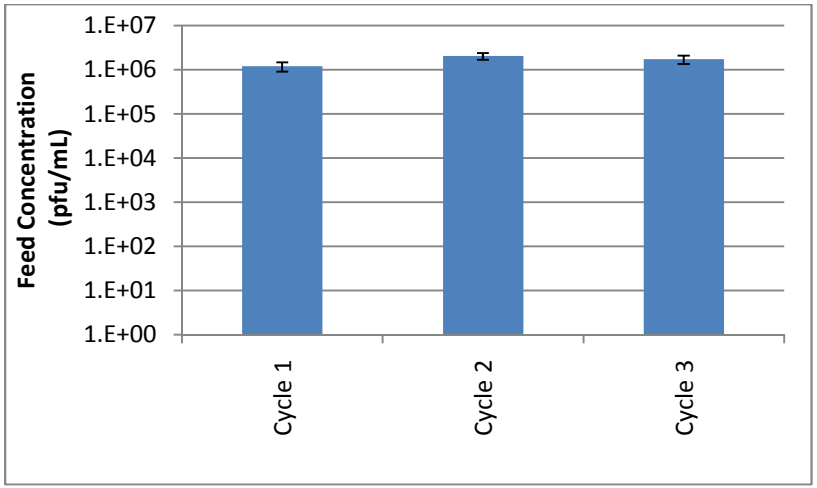

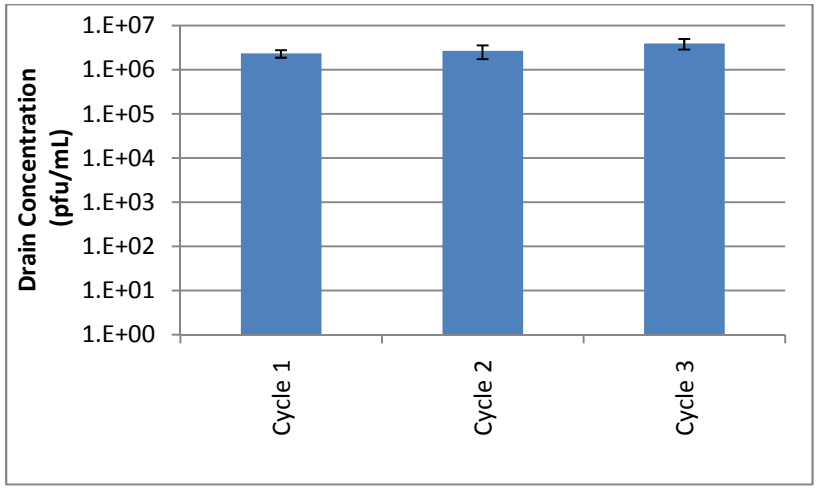

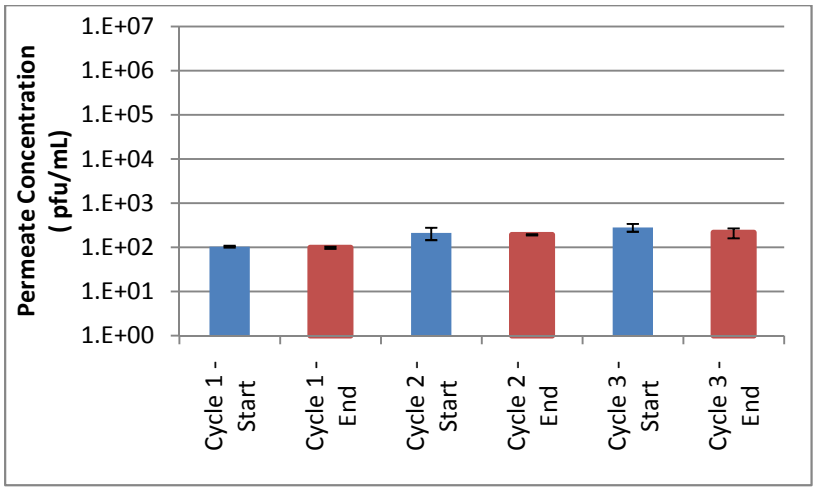

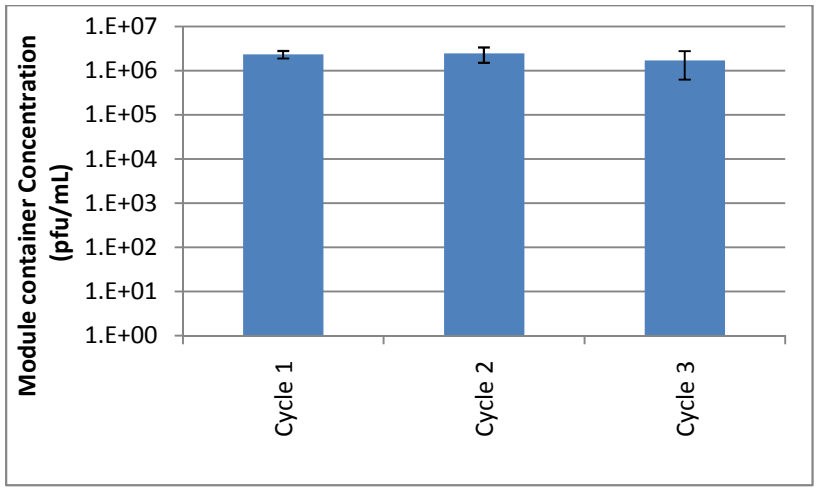

Georgian Bay experiment (November 2010) fourth spiking:

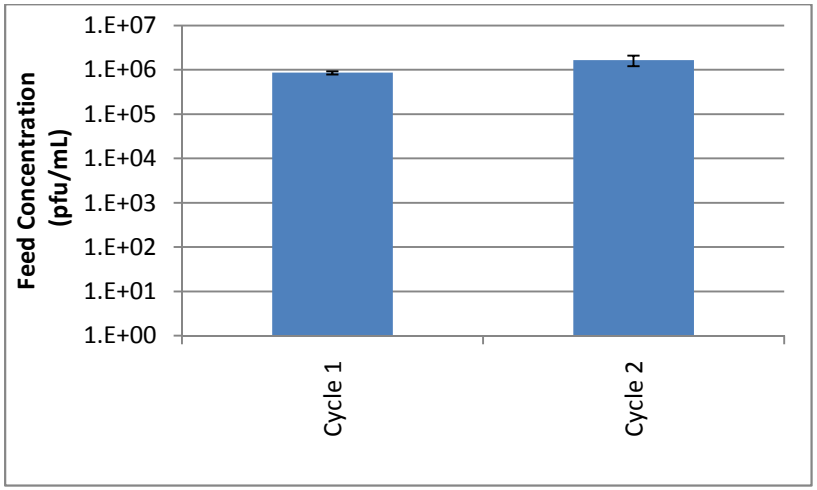

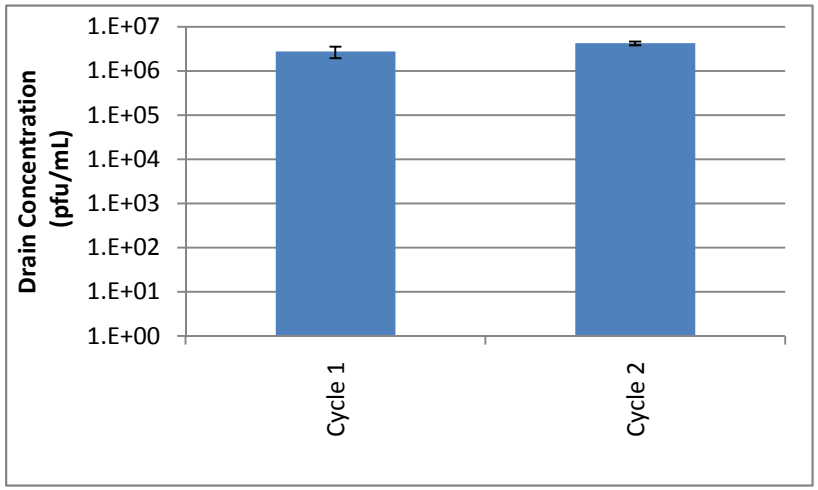

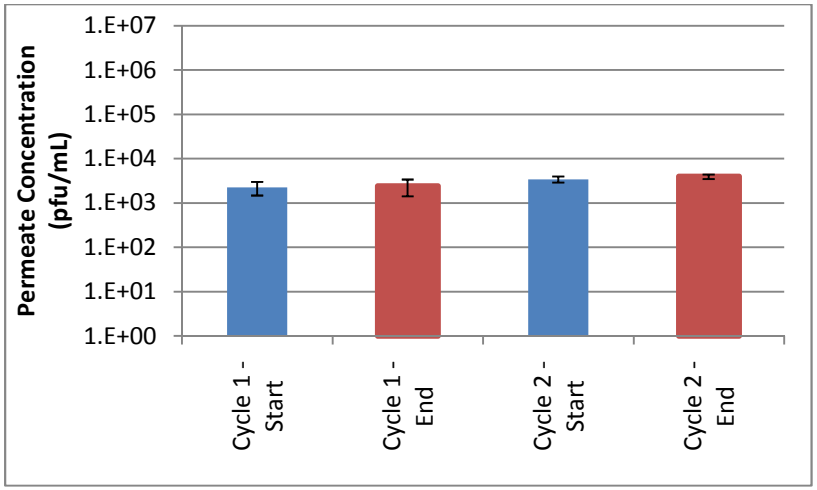

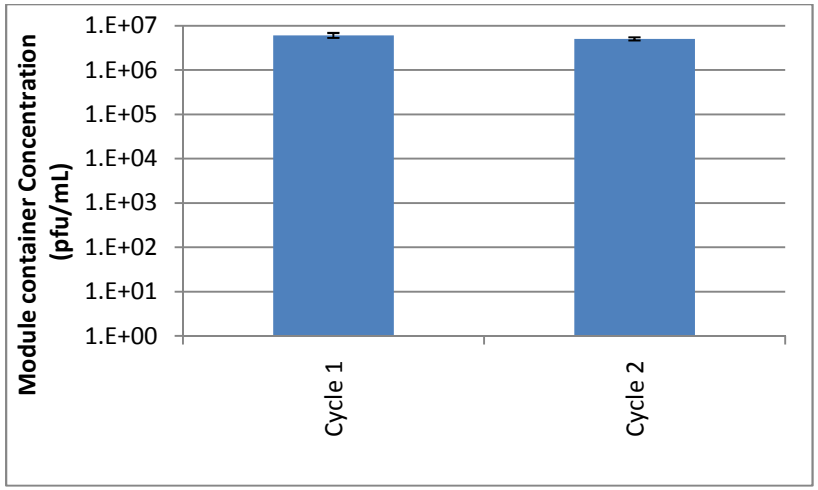

Georgian Bay experiment (November 2010) fifth spiking:

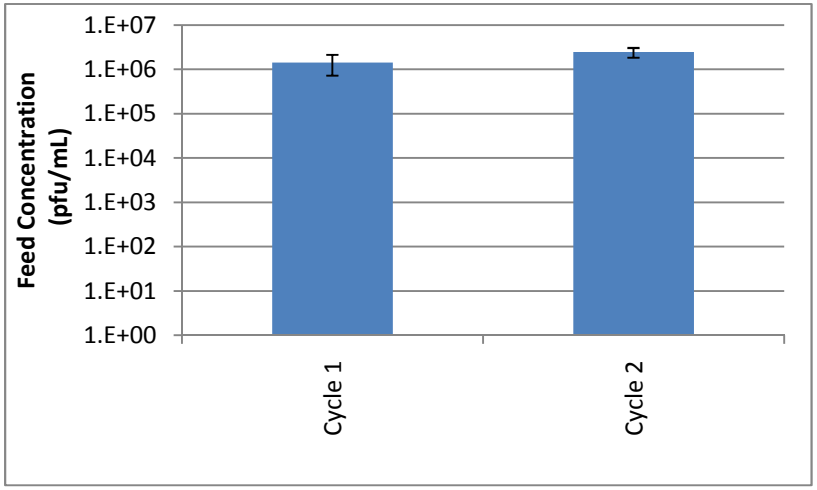

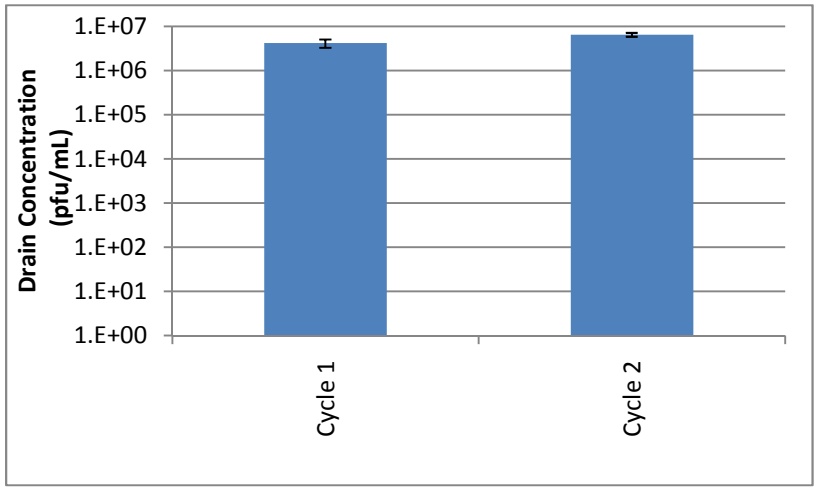

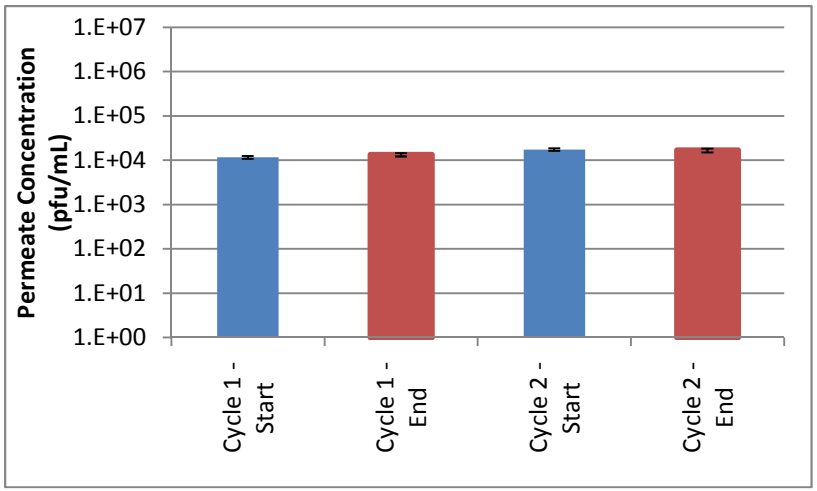

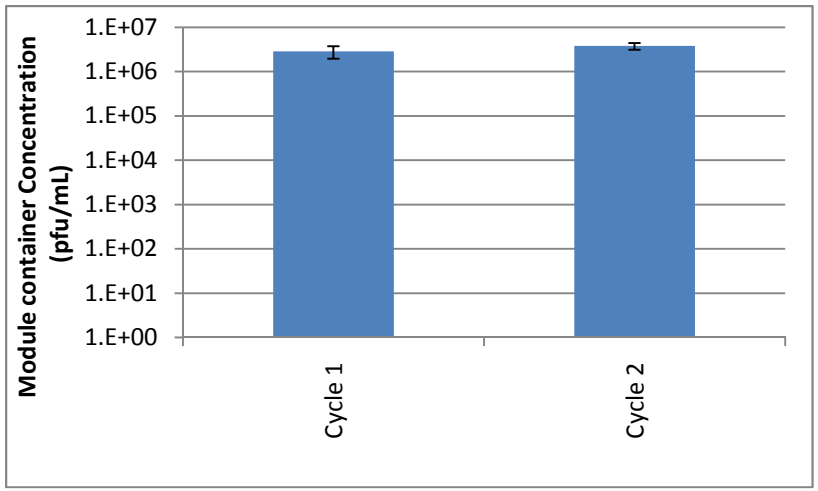

R^2 values for fitting TMP data for random filtration cycles within the second fouling experiment of the Grand River water (September 2010) to the different fouling mechanisms models (Best fit is the shaded cell).

Cycle Number	Standard blockage (n=1.5)	Intermediate Blockage (n=1)	Complete blockage (n=2)	Cake Layer formation (n=0)
5	0.8114	0.8102	0.8123	0.8073
15	0.7789	0.7798	0.7779	0.7811
29	0.8223	0.8236	0.8208	0.8255
45	0.857	0.8588	0.855	0.8612
80	0.9128	0.9146	0.9107	0.9175
115	0.9435	0.946	0.9407	0.9504
140	0.9441	0.9465	0.9414	0.9505
180	0.9544	0.9568	0.9518	0.961
200	0.9285	0.9316	0.9251	0.9375

R^2 values for fitting TMP data for random filtration cycles within the Georgian Bay fouling experiment (November 2010) to the different fouling mechanisms models (Best fit is the shaded cell).

Cycle Number	Standard blockage (n=1.5)	Intermediate Blockage (n=1)	Complete blockage (n=2)	Cake Layer formation (n=0)
5	0.8626	0.8621	0.8629	0.8606
15	0.6888	0.6886	0.6888	0.6882
29	0.6119	0.613	0.6109	0.6149
45	0.7038	0.7033	0.7042	0.7022
80	0.878	0.8796	0.8763	0.8825
115	0.8086	0.8104	0.8067	0.8137
140	0.8484	0.8504	0.8484	0.854
180	0.8522	0.8549	0.8494	0.8601
200	0.9182	0.9195	0.9169	0.9216
225	0.9362	0.9375	0.9348	0.9396
250	0.8812	0.8825	0.8798	0.8848
300	0.8615	0.8627	0.8602	0.8648
350	0.8785	0.8801	0.8768	0.8832

Bibliography

Adham, S. (2005) Development of a microfiltration and ultrafiltration knowledge base, AWWA Research Foundation and American Water Works Association, Denver, CO.

Arkhangelsky, E. and Gitis, V. (2008) Effect of transmembrane pressure on rejection of viruses by ultrafiltration membranes. Separation and Purification Technology 62(3), 619-628.

A.P.H. Association, Eaton, A.D., Clesceri, L.S., Greenberg, A.E., Franson, M.A.H., A.W.W. Association, and W.E. Federation, (1998) Standard methods for the examination of water and wastewater, American Public Health Association, Washington, DC.

AWWA (2005) Microfiltration and ultrafiltration membranes for drinking water, American Water Works Association, Denver, CO.

Binnig, G., Quate, C.F. and Gerber, C. (1986) Atomic Force Microscope. Physical Review Letters 56(9), 930.

Bowen, W.R., Calvo, J.I. and Hernández, A. (1995) Steps of membrane blocking in flux decline during protein microfiltration. Journal of Membrane Science 101(1-2), 153-165.

Bowen, W.R., Hilal, N., Lovitt, R.W. and Williams, P.M. (1996) Atomic Force Microscope Studies of Membranes: Surface Pore Structures of Diaflo Ultrafiltration Membranes. Journal of Colloid and Interface Science 180(2), 350-359.

Bungay, P.M. and Brenner, H. (1973) The motion of a closely-fitting sphere in a fluid-filled tube. International Journal of Multiphase Flow 1(1), 25-56.

Burns, D.B. and Zydney, A.L. (2001) Contributions to electrostatic interactions on protein transport in membrane systems. AIChE Journal 47(5), 1101-1114.

Carrillo-Tripp, M., Shepherd, C.M., Borelli, I.A., Venkataraman, S., Lander, G., Natarajan, P., Johnson, J.E., Brooks, C.L. and Reddy, V.S. (2009) VIPERdb2: an enhanced and web API enabled relational database for structural virology. Nucleic Acids Research 37(suppl 1), D436-D442.

Casella, G. and Berger, R.L. (2002) Statistical inference, Thomson Learning, Australia; Pacific Grove, CA.

Cho, J., Amy, G. and Pellegrino, J. (2000) Membrane filtration of natural organic matter: Factors and mechanisms affecting rejection and flux decline with charged ultrafiltration (UF) membrane. Journal of Membrane Science 164(1-2), 89-110.

Costa, A.R., de Pinho, M.N. and Elimelech, M. (2006) Mechanisms of colloidal natural organic matter fouling in ultrafiltration. Journal of Membrane Science 281(1-2), 716-725.

Crittenden, J.C. and Montgomery Watson Harza (Firm). (2005) Water treatment principles and design, J. Wiley, Hoboken, N.J.

De la Rubia, A., RodriÌ guez, M., LeoÌ n, V. and Prats, D. (2008) Removal of natural organic matter and THM formation potential by ultra- and nanofiltration of surface water. Water Research 42(3), 714-722.

Dechadilok, P. and Deen, W.M. (2006) Hindrance Factors for Diffusion and Convection in Pores. Industrial & Engineering Chemistry Research 45(21), 6953-6959.

Deen, W.M. (1987) Hindered transport of large molecules in liquid-filled pores. AIChE Journal 33(9), 1409-1425.

Dietz, P., Hansma, P.K., Inacker, O., Lehmann, H.-D. and Herrmann, K.-H. (1992) Surface pore structures of micro- and ultrafiltration membranes imaged with the atomic force microscope. Journal of Membrane Science 65(1-2), 101-111.

Egerton, R.F. (2005) Physical principles of electron microscopy : an introduction to TEM, SEM, and AEM, Springer Science+Business Media, New York.

Fiksdal, L. and Leiknes, T. (2006) The effect of coagulation with MF/UF membrane filtration for the removal of virus in drinking water. Journal of Membrane Science 279(1-2), 364-371.

Flemming, H.C. (1997) Reverse osmosis membrane biofouling. Experimental Thermal and Fluid Science 14(4), 382-391.

Flemming, H.C., Schaule, G., Griebe, T., Schmitt, J. and Tamachkiarowa, A. (1997) Biofouling - The Achilles heel of membrane processes. Desalination 113(2-3), 215-225.

Fong, T.-T. and Lipp, E.K. (2005) Enteric Viruses of Humans and Animals in Aquatic Environments: Health Risks, Detection, and Potential Water Quality Assessment Tools. Microbiol. Mol. Biol. Rev. 69(2), 357-371.

Freedman, D. and Diaconis, P. (1981) On the histogram as a density estimator: L2 theory. Probability Theory and Related Fields 57(4), 453-476.

Grabow, W.O.K. (2001) Bacteriophages: Update on application as models for viruses in water. Water Sa 27(2), 251-268.

Gutierrez, L., Li, X., Wang, J., Nangmenyi, G., Economy, J., Kuhlenschmidt, T.B., Kuhlenschmidt, M.S. and Nguyen, T.H. (2009) Adsorption of rotavirus and bacteriophage MS2 using glass fiber coated with hematite nanoparticles. Water Research 43(20), 5198-5208.

Haberkamp, J., Ernst, M., Makdissy, G., Huck, P.M. and Jekel, M. (2008) Protein fouling of ultrafiltration membranes — investigation of several factors relevant for tertiary wastewater treatment. Journal of Environmental Engineering and Science 7(6), 651-660.

Hallé, C., Huck, P.M., Peldszus, S., Haberkamp, J. and Jekel, M. (2009) Assessing the performance of biological filtration as pretreatment to low pressure membranes for drinking water. Environmental Science and Technology 43(10), 3878-3884.

Hallé, C. (2010) Biofiltration in Drinking Water Treatment: Reduction of Membrane Fouling and Biodegradation of Organic Trace Contaminants, University of Waterloo, Waterloo.

Hayama, M., Kohori, F. and Sakai, K. (2002) AFM observation of small surface pores of hollow-fiber dialysis membrane using highly sharpened probe. Journal of Membrane Science 197(1-2), 243-249.

Health Canada (2004) Guidelines for Canadian Drinking Water Quality: Supporting Documentation — Enteric Viruses, Water Quality and Health Bureau, Healthy Environments and Consumer Safety Branch, Health Canada, Ottawa, Ontario.

Health Canada (2010) Enteric Viruses in Drinking Water - Document for Public Comment. Water, F.-P.-T.C.o.D. (ed), Water Quality and Health Bureau, Healthy Environments and Consumer Safety Branch, Health Canada, Ottawa, Ontario.

Herath, G., Yamamoto, K. and Urase, T. (1999) Removal of viruses by microfiltration membranes at different solution environments, pp. 331-338.

Hermia, J. (1982) Constant pressure blocking filtration laws - application to power-law non-newtonian fluids. TRANS INST CHEM ENG V 60(N 3), 183-187.

Hernandez, A., Calvo, J.I., Pradanos, P. and Palacio, L. (1999) Surface chemistry and electrochemistry of membranes. Sørensen, T. (ed), M. Dekker.

Hirasaki, T., Yokogi, M., Kono, A., Yamamoto, N. and Manabe, S. (2002) Removal and determination of dispersion state of bacteriophage phi X174 in aqueous solution by cuprammonium regenerated cellulose microporous hollow fiber membrane (BMM (R)). Journal of Membrane Science 201(1-2), 95-102.

Hlavacek, M. and Bouchet, F. (1993) Constant flowrate blocking laws and an example of their application to dead-end microfiltration of protein solutions. Journal of Membrane Science 82(3), 285-295.

Hong, S. and Elimelech, M. (1997) Chemical and physical aspects of natural organic matter (NOM) fouling of nanofiltration membranes. Journal of Membrane Science 132(2), 159-181.

Howe, K.J. and Clark, M.M. (2002) Fouling of Microfiltration and Ultrafiltration Membranes by Natural Waters. Environmental Science & Technology 36(16), 3571-3576.

Hu, J.Y., Ong, S.L., Song, L.F., Feng, Y.Y., Liu, W.T., Tan, T.W., Lee, L.Y. and Ng, W.J. (2003) Removal of MS2 bacteriophage using membrane technologies, pp. 163-168.

Huang, H., Young, T.A. and Jacangelo, J.G. (2007) Unified Membrane Fouling Index for Low Pressure Membrane Filtration of Natural Waters: Principles and Methodology. Environmental Science & Technology 42(3), 714-720.

Huang, H., Schwab, K. and Jacangelo, J.G. (2009) Pretreatment for Low Pressure Membranes in Water Treatment: A Review. Environmental Science & Technology 43(9), 3011-3019.

Huber, S.A., Balz, A., Abert, M. and Pronk, W. (2011) Characterisation of aquatic humic and non-humic matter with size-exclusion chromatography - organic carbon detection - organic nitrogen detection (LC-OCD-OND). Water Research 45(2), 879-885.

ICTVdB Management (2006a) 00.042. Microviridae. In: ICTVdB The Universal Virus Database, version 3. Büchen-Osmond, C. (Ed), Columbia University, New York, USA.

ICTVdB Management (2006b) 00.037.0.01.001. Enterobacteria phage MS2. In: ICTVdB The Universal Virus Database, version 4. Büchen-Osmond, C. (Ed), Columbia University, New York, USA.

International Organization for Standardization (1995) ISO 10705-1, Detection and enumeration of bacteriophages. Part 1: Enumeration of F-specific RNA bacteriphages.

Isbister, J.D., Simmons, J.A., Scott, W.M. and Kitchens, J.F. (1983) A simplified method for coliphage detection in natural waters. ACTA Microbial Polonica 32, 197-206.

Jacangelo, J.G., Adham, S.S. and Laine, J.M. (1995) Mechanism of Cryptosporidium, Giardia, and Ms2 Virus Removal by Mf and Uf. Journal American Water Works Association 87(9), 107-121.

Jacangelo, J.G., Patania Brown, N.L., Madec, A., Schwab, K., Huffman, D., Amy, G., Mysore, C., Leparc, J. and Prescott, A. (2006) Micro- and ultrafiltration performance specifications based on microbial removal, Awwa Research Foundation : American Water Works Association ; IWA Pub., Denver, Colo.; S.l.

Jarusutthirak, C., Mattaraj, S. and Jiraratananon, R. (2007) Influence of inorganic scalants and natural organic matter on nanofiltration membrane fouling. Journal of Membrane Science 287(1), 138-145.

Jermann, D., Pronk, W., Meylan, S. and Boller, M. (2007) Interplay of different NOM fouling mechanisms during ultrafiltration for drinking water production. Water Research 41(8), 1713-1722.

Jucker, C. and Clark, M.M. (1994) Adsorption of aquatic humic substances on hydrophobic ultrafiltration membranes. Journal of Membrane Science 97, 37-52.

Kang, S., Asatekin, A., Mayes, A.M. and Elimelech, M. (2007) Protein antifouling mechanisms of PAN UF membranes incorporating PAN-g-PEO additive. Journal of Membrane Science 296(1-2), 42-50.

Kennedy, M.D., Kamanyi, J., Salinas, S.G., Lee, N.H., Schippers, J.C. and Amy, G. (2008) Advanced membrane technology and applications. Li, N.N. (ed), John Wiley & Sons, Hoboken, N.J.

Khayet, M. and Matsuura, T. (2001) Preparation and Characterization of Polyvinylidene Fluoride Membranes for Membrane Distillation. Industrial & Engineering Chemistry Research 40(24), 5710-5718.

Khulbe, K.C., Feng, C.Y. and Matsuura, T. (2008) Synthetic polymeric membranes : characterization by atomic force microscopy, Springer, Berlin [u.a.].

Kim, J.Y., Lee, H.K. and Kim, S.C. (1999) Surface structure and phase separation mechanism of polysulfone membranes by atomic force microscopy. Journal of Membrane Science 163(2), 159-166.

Kim, K.J., Fane, A.G., Fell, C.J.D., Suzuki, T. and Dickson, M.R. (1990) Quantitative microscopic study of surface characteristics of ultrafiltration membranes. Journal of Membrane Science 54(1-2), 89-102.

Knoell, T., Safarik, J., Cormack, T., Riley, R., Lin, S.W. and Ridgway, H. (1999) Biofouling potentials of microporous polysulfone membranes containing a sulfonated polyether-ethersulfone/polyethersulfone block copolymer: correlation of membrane surface properties with bacterial attachment. Journal of Membrane Science 157(1), 117-138.

Kuzmanovic, D.A., Elashvili, I., Wick, C., O'Connell, C. and Krueger, S. (2003) Bacteriophage MS2: Molecular Weight and Spatial Distribution of the Protein and RNA Components by Small-Angle Neutron Scattering and Virus Counting. Structure 11(11), 1339-1348.

Langlet, J., Gaboriaud, F., Duval, J.F.L. and Gantzer, C. (2008) Aggregation and surface properties of F-specific RNA phages: Implication for membrane filtration processes. Water Research 42(10-11), 2769-2777.

Langlet, J., Ogorzaly, L., Schrotter, J.C., Machinal, C., Gaboriaud, F., Duval, J.F.L. and Gantzer, C. (2009) Efficiency of MS2 phage and Q beta phage removal by membrane filtration in water treatment: Applicability of real-time RT-PCR method. Journal of Membrane Science 326(1), 111-116.

Lee, N., Amy, G., Croué, J.-P. and Buisson, H. (2004) Identification and understanding of fouling in low-pressure membrane (MF/UF) filtration by natural organic matter (NOM). Water Research 38(20), 4511-4523.

Lee, N., Amy, G., Croué, J.-P. and Buisson, H. (2005) Morphological analyses of natural organic matter (NOM) fouling of low-pressure membranes (MF/UF). Journal of Membrane Science 261(1-2), 7-16.

Lee, N., Amy, G. and Croué, J.-P. (2006) Low-pressure membrane (MF/UF) fouling associated with allochthonous versus autochthonous natural organic matter. Water Research 40(12), 2357-2368.

Lewandowski, Z. and Beyenal, H. (2005) Biofilms: their structure, activity, and effect on membrane filtration. Water Sci Technol. 51(6-7), 181-192.

Li, Q. and Elimelech, M. (2004) Organic fouling and chemical cleaning of nanofiltration membranes: Measurements and mechanisms. Environmental Science and Technology 38(17), 4683-4693.

Lytle, C. and Routson, L. (1995) Minimized virus binding for tests of barrier materials. Appl. Environ. Microbiol. 61(2), 643-649.

Madaeni, S.S., Fane, A.G. and Grohmann, G.S. (1995) Virus removal from water and wastewater using membranes. Journal of Membrane Science 102, 65-75.

Madaeni, S.S. (1997) Mechanism of virus removal using membranes. Filtration & Separation 34(1), 61-65.

Makdissy, G., CroueÌ , J.P., Amy, G., Lee, N., Habarou, H. and Buisson, H. (2002) Advances in knowledge of fouling of an ultrafiltration membrane. Proc. AWWA WQTC.

Matsuura, T. (1994) Synthetic membranes and membrane separation processes, CRC Press, Boca Raton.

McKenna, R., Xia, D., Willingmann, P., Iiag, L.L., Krishnaswamy, S., Rossmann, M.G., Olson, N.H., Baker, T.S. and Incardona, N.L. (1992) Atomic structure of single-stranded DNA bacteriophage [Phi]X174 and its functional implications. Nature 355(6356), 137-143.

Mehta, A. and Zydney, A.L. (2005) Permeability and selectivity analysis for ultrafiltration membranes. Journal of Membrane Science 249(1-2), 245-249.

Mehta, A. and Zydney, A.L. (2006) Effect of Membrane Charge on Flow and Protein Transport during Ultrafiltration. Biotechnology Progress 22(2), 484-492.

MF-Millipore™ (MF-Millipore Membrane Filter) Retrived from (http://www.millipore.com/catalogue/item/vmwp04700).

Otaki, M., Yano, K. and Ohgaki, S. (1998) Virus removal in a membrane separation process. Water Science and Technology 37(10), 107-116.

Pearce, G. (2007) Introduction to membranes: Filtration for water and wastewater treatment. Filtration & Separation 44(2), 24-27.

Peiris, R.H., Hallé, C., Budman, H., Moresoli, C., Peldszus, S., Huck, P.M. and Legge, R.L. (2010) Identifying fouling events in a membrane-based drinking water treatment process using principal component analysis of fluorescence excitation-emission matrices. Water Research 44(1), 185-194.

Penrod, S.L., Olson, T.M. and Grant, S.B. (1996) Deposition kinetics of two viruses in packed beds of quartz granular media. Langmuir 12(23), 5576-5587.

Pham, M., Mintz, E.A. and Nguyen, T.H. (2009) Deposition kinetics of bacteriophage MS2 to natural organic matter: Role of divalent cations. Journal of Colloid and Interface Science 338(1), 1-9.

Pierre, G., Causserand, C., Roques, C. and Aimar, P. (2010) Adsorption of MS2 bacteriophage on ultrafiltration membrane laboratory equipments. Desalination 250(2), 762-766.

Pujar, N.S. and Zydney, A.L. (1997) Charge Regulation and Electrostatic Interactions for a Spherical Particle in a Cylindrical Pore. Journal of Colloid and Interface Science 192(2), 338-349.

Richard Bowen, W., Hilal, N., Lovitt, R.W. and Williams, P.M. (1996) Atomic force microscope studies of membranes: Surface pore structures of Cyclopore and Anopore membranes. Journal of Membrane Science 110(2), 233-238.

Sahely, B. (2005) Hundreds of millions of membrane fibres in Ontario, but who's counting?

Saksena, S. and Zydney, A.L. (1995) Pore size distribution effects on electrokinetic phenomena in semipermeable membranes. Journal of Membrane Science 105(3), 203-215.

Schijven, J.F. and Hassanizadeh, S.M. (2000) Removal of viruses by soil passage: Overview of modeling, processes, and parameters. Critical Reviews in Environmental Science and Technology 30(1), 49-127.

Sheldon, J.M. (1991) The fine-structure of ultrafiltration membranes. I. Clean membranes. Journal of Membrane Science 62(1), 75-86.

Smith, F.G. and Deen, W.M. (1983) Electrostatic effects on the partitioning of spherical colloids between dilute bulk solution and cylindrical pores. Journal of Colloid and Interface Science 91(2), 571-590.

Sun, W., Chen, T., Chen, C. and Li, J. (2007) A study on membrane morphology by digital image processing. Journal of Membrane Science 305(1-2), 93-102.

Urase, T., Yamamoto, K. and Ohgaki, S. (1994) Effect of pore-size distribution of ultrafiltration membranes on virus rejection in cross-flow conditions, pp. 199-208, Pergamon-Elsevier Science Ltd.

Urase, T., Yamamoto, K. and Ohgaki, S. (1996) Effect of pore structure of membranes and module configuration on virus retention. Journal of Membrane Science 115(1), 21-29.

USEPA (2001a) LOW-PRESSURE MEMBRANE FILTRATION FOR PATHOGEN REMOVAL: APPLICATION, IMPLEMENTATION, AND REGULATORY ISSUES. Agency, U.S.E.P. (ed).

USEPA (2001b) Method 1602: Male-specific (F+) and somatic coliphage in water by single agar layer (SAL) procedure, EPA 821-R-01-029, Office of Water, Washington DC.

Valegard, K., Liljas, L., Fridborg, K. and Unge, T. (1990) The three-dimensional structure of the bacterial virus MS2. Nature 345(6270), 36-41.

van Voorthuizen, E.M., Ashbolt, N.J. and Schafer, A.I. (2001) Role of hydrophobic and electrostatic interactions for initial enteric virus retention by MF membranes. Journal of Membrane Science 194(1), 69-79.

Veeco Instruments Inc. (2004) SPM Training Notebook.

Verliefde, A.R.D., Cornelissen, E.R., Heijman, S.G.J., Petrinic, I., Luxbacher, T., Amy, G.L., Van der Bruggen, B. and van Dijk, J.C. (2009) Influence of membrane fouling by (pretreated) surface water on rejection of pharmaceutically active compounds (PhACs) by nanofiltration membranes. Journal of Membrane Science 330(1-2), 90-103.

Vincent, L. (1991) Watersheds in Digital Spaces: An Efficient Algorithm Based on Immersion Simulations. IEEE Transactions on Pattern Analysis and Machine Intelligence 13, 583-598.

Vrouwenvelder, H.S., van Paassen, J.A.M., Folmer, H.C., Hofman, J.A.M.H., Nederlof, M.M. and van der Kooij, D. (1998) Biofouling of membranes for drinking water production. Desalination 118(1-3), 157-166.

Wickramasinghe, S.R., Bower, S.E., Chen, Z., Mukherjee, A. and Husson, S.M. (2009) Relating the pore size distribution of ultrafiltration membranes to dextran rejection. Journal of Membrane Science 340(1-2), 1-8.

Yamamura, H., Kimura, K. and Watanabe, Y. (2007) Mechanism Involved in the Evolution of Physically Irreversible Fouling in Microfiltration and Ultrafiltration Membranes Used for Drinking Water Treatment. Environmental Science & Technology 41(19), 6789-6794.

Yuan, W. and Zydney, A.L. (1999) Humic acid fouling during microfiltration. Journal of Membrane Science 157(1), 1-12.

Zeman, L.J. and Zydney, A.L. (1996) Microfiltration and ultrafiltration : principles and applications, M. Dekker, New York.

Zheng, X. (2010) Major Organic Foulants in Ultrafiltration of Treated Domestic Wastewater and their Removal by Bio-filtration as Pre-treatment, Technischen Universität Berlin.

Zheng, X., Ernst, M., Huck, P.M. and Jekel, M. (2010) Biopolymer fouling in dead-end ultrafiltration of treated domestic wastewater. Water Research 44(18), 5212-5221.

Zodrow, K., Brunet, L., Mahendra, S., Li, D., Zhang, A., Li, Q. and Alvarez, P.J.J. (2009) Polysulfone ultrafiltration membranes impregnated with silver nanoparticles show improved biofouling resistance and virus removal. Water Research 43(3), 715-723.

Zularisam, A.W., Ismail, A.F. and Salim, R. (2006) Behaviours of natural organic matter in membrane filtration for surface water treatment -- a review. Desalination 194(1-3), 211-231.